University of Glasgow

Hudson-McAulay, Kate J. (2016) *The structural and mechanical integrity of historic wood.* PhD thesis.

http://theses.gla.ac.uk/7529/

The structural and mechanical integrity of historic wood

Kate J Hudson-McAulay

BSc (Hons), MSc

Submitted in fulfilment of the requirements for the

Degree of Doctor of Philosophy

School of Chemistry

College of Science and Engineering

University of Glasgow

August 2016

Abstract

Little is known about historic wood as it ages naturally. Instead, most studies focus on biological decay, as it is often assumed that wood remains otherwise stable with age. This PhD project was organised by Historic Scotland and the University of Glasgow to investigate the natural chemical and physical aging of wood.

The natural aging of wood was a concern for Historic Scotland as traditional timber replacement is the standard form of repair used in wooden cultural heritage; replacing rotten timber with new timber of the same species. The project was set up to look at what differences could exist both chemically and physically between old and new wood, which could put unforeseen stress on the joint between them. Through Historic Scotland it was possible to work with genuine historic wood from two species, Oak and Scots pine, both from the 1500's, rather than relying on artificial aging. Artificial aging of wood is still a debated topic, with consideration given to whether it is truly mimicking the aging process or just damaging the wood cells.

The chemical stability of wood was investigated using Fourier-transform infrared (FTIR) microscopy, as well as wet chemistry methods including a test for soluble sugars from the possible breakdown of the wood polymers. The physical properties assessed included using a tensile testing machine to uncover possible differences in mechanical properties. An environmental chamber was used to test the reaction to moisture of wood of different ages, as moisture is the most damaging aspect of the environment to wooden cultural objects. The project uncovered several differences, both physical and chemical, between the modern and historic wood which could affect the success of traditional 'like for like' repairs. Both oak and pine lost acetyl groups, over historic time, from their hemicellulose polymers. This chemical reaction releases acetic acid, which had no effect on the historic oak but was associated with reduced stiffness in historic pine, probably due to degradation of the hemicellulose polymers by acid hydrolysis. The stiffness of historic oak and pine was also reduced by decay. Visible pest decay led to loss of wood density but there was evidence that fungal decay, extending beyond what was visible, degraded the S2 layer of the pine cell walls, reducing the stiffness of the wood by depleting the cellulose microfibrils most aligned with the grain. Fungal decay of polysaccharides in pine wood left behind sugars that attracted increased levels of moisture.

 The degradation of essential polymers in the wood structure due to age had different impacts on the two species of wood, and raised questions concerning both the mechanism of aging of wood and the ways in which traditional repairs are implemented, especially in Scots pine. These repairs need to be done with more care and precision,

especially in choosing new timber to match the old. Within this project a quantitative method of measuring the microfibril angle (MFA) of wood using polarised Fourier transform infrared (FTIR) microscopy has been developed, allowing the MFA of both new and historic pine to be measured. This provides some of the information needed for a more specific match when selecting replacement timbers for historic buildings.

Table of Contents

List of Tables

List of Figures

Acknowledgement

Author's declaration

I declare that, except where explicit reference is made to the contribution of others, this PhD project is the result of my own work and has not been submitted for any other degree at the University of Glasgow or any other institution.

Kate Hudson-McAulay

Glossary of Abbreviations:

ANOVA- Analysis of Variance

D- Density

FTIR Spectroscopy – Fourier Transform Infrared Spectroscopy

MFA – Microfibril Angle

MOE-Modulus of Elasticity

NIR-Near Infrared Spectroscopy

PEGcon – Polyethylene glycol concentrate

RH – Relative Humidity

SD – Standard deviation

SEM-standard error of mean

UV – Ultraviolet

WAXS-Wide Angle X-ray Scattering

XRD- X-ray Diffraction

Probability values

Probability values given in this thesis have the following meanings:

P >0.05 – No significant difference

P < 0.05 –Significant - there is less then 5% probability that the difference in the results occurred by chance.

P < 0.01 Very significant – there is less than 1% probability that the difference occurred by chance.

P <0.001 Highly significant - there is less than 0.1% probability that the difference occurred by chance.

Chapter 1

Introduction

1.1 Scope of the thesis

Historic wood is one of the most important materials in our cultural heritage. Without it we would not have any of the wooden buildings (figure 1.1) or ships that are greatly admired today (figure 1.2). There are still many structures standing today that contain historic wood (Grimsdale, 1985).

Wood is still favoured for a lot of building work today due the fact that it is extremely strong and light in weight. It is also an easy material to work with in regard to cutting and shaping (Krauss et al., 2011; Kisternaya and Kozlov, 2006; Mitchell, 1985). Durability depends on species, chemical composition and environment (Yilgor et al., 2013).

As wood is an organic material its properties are all interlinked (Lasserre et al., 2009; Zwerger, 1997, p. 10). The intention of this research is not only to examine the mechanical properties of historic wood, but also to examine the wood at a cellular level to uncover how its performance changes with age.

Little is known about historic wood as it ages. Most published research focuses on biological decay. It is generally thought that without the influence of biological decay, wood would not age. However there is some evidence for chemical degradation (Erhardt et al., 1996; Gereke et al., 2011).

Figure 1.1: Stirling Castle (Carpenter Oak and Woodland, 2003)

Figure 1.2: HMS Victory (McGowan, 1999)

1.2 Timber sources and trade routes

Historically speaking the definition of wood is the material from small diameter coppiced trees where most commonly the whole stem is used. The technique of coppicing can only be carried out on hardwood trees. Historically timber is referred to as pieces cut from larger trees. These terms are not used with these strict historical definitions throughout this thesis and are more broadly used according to the more modern generalisation of the terms.

The most commonly found historic wood species in England is oak. Oak was the most abundant wood available until softwoods began to be shipped in during the Georgian period, when England's supply of oak was fast running out (Stevenson, 2009). Oak was then becoming scarcer due to competition for its use in the construction of houses and of ships for the wars with France (Yeomans, 1985).

Oak was not only preferred due to its abundance. Oak is a dense wood which is durable and extremely strong in tension and compression, making it a preferred material in the construction of timber framed buildings (Zwerger, 1997, p.36).

Scotland's timber heritage does not follow the same pattern that is seen in England. It is linked more to building traditions on the Continent such as those of the Netherlands, Germany and France. It is thought that this occurred through contact with these nations when they were at war with England (Brentnall, 2008).

Scotland began to import wood long before England, in the 15th century. This was due to the relatively poor quality of oak in Scotland, which has a tendency to grow more twisted making it unsuitable for structural use, and with the constant wars with England, the Scots looked elsewhere for the resource. Dendrochronological evidence shows that oak was imported principally from the Scandinavian regions (Mills and Crone, 2012). Local records of forest land are less readily available in Scotland than in England, but the combination of records and dendrochronology can give a lot of details about the history of a forest, including dates when more trees were felled or cleared for grazing by burning (Davis and Watson, 2007, p.1782).

Evidence for Scots pine in Scotland stems back to over 8000 years ago. In the mid Holocene there was around 1,500,000 ha of pine forest, of which only an estimated 1% remains (Wilson et al., 2011). This is believed to be due to major climatic changes, with harsh winds and increased rainfall (Wilson et al., 2011; Smout, 2015), as well as the gradual expansion of blanket bog. Birch then out-competed Scots pine as it can withstand wet soils (Smout, 2015). As the soils began to dry out about 4,500 years ago the pine resource began to recover (Smout, 2015).

Pine wood has been used locally over the course of history, but during the late eighteenth century Scots pine from northern Scotland was used more widely to support the ship building industry, and later for sleepers for railway lines (Smout, 2015). But evidence of imported Scots pine can be seen as far back as the 1460's from Finland. More frequent use of imported timber began in the 16th century from Scandinavia (Crone, 2008; Mills and Crone, 2012). Local knowledge allowed Scots pine to be grown in the Highlands producing wood with relatively few knots, but the trees were difficult to extract from the Highland glens. Dendrochronological evidence for the use of native Scottish pine in surviving medieval buildings is therefore very limited. Dendrochronological evidence shows that Scotland relied heavily on imported pine until the 18th century, when the infrastructure to use the native resource was developed (Mills and Crone, 2012). Therefore the wood obtained for this project, dated to the 15th and 16th century, is most likely Scandinavian imports.

1.3 Structural properties of historic timber roofs

The design of timber roofs in Scotland was influenced, much like anywhere else, by the timber resources available. Timber throughout the Medieval period was in short supply in Scotland, especially long straight timbers, and when these were available they were very expensive, whether home-grown or imported (Mills and Crone, 2012; Gomme, 2002).

Timber roof structures are a complex piece of engineering. Even the simplest of roofs have a very precise function with each element working together to keep the whole structure stable. At any one time there are three forms of loads on a roof structure: superimposed loads, meaning the weight of the roof covering; the weight of the frame itself; and the force of the elements such as wind (Brunskill, 2004, p20). The weight of the roof material, for example slate or thatch, puts a considerable load on the timber framework supporting it (Brunskill, 2004, p20). This weight can be resolved into a bending stress on the rafter and an outward force at the bottom of the rafter, which can topple the supporting walls. This is the main problem of construction that had to be overcome for a building design to be successful (Brunskill, 2004, p20). From an early date there were two very simple solutions common in Scotland, the cruck frame and the tie beam. More complex solutions including hammer beam roofs evolved later.

1.3.1 Cruck Roofs

Cruck design is thought to have stemmed from an extremely primitive approach of just tying two poles together and then thatching the roof, but its origins cannot be traced in

detail as there is little evidence of timber structures from before 1200 (Harris, 2010, p.9; Fenton, 1976, p.181).

Figure 1.3: Cruck frame seen at Prior's Lynn, Dumfries-shire (Dixon, 2002).

Generally cruck frames (figure 1.3) (cruiks in Scots) were used in vernacular buildings. But there have been examples found in a wide range of Scottish buildings from barns and cottages to castles (Dixon, 2002; Martin, 1987, p144). There a number of different designs for a cruck frame but in the basic design the roof is supported by pairs of curved timbers springing from the ground (Russell, 1993; Hanke 2008b; Fenton, 1976, p.183). The outward force caused by the weight of the roofing is transmitted down to ground level, or to near the base of the wall if the cruck stops short of the ground (Hay 1974, p33; Brunskill, 2004, p40). In Scotland cruck frames were most often used in conjunction with dry stone walling, which is stable under compression but not when subjected to an outward (shear) force. It was difficult to get large curved timbers to make taller buildings, and most were single-story. In the 12th century the cruck blades were brought directly down to the earth but in the 13th to 14th century they were shortened and were raised upon stone foundations (Dixon 2002). The crucks support the roof purlins. Over time there were many different designs. In some the cruck blades carry the lowest purlin or a wall plate and in others they hold the ridge purlin (Hay, 1976, p.33).

There are regional differences in the design of cruck systems (Walker, 1976, p.56) but the roofs themselves were generally thatched (Fenton, 1976, p.182). Sometimes the large curved timbers were simply tied or pegged together at the apex of the roof, but in other cases they were held together by a tie beam or a collar beam (Grant, 1961, p.144; Matin, 1987, p.145; Brunskill, 2004, p.40). The tie or collar beam reduces the bending

stress on the cruck timbers. Tenon joints were used to connect the tie beam with the cruck (figure 1.4) (Brunskill, 2004, p.43).
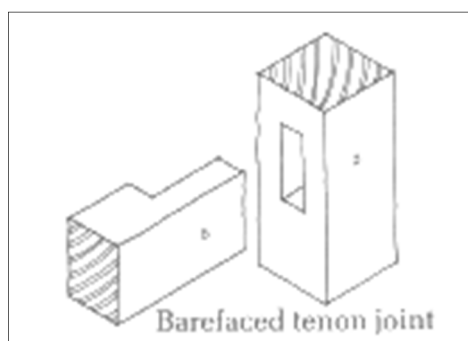
Figure 1.4: Example of a Tenon joint
(Brunskill, 2004, p. 142)

Over time cruck design developed into the jointed cruck, with very simple joints, usually dovetail joints for the main crucks, but some used pegged, halved joints which would help alleviate bending stress on the timbers. Jointed crucks were adopted to enable cruck systems to be used when the timbers available were not as curved or as long as usually required (Hay, 1976, p.33; Brunskill, 2004, p.42-43). Builders would travel miles searching for a tree growing in the manner they wanted for the curved timbers (Grant, 1961, p.149).

1.3.2 Tie beam or A-frame roofs

The tie beam system was popular because it overcame the issue of the outward force at the bases of the rafters, carrying this force in a tie-beam between them. This was the most common solution found in Scotland, particularly in parish churches and smaller castles, as the span of the roof could be no more than the length of the timbers available for the tie beams (Brunskill, 2004, p.62). This roof had many different designs but the general principle has two inclined principal rafters tied together with either a tie beam connecting the base of the rafters, or a collar connecting them at a higher level (Brunskill, 2004, p.115).

From the 15th century a number of tie beam roofs survive in Scotland; these essentially tie the rafter together at the base stretching from the top of each wall. There are also simple A-frame designs tying the rafters with a collar; a good example of this can be seen in figure 1.5 (Fawcett, 2002, p.245; Gomme 2002).

Figure 1.5: A-frame roof at Doune Castle
(Tabraham, 1986, p.10)

The main problem of this construction was the lack of any longitudinal tie. This allowed the rafters to deflect from vertical under pressure from the elements, which has caused a number of these roofs to collapse (Oldrieve and Scot, 1916; Brunskill, 2004, p.62). Aside from this there are other design problems with tie beam construction. The tie beam itself is under tension load. This makes it difficult to ensure that the rafters are well attached to it, as most kinds of joint will be pulled apart rather than forced together. Lap joints were used where the brace meets the rafter (Brunskill, 2004, p. 142). In the case of the pegged lap joint (figure 1.6) the key to this joint's success is the pegs, but these can become compromised with time as they can become loose from the swelling and shrinkage of the wood in changing humidity. Although the pegs used in joints were not always of the same wood as the frame, this could be a larger problem for pine structures from the results found in Chapter 4. This is discussed further in Chapter 11.
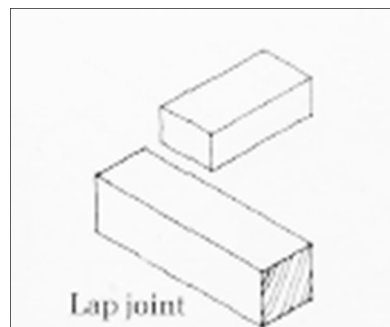
Figure 1.6: Example of a lap joint
(Brunskill, 2004, p.142)

1.3.3 More complex roofs

In larger church buildings, excessively long timbers would be needed for the tie beams (41% longer than the rafters, if the roof pitch is 45 degrees). A tie beam is also incompatible with a stone vault that comes above the level of the wall head, and other solutions were necessary. None of the Scottish abbey churches kept their roofs after the Reformation. However the 13th century roof of Glasgow cathedral survived until it was renewed sometime in the 1900s (Fawcett, 2002, p244; Oldrieve and Scot, 1916). It is a form of scissor beam roof. The scissor beams in combination with the collar beam prevent the outward force at the base of the rafters, which are not in tension like the truss systems which were common from the 19th century in Scotland (Oldrieve and Scot, 1916). These roofs found in the nave and choir of Glasgow cathedral (figure 1.7) are very similar to designs seen in France at Bayeux Cathedral (figure 1.8) and Tours Cathedral (figure 1.9) which have been suggested to be the predecessors of hammer beam roofs in England (Courtney, 1999, p.100).These French roofs are similar to hammer beam roofs in that they allow space for stone vaults to be constructed below them, although they are simpler in design. The triangle at the base of the rafters was supported by the walls as at Glasgow (Fawcett, 2002, p.244; Oldrieve and Scot, 1916; Hay, 1974, p.28). Further rafters were then placed between the principals to support the roof covering (Oldrieve and Scot, 1916). This, along with a sole plate, allows the load to be spread evenly along the head of the wall (Hay, 1974, p.28). A design feature which did not survive the test of time was the triangle at the base of the rafters on top of the main supporting wall. This rested on the sole plate which was actually built into the masonry, which allowed water to become trapped around the timbers and rot to set in, causing some of these roofs to be destroyed (Fawcett, 2002, p.246).
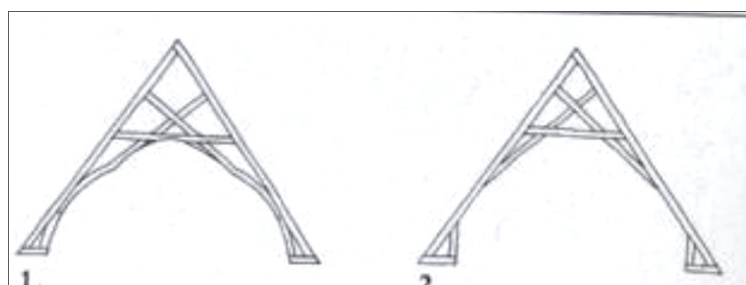
Figure 1.7: Design of Glasgow cathedral choir and nave roofs (Fawcett, 2002, p. 243)
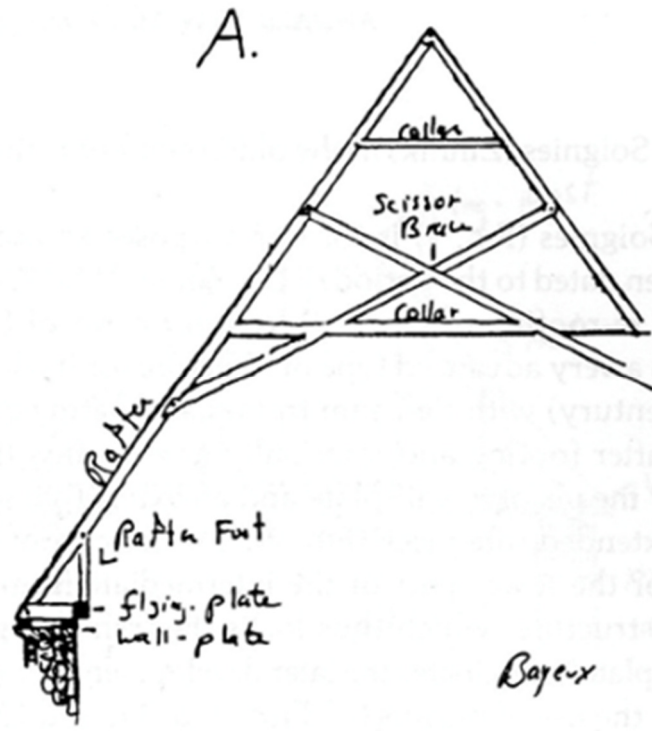
Figure 1.8: Roof of Bayeux cathedral (Courtney, 1999, p. 99)
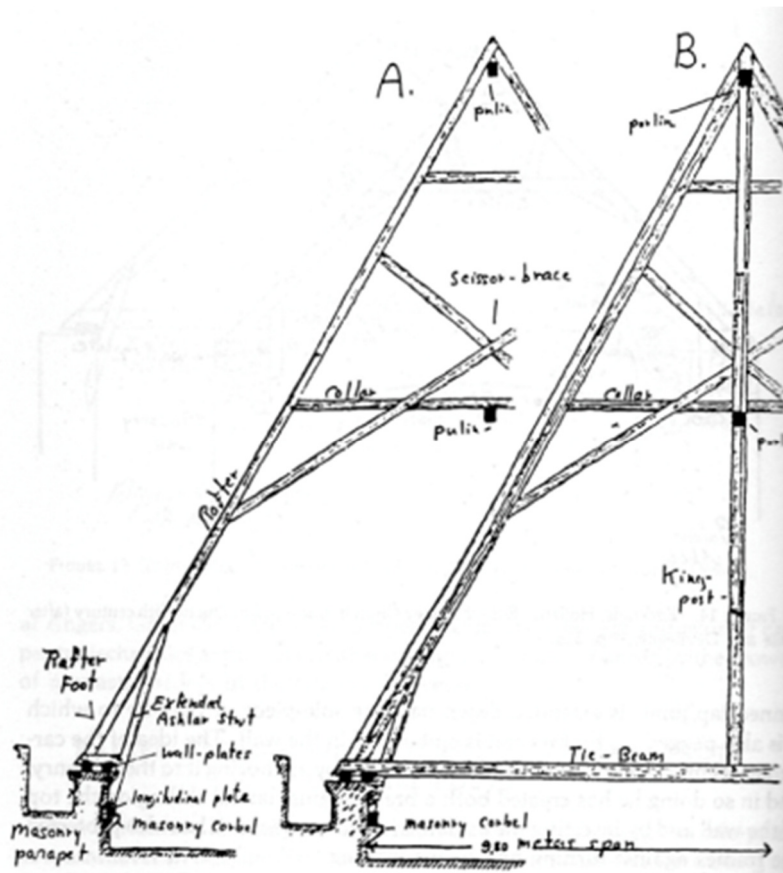
Figure 1.9: Roof of Tours cathedral (Courtney, 1999, p.108)

There is evidence in Scotland for evolution in roof design as the desire for wider halls developed. An example of this is at Randolph's Hall in Darnaway Castle (1387), where tie beams were used in conjunction with crown posts (Hay, 1974, p.29). However there is some debate over whether Darnaway is considered to be a hammer beam roof or not, as the hammer beams appear to be only decorative items (Gomme, 2002).

These roofs then evolved into the ornate hammer beam roofs which are often considered to be uniquely English (Courtney, 1999, p.89). The number of surviving hammer beam roofs in Scotland is small as they were very rare in Scotland to begin with (Gomme, 2002), and they were restricted to large castle halls and churches as they were very expensive and ornate (Brunskill, 2004, p.72). The development of the hammer beam roof in Scotland is thought to have arisen from the desire for halls that were becoming wider as well as taller (Courtney, 1999, p.94). The restricted availability of timber in Scotland also may have driven this move towards hammer beam roofs, as tie beam roofs cannot be made any wider than the logs used for the tie beam (Hay, 1974, p.29). But in a hammer beam roof the longest member is actually the rafters, whereas the rest of the structure is made up of short heavy timbers which are often curved.

The hammer beams roofs of this period were reserved for ornate purposes in buildings of high status (Russell, 1993; Yeomans, 2009, p.174). Hammer beam roofs (figure 1.10) were complex. It was necessary to find a way to support the arcade plate. This is the longitudinal beam attached as a wall plate in truss systems. One solution was to support the arcade plate on short posts known as the hammer posts, which rest on a short beam, the hammer beam. This has a cantilevered effect inward from the top of the outside wall and braces against it (Harris, 2010, p.10-11; Gomme, 2002). Most hammer beam roofs are double framed systems in which the common rafters are supported by an inner framework, composed of pairs of strong rafters called principals to which purlins are attached and which are further strengthened by braces (Raphael, 1877, p.20; Courtney, 1999, p.90).

Figure 1.10: Hammer beam roof of the great hall at Edinburgh castle (RCAHMS, 1999)

These are extremely complex structures with a series of complex stresses working within them. The joints between the timbers are very costly due to their complexity (Courtney, 1999, p.90) and repairing or replacing an element within this structure will need to be done with extreme care so as not to distort the rest of the structure. If the replacement timber used in a repair had different MFA and as a result differential shrinkage compared with the original, this would potentially have a warping effect on the whole roof structure.

1.3.4 Post-Medieval roofs

From the 16th century onward, Scottish roof design tended to become simpler with gabled ends and closely spaced rafters, often using an A-frame design made from timbers which had a square uniform scantling with no obvious difference between principal and common rafters. The whole structure was hidden behind plaster ceilings, which were often decorated in state buildings by painting (Serafini and Gonzalez-Longo, 2015; Hanke, 2008a, p.13). An exception to this was the roof of Parliament Hall, built in false hammer beam design; it was an extremely elaborate complex design where two elements of the roof act independently (Gomme, 2002).

These roofs were reliant on the gable wall ends for their longitudinal rigidity, having no wall plate, tie-beams or purlins. The rigidity of the structure also relied on the sarking, usually two layers of sawn wood that ran horizontally and vertically, separated by insulation which usually consisted of fleece. (Serafini and Gonzalez-Longo, 2015; Hanke, 2008; Dixon, 2002).

The common rafter form of building was extremely persistent in Scotland and can be found in buildings constructed up until the 18th century, when other countries such as England had moved to king and queen post truss systems (Serafini and Gonzalez-Longo, 2015).

The first record of the king post truss system appearing in Scotland was drawn by William Adam in 1720 for the New College library in Glasgow (figure 1.11), (Serafini and Gonzalez-Longo, 2015; Hanke, 2008) but this was never put into place. It is thought that the local carpenters had no idea how to construct a roof to this design (Serafini and Gonzalez-Longo, 2015).
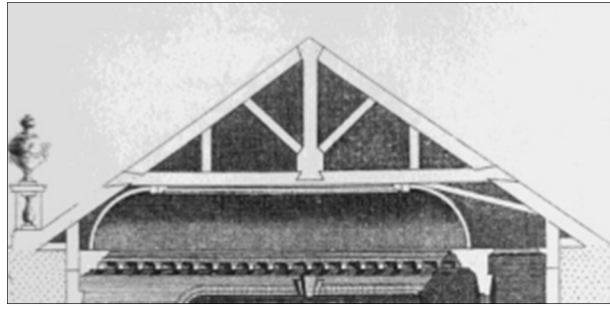
Figure 1.11: Adams design for the Glasgow New College Library, 1720 (Serafini and Gonzalez-Longo, 2015)

More complex trusses began to appear in the mid-18th century in Scotland and are believed to show English influence in their design (Serafini and Gonzalez-Longo, 2015; Dixon, 2002; Harris, 2010, p.81). There are many different variants of the truss system. The two main designs seen in Scottish timber roofs during the mid-18th century are the king post truss and the queen post truss (Russell, 1993). The king post truss (figure 1.12) gives direct support to the roof by having the king post rise from the tie beam. The principal rafters then rise from each side of the tie beam into the king post. The purlins are usually slender and are trenched into the principal rafters (Harris, 2010, p.81; Serafini and Gonzalez-Longo, 2015; Hanke, 2008a, p.20).
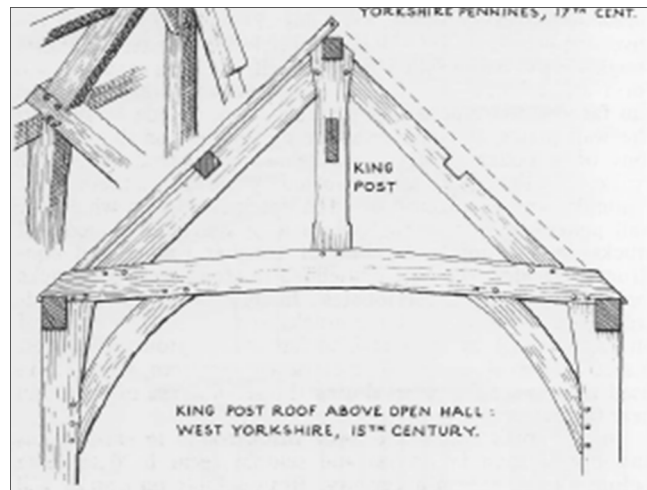
Figure 1.12: Example of a King post truss system (Harris, 2010, P.78)

Queen post trusses (figure 1.13) have vertical posts supporting the main roof plate or purlin, but instead of reaching to the ground they are supported on the tie beam (Harris 2010, p.85). The principal rafters support the purlins and are joined by a collar. The joint between the tie beam and queen posts is often enlarged (Harris, 2010, p.86).
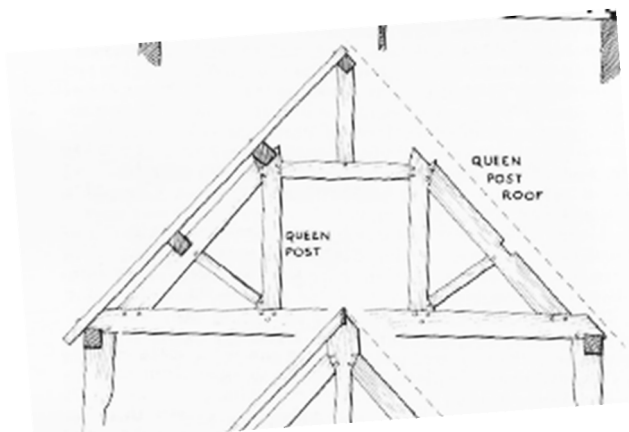
Figure 1.13: Example of a Queen post truss
(Harris, 2010, p. 84)

The earliest truss roof known to be built in Scotland was a queen post truss at Oakshaw Trinity Church in Paisley (1750). It has been suggest that this actually inspired the use of truss system in Scotland, leading to the roof of Auchinleck house (1758) being built in the king post truss style (Serafini and Gonzalez-Longo, 2015). Adoption of these was gradual, and common rafter roofs were still being built throughout the same time period, although there are some cross overs between the two designs (Serafini and Gonzalez-Longo, 2015; Hanke, 2008a, p.13).

The truss systems came into favour because they were light in weight and could replace the need for traditional purlins and ceiling joists. Often the trusses could be assembled before installation (Desch and Dinwoodie, 1996, p.195). In many buildings they were covered by plaster and lath ceilings (Raphael, 1877, p.18-19; Hay, 1974, p.31).

These highly engineered truss systems are believed to have become popular not only for design reasons but also due to the new possibility of getting great lengths of imported softwood timber from North America. This allowed larger spans to be bridged in timber and introduced the possibility of low pitched roofs (Russell, 1993). In Scotland from the mid 18th century through to the 19th century and beyond these became the most favoured system. In consequence, the craft of traditional carpentry came to an end in the late 18th to early 19th century (Harris, 2010, p.3; Dixon, 2002), although the hammer beam roof made a short comeback in the Victorian high gothic period for use in elaborate halls and churches (Russell, 1993; Yeomans, 2009, p.174).

1.3.5 Ceilings and flooring

In the 15th century elaborate ceilings were used to hide the structural timbers of the roof in high status buildings such as churches and castles. One of the more common

features in smaller churches was the timber barrelled ceiling (figure 1.14) (Fawcett, 2002, p.239).
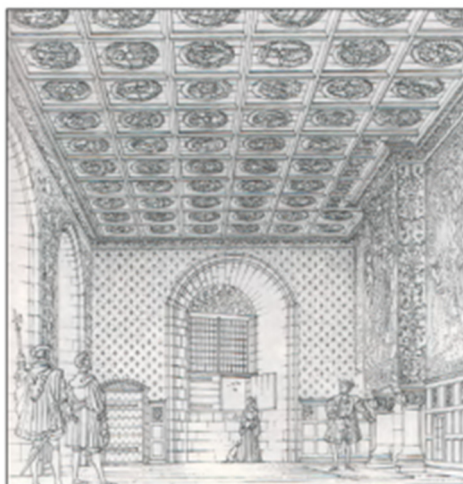
Figure 1.14: Coffered ceiling of the Great Hall
of Stirling Castle (Hanke, 2008a, p.25)

During the 16th century Renaissance, coffered ceilings were also used in high status buildings to hide the heavy beams supporting the roof (Hanke, 2008a, p.24; Raphael, 1877, p.16). A temporary scaffold platform was used to fix the ceiling panels and the framing ribs to the load bearing structural beams. This operation demanded considerable skills and precise work to be successful, and to avoid distorting the decorative works on the ceiling (Hanke, 2008a, p.28). The most famous example of a coffered ceiling in Scotland is from Stirling Castle (Hanke, 2008a, p.25; Hanke, 2008b). A lesser version of these decorated timber ceilings was widely popular from the 1580s. These were constructed simply by nailing painted boards onto the structural joists of the floor above (Hanke, 2008a, p. 29). During this time period it was becoming expected that the flooring would provide a decorative ceiling for the room below (Brunskill, 2004, p.75-76).

Most of the simpler floors were constructed from boards laid directly on floor joists spanning the gap between the walls (Brunskill, 2004, p.76). Huntingtower Castle (figure 10) is a fine example of this floor design and had an elaborate painted ceiling underneath, the joists and the panels between them being elaborately painted. Alternatively the joists could be supported by binder or bridging joists, which were larger timbers that spanned the width of the building from wall to wall (Brunskill, 2004, p.99).

Figures 1.15 and 1.16 show different ways in which floor joists were supported. Figure 14 shows a stone ledge built out of the left side of the wall, for a timber wall plate on which the joists would rest. Figure 1.17 shows holes left in the masonry to house the ends of the floor joists. A third alternative was to support a timber wall plate on corbel stones seen in figure 1.18. This alternative allowed a freer flow of air around the

vulnerable ends of the joists and reduced the chance of decay. The timber samples made available for this project are from these types of timber joists (figure 2.6).

Figure 1.15: Painted ceiling of the Lord's hall, Huntingtower Castle; Scotland's oldest surviving example (Tabraham, 1986, p.57)

Figure 1.16: Painted joists from Old Gala House (RCAHMS, 1957)

Figure 1.17: Ledge on left side of the building to support floor joists at Skipness Castle (RCAHMS, 1971)

Figure 1.18: Holes in the masonry for supporting the floor joists at Tarbert Castle (RCAHMS, 1971)

Unfortunately many timber structures and roofs have been lost through neglect and decay, because they were not seen as an important part of the building and were hidden away behind plastered ceilings. Further, many roofs and floors have been subject to inappropriate repair, replacement or in some case even demolition (Cestari et al., 2011). This is a very different view from that of their historical builders, when in the medieval period the timber parts of the building were by far the most valuable (Grant, 1961, p.142).

Mechanical failure requiring repairs, within roofs and other timber structures, is usually caused by movement such as twisting of the timber frame, which placed excessive loads on some part of the structure. Problems like this may be caused by failure in the

bracing of the frame or by movement of the foundations (Russell, 1993), but most often by decay when the timber is not sufficiently dry and well ventilated. Joist ends inserted into sockets in cold, damp stone are a typical problem.

Other structural problems can be caused by bad interventions, where for example the load-bearing timber members have been cut through to insert extra floors, doors and windows or for adding services to the building (Russell, 1993).

1.4 Wood Anatomy

Wood and woody plants are extremely abundant in the world with over 20,000 different species, each having different properties and value depending on the slight differences within their anatomy and extractives leading to their suitability for different uses (Wiedenhoeft, 2010).

The first thing to remember about wood is that it does not grow for our use. Everything about wood and its anatomy serves its function as the trunk of a tree and is specialised to support and protect the tree (Paris, et al., 2010; Wiedenhoeft, 2010). The structure of wood is the result of continuous growth of a living organism. Before we can understand the properties of historic wood and the effect of aging we have to understand how it is produced and how it once functioned in a living tree (Wright, 2005, p. 14).

The tree trunk consists of bark (phloem) and woody tissue (xylem). Both xylem and phloem cells are produced by the vascular cambium which is located between the wood and the inner bark and is too thin to be visible to the naked eye. Here in the cambial zone new cells are produced by repeated cell division (Wilson and White, 1986, p. 11). These tube-like cells, glued together along the middle lamella, form the structural basis of the tree (Varner et al., 2012).

Both the xylem and the phloem, produced from the cambium, are known as vascular tissues (figure 1.19). The primary cambial cells become differentiated into the two types of vascular tissue. The secondary growth stage is where the tree begins to add thickness by making these new tissues (Esau, 1977, p.101).
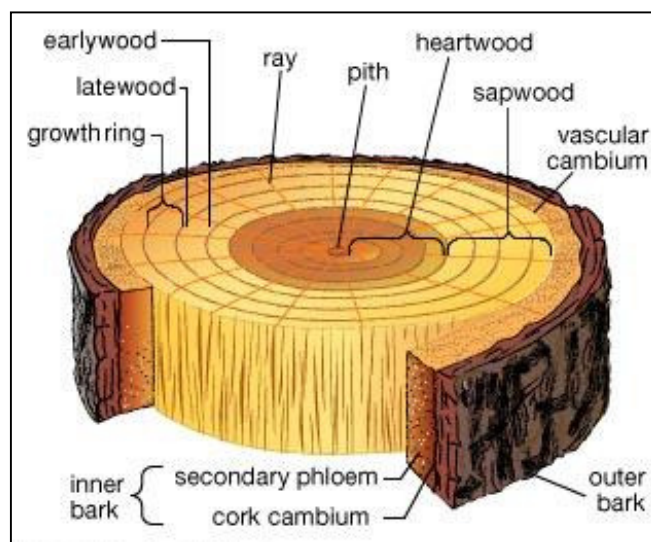
Figure 1.19: Cross section of the trunk of a tree (Britannica, 2006)

The role of the wood (xylem) is critical to the survival of the tree as it provides mechanical support for the tree, which needs to carry branches whilst the tree is growing in height to compete for light (Spicer and Groover, 2010).

Figure 1.20: Knots in Pine wood (Desch and Dinwoodie, 1996, p. 13)

The growth of the xylem occurs with annual growth rings. There are two stages of annual growth, the earlywood which grows during the spring and latewood which is produced in summer. The earlywood has wide cells for the fast transport of water and nutrients when the tree is in the first and quickest part of the growing season (Esau, 1977, p.106). The latewood gives the tree structural support. The latewood cell walls become thicker and the wood becomes more dense and stiffer (Wilson and White, 1986, p. 12).

In the secondary xylem there are two distinct types of tissues. The axial system is vertical and makes up the main body of cells in the trunk (Esau, 1977, p.101). The ray cells are orientated radially from pith to bark (Varner et al., 2012; Hiziroglu, 2009). Knots (figure 1.20), form at the base of live or dead branches and are considered a problem in wood working and in assessing the quality of wood. There are different types of knot in that the knot from a living branch cannot be pushed out of the wood whereas dead knots are loose and likely to fall out. Loose knots can be very undesirable depending on how the wood is to be used (Wilson and White, 1986, p. 18).

1.4.1 Differences between hardwood and softwood

The axial system includes tracheary cells which are the most specialised cells in the xylem. Their function is the conduction of water. There are two unique types of these cells, the tracheids found in softwoods and the vessel cells found in hardwoods (figure 1.21) (Unger et al., 2001, p. 12). The vessel and tracheid cells act like the blood vessels of the tree, transporting water and inorganic nutrients from the roots to the crown (Thibaut et al., 2001). These cells differ in the way they transport water. The tracheids are cells with closed ends, which transport water through what are called bordered pits in the sides of the cells. The pits pass water from one cell to another (figure 1.22). The pits are bordered to prevent them from acting as weak points in the cell wall and in times of drought they can be closed by a torus to stop loss of water and to prevent air from entering the cells (Carlquist, 2010).
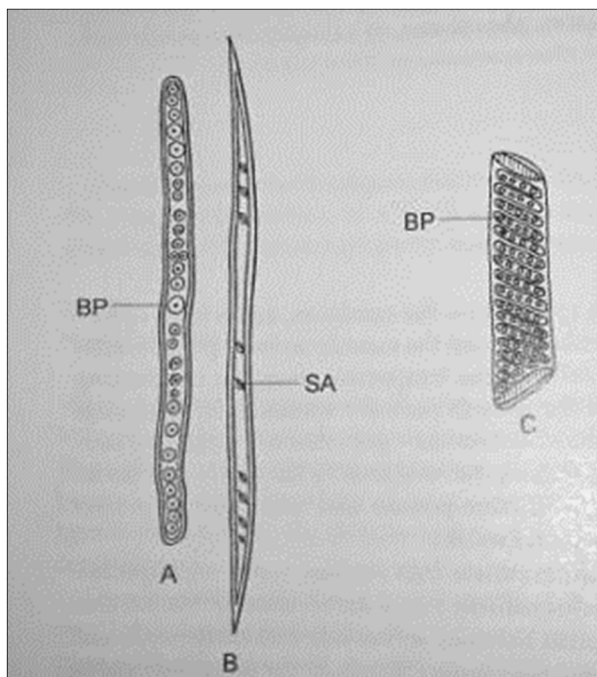
Figure 1.21: A: Pine earlywood tracheid, B: pine latewood tracheid and C: hardwood vessel cell (BP: bordered pits and SA slit appiture) (Unger et al., 2001, p.12)

Figure 1.22: Bordered pits, x150 magnification (Desch and Dinwoodie, 1996, p.16)

The vessel cells found in hardwoods, on the other hand, are cells which are open at each end and connect together to allow a continuous flow of water (Unger et al., 2001, p.12).

Softwoods and hardwoods are also differentiated by density. Softwoods tend, on average, to be less dense than hardwoods, although this does not mean that every hardwood is harder than softwoods (Desch and Dinwoodie, 1996, p. 78).

Due to the difference in density softwoods are sometimes easier to work than the more dense hardwoods (Jackson and Day, 1989, p.17), but some hardwoods such as oak have the advantage of being particularly resistant to decay (Wright, 2005, p. 13).

Identifying both hardwood and softwood species taken from a historic building is done mainly through light microscopy. A trained person can identify species by the way in which pores in the wood are distributed throughout the growth rings in the latewood (Desch and Dinwoodie, 1996, p. 61). Due to chemical differences between the hemicellulosic polymers in softwood and hardwoods is it possible to distinguish between the two using Fourier transform infrared (FTIR) spectroscopy (Barker and Owen, 1999; Pandey, 1998).

1.5 Wood cell wall structure

1.5.1 Wood cell anatomy

Wood cells (figure 1.23) form a wide variety of shapes, sizes and wall thickness to service the current needs of the tree (Burgert, 2006; Fratzl et al., 2004).

Wood cell walls are made up of several different layers centred round the lumen, the cavity originally occupied by the living cell, and the organisation of the cellulose microfibrils and matrix material differ with each cell wall layer. The outermost layer of the cell wall is known as the primary wall. It contains cellulose microfibrils in thin aggregates which cross over each other. One of the main roles of the primary wall is to stand up to the internal pressures of the living cell and control the expansion of the cell during its growth (Burgert, 2006, Thomas et al., 2013). The secondary wall is divided into three layers, the S1, S2 and S3 layers (figure 1.24) (Unger et al, 2001, p. 13; Cowdrey and Preston, 1966).
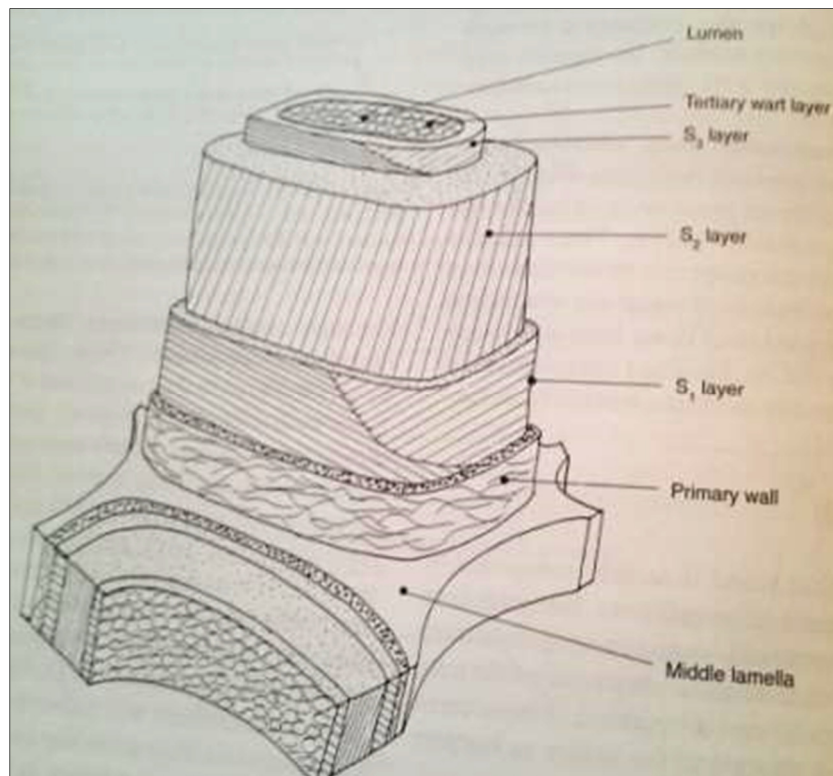
Figure 1.23: The layers of a wood cell wall (Ridout, 2000, p. 6)
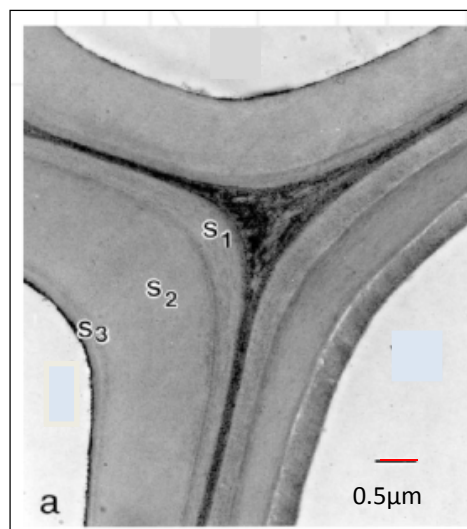
Figure 1.24: Scanning Electron
Microscope image of wood cell walls
(Tabet and Aziz, 2013)

The S1 layer is made up of laminations, in which the microfibrils are arranged in a flat helix. This helix changes direction in every lamination. The S1 layer itself is so thin that it usually cannot be seen under light microscopy (Ridout, 2000, p.6), generally around 0.1-0.35 μm in thickness. It has been observed that the microfibrils in this cell-wall layer are orientated at a large angle, around 60°–80°, to the long axis of the tracheids (Khalili et al., 2001; Tabet and Aziz, 2013; Rusinb and Tulika, 2005; Donaldson, 2008).

The cellulose chains in the S2 layer of the cell wall are laid down approximately parallel to the cell axis, which gives the wood greater mechanical strength and stiffness along the grain (Simonović et al., 2011; Ricardo et al., 2011; Bjurhager et al., 2012). Although they are roughly parallel to the cell axis they wind helically around the cell, at a helical angle called the microfibril angle (MFA), as shown in figure 1.25 (Bader et al., 2012; Krauss et al., 2011; Burgert, 2006; Verrill and Kretschmann, 2011; Fratzl et al., 2004; Donaldson, 2008; Altaner and Jarvis, 2008; De Borst et al., 2013). The S2 layer is the thickest cell wall layer, usually between 1 and 10 μm thick and making up 75–85% of the total cell-wall thickness. As a result the S2 layer has an important role in mechanical support. The microfibril angle of this layer is small and usually will never exceed 30° (Rusinb and Tulika, 2005).
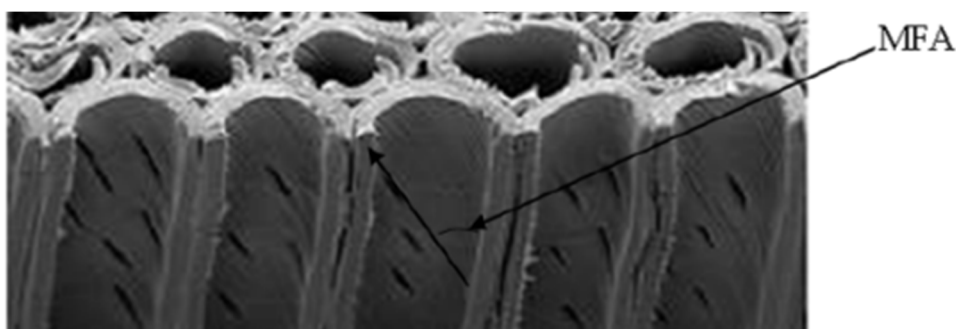
Figure 1.25: View of the MFA by Scanning Electron microscopy (SEM). The MFA can be seen from the bordered pits which appear as slits in the cell wall following the direction of the microfibrils (Tabet and Aziz, 2013).

The S3 layer of the cell wall is thinner than the S1 layer, usually between 0.5–1.0 μm. The cellulose microfibrils in this layer are in a parallel arrangement but not so strictly as in the S2 layer, at an angle between 60°–90° to the cell axis (Rusinb and Tulika, 2005; Barnett and Bonham, 2004). The innermost surface against the lumen in some species has a warty appearance (Unger et al., 2001, p.14).

The cells being layered in this manner give wood its unique stiffness for its weight. The microfibril orientations in the S1 and S3 wall layers are also important and are believed to prevent the cell from bursting. The S1 layer in particular is thought to have the main role in protecting the cell from water tension forces and crushing (Donaldson, 2008). So although the microfibril orientation in the S1 and S3 cell-wall layers is not as significant for the mechanical properties, these layers still have a crucial role to play in the tree's overall survival and success.

These layers make up the wall of a single wood cell. The cells are attached to one another by a matrix known as the middle lamella, but this is hard to distinguish under the microscope from the primary cell wall, which often leads to them being classed together. The middle lamella is lignin rich. This lignin is chemically linked to the

hemicellulose polysaccharides acting as a binding matrix holding the wood cells attached to one another (Ridout, 2000, p.7).

It is the unique microfibril orientation and cell wall structure that makes wood such a desirable material in terms of its mechanical properties, perfect for a building material. Yet wood, once it has been dried, also has a low density relative to its strength and stiffness (Fratzl et al., 2004).

1.5.2 Wood Polymers

Wood cell walls are made up of three main polymer classes: cellulose, hemicellulose and lignin. Cellulose and the hemicelluloses are sugar based polymers whereas lignin is an aromatic polymer (Barker and Owen, 1999; Tabet and Aziz, 2013; de Borst et al., 2013; Varner et al., 2012**).**

The main polymer responsible for the strength of wood cell walls is cellulose. Cellulose is made up of glucose units joined together in a chain. The chain structure of cellulose is almost exactly the same as starch, bar one difference; every alternate glucose in the sequence of cellulose is joined upside down (Hinterstoisser et al., 2001; Zabler et al., 2010). This subtle difference in the chain structure makes cellulose an entirely different polymer with a completely different range of properties, making cellulose the strongest of the wood polymers (Varner et al., 2012; Ridout, 2000, p. 5).

Cellulose forms microfibrils. What gives cellulose its great stiffness and strength is the structure of the microfibrils. The crystalline cellulose at their core has great rigidity in the direction parallel to their axis (Krauss et al., 2011; Fernandes et al., 2011). Cellulose microfibrils are tightly held together by hydrogen bonds which tie the adjacent chains together forming the crystalline structure of the microfibril (Altaner and Jarvis, 2008; Tabet and Aziz, 2013). Cellulose microfibrils are often referred to as being crystalline but they do not form a perfect crystal. They also contain disordered domains, the structure of which is still not fully understood (Fernandes et al., 2011; Thomas et al., 2014).

The microfibrils aggregate together to form microfibril bundles. These are the principal structural unit of the cell wall, differing between softwoods and hardwoods (Thomas et al., 2014; Fernandes et al., 2011). Between the bundles of microfibrils are the hemicellulosic matrix polymers (figure 1.26). These are of lower molecular weight. Although they resemble cellulose in structure they are branched and do not form crystalline microfibrils.
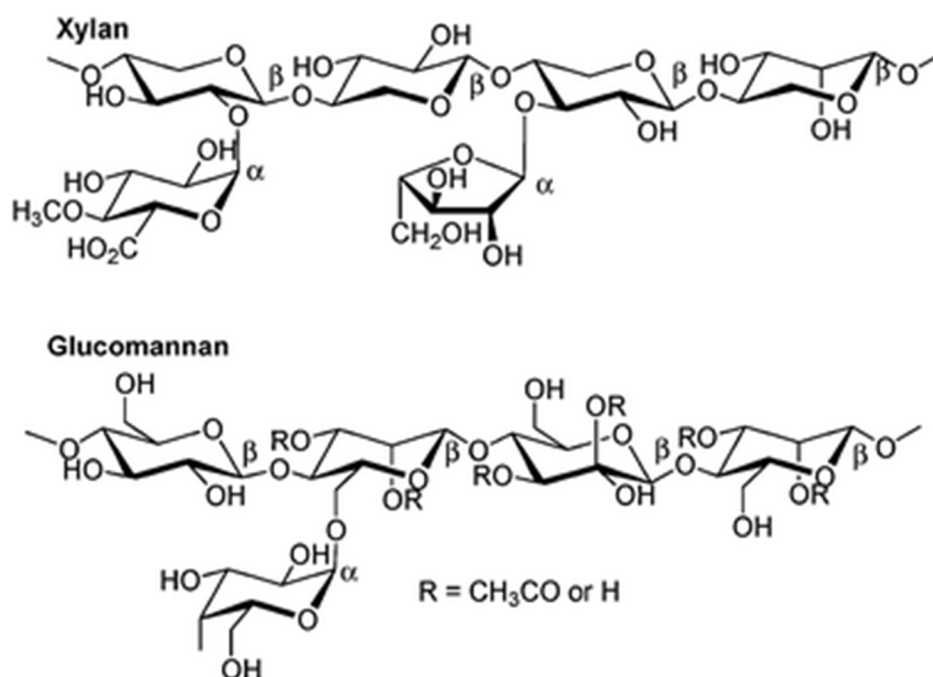
Figure 1.26 Structures of the two main hemicelluloses found in softwoods (Dutta et al., 2012)

The hydrogen bonding between the cellulose polymer and the hemicellulose polymers is also one of the key factors controlling the mechanical properties of wood (Hinterstoisser et al., 2001; Aydin, 2007).

Hemicelluloses are the second most abundant polymer group in wood and can comprise 10-30 % of the dry biomass depending on the species (Schädel et al., 2010). Hemicelluloses are more affected by the moisture content than lignin or cellulose. This has been seen even at normal humidity levels when hemicelluloses have more tendency to rearrange than cellulose (Salmén, 2004).

There are three main sugar units that form hemicelluloses in wood. These are xylose, glucose and mannose and they differ in amount in hardwoods and softwoods. Xylans (glucuronoxylans) are the most abundant hemicelluloses in hardwoods and can make up 23-33% of the dry mass of the wood (Gabrielii et al., 2000; Marchessault, 1962). The two main hemicelluloses in softwoods are glucomannans and xylans (glucuronoarabinoxylans). Some observations have shown that softwood xylans are more associated with lignin and glucomannans are associated with the cellulose polymers (Schädel et al., 2010; Fratzl et al., 2004). The hemicellulose chains are thought to cross-link cellulose microfibrils (Fratzl et al., 2004; Aydin, 2007) or microfibril bundles (Fernandes et al., 2011). It has recently been revealed that glucuronoxylan has an acetylated backbone which forms a flat-ribbon; 2-fold helix when it bonds to the cellulose polymer at its hydrophilic faces (Busse-Wicher et al., 2014; Bromley et al., 2013; Cosgrove and Jarvis, 2012). It is thought that the acetyl groups are on the outside

of the chain, attached at the 2-OH and 3-OH positions of alternate xylose units, while the inside is hydrogen bonded to the cellulose polymer (Cosgrove and Jarvis, 2012; Busse-Wicher et al., 2014). Glucoronoxylan chain segments between those that are bound do not have this pattern of aceylation. The two kinds of segments within one chain, permit crosslinking of cellulose by the glucuronoxylans in hardwoods (Pinto et al., 2005; Kulkarni et al., 2012). So far this has not been found in softwoods but it is likely to occur in softwoods as well.

The final main polymer is lignin. Lignin is a complex polymer. It forms a 3D network in the cell walls, binding to the hemicelluloses. Lignin is not formed from sugar like the polysaccharides; it is formed from three cinnamyl alcohols, 4-coumaryl alcohol, coniferyl alcohol and sinapyl alcohol. The proportions of these three building blocks are different in softwoods and hardwoods; in softwoods lignin is mainly formed from guaiacyl units and results from the polymerisation of coniferyl alcohol, whereas hardwood lignin, a guaiacyl-syringyl polymer, is the result of co-polymerisation of coniferyl alcohol and sinapyl alcohol (Fratzl et al., 2004; Unger et al., 2001, p. 18; Aydin, 2007).

1.6 Structural Origins of the Mechanical Properties of Timber

For a long time in wood science, density was considered to be the key property determining mechanical properties, until routine methods became available to determine microfibril angle (MFA). Although MFA is now known to be the principal factor controlling mechanical qualities of wood such as stiffness and strength; density still plays a major role (Evans and Ilic, 2001; Rinn et al., 1996; Roszyk et al., 2010; Dutilleul et al., 1998; Vavrčík et al., 2009; Ricardo et al., 2011).

Density varies greatly, not just in different species but also within each tree (Treacy et al., 2000). It depends on the growth history of the tree (Reiterer and Stanzl-Tschegg 2001; Zhang, 1993; Machado et al., 2014; Treacy et al., 2000). The growth history determines anatomical factors such as the proportions of early and latewood in each growth ring. In softwoods, latewood cells have much thicker cell walls than earlywood, resulting in a higher density (Bergés et al., 2008; Cown et al., 2005; Rinn et al., 1996; Vavrčík et al., 2009; Mansfield et al., 2009; Hein et al., 2013). These growth features depend on silivculture and on the proportion of mature and juvenile wood in a tree, which in turn varies with genetics, growth rate and height within the stem (Gapare et al., 2012; Dutilleul et al., 1998; Cown et al,. 2005). Wood density has also been found to be sensitive to the climate in which the tree is grown and any changes in climatic stress in the growing season (Bouriaud et al., 2003; Auty et al., 2014; Kellomäki et al., 1999; Silva et al., 2014a).

Hardwoods and softwoods differ in density properties due to their anatomy. In ring porous hardwoods such as oak the density and the width of seasonal growth in each ring change from pith to bark. Density tends to increase with ring width as the amount of porous latewood is lower, but it decreases with ring number from the pith leaving the central part of the tree having the highest density (Vavrčík et al., 2009; Knapic et al., 2007; Guilley et al., 1999; Kellomäki et al., 1999; Miyajima, 1955). In contrast softwoods with wider ring width give lower density wood, resulting in denser wood toward the bark of the tree (Kellomäki et al., 1999; Dutilleul et at., 1998; Beets et al., 2001; Krauss et al., 2011). In Scots pine, after the initial slow growth leaves a few dense rings near the pith, density is low in juvenile wood, then it tends to increase before becoming more stable within the mature wood (Auty et al., 2014; Hannrup et al., 1998). Pine has a general tendency to increase in density as the tree grows, whereas this gradient in hardwood species has been seen to be smaller (Evans et al., 2000; Repola, 2006).

Although MFA and density work together to dominate wood properties such as stiffness and strength, there is not much correlation between them. This shows that they are most likely controlled independently by the tree to serve different needs. It may then be possible to breed trees to be better in one of the two properties (Evans et al., 2000; Alteyrac et al., 2006; Tabet and Aziz, 2013). Density is still considered to be a key property of wood especially in the forest industry, as it has a major impact on the quality of the wood and the value of wood products, as well as showing an inverse relationship with yield (Alteyrac et al., 2006).

MFA is believed to be the dominant property for the longitudinal stiffness of wood, not density (Penttilä et al., 2013). There have been experiments using polarised FTIR spectroscopy to find out the relative orientation of the hemicellulose and lignin polymers in relation to the microfibrils and the cell axis (Stevanic and Salmén, 2009; Simonović et al., 2011). Some of these polymers appear to have a parallel relationship with the microfibrils. It is assumed that the peak at 1160cm^{-1} is derived from cellulose, but as some chemical bonds within hemicelluloses are the same it is logical that hemicelluloses might also contribute to this peak. It has also been suggested the lignin follows the parallel orientation of the cellulose microfibrils, but data presented in Chapter 5 of this project showed no polarisation of the lignin peak at 1510cm^{-1} which would suggest a contradiction to the experiments described by Stevanic and Salmén, (2009) and Simonović et al., (2011).

The strength and flexibility of microfibrils are remarkable; they stretch elastically to a small extent when a load is applied but thereafter the matrix polymers experience some more permanent rearrangement allowing the microfibrils to slide past one another. The

cell wall then shows what is known as plastic deformation (Burgert and Fratzl, 2009; Fernandes et al., 2011; Roszyk et al., 2010).

It has been observed that the MFA correlates broadly with the mechanical stresses that are present in the different stages of the tree's growth. For example juvenile wood needs to be flexible and bend without breaking, which is made possible by it having a higher MFA than mature wood. Mature wood needs to have a lower MFA to be able to withstand the compression force exerted by the weight of the tree (Chaffey, 2000; Via et al., 2009; Burgert, 2006). The higher MFA in juvenile wood leads to it being considered inferior to mature wood for many purposes. Juvenile wood is usually the first 5 -25 annual rings, depending on the species, produced by a tree during its initial period of rapid growth (Chaffey, 2000; Altaner and Jarvis, 2008). Although the juvenile wood has lower strength and stiffness than the rest of the heartwood, the cells known as the sapwood, laid down later by the growing tree, are also less durable than the heartwood cells (Mansfield et al., 2009; Wiedenhoeft, 2010).

Sapwood consists of cells which are physiologically active and transport water. Although many of the cells are dead, the parenchyma cells which reside in the rays remain alive until they are no longer needed for storage (Desch and Dinwoodie,1996, p. 19) whereas the heartwood cells are normally dead (although not always nor in every species) (Unger et al., 2001, p. 9; Wiedenhoeft, 2010).

Figure 1.27: Colour change from sapwood to heartwood. (General Botany Laboratory, 2011)

The heartwood of a tree was historically the most desirable part and in a lot of species it is easy to locate in the tree because the cells are darker in colour in comparison to the sapwood (figure 1.27) (Wilson and White, 1986, p.13).

The colour of heartwood is thought to be produced when extractives such as tannins, produced in the sapwood close to the heartwood-sapwood boundary, infiltrate the heartwood causing it to become more strongly coloured. Dark colour is part of what

makes certain woods, for example mahogany, more desirable in decorative functions such as furniture (Grabner et al., 2005; Brazier, 1985; Wiedenhoeft, 2010). High extractive content can also make some wood species more durable, which for some functions makes them a more desirable choice (Grabner et al., 2005). The sapwood of the tree is traditionally considered inferior and in a lot of work with wood, especially furniture making, it is cut away as it is more susceptible to biological decay by insect pests and fungi (Jackson and Day, 1989, p.11) The sapwood contains more residual nutrients than the heartwood, and this is why it is more easily attacked by beetles and fungi. Part of the seasoning process in medieval times involved stripping the sapwood from that heartwood (Wright, 2005, p. 16). This process has also been done in standing buildings as a method of stopping infestation by deathwatch beetle, as the beetles cannot attack the heart wood if it has not already been attacked by micro-organisms (Ridout, 2000, p.50).

The shrinkage and distortion of wood are also a concern in timber conservation and are influenced by wood anatomy. Certain growth characteristics can affect the distortion of wood such as MFA, areas of compression or tension wood, spiral grain and the presence of knots. These factors do not affect the living tree but once the wood goes through the drying process to produce useable timber the loss of moisture causes deformation, as shown in figure 1.28 (Cave, 1972).
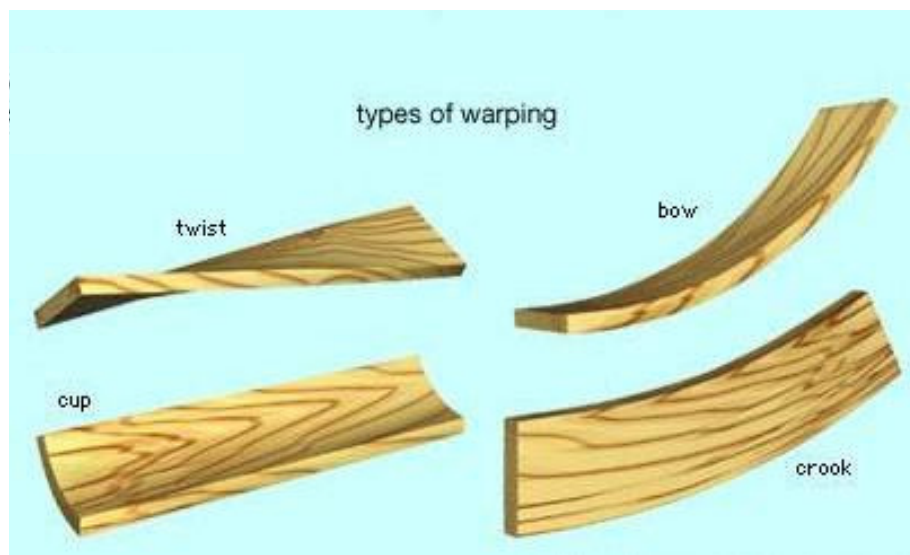
Figure 1.28: The different kinds of distortion of wood (Encyclopaedia Britannica, 2000)

It is not the cellulose microfibrils which shrink but the matrix materials. This results in the MFA having an impact on the direction of distortion (Yamamoto et al., 2001). Shrinkage is known to be uneven for the different wood directions. Typical shrinkage levels from green to dry are generally believed to the about 0.5% longitudinally, 4% radially and 6% tangentially. Much research has gone into why shrinkage in the radial

and tangential directions are so different but the reason is still unclear today (Patera et al., 2013; Leonardon et al., 2009; Babinski, 2011; Kifetew et al., 1998).

Changes in humidity within a historic building will allow the wood's moisture content to increase or decrease (Desch and Dinwoodie, 1996, p. 87). This, when coupled with natural differences in the wood on opposite sides of a piece of timber, such as MFA and knots, can cause distortion of various kinds shown in figure 1.12. Shrinkage of wood is also a problem in conservation when differential movement between two joined pieces of timber results from fluctuations in relative humidity. When a new piece of timber is fastened to a historic piece in a repair, and the old and new pieces have different shrinkage properties, this would put extra stress on the new joint at the interface between old and new material.

1.7 Timber Seasoning.

It is thought that until the later 15th century wood was felled and then used green. The custom of seasoning and drying came after this; however it is not known exactly when it became the custom to dry wood before using it (Zwerger, 1997, p. 20).

Figure 1.29: Air drying of timber (Ridout, 2000, p.121)

Seasoning is the traditional process in which moisture in the felled wood is removed by slow air drying (figure 1.29). Prior to air drying some timbers were seasoned by soaking the wood in fresh or salt water, and in some cases even in peat bogs. It is thought these methods were used to remove soluble nutrients from the wood (Tredgold, 1985).

Modern day timber is rarely seasoned but is usually dried in kilns to remove the unwanted moisture.

To many people who work with wood today it is an obvious fact that the presence of moisture in wood will result in rotting amongst other problems. Even without all the science known today, wood workers in history also knew this fact which is why they

began to season wood (Wright, 2005, p.17). The process of removing the sapwood as the wood was being prepared for seasoning also went out of practice at an early date (Wright, 2005, p. 17).

The simplest traditional way to season timber was by air drying. Timber would be cut into planks or beams and then stacked on the ground in piles with spacers ('stickers') between the layers of wood. It was sheltered from the rain and allowed to dry out by the natural air flow through the piles. It would take about 1 year to dry hardwoods boards 25mm thick to a moisture content of 14-16%. The wood was then often moved to the site in which it was to be used, to allow it to acclimatise to the area before use (Jackson and Day, 1989, p. 13).

1.8 Timber durability

Degradation of dead wood in a forest is a natural process but when it occurs in a building it is in most cases through human negligence, either in buildings that have been abandoned or fallen into disrepair, or due to poor maintenance routines (Bucşa and Bucşa, 2008; Kisternaya and Kozlov, 2007). Decay occurs when wood is exposed to conditions favourable to fungal growth, usually damp conditions, although some fungi can survive with very little water (Blanchette, 1995; Clausen, 2010).

Wood is a unique material and some wood species can stand up to biological decay better than others. As with everything the level of resistance can also depend on the individual tree and its properties. No two pieces of wood are ever the same, even from the same tree (Bader et al., 2012; Ridout, 2000, p. 3).

For example the extractives found in oak allow it to be less susceptible to fungal decay in comparison to pine (Carvalho et al., 2009; Clausen, 2010). When fungal decay sets in, the wood will in some cases lose mechanical strength sooner than it loses density. The traditional way of assessing decay is through mass loss but in some cases this may not be enough (Bader et al., 2012; Oberle et al., 2014; Green, 2001; Curling et al., 2001). Although finding mechanical issues with the wood may not be simple, they can still be present and problematic, whereas trying to find chemical changes to the wood can be a more difficult process (Fackler and Schwanninger, 2012). Decay in the microstructure of wood can affect macroscopic mechanical properties (Bader et al., 2012). Once fungi have penetrated into the wood, incubation experiments have shown that the risk of mechanical degradation rises extremely fast if the conditions for fungal growth are allowed to continue (Brites et al., 2013; Hastrup, et al., 2012).

1.9 Microbial degradation of timber

1.9.1 Wet waterlogged wood:

Wet waterlogged wood found in sunken ships such as the Mary Rose and the Vasa can survive under sea bed conditions for hundreds or even thousands of years. Natural changes are expected to be seen in the structure of the wood, depending on the species and burial length (Passialis, 1997; Esteban et al., 2010; Greaves, 1971).

Changes in the chemical composition of wet waterlogged wood are due to slow enzymatic hydrolysis of the carbohydrate polymers of the wood, which leads to the loss of these polymers, a higher lignin content and a lower density (Čufar et al., 2008; Passialis, 1997). Wet waterlogged wood will also contain inorganic materials such as salts, and thus far more ash than recent wood (Passialis, 1997). In wet environments hemicelluloses are found to be degraded far more than cellulose (Gelbrich, et al., 2008).
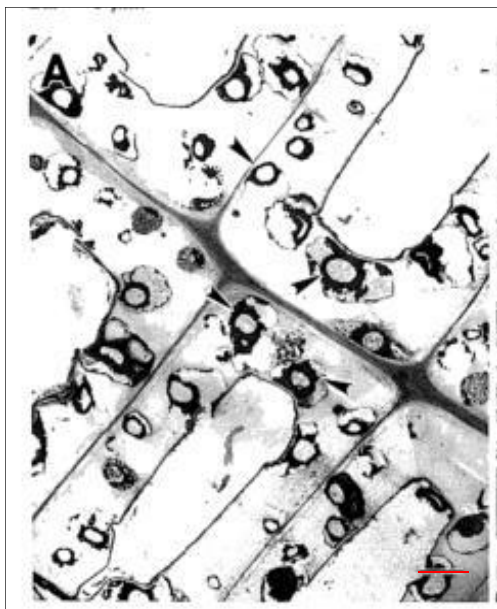
Figure 1.30: Damage done by erosion bacteria, scale bar 3 μm (Blanchette et al., 1985)

Although, unlike historic wood, waterlogged wood is not degraded by fungi due to the anaerobic conditions, tunnelling bacteria (figure 1.30) or erosion bacteria can be causes for concern in waterlogged wood. They can be seen in the transverse section of the wood and show a chequered pattern of decay (Greaves, 1971; Passialis, 1997; Björdal et al., 2005; Čufar et al., 2008). They attack from the cell lumen and penetrate through the S3 layer of the cell walls. The S2 layer is slowly turned into amorphous material which is thought to be a combination of bacterial slime, bacteria and left-over lignin. They get into the wood fibres via the pits in the ray cells (Björdal et al., 2005; Lionetto

et al., 2013; Kretschmar et al., 2008; Greaves, 1971). The decayed regions align themselves with the microfibrils and the erosion is usually seen following these. The bacteria attack the S2 layer more due to its elevated cellulose and hemicellulose content (Björdal et al., 2005; Lionetto et al., 2013; Čufar et al., 2008). This leads to a spongy material which is likely to collapse if the wood is allowed to dry out (Lionetto et al., 2013).

Allowing this wood to dry out without some form of treatment will result in large dimensional changes. Almost double the amount of shrinkage compared to recent wood can be seen in these cases (Kolař et al., 2014). This problem is usually controlled with the use of an impregnation solution which controls the level of shrinkage. PEG or polyethylene glycol is the most commonly used solution in the UK. PEG can be obtained in different molecular weights of 200-4000 grams per mole, and is adjustable for species and amount of decay as calculated by a programme called PEGcon (polyethylene glycol concentration) (Babinski, 2011). But this system is not without its faults as it does not take into account the differential shrinkage seen within untreated wood (Babinski, 2011). For the treatment to be successful it requires prior removal of the salts left by the sea water from the wood. Salts and iron acquired from the environment can cause huge problems in the treatment of waterlogged wood (Macchioni et al., 2013).

1.9.2 Archaeological (buried) wood:

In buried wood, decay generally leads to the loss of the carbohydrate polymers and a relative increase in lignin (Kolař et al., 2014). There is also an increase in the porosity of buried wood resulting from microbial degradation (McConnachie et al., 2008). The degradation also depends on the soil conditions and in some cases on the history of the wood and its use (Čufar et al., 2008). It has also been found that the outside surface of buried wood has a much higher content of ash infiltrating from the surrounding soil, together with higher nitrogen and phosphorus content (Macchioni et al., 2013; Gelbrich et al., 2012; Kretschmar et al., 2008; Gelbrich et al., 2008). The pH of the soil has also been found to influence the decay of the wood, which is worst at a slightly alkaline pH 7-8.3. This is the optimum pH range at which soil bacteria and fungi can flourish (Kretschmar et al., 2008).

Erosion bacteria attack archaeological wood in areas such as foundation piles where the oxygen content of the soil is too low for wood-degrading fungi to attack. There, bacterial degradation can be identified by the checked pattern of decay seen in the transverse section of the wood, and by increased moisture content and lower density (Esteban et al., 2010; Björdal et al., 2005; Čufar et al., 2008; Gelbrich et al., 2008). As in bacterial attack on wet wood, they invade from the cell lumen aligning themselves with the microfibrils in the S2 layer and attack from the ray cells through the bordered

pits (Greaves, 1971; Macchioni et al., 2013). When degraded samples were compared to sound wood they showed a reduction in phenolic compounds and soluble sugars and a higher content of lignin (Gelbrich et al., 2008; Gelbrich et al., 2012). The breakdown of hemicellulose has also found to be more severe in archaeological wood compared to the breakdown of the cellulose (Gelbrich et al., 2008).

Bacterial degradation of wood is very slow in comparison with fungal decay and it is questionable whether bacteria perform any important role in the degradation of wood in oxygenated conditions (Greaves, 1971). Shrinkage can be almost doubled compared to recent wood if buried wood is allowed to dry without prior treatment (Kolař et al., 2014).

1.9.3 Historic wood

It is widely agreed that the most common forms of decay to timber in historic buildings are dry rot and decay caused by the deathwatch beetle. For wood to be affected by fungi, insects or bacteria there have to be specific conditions. Decay organisms are living things and like all living things they need a certain environment to survive in. Timber decay is closely linked to conditions suitable for these types of biological decay (Feilden, 2003).

Figure 1.31: Dry rot on roof beams (Ridout, 2000, p.190)

Figure 1.32: Brown rot, identifiable by the cube-like degradation pattern (Deacon, 2005)

Fungi do not survive to attack wood if the moisture content is below 22%, but most wood boring insects are able to survive in moisture contents low as 12 %. It is believed that some insects can even attack the wood in moisture levels as low as 8% (Ridout, 2000, p.23). The moisture available in wood equilibrates with atmospheric moisture, which is quantified as relative humidity (RH). RH is the ratio of the actual partial pressure of water vapour to the equilibrium vapour pressure of water at the same temperature.

Dry rot (figure1.31) can easily be controlled at the right moisture content, but in historic buildings it is not always simple to put that concept into practice, especially in church buildings which are only in use a few days a week. Dry rot can also be hard to find in church buildings as it attacks the wood panelling from behind, destroying the wood while the occupants are none the wiser (Cullen, 1996).

Most conservators will aim to keep historic and archaeological wood in conditions which allow a temperature between 18-20°C, and a relative humidity between 50-55% +/-5, (Gerrish, 2011). This however is difficult to do in conditions outside a museum, such as in historic ships and buildings. It is important when trying to analyse the possibility of a biological decay problem, that the timbers people are concerned about should not just be checked for moisture content at the surface, but the timber should also be checked internally, in case there are any voids that are concealing moisture which could lead to decay (Demaus, 1995).

All fungi grow first by producing hyphae which enter the cell lumina and push into the S2 layer. Under the microscope these hyphae look like tiny strands of hair (Clausen, 2010). White rot fungi are unique in removing the lignin as well as the holocellulose. They successfully decompose the entirety of the cell wall polymers, starting with the lignin as it impedes access to the more nutritious carbohydrate polymers (Blanchette et al., 1985; Faix et al., 1991; Hastrup et al., 2012). White rot fungi do not break down cellulose as much as the other wood polymers, so in white rots the modification of lignin and the depolymerisation of the hemicellulose are the principal changes (Fackler and Schwanninger, 2012; Yilgor et al., 2013). White rot fungi have a greater tendency to attack hardwoods than softwoods, but will attack both in the right conditions. They are known as white rots because, by degrading lignin, they leach the colour out of the wood leaving it white. If the wood is white it is beyond repair (Clausen, 2010).

Brown rot fungi (figure 1.32) are the most destructive form of fungi towards buildings in the UK and in most of the northern hemisphere. Brown rot fungi will attack and break down the polymer structure of cellulose and hemicelluloses. The worst damage caused by these fungi can be seen in the S2 layer, although the fungal mycelium will have mostly grown in the lumina of the wood cells (Xu and Goodell, 2001; Enoki et al., 1988, Curling et al., 2001; Hastrup et al., 2012).

Although these two classes of fungi work in very different ways in the breakdown of the wood structure, they all do considerable damage to the strength of wood (Srpčič, 2008; Hastrup et al., 2012). The dry rot fungus *Serpula lacrymans* (Wulfen: Fr.) Schroeter is a type of brown rot which holds a special notoriety in the built environment due to its vitality, its destructive potential and the huge costs involved in rectifying the damage caused (Strätling et al., 2008).

The most common place to find decay is where a beam end enters a stone wall. Here the wood can get damp from the masonry and rot sets in. However the most problematic and dangerous place to get rot is in the joints between members of a wood structure. If these become weakened the whole structure will become unstable, particularly if it was built without diagonal reinforcement (Brites et al 2013). In this way, problems can spread throughout a timber structure very quickly (Sousa et al., 2014).

1.10 Timber degradation: from pests

The deathwatch beetle (figure 1.33) causes huge amounts of damage in timber. The flight holes left are extremely large and very distinctive. Unlike other types of wood-boring beetle it can be hard to tell if an infestation has been remedied, as the deathwatch beetle will use existing flight holes.

Figure 1.33: The deathwatch beetle (Ridout, 2000, p.37)

It is not the beetles themselves that cause the damage; it is the larvae that eat through the wood. Once they have fed enough, which can take anything from 5-7 years, the larvae develop into pupae and emerge as beetles. The beetles do not live long, usually around two weeks, in which time they mate and the female will then lay 50-100 eggs again in the timber to begin the life cycle over again (Unger et al., 2001, p.66), providing another 50-100 larvae which will feed off the wood for another 5-7 years. One of the main reasons why the deathwatch beetle causes the most damage is its mating requirements. A female beetle will not mate with a male beetle unless the male has enough weight, as the male beetle will transfer its spermatophores to the female to provide the nutrients needed for the development of their eggs. Therefore if the male larvae have not eaten enough to reach a suitable weight for the female they will not be able to mate (Ridout, 2000, p.46).

A series of tests were done concerning the deathwatch beetle by Ridout, B (2000) which showed that when given a choice the deathwatch beetle would attack medieval wood in preference to modern wood. This was thought to be due to the combination of fissures

in older oak, providing easier access, and the greater incidence of fungal decay which makes it easier for the beetle to attack (Ridout, 2000, p42-43).

The heartwood of a tree is not readily affected by attack from beetles as it retains the extractives, the tree's natural defences stored when it was living. These usually prevent beetles from attacking the wood any further than the sapwood, but they can be degraded. Certain types of fungi and bacteria attack the heartwood allowing it to become more susceptible to beetle attack. Figure 1.34 shows where the pith region of a beam has been attacked by pests. This is unusual and occurs only if the tree was infected before it was cut down. In a growing tree the pith is more susceptible to fungi that can overcome the heartwood's defences. Once the tree is cut down this allows the pest to continue the decay (Ridout, 2000, p. 44).The microbial attacks can be stopped by controlling the environment but once the protection from the extractives in the heartwood has been destroyed it will not recover, leaving the heartwood more open to attack (Ridout, 2008, p.162).

Figure 1.34: Pith attacked by pests (Ridout, 2000, p.44)

Experiments have shown that wood which has been eaten by insects (xylophages) will absorb higher amounts of water, which favours pest development, deteriorating the wood faster (Sandu et al., 2003).

Figure 1.35: Rotten beam end at the base of a wall (Pizzo and Schober, 2008)

It takes a great deal of moisture to keep fungi and beetles alive and able to continue their consumption of the timber, therefore poorly maintained buildings are a key target. To insects, wood in a damp building is just the same as a forest floor. Therefore having a good maintenance programme and the correct environmental conditions around the timber is essential to ensure that biological attack will not occur (Ridout, 2005).

If historic wood ever becomes wet, which is likely as it is a building material suitable for roofs and ships, it is essential that the wood is allowed to dry out again as quickly as possible. If wood remains wet for long periods of time then the effect of decay becomes far worse and harder to control (Zwerger, 1997, p.23). This happens particularly to beam ends housed directly in sockets in the masonry as the surrounding stone will hold enough moisture for the timber to rot (figure 1.35).

Biological attack on wood and the resulting decay can be prevented by keeping historic buildings weather-tight and in a good state of repair. This can be the key to their preservation (Newton, 2011, p.27), but it is not a simple process, especially concerning beam ends that are directly inserted into stone. In Scotland a historic system known as harling was used to keep buildings weather proof (Fisher, 1976, p17). Harling is a slaked lime coating over rubble stonework, to both decorate the surface of the building and provide a waterproofing system (Frew, 2013) but the harling has been lost from a large and uncertain proportion of Scottish buildings (Frew, 2013).

1.11 Timber degradation: chemical changes

Degradation of wood has been researched in depth when it has concerned insect pests, fungi and bacteria. If the wood has not been affected by any of these, there is little known about its degradation during aging.

Wood, like many other materials, suffers from physical and chemical decay. One of these forms of decay is through visible light and ultra violet (UV) degradation. This degradation only affects the surface of the wood as UV light can only penetrate around 0.05 to 0.5 mm (Ridout, 2000, p.32). Lignin suffers most from this form of degradation, which causes the silvery grey appearance of aged wood (Unger et al., 2001, p.47; Kisternaya and Kozlov, 2007).

In UV radiation, cellulose undergoes auto-oxidation which leads to a weakening effect on the wood. The cellulose itself does not absorb the UV. The lignin acts as a photo-sensitizer, transferring the energy to the cellulose. This causes some of the long cellulose chains to break and lowers the degree of polymerisation, weakening the wood but only at the surface (Ellison, 2000; Unger et al., 2001, p. 47). UV degradation can be monitored by FTIR. The degradation of lignin as a function of duration of UV exposure can be monitored by the loss of intensity from lignin bands at 1506cm^{-1} and 1601cm^{-1} in the FTIR spectra, which represent a vibration of the aromatic rings in lignin (Evans et

al., 1992; Tolvaj, 2009). Other effects of weathering have been monitored by FTIR spectroscopy as it is sensitive enough to detect small changes in the composition of the weathered surface layer. Lionetto et al (2012) used FTIR in this way to show that cellulose crystallinity increased at the expense of amorphous cellulose.

One of the concerns arising from the chemical degradation of wood is the production of acetic acid. The problem of wood releasing acetic acid has been known by conservators for years, although it has not previously been considered as causing a problem for the wood itself. For conservators currently the problem is that the acid produced from the wood actively corrodes metals, therefore any metal objects in wooden cases are at risk (Zelinka et al., 2008). Acetic acid is released by hydrolysis of the acetyl groups from the hemicellulose polymers and the resulting acid conditions can catalyse the depolymerisation of the hemicellulose chains, and probably also cellulose (Hosseinaei et al., 2012). The effect on the chemical aging of wood is one of the key things that this research aims to uncover and is discussed in Chapter 11.

1.12 Timber conservation

The current conservation methods available for timber structures are traditional carpentry repairs, steel repairs and resin repairs. It is well known that the green wood used in most oak framed historic buildings will shrink with age from loss of moisture, loosening joints in the timber frames (Zwerger, 1997, p.18).

In the past conservators tended to think that these loosened joints needed to be strengthened. This had bad effects on certain structures which needed the freedom to move. For example bell frames were designed to shrink to get a better swinging motion for the bell ringing. If at any time they became too loose, they used to be stiffened a little by wedging small wooden pieces in the gaps. The modern method of strengthening with steel has affected the way the frame works, which can even change the way the bells were meant to sound (Morton, 2009). Gaps between the joints can allow moisture to pool, which will allow the correct conditions for biological decay (Brites el al., 2013, Pizzo, 2008). Biological decay at loose joints can be extremely damaging, as loss of strength from decay can cause buildings to settle, removing support from the whole structure. Shrinkage is a key consideration as different pieces of wood shrink differently. Therefore it is logical that historic and modern wood will move differently, with potential effects on the traditional repairs favoured in conservation. This is discussed in Chapter 5.

In the effort to conserve historic timber ships and buildings, current conservation practice is to cut the rotten or damaged piece of wood out of a frame and splice in a new piece of timber. This is the standard, accepted approach to repairs but it has never

really been scientifically looked at with respect to the impact of mixing historic wood with modern wood.

1.12.1 Traditional carpentry repairs

One of the major problems with the shrinkage of historic wood has arisen as recently as the 20th century, with the development of central heating. When this was put into many historic houses warping began to be seen, especially in the wooden floor boards around the radiator and water pipes. Today the gaps which have been caused by the addition of central heating are usually filled by adding new timber pieces, although this is only done when completely necessary. Standard practice with floor boards, unlike timber frames, is to match the timber with antique or well seasoned pieces (Weldon, 2009). How these repairs are carried out to maintain the integrity of the entire timber structure, and how findings from this research should be considered in the future, is discussed in Chapter 12 with Section 12.3 focusing on how this will affect timber joints. Here the current approach to traditional repairs is discussed with respect to historic timber.

Differences in atmospheric temperature cause changes in RH, which affect the moisture content of the wood and often need to be taken into account in traditional carpentry repairs. There will be a difference in wood shrinkage depending on whether the wood is inside or outside the building. Timber roof beams can be partly inside and partly outside (Bell, 1992). Timber frames were designed to stand on their own acting as one unit, therefore in conservation the preferred option is that any work done to a timber frame should keep this unity, resulting in the frame acting as it always has throughout its life (Russell, 1993).

In timber framed buildings it is often found that the sole plate has suffered severe decay, due to the fact that it can pick up moisture very easily from the ground causing it to be extremely susceptible to fungal and pest decay (Morton, 2009).

Figure 1.36: Traditional carpentry repair with new wood spliced in. (Simons, 2007)

The other main area in a timber building that is highly susceptible to decay is the ends of beams recessed into the masonry. Here the wood is susceptible to moisture diffusing from the wet masonry exterior. Masonry can cause a further problem for decay without being wet itself. Outside walls are generally colder. Wood can transport moisture in its vapour phase through open air spaces. Water vapour may therefore move through the wood from warmer areas towards the colder beam ends in their masonry sockets, where it will condense. The higher moisture content might then lead to decay. Splice repairs to beam ends are most common (Pizzo and Schober, 2008; Pizzo, 2008).

Current conservation practice is to replace timber at decayed joints with green oak to keep the feel of the wooden structure (figure 1.36). It is usually not done using seasoned oak as a piece of seasoned oak of the correct size would be extremely expensive (Russell, 1993), but as the green oak shrinks after installation, stresses may arise.

As in all methods of conservation it is the ethical responsibility of the conservator not to remove any of the historic material unless completely necessary, or unless the material is so damaged that it can no longer carry out its purpose (Tomback, 2007, p.209). In these cases the standard practice is to try and keep the complete timber structure where possible but if this is not possible the decayed part of the timber will be cut away and a new piece of timber will be spliced on to the end, at least keeping the species the same. It is also necessary to assess why the timber has decayed. In buildings the major cause is that timber beam ends have been built into the wall causing moisture to become trapped in them (Morton, 1999).

The reason why these splice repairs are so highly regarded in building conservation is as an answer to the problems caused by decayed timber, allowing the impact of the conservation measures to be kept to a minimum and avoiding diverting people's attention from the historic importance of the object. By using these forms of splice repairs to a building a lot of the original timber structure can be retained and if the timber selected for the new, spliced-in piece is chosen carefully it can even be matched so closely in colour as not to detract from the original appearance of the building (Hayden and Lund, 1998).

Problems can occur with these types of repairs. For example buildings with a complete timber frame, rather than just a timber roof, are able to cope with the load put on them in extraordinary ways. If a timber component has decayed the frame will often change its load pattern throughout the building to compensate for this. Therefore when the conservators go in and add a fresh splice while removing the decay from the timber, the older structure of the building will now need to change its load pattern again, which can cause more damage to the foundations (Morton, 2007). There is also the question of

instability occurring due to differential shrinkage between the historic and new timber members (Kozlov and Kitsernaya, 2013; Buck, 1952).

The aim of the splice joint is to leave much of the original structure in place. Some repairs to historic buildings are done using green oak which is then stained to make it appear closer to the colour of the historic wood, making the repairs less visible to the public and thus less likely to detract from the original historic material (Hayden and Lund, 1998).

A lot of people love the weather-worn look of old buildings and timbers with the natural patina they develop over time. The splice joints aim to keep as much of this intact as possible, trying to retain the authenticity and historic importance of the original timbers (Knut and Marstien, 2000, p. 12).

Many splice joints involve the use of synthetic resins as a form of adhesive. Most commonly used for these repairs is epoxy resin to stabilise the stainless steel pegs used to hold the joint together (figure 1.37). It is also widely argued that we don't know the long term effects of these synthetic materials nor how stable they will be over time. Although epoxy resin has been widely tested some conservators are still not convinced of its utility (Charles and Charles, 1990, p.12).Resins have to provide structural support for the wood-wood bonded area as well as having safe and stable interaction with very different materials, and are expected to behave well with all of them. Careful surface preparation is needed before the resins are applied (Custodio et al., 2009).

Traditional carpentry repairs may involve a lot of stripping back of material to get access to the decayed areas. They may also involve cutting away enough of the historic timber to get rid of all the decayed material and to provide a good bond surface for repairs with resins. These drastic carpentry repairs may be the most obvious choice but they can be the least conservative (Brentnall, 2008, p. 172).

1.12.2 Resin repairs

The impregnation of wood with resins is another method for keeping the historic timbers in place rather than removing them, keeping to the principle of maintaining the historic fabric intact.

Figure 1.37: Resin and steel rod repairs (Schober, 2008)

Using resin impregnation has a number of advantages. It can be useful in preserving important evidence of historic techniques such as tool marks from construction, which can add historical value to the building (Larsen and Marstein, 2000, p.14; Custodio et al., 2009). Although resin repairs have certain good qualities they should always be considered with a certain amount of care and, some believe, only where carpentry is impractical (Larsen and Marstein, 2000, p.48). They have not been in use in conservation for as long as carpentry repairs, but they have been in use for more than 30 years now. There has yet to be a consistent study of their performance in use when compared to more traditional repairs (McCaig, 2006; Pizzo, 2008).

There are two main resins used in structural conservation, epoxy resins and polyester resins. Polyester resin is the cheaper option of the two and it is more used to strengthen material in pre-decorated areas where the repair itself can be concealed (McCaig, 2006; Custodio et al., 2009).

Epoxy resins in conservation are being considered more important for structural repairs. They have low shrinkage when they cure and are highly resistant to chemicals, as well as being very high in strength (Unger et al., 2001, p. 487). The main reasoning behind using epoxy is that it has the ability to be used in strengthening the historic timbers while leaving them *in situ*, without too much disturbance of the historic material (McCaig, 2006). Epoxy resins have a lower visual impact than steel and timber repairs but they do cause darkening of the original material due to saturation of the pores in the wood (Horie, 1987, p.175). Depending on the amount of decay in the timber, epoxies can be easily used by injecting the resin directly into the decayed material

(Pizzo, 2008), although this is not without problems because frass, which is left by pest infestation, can cause blockages when using resin of high viscosity. Lower viscosity resins are not without problems if they are not properly cured, as they can leak out with temperature changes (Horie, 1987, p.171-172). Epoxy resins have other disadvantages as they can cause moisture to be trapped in the wood, which can cause decay (Larsen and Marstein, 2000, p.48). Epoxy resin also goes against one of the principles of conservation, that repairs should be reversible where possible (Charles and Charles, 1990, p.12). In theory epoxy resin treatment is reversible, as in certain solvents epoxies will swell and it is possible to remove them mechanically, but once they have been used for consolidation it becomes far too difficult to put this theory into practice (Horie, 1987, p.173). Although epoxies have their problems, they do leave the wood workable so that added strengthening devices can be used, such as wooden pegs, which can benefit the structure's security (Unger et al., 2001, p.481).

One of the advantages of epoxy resins is that if they fail under a new load put on the timber, then the usual timber to timber or steel repairs can take place afterwards, although at increased cost (McCaig, 2006). Epoxy repairs are also very sensitive to the climate in which they are left to cure. Under optimum laboratory conditions perfect setting is possible, and careful application with brushes to impregnate small areas of decay can be done very delicately (Lionetto and Frigione, 2012). However when used in the field, if the temperature is too cold or too hot the resin will not set correctly, especially if there is too much moisture in the wood. Over about 22% moisture the bond will not reach its greatest potential (Stoeckel et al., 2013; Broughton and Hutchinson, 2001; Custódio and Broughton, 2008). Over 30% moisture content there will be no bonding at all. Again there are problems with differential movement. Wood will always swell and shrink with changing moisture in the environment. Resin does not do this. In a building where the RH is allowed to fluctuate this can cause serious damage to the bond between wood and resin (Custodio et al., 2009) especially if resins are used to fill large voids within in the wood.

Synthetic resins, such as epoxy resin, have their time and place in the conservation of historic wood. For example, epoxy resin can be used successfully by injecting it into a beam end entering the wall, so that it can be protected from moisture. The further the resin can be injected into the wood, the better the mechanical interlock between the wood and the resin (Feilden, 2003, p. 37).

Traditional carpentry repairs are something that has always been part of standard conservation practice, involving the minimum necessary intervention in the building fabric (Taylor, 1999). Some believe that our historic structures are like documents from the past and should be kept as authentic as possible for the future (Knut and Marstien, 2000, p. 12). In most historic building repairs this will be the main aim but no one has

ever looked into the possible effects of adding new timber to old timber. As new and old wood of any one species are thought of as being the same material, in practice they are expected to react in the same way, but the author intends to explore what differences may be present. After all, the newer wood may be hundreds of years younger than the original and may have been grown in completely different conditions. Can we just assume that they function identically? The research described in this thesis tests both historic and modern wood to find out if differences occur, and if replacing 'like with like' is in fact the best method for the survival of our historic wood heritage.

1.12.3 Steel repairs

Steel repairs are used today in preference to other techniques because of the strength they can provide to historic timber so that it can remain *in situ*. Many steel repairs fit in to one of the main conservation principles of conservation which is, that the work should be reversible. The use of steel repairs has been taking place since the 19th century with a good success rate in most cases (Larsen and Marstein, 2000, p.49).

Figure 1.38: Steel repair to strengthen a bell tower (Morton, 2009)

Splicing and steel repairs can be used together to strengthen historic timbers. The pieces would usually be spliced together and steel pins would be used to secure the joint between the new piece and the historic timber (Warren, 2002; Schober 2008). Although steel repairs can have an undesirable visual effect on the building, they can be covered with oak cladding. An example of this can be seem at Bucknall Church (figure 1.38), (Warren, 2002), but this approach can also cause problems. Steel repairs can be very good when a new load would require a timber far too big to fit in with the building, leaving it looking out of scale (Warren, 2002). Although this form of strengthening of historic timbers will leave them *in situ*, therefore preserving more of the historic material, problems can still occur where areas of decayed timber have been strengthened and a new load has been put back on the historic structure. If this load is too much for the timber, it may break but not in the same place as before. As the strengthened repair is more rigid, it will result in the historic fabric breaking first

(Larsen and Marstein, 2000, p. 49). Other disadvantages of this method are that problems can occur when the wood flexes with season and moisture content. Steel does not have this reaction as it is not organic and does not absorb moisture. In certain climates this can cause damage to historic timbers (Larsen and Marstein, 2000, p. 49). Where it is possible steel repairs should be kept accessible for inspection to prevent irreversible decay from occuring through trapped moisture (Russell, 1993).

Repairs with steel wire can be done in a relatively short amount of time and can often be done without dismantling the timber structure, but these repairs can fail if they rely on adhesive bonds between the wire and the timber. This does not work well in a fractured area in the timber, which is most likely to be the point of the repair (Borri and Corradi, 2011).

1.13 Thesis Aims

Little is known about how wood ages and what processes are taking place within the wood at cellular level, nor how its age affects its mechanical stability. This PhD research was intended to find some of the answers to these questions. It was hoped that the outcomes would help to show whether traditional carpentry repairs, used in the conservation and restoration of historic structures, are the correct method to keep these buildings alive.

One of the reasons why so little is known about historic wood is that what has survived through time is usually part of a structure and is not available for destructive testing. The historic samples of Scots pine and Oak were obtained from Historic Scotland, but were of much smaller dimensions than was originally envisaged. A full description of the samples is given in Chapter 2. They had previously been analysed for Historic Scotland by dendrochronologist Anne Crone, and were dated to the 15th and 16th centuries.

Even with access to some historic wood samples provided by Historic Scotland, the testing had to be done on a very small scale to get as much information as possible out of the small amount of historic wood that could be spared for experimental purposes. It was therefore necessary to greatly reduce the scale of a number of the accepted mechanical testing methods, and to validate these methods at the smaller scale used. The mechanical tests were chosen to determine if there was any difference in mechanical properties between the historic and modern samples. The main test initially chosen was the 3-point bend test, which is the industry standard for testing stiffness, but after attempting to validate this test on small scale samples it was found that the length of the Scots pine samples available was inadequate. Therefore a novel miniature compression test was set up. Hardness testing was also carried out on oak, as hardness is important in replacement floor boards. It is widely held that oak becomes harder with age and this theory was tested quantitatively.

A further objective was to compare shrinkage and moisture uptake between historic and new samples, because any large differences in these properties could cause serious damage to traditional repairs and, in the case of moisture which is discussed in Chapter 4, could enhance biological decay due to water pooling in joints between old and new wood.

The density and microfibril angle of historic and modern oak and Scots pine were compared, with the initial aim to uncover how the original quality of wood might have differed in historic times due to different forest management and climate. It was expected that any changes with age could only be seen once such differences in quality at the time of felling had been taken into account. Microfibril angle and polymer composition were measured by FTIR microscopy on sample series from pith to bark. Unexpectedly, these measurements made it possible to distinguish between sound wood and wood affected by decay. This allowed us to distinguish the effects of decay on mechanical properties from any direct effect of age.

The final aim of these experiments was to provide insights into conservation practice by relating chemical and biological degradation to the mechanical properties of wood (Grabner and Kotlinova, 2008). Such insight into the material might lead to better conservation treatments (Monaco et al., 2013), and make it possible to predict whether any treatment could damage the material in the long run (McConnachie et al., 2008).

Chapter 2

Sample History

Historic wood is wood which has spent its full life in service within an existing building or structure, whereas archaeological wood is wood which has either been buried in the soil or discovered through archaeological excavation. Wet or waterlogged wood is wood which has been submerged under water, sometimes for hundreds of years. For example the structure of HMS Victory (figure 2.1) is historic wood because it has always been in service, not buried or waterlogged, while the structure of the Mary Rose (figure 2.2) is waterlogged wood removed from the sea bed completely saturated with water, and finally the Dover Bronze Age boat (figure 2.3) comprises archaeological wood dug out of a main road in Dover.

Each of these different environments affects mechanical and chemical properties of the wood very differently, as degradation depends on the conditions that the wood is subjected to (Popescu et al., 2006; Kretschmar et al., 2008). For example historic wood has been preserved in aerobic conditions compared to waterlogged and archaeological wood which have been preserved in anaerobic conditions, leading to completely different decay mechanisms as explained in Chapter 1.
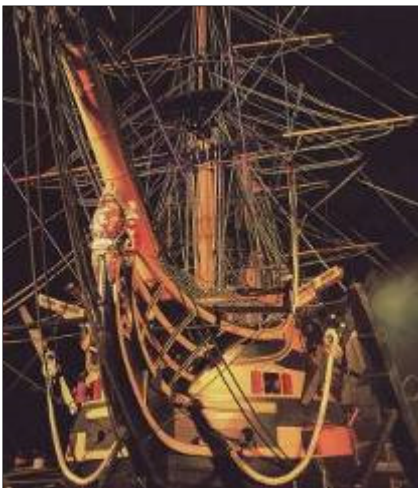
Figure 2.1: HMS Victory (McGowan, 1999)

Figure 2.2: The Tudor warship Mary Rose (Cawthorne, 2012)

Figure 2.3 Dover bronze age boat (Dover Museum, 2000)

The historic wood samples provided by Historic Scotland were beam ends which had previously been given to Dr Anne Crone (AOC Archaeology) for dendrochronological analysis. As they had already been analysed by dendrochronology, the dates of the samples were known but there was also more information on their history. The approximate provenance of the wood can often be determined, and the wood structure itself can also tell us a lot about the environment when the wood was still a growing tree accumulating rings through the passing years (Nilsson and Rowell, 2007).

The historic wood beam ends provided for this project are from three different sites in Scotland:

2.1 Abbey Strand Sanctuary – Edinburgh

Abbey Strand Sanctuary (figure 2.4) is a three storey building. It dates back to the late 15th / early 16th century. The building was partly rebuilt in 1544 and was heavily restored in 1916 (Historic Scotland, 2012).

Abbey Strand is one of the sanctuary buildings located around Holyrood. The sanctuary zone was created by the Abbey as a religious sanctuary free from civil law. Most of the people coming here to seek asylum were debtors. People wishing to claim sanctuary had to apply to the Bailie of Holyrood and pay a booking fee. If you were then accepted you received a letter of protection and could live free of threat inside the sanctuary zone. The law changed in 1880 when debtors could no longer be imprisoned, and so the need for the sanctuary ceased (Davidson, 2014, p. 593). The wood samples came from floor joists from the old Abbey court house, which has a fine example of a refurbished fore-stair and still bears the arms of Scotland including the monogram of James IV (RCAHMS, 2013).
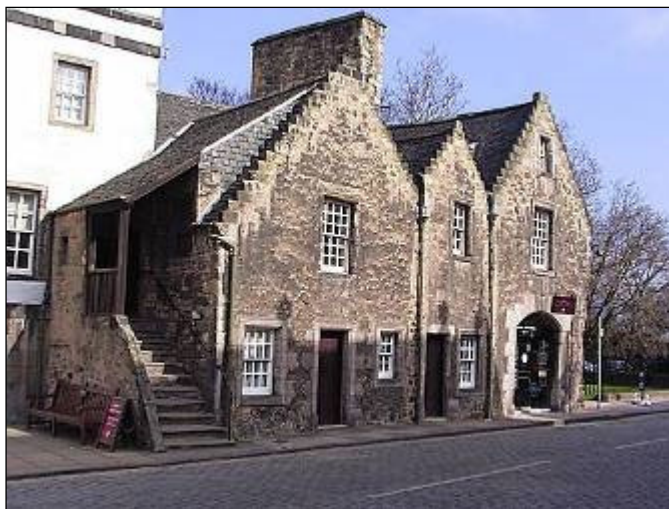
Figure 2.4: Abbey Strand – Edinburgh (Historic Scotland, 2012)

2.2 Bay Horse Inn – Fife, Kirkcaldy

Bay Horse Inn (figure 2.5) is a compact two storey domestic building which is dated to 1583. The building has two painted ceilings which were restored in 1969-70. One can be seen in figureFigure 2.6. It is the wood removed from these ceilings from which a sample has been provided; with a dendrochronological date in the 16th century (Canmore, 2013).

Figure 2.6: Painted ceiling from Bay horse Inn (Canmore, 2013).

Figure 2.5: Bay Horse Inn (Canmore, 2013).

2.3 Carnock House –Stirling

Carnock House (figure 2.7) was originally a simple rectangular building with two stair towers, built in 1548 by Robert Drummond. Extensive additions have been made to the building starting in 1634 and carrying on through the 17th century. The house was eventually demolished in 1941 (Canmore, 2008).

The samples came from oak beams forming part of a painted ceiling that has been dendrochronologically dated to 1588-1589; evidence strongly suggests that the ceiling was installed in the house in 1589. The oak beams themselves ranged between 88 and 272 years old (Crone, 2011). This is the felling age of the tree. There was a little difficulty counting all of the outside rings as they became unclear towards the bark edge.

Figure 2.7: Carnock House (Canmore, 2013).

2.4 Eighteenth century samples

The samples of oak tested from the 18th century were obtained from English town churches which were being renovated. The church pews themselves were removed to allow the wood to be re-used. The church pew from Norwich was dated to 1830 and the church pew from Tunbridge Wells to 1840. Both pews were oak and in extremely good condition with no evidence of decay from pest or fungal degradation, making them good examples of naturally aged wood from this time period.

2.5 Modern Samples

Modern samples of green oak were surprisingly difficult to obtain in Scotland, as the main commercial timber species grown here are soft woods such as Scots Pine and Sitka Spruce. A timber frame building company called Carpenter Oak and Woodland specialise in the making of new timber frames in oak and the repair of old timber structures. They are based at Loch of Lintrathen, Kirriemuir, and have kindly provided 5 beam ends from green French-grown oak for this project. Carpenter Oak and Woodland have been involved in a number of projects in the restoration of historic timber framed structures. The best known was the reconstruction of the roof of the great hall at Stirling Castle. After wood identification the oak species of the modern samples used in this project is sessile oak (*Quercus sessiflora*) as shown in figure 2.8 with the published comparison in figure 2.9.

Figure 2.8: Modern oak sample identified as Sessile Oak scale bar 0.5mm. Image: K Hudson-McAulay
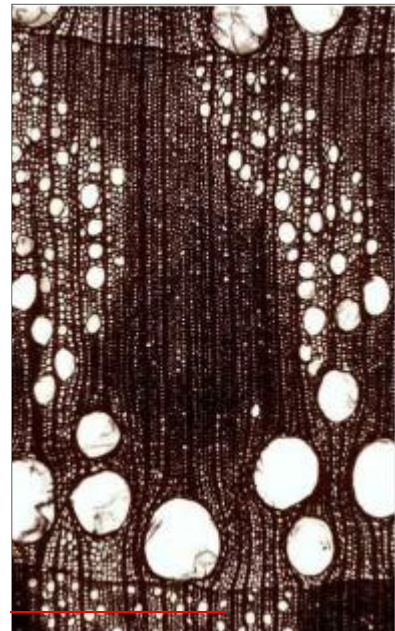
Figure 2.9: Published micrograph of Sessile Oak 5 mm scale bar from Schoch et al., 2004.

Modern Scots pine for this work was obtained from B&Q Abbotsinch Retail Park, 1 Washington Road, Paisley, Renfrewshire PA3 4EP and had been sawn by BSW Timber Ltd. BSW's Scots pine is mostly from northeast Scotland and is processed at their Grantown on Spey sawmill.

2.1 Light microscopy of samples

The use of light microscopy to examine wood is a powerful tool, not only in the identification of wood but also in the diagnosis of fungal attack, when evidence can be seen of deterioration of the wood cells (Reffner et al., 1995; Anagnost, 1998). The images for this project were taken using a Leica ATC 2000 light microscope with objective magnification up to 100x. The microscope was fitted with a Nikon Coolpix 990 3.34 megapixel camera. The samples were prepared in transverse section 19µm thick using a Leica RM2255 microtome fitted with a solid steel blade. Unfortunately it was not possible to assess the decay quantitatively by light microscopy on these samples. The images here are to show visually some of the effects of decay found in the historic samples, as assessed qualitatively in table 2.1.

Table 2.1: Visual assessment of the decay in the historical samples

Sample	Decay present
HP-1500-01 Historic (H) Scots pine (P) from the 1500s sample 1 (01) from Carnock house	Visible signs of pest damage within the sapwood but no visible signs of fungi present
HP-1500-02 Historic (H) Scots pine (P) from the 1500s sample 2 (02) from Carnock house	Visible signs of pest damage within the sapwood but no visible signs of fungi present
HP-1500-03 Historic (H) Scots pine (P) from the 1500s sample 3 (03) from Carnock house	No visible signs of pest or fungal decay present
HP-1500-04 Historic (H) Scots pine (P) from the 1500s sample 4 (04) from Bay Horse Inn	Visible signs of pest damage within the sapwood but no visible signs of fungi present
HP-1500-05 Historic (H) Scots pine (P) from the 1500s sample 5 (05) from Bay Horse Inn	Visible signs of pest damage within the sapwood but no visible signs of fungi present
HO-1500-01 Historic (H) Oak (O) from the 1500s sample 1 (01) from Abbey Strand	No visible signs of pest or fungal decay present

HO-1500-02 Historic (H) Oak (O) from the 1500s sample 2 (02) from Abbey Strand	No visible signs of pest or fungal decay present
HO-1500-03 Historic (H) Oak (O) from the 1500s sample 3 (03) from Bay Horse Inn	No visible signs of pest or fungal decay present
HO-1500-04 Historic (H) Oak (O) from the 1500s sample 4 (04) from Carnock House	Visible signs of pest damage within the sapwood but no visible signs of fungi present
HO-1500-05 Historic (H) Oak (O) from the 1500s sample 5 (05) from Carnock House	No visible signs of pest or fungal decay present
HO-1800-01 Historic (H) Oak (O) from the 1800s sample 1 (01) from Norwich Church	No visible signs of pest or fungal decay present
HO-1800-02 Historic (H) Oak (O) from the 1800s sample 1 (01) from Tunbridge Wells Church	No visible signs of pest or fungal decay present

2.1.1 Light microscopy of oak samples

Figure 2.10: Historic Oak, HO-15-01 heartwood. Scale bar 0.5mm
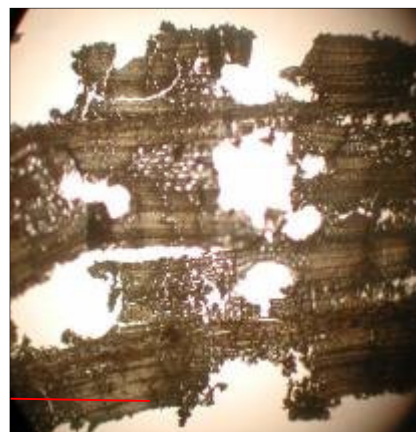
Figure 2.11: Historic Oak HO-15-03 sapwood showing biological damage. Scale bar 1 mm

Figure 2.10 shows the heartwood of 15th century oak and figure 2.11 shows the sapwood of the same oak sample. It can be seen in these images that the sapwood cell walls of the historic wood are in a much more decayed state and that pest and fungal decay have destroyed some of the cell walls completely.
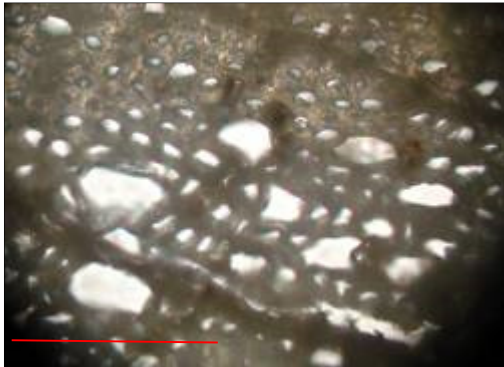
Figure 2.12: Image of damage to latewood in the sapwood of the historic Oak HO-15-02. Scale bar 0.5 mm
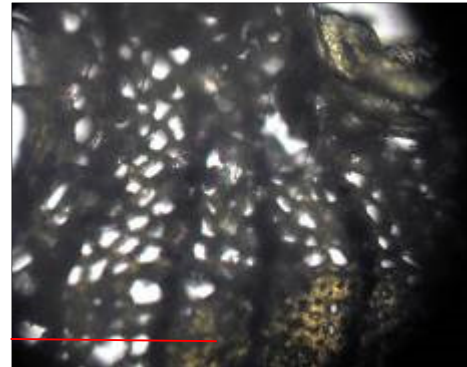
Figure 2.13: Image of damage to earlywood in the sapwood of the historic Oak HO-15-4. Scale bar 0.5 mm

Images of the latewood (figure 2.12) and the earlywood (figure 2.13), at higher magnification show damage to the cell walls. Light can be seen coming through the cell walls where areas of the S2 layer have been destroyed by biological decay. This is most likely due to fungal decay as insect pests cause larger-scale destruction, as seen in figure 2.14, showing a pest hole in one of the oak samples.
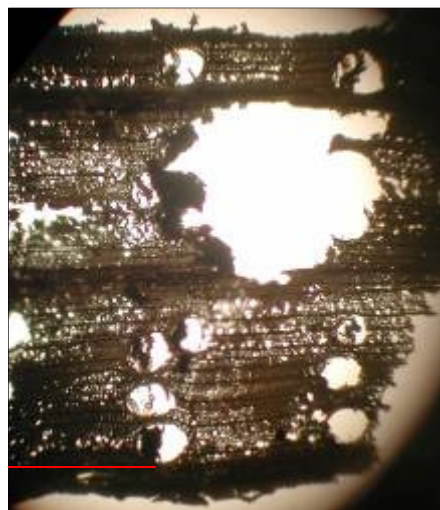
Figure 2.14: Image of damage left by pest infestation. Scale bar 1 mm HO-15-01

2.1.2 Pine
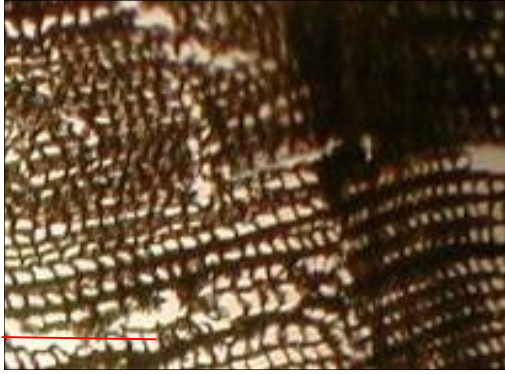
Figure 2.15: Historic Scots pine HP-15-02 heart wood. Scale bar 1 mm

Figure 2.16: Historic Scots pine HP-15-01 sapwood. Scale bar 1mm

Figure 2.15 shows the heartwood and figure 2.16 shows the sapwood of a 16th Century Scots pine sample. The sapwood again is far more extensively destroyed by biological attack with many of the cells appearing almost threadbare, where the carbohydrate-rich layers of the secondary cell walls have been eaten away, leaving behind the primary cell walls.
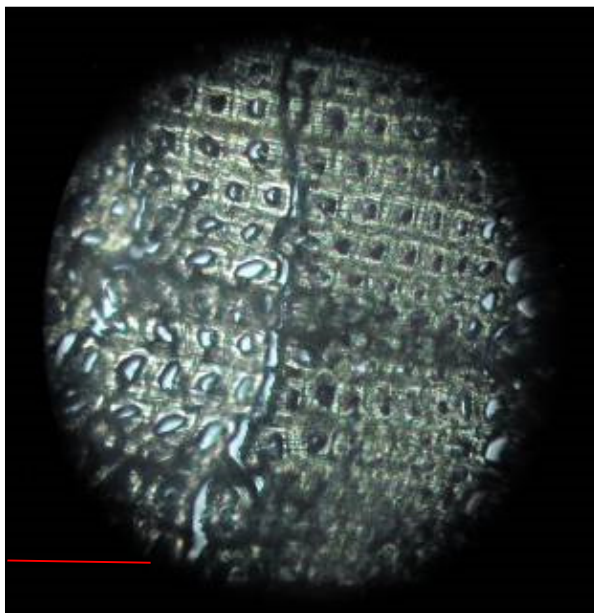
Figure 2.17: Image of damage to latewood in the sapwood of the historic Scots pine HP-15-03. Scale bar 0.5 mm

Figure 2.18: Image of modern Scots pine MP-02 showing no damage to its wood cells. Scale bar 0.5 mm

Figure 2.17 shows the latewood of a 16th Century sapwood sample, which can be compared with the modern Scots pine sample in figure 2.18. Damage to the latewood can easily be seen as the light is shining directly through the cells where the S2 layer

has been depleted. This is not seen in the modern sample. Again, this is due to fungal decay as pest damage leads to complete destruction of the cell walls, as can be seen in figure 2.19.
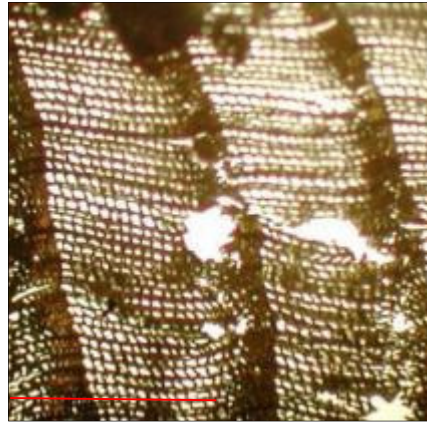
Figure 2.19: Image of damage left by pest infestation HP-15-04 scale bar 1 mm

Chapter 3

Analysis of Chemical Changes using FTIR Spectroscopy

There are many different types of spectroscopic analysis applicable to wood. These include ultraviolet (UV), near infrared (NIR), mid-range Fourier-transform infrared (FTIR) and solid-state nuclear magnetic resonance (NMR). Each of these has its own benefits and flaws depending on what we want to discover about historic wood samples. Here, as most spectroscopy methods are used on solution state samples, these have been adapted for use on solid materials. Due to the density of solid materials the sample needs to be either powdered, the most common method, or prepared as thin sections which take skill to produce (Fackler and Schwanninger, 2012; Pandey and Theagarajar, 1997; Altaner et al., 2010). Infrared spectroscopy is a powerful tool for investigating the chemical makeup of wood and has been in use since the early 1950s. FTIR has been widely used since the 1960's, replacing simpler forms of IR due to its availability and relative ease of use for testing inorganic and organic compounds (Barker and Owen, 1999; Casadio and Toniolo, 2001; Doménech Carbó et at., 1996). FTIR is a relatively common analytical technique for wood as it can identify the various functional groups on the molecules that make up the polymers of wood. The FTIR microscopy method used here has the great advantage of allowing the precision of FTIR with solid samples, and being able to set up the area of the wood sample you particularly want to test allowing for local changes in the wood, for example between ring boundaries (Fackler and Schwanninger, 2012; Reffner et al., 1995; Chang et al., 2014).

FTIR microscopy has many advantages in cultural heritage studies, being a very powerful tool, yet in most cases needing only very small samples on which to work, as well as being non-destructive towards the sample tested. That and the speed of analysis can make it outstanding monitoring equipment (Faix, 1991; Derrick et al., 1995, p. 13; Gruchow et al., 2009; Pandey and Theagarajar, 1997). FTIR works by stimulating the atoms joined by chemical bonds into vibrational motion. At different IR wavelengths, different chemical bonds give rise to spectral peaks as their characteristic vibrational frequency depends on their rigidity (Fackler and Schwanninger, 2012; Ali et al., 2001). The mid-infrared spectral range used to examine wood is between 600 cm^{-1} and 4000 cm^{-1} in frequency. In this range there are specific peaks that have been assigned to the different polymers in wood (Sun et al., 2001; Edith and Maryse, 2009; Chang et al., 2014).

Wood is a complex biological material which is made up of the polymers lignin, hemicelluloses and cellulose. FTIR has the ability to pick out structural differences between these polymers if they break down or change with time. It is even possible to pick up subtle differences in polymer structure between different species (Blanchette, 1995; Barker and Owen, 1999; Pandey, 1998).

The most informative region of an FTIR spectrum of wood is called the fingerprint region (Fackler and Schwanninger, 2012; Marchessault, 1962). The lower-frequency part of the fingerprint region below a frequency of 1460 cm^{-1} is difficult to understand as many of the peaks arise from O-H bending and C-O-C stretching vibrations that occur in both cellulose and hemicelluloses, making these polymers difficult to distinguish (Pandey and Theagarajar, 1997).

Bands specific for hemicellulosic xylans include the absorption at 1045 cm^{-1} assigned to the stretching of C-O and C-C bonds in the sugar ring with some contribution from O-H bonds in the xylan polymer (Sun et al., 2001; Evans et al., 1992). There are other wavelengths attributed to other structural features of hemicelluloses, for example the ester C=O stretching band at 1738cm^{-1} associated with acetyl groups (Pandey, 1998; Gruchow et al., 2009; Pandey and Theagarajar, 1997; Simonović et al., 2011).

Lignin has specific bands in the spectrum assigned to aromatic ring stretching vibrations, coming from the benzene ring of the lignin polymer, which can been seen at around 1505 and 1593 cm^{-1} (Gruchow et al., 2009; Pandey and Theagarajar, 1997; Pandey, 1998; Barker and Owen, 1999). There are also bands at 1265 and 1237cm^{-1} which are associated with the C—O stretching region of the lignin polymer (Pandey and Theagarajar, 1997; Gelbrich et al., 2008), but these overlap with cellulose bands so the 1510^{-1} band is most frequently used.

Another advantage of using FTIR is the ability to use the spectra quantitatively allowing comparison of the chemistry in old and new wood (Leonardon et al., 2009; MacKinnon et al., 2006; Sturcove et al., 2006; Faix et al., 1991). As spectra from old and new wood are very similar, distinguishing these will depend on good quality of the spectral data and on statistical analysis (Esteban et al., 2005; Pandey, 1998; Penttilä et al., 2013; Chauhan et al., 2001).

The data richness gained from FTIR analysis can give conservators the ability to diagnose the degradation of cultural materials and provide a better treatment response (Doménech Carbó et al., 1997).

3.1 Sample preparation

The need for specialised methods of sample preparation for the FTIR microscope is both an advantage and disadvantage, for various reasons. Traditionally FTIR spectroscopy requires a potassium bromide (KBr) disk in which a tiny amount of the sample material is incorporated. KBr is used because it does not absorb in the FTIR spectral range.The sample material, usually around 0.5 mg (Doménech Carbó et al., 1996), is ground with the KBr into a fine powder and then pressed to make up the disk. This can be laborious and due to differences in the particle size of the powder it is not always effective (Altaner et al., 2010; Faix and Böttcher, 1992). This technique is appealing for conservators because only a very small sample amount needs to be taken from a discrete area of a historic object. This form of FTIR is a bulk testing technique, but the FTIR microscope used in the present experiments allows for more precise control over the location from which the spectrum is obtained in the wood section.

The FTIR microscope is at its best with thin longitudinal sections of wood. It gives unsatisfactory flattened spectra from transverse sections due to the heterogeneity of the wood, leading to saturated absorption of the IR beam. Longitudinal thin sections have advantages over the other sample preparation methods for precision measurements, allowing you to pin point any spatial changes in composition accurately throughout the samples, but to prepare the thin sections skill with a microtome is needed. The sections need to be cut to around 20 μm or one double cell wall thick for good spectra to be obtained. Usually thin sections of softer biological materials are prepared after resin embedding of the samples but this causes issues with wood due to the resin entering the cell lumen and interfering with the FTIR spectra. Therefore it was not used here. Samples were cut without the embedding process (Barker and Owen, 1999; Altaner, et al., 2010; Gruchow et al., 2009). The spatial precision makes it possible to pin point any area of the cells, for example cells in the latewood or earlywood, which is why this method is favoured here.

For this experiment three samples were taken from each of the beam ends; one pith, one heartwood and one sapwood. Cubical blocks 5 mm x 5 mm x 5 mm were cut first in order to fit in the clamp of the microtome. The blocks were then soaked for 12 hours in water to soften the wood (Faix and Böttcher, 1992). Thin sections 19 μm thick were then cut from the blocks using a Leica RM2255 microtome fitted with a solid steel blade (Casadio and Toniolo, 2001; Fackler and Schwanninger, 2012). Samples were cut in the axial-tangential direction. They needed to be as thin as this in order for the IR beam to be able to pass through the samples, giving clear spectra without saturation of the more intense absorption bands. As earlywood cells are usually about 30 μm in diameter,

cutting a section 19 μm thick provides half a cell including two adherent cell walls in thickness, and provides a maximum FTIR absorbance usually around 1 in the fingerprint region, giving good quality spectra. Thicker samples cause too much saturation making quantitative comparisons unreliable. Using pith to bark sequences of blocks can allow a series of measurements that reveal any chemical changes that occur across a section of the beam.

3.2 Procedure

The spectra were collected using a Nicolet Nexus FTIR spectrometer attached to a Nicolet Continuum Microscope with an MCT detector which is cooled using liquid nitrogen. The Nicolet Omnic version 7,2a software was used, both to control the spectrometer and to process the spectra. The spectrometer was set to scan 32 times per spectrum, with a spectral range of 800cm^{-1} – 4000cm^{-1} and a spectral resolution of 2 cm^{-1}. This FTIR microscope has a theoretical spatial resolution of 3 μm due to the wavelength of the radiation, but due to scattering within the microscope optics, in practice the spatial resolution is limited to around 10 μm. Using an IR beam with larger dimensions than this gives better signal/noise and for these experiments the beam window was set at 100 μm square. The spectra were saved in their raw .CSV form and then further processed in Microsoft Excel. The FTIR microscope was set up in transmission mode where the infrared beam has to pass twice completely through the sample (Edith and Maryse, 2009).This is due to the optical geometry of the microscope, which has a condenser set up using mirrors rather than lenses. Three different 100 μm x100 μm areas of each section were measured to get good coverage of the whole sample. Using this method in transmission mode the data produced from the spectra could then be analysed in a quantitative manner (Edith and Maryse, 2009). Even though the samples were produced using a microtome they still varied in thickness. Therefore it was necessary to ratio the absorbances against the total absorbance of the representative carbohydrate region within each spectrum. The level of replication that was used allowed for better data analysis and results that could be used, with statistical analysis, to uncover what was occurring due to age, and what could be attributed to biological attack and natural variation between trees.

3.3 Data analysis

Spectral data obtained from the samples first had to be baseline corrected in Microsoft Excel. It is possible to baseline-correct the spectra in bulk so that linear baselines are drawn between the same frequencies for each spectrum, resulting in more reproducible

analysis of the peaks and normalisation of the spectra (Faix and Böttcher, 1992; Yilgor et al., 2013). In contrast, although most software attached to spectrometers has a function to baseline correct the samples, due to different end frequencies for each segment's baseline, quantitative analysis of large groups of spectra is inaccurate. In this data analysis the spectra were baseline corrected using the equation below in Excel.

3.3.1 Baseline Correction Equation:

OA – (IF(F>FF1, FF1A, IF(F>FF2, FF1A + (FF2A-FF1A) * (F-FF1) / (FF2-FF1), IF(F>FF3, FF2A + (FF3A-FF2A) * (F-FF2) / (FF3-FF2), IF(F>FF4, FF3A + (FF4A-FF3A) * (F-FF3) / (FF4-FF3), IF(F>FF5, FF4A + (FF5A-FF4A) * (F-FF4) / (FF5-FF4), IF(F>FF6, FF5A + (FF6A-FF5A) * (F-FF5) / (FF6-FF5), IF(F>FF7, FF6A + (FF7A-FF6A) * (F-FF6) / (FF7-FF6), FF7A)))))))

Key:

OA = Original Absorbance (or lower spectral limit, usually at 800 cm^{-1} frequency for wood)

IF = Excel comparison command

F =Frequency

FF1 = Flattening Frequency1 (for using baseline with wood this is 3764)

FF2 = Flattening Frequency 2 (for using baseline with wood this is 3003)

FF3 = Flattening Frequency 3 (for using baseline with wood this is 2635)

FF4 = Flattening Frequency 4 (for using baseline with wood this is 1810)

FF5 = Flattening Frequency 5 (for using baseline with wood this is 1538)

FF6 = Flattening Frequency 6 (for using baseline with wood this is 1186)

FF7 = Flattening Frequency 7 (for using baseline with wood this is 918)

FF1A = Flatting Frequency 1 Absorbance (the absorbance level of the spectra corresponding to this frequency).

FF2A = Flatting Frequency 2 Absorbance

FF3A = Flatting Frequency 3 Absorbance

FF4A = Flatting Frequency 4 Absorbance

FW5A = Flatting Frequency 5 Absorbance

FW6A = Flatting Frequency 6 Absorbance

FW7A = Flatting Frequency 7 Absorbance
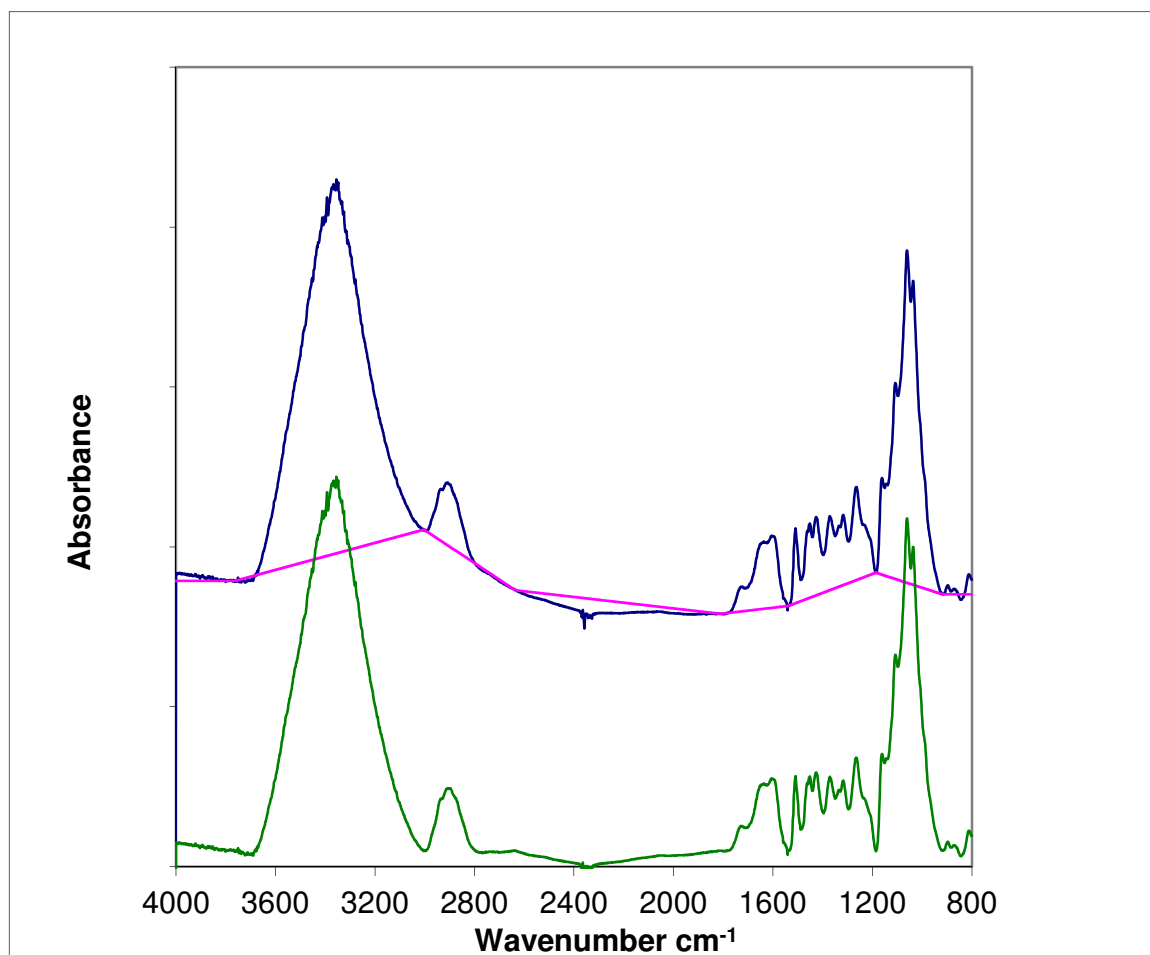
Figure 3.1: The principle of the baseline correction. The baseline shown coloured in red is constructed by running straight lines between fixed frequencies in the uncorrected (blue) spectrum and was subtracted from the uncorrected spectrum to produce the baseline-corrected (green) spectrum.

The baseline correction using the equations above was carried out as shown in figure 3.1 and applied to all of the spectra before further analysis took place.

3.3.2 Ratio Development:

After baseline correction it was possible to calculate ratios between significant peak areas. The peaks tested here are the C=O stretching band from hemicellulose acetyl groups at 1727 cm^{-1} and the 1509 cm^{-1} C=C benzene ring vibration band from lignin.

These peaks were chosen based on results from the RH testing experiments in Chapter 4.

Lignin Ratio:

To obtain the ratio for the lignin peak firstly the average was taken of the entire fingerprint region of the spectra, from the 1186 cm^{-1} peak to the 1586 cm^{-1} peak (figure 3.2).

The average was then taken for the lignin peak between 1504 cm^{-1} and 1513 cm^{-1}, considered as the boundaries of the peak at 1509 cm^{-1}. This peak is assumed to be specific for lignin because it corresponds to a stretching vibrational mode across the benzene ring, which is mainly seen in the lignin polymer (Faix 1991; Pandey and Theagarajar, 1997; Evans et al., 1992). The averaged fingerprint and 1509 cm^{-1} absorbances were then ratioed:

Lignin Ratio = Lignin Average/Fingerprint Average
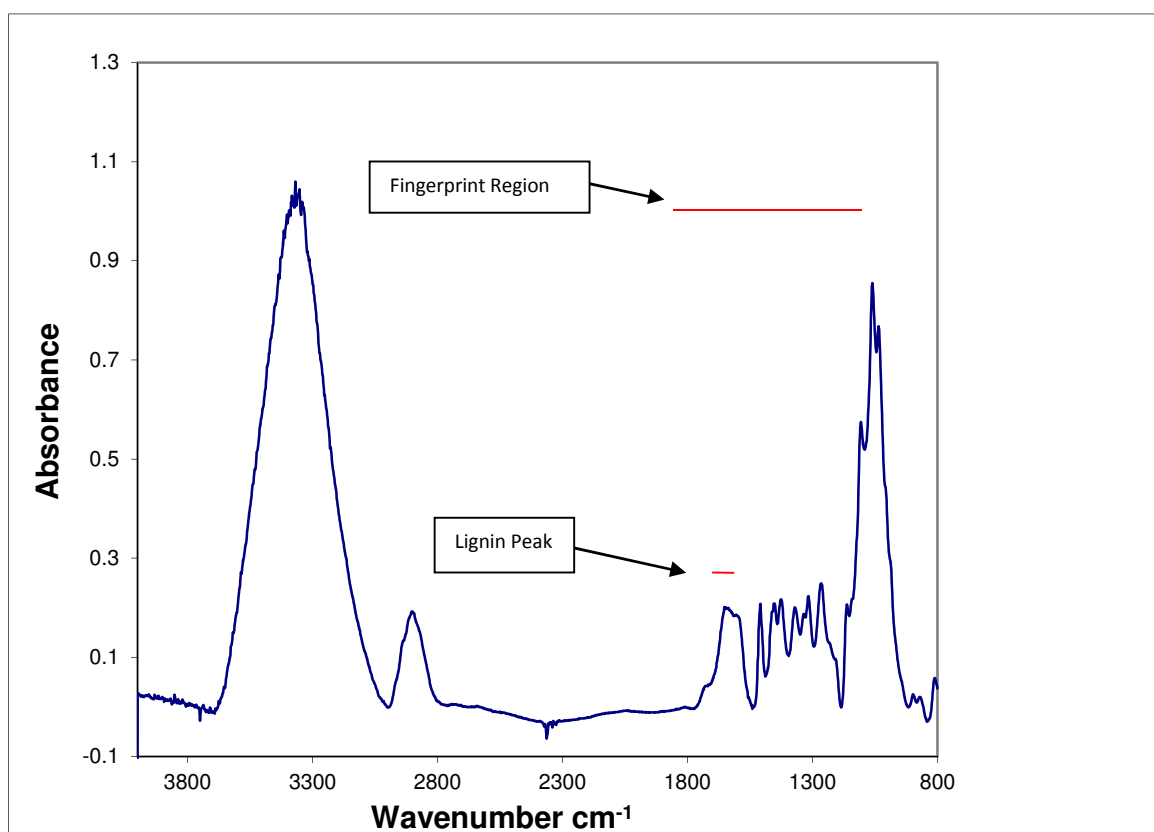
Figure 3.2: Spectrum showing the lignin peak between 1504 cm^{-1} and 1513 cm^{-1}, whose area was divided by the area under the fingerprint region from the 1186 cm^{-1} peak to the 1586 cm^{-1} peak to produce the lignin ratio.

Hemicellulose (acetyl) Ratio:

For the acetyl ratio the same procedure was applied using the average of the fingerprint region between 1186 cm^{-1} and 1586 cm^{-1}, as with the lignin peak (figure 3.3).

The average was calculated for the acetyl C=O stretching peak of the hemicellulose polymers between 1724 cm^{-1} and 1727 cm^{-1}. There are other peaks in the spectra that are related to hemicelluloses, but as the hemicellulosic polymers are so similar to cellulose these peaks cannot be used to distinguish between the two polymers. The 1726 cm^{-1} peak relates to the acetyl groups which are found on the hemicellulose polymers (Faix, 1991; Pandey and Theagarajar, 1997; Evans et al., 1992; Altaner et al., 2010). These acetyl groups are attached to the 2- and 3- positions on xylose in hardwood glucuronoxylans. In softwoods there are two types of hemicellulose, the glucomannans and the smaller glucuronoxylans. It is believed that only the glucomannans are acetylated (Parente et al., 2014; Pawar et al., 2013). The absorbance ratio was then calculated:

Acetyl Ratio = Acetyl Average/ Fingerprint Average
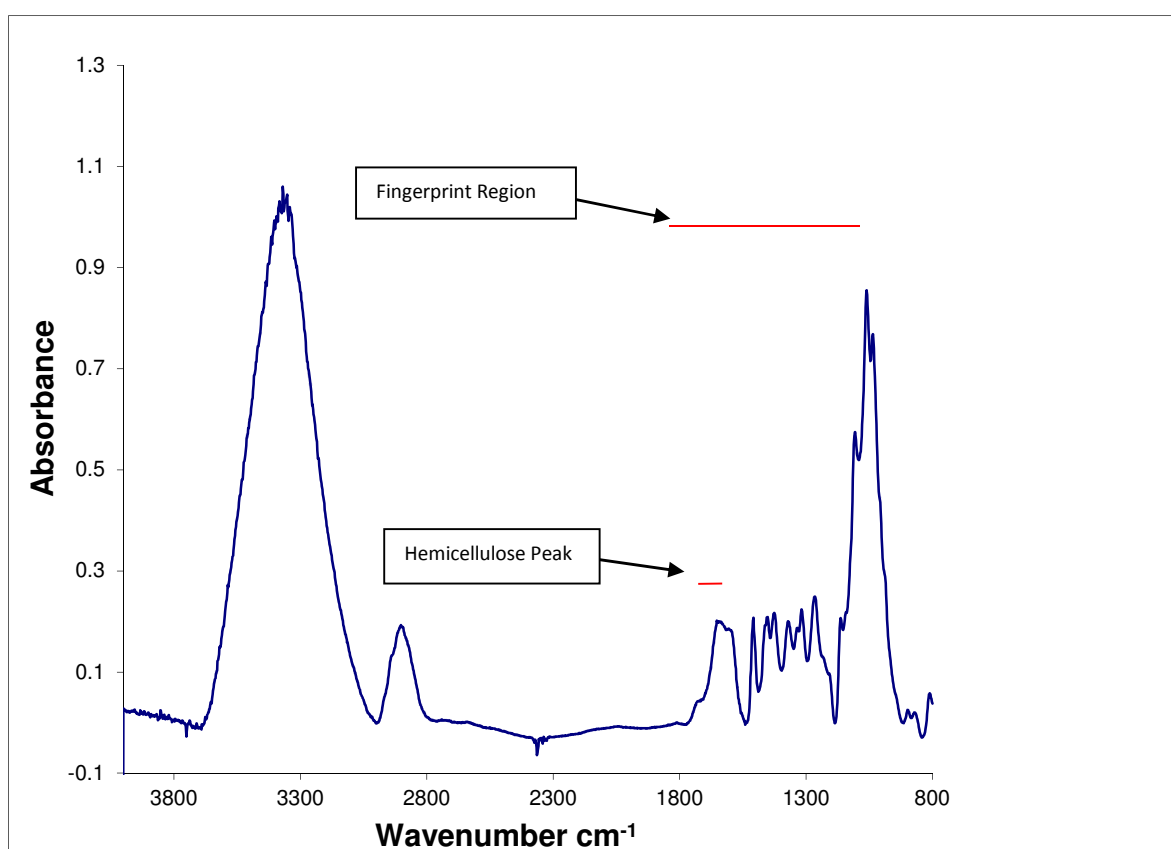
Figure 3.3: Spectrum showing the acetyl C=O stretching peak of the hemicellulose polymers between 1724 cm^{-1} and 1727 cm^{-1}, which was divided by the fingerprint region from the 1186 cm^{-1} peak to the 1586 cm^{-1} peak to produce the hemicellulose (acetyl) ratio.

The ratios were then used to plot the following results;

3.4 Results

3.4.1 Oak lignin
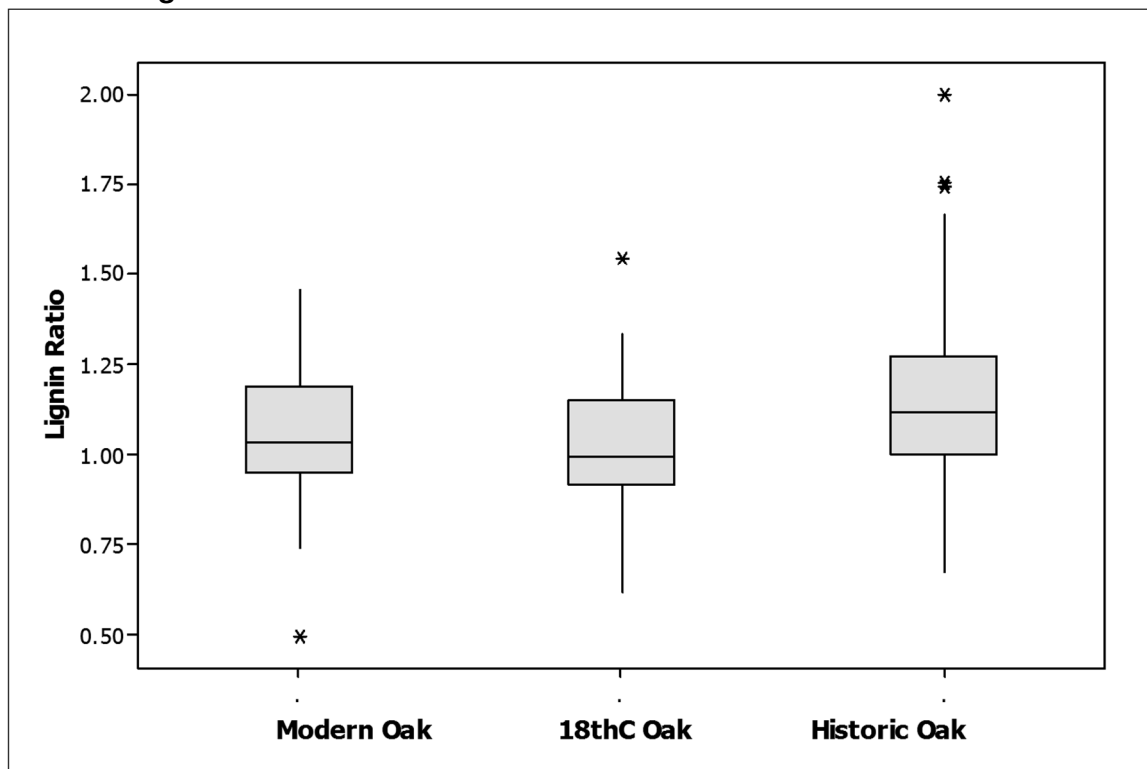
Figure 3.4: Box plot showing the difference in relative lignin content, as determined by the lignin ratio, in the different sample ages of oak.

In a box plot the top and bottom of the box represent the first and third quartiles of the data and the band inside is the median. The lines extending upward and downward from the box, known as whiskers, indicate variability outside the upper and lower quartiles and the asterisks represent outliers within the data.

	Modern Oak	18Th C Oak	Historic Oak
Lignin Ratio	1.054 a	1.024 a	1.175 b

Table 3.1: Mean lignin ratio of oak samples of different ages.

Means followed by the same letter are not significantly different, Fisher LSD (P>0.05).

Figure 3.4 shows the FTIR ratios follows the literature finding that the lignin content slightly increases with age. The results of one way analysis of variance show that the lignin contents of the three age groups contain at least one statistically very significant difference (P < 0.001). The Fisher test showed that the lignin content of the modern

wood was significantly different (Fisher LSD p<0.05) from the historic wood but not the 18th C wood. The historic wood was also significantly different from the 18th century wood. Therefore there appears to be slightly more lignin in the older oak samples. The increase was relatively small. Increased lignin in historic wood samples has been noted in the literature (Popescu et al., 2006; Fackler and Schwanninger, 2012).
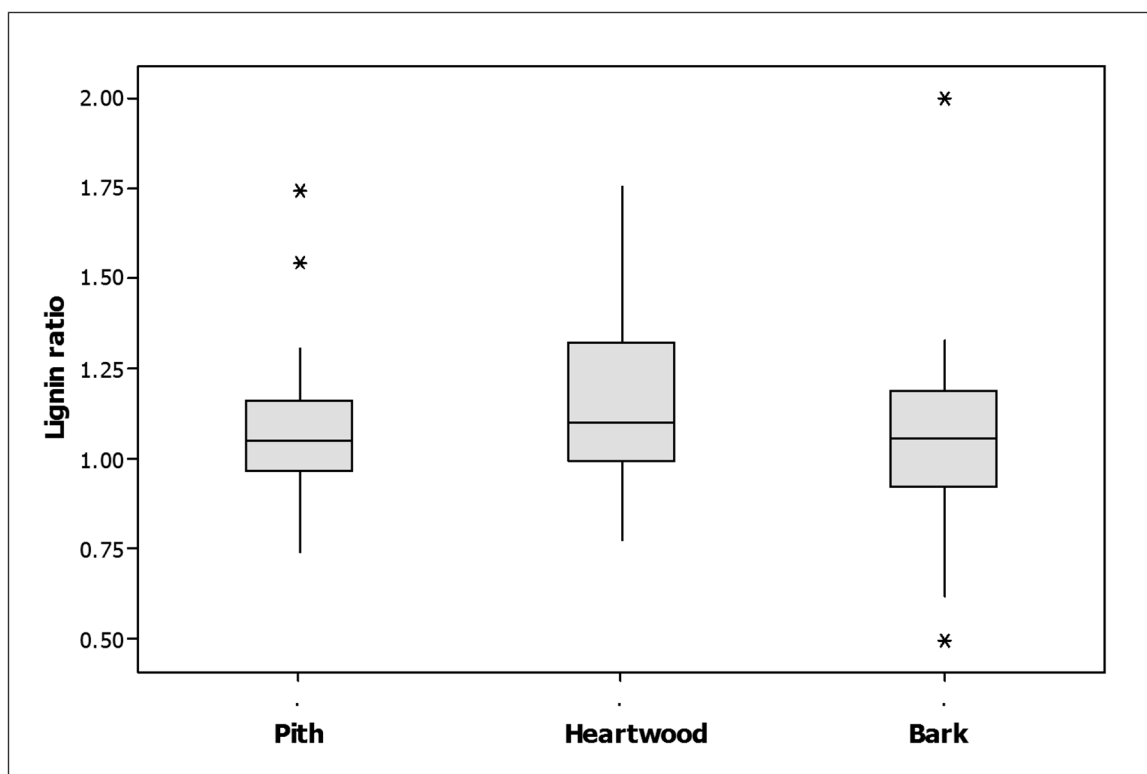
Figure 3.5: The relative lignin content as determined by the lignin ratio, throughout the cross section of the historic oak beams.

	Pith	Heartwood	Bark
Lignin Ratio	1.134	1.108	1.052

Table 3.2: Mean revised lignin ratio through the cross section of historic oak beams.

There were no significant differences between the means (ANOVA P>0.05).

The ratio was then looked at from pith to bark of the historic oak (figure 3.5), to find out if the increase in lignin was happening throughout the beams or in a particular area which could be linked to biological attack. The one way analysis of variance shows there is no significant difference between the different areas (table 3.2). This shows that the increase in lignin seems to be spread throughout the wood rather than restricted to the sapwood, as would be expected if it was due to biological decay. This increase in lignin

has no obvious explanation but the lignin ratio is compared to the fingerprint region which represents cellulose and hemicelluloses. Any loss of hemicelluloses due to age or fungi would make it appear that the lignin was increasing. The ratio for lignin was therefore re-run using different frequencies to see if this was correct.
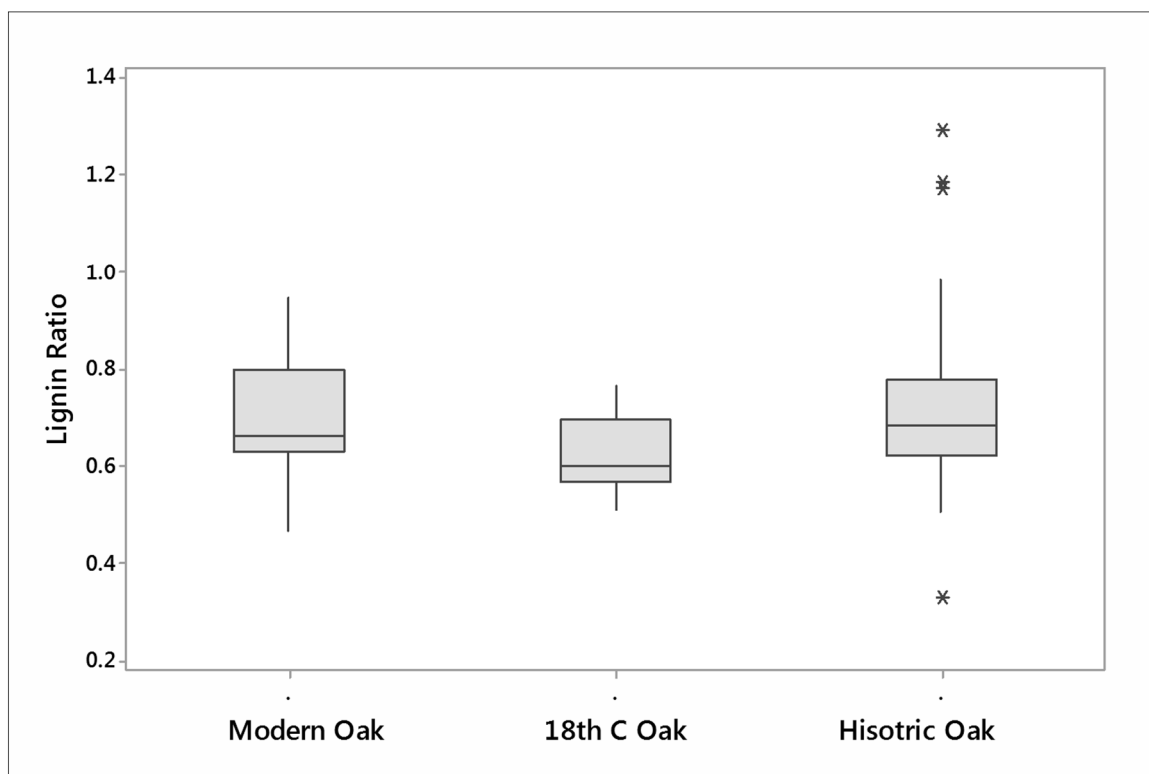
Figure 3.6: The revised lignin ratio using the lignin peak between 1504 cm^{-1} and 1513 cm^{-1} divided by the 1425 cm^{-1} cellulose peak to representing the relative lignin content in the different ages of oak.

	Modern Oak	18Th C Oak	Historic Oak
Lignin Ratio	0.697 ab	0.625 b	0.721 a

Table 3.3 Mean revised lignin ratio of oak samples of different ages.

Means followed by the same letter are not significantly different, Fisher LSD (P>0.05).

The analysis of the lignin peak was re-done using the same lignin peak as before but comparing this peak with the peak associated with cellulose at 1425 cm^{-1}(figure 3.6). The results shown in the box plot above show a slight dip in lignin in the 18th century oak. One way analysis of variance showed that there was a significant difference in lignin with age with a significant P value < 0.05. Fisher test was carried out at 95%

confidence limits showed decreased lignin in the 18th century oak compared to the historic oak (table 3.3). This is most likely not due to any aging effect but due to natural variation in the trees as there were only two 18th century trees here and they only differ significantly from the historic oak. It might be that the 18th century trees in the sample set have more tension wood, which has a lower lignin content (Joseleau et al., 2004).

3.4.2 Oak Hemicellulosic Acetate
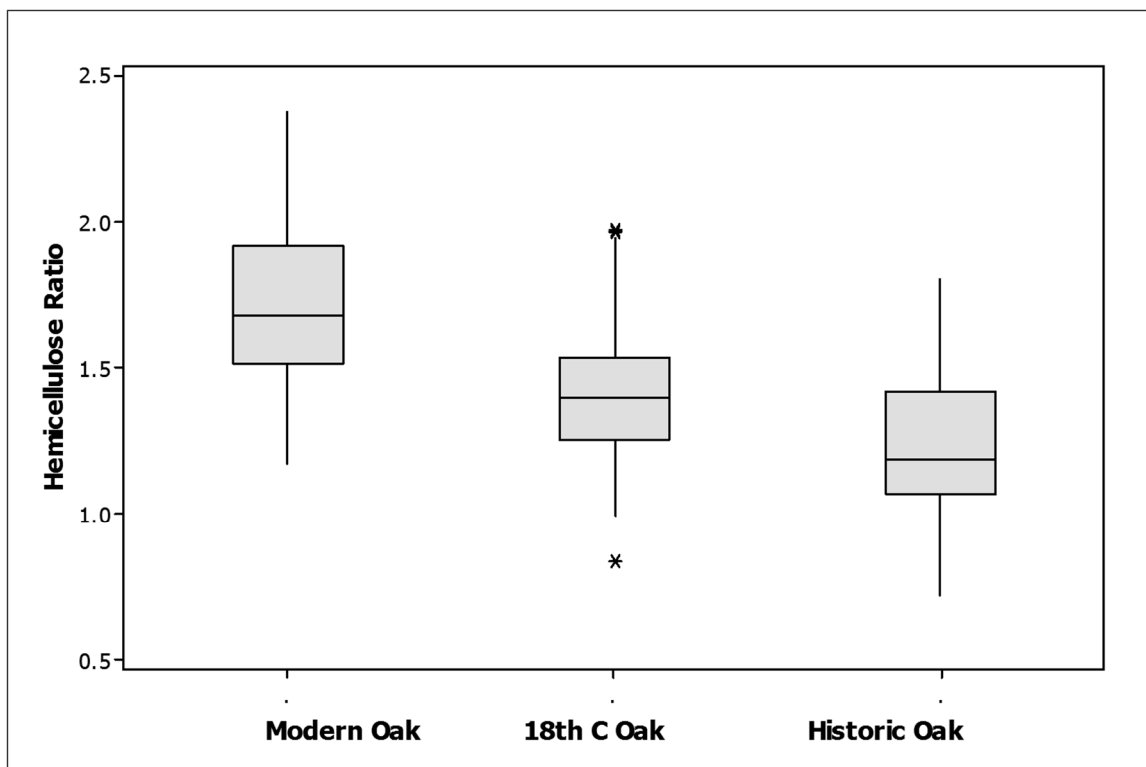
Figure 3.7: The difference in relative acetyl content as determined by the hemicellulosic acetyl ratio, in the different sample ages of oak.

	Modern Oak	18[Th] C Oak	Historic Oak
Hemicellulose acetyl Ratio	1.707 a	1.421 b	1.240 c

Table 3.4: Mean hemicellulosic acetyl ratio of oak samples of different ages.
Means followed by the same letter are not significantly different, Fisher LSD (P>0.05).

Figure 3.7 shows the relative hemicellulosic acetyl content based on the 1724 cm^{-1} absorbance peak. This is the region of the C=O stretching vibration from acetyl groups. The box plot and the one way analysis of variance (table 3.4) show that there was a clear loss of acetyl groups with aging of the wood, giving a highly significant P Value

<0.001. The Fisher test showed that all the different age groups are significantly different from each other (Fisher LSD P<0.05). For oak this seems to mean that it gives off acetic acid progressively as it grows older. Any increase in acetic acid being given off with age is a concern for conservation as any metal wall mount or display near beams may be affected. Acetic acid accelerates the corrosion of metals, especially iron.
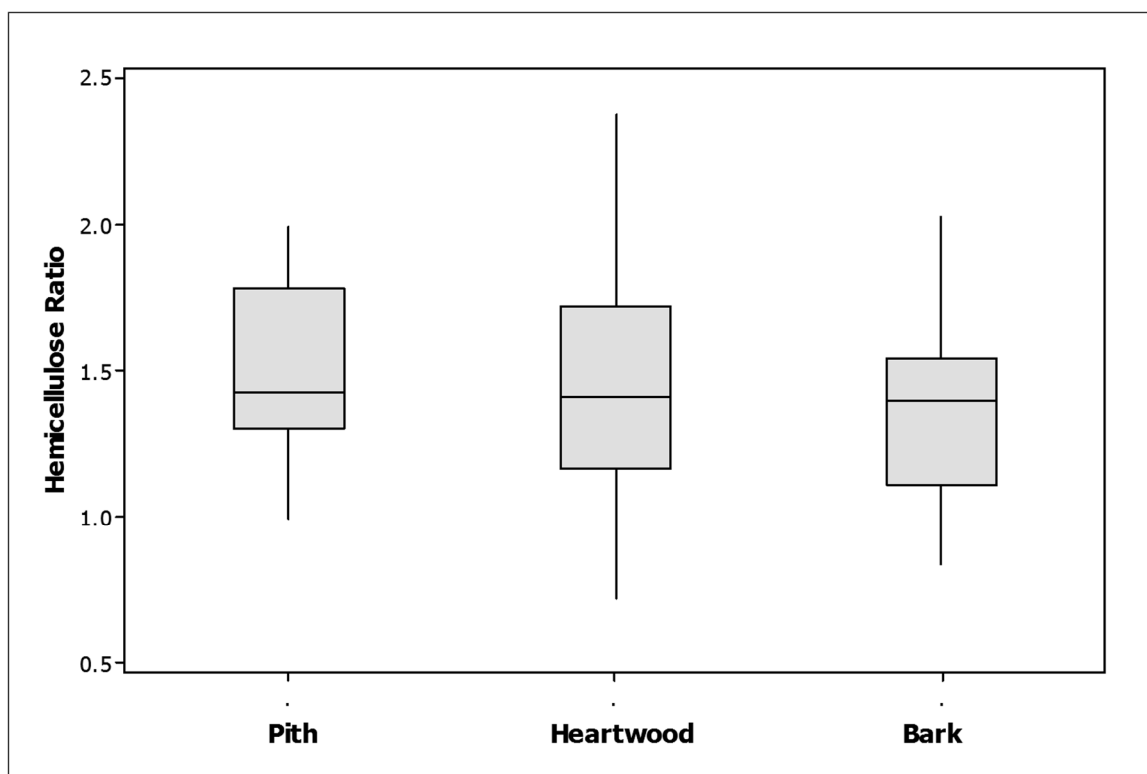
Figure 3.8: The relative acetyl content as determined by the hemicellulosic acetyl ratio, throughout the cross section of the historic oak beams.

	Pith	Heartwood	Bark
Hemicellulose Ratio	1.455	1.449	1.401

Table 3.5: Mean hemicellulosic acetyl ratio through the cross section of historic oak beams.

There were no significant differences between the means (ANOVA P>0.05).

From figure 3.8 it appears that there was a slight decrease in acetyl groups from the pith to the bark but the one way analysis of variance showed this to be non significant (table 3.5) due the scatter within the samples.

3.4.3 Pine Lignin
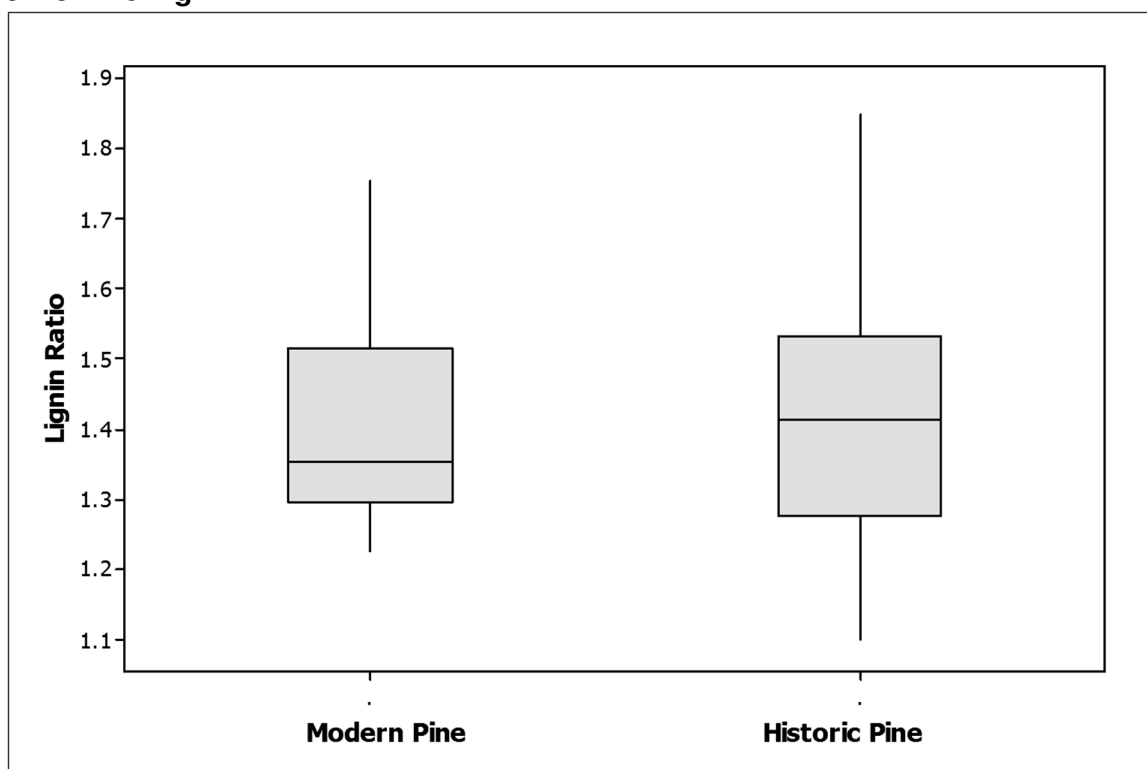
Figure 3.9: Relative lignin content as determined by the lignin ratio, in the different sample ages of Scots Pine.

	Modern Pine	Historic Pine
Lignin Ratio	1.408	1.416

Table 3.6: Mean lignin ratio through the cross section of historic pine beams.

There were no significant differences between the means (ANOVA P>0.05).

From figure 3.9 it can be seen that there was no evident difference in lignin content between the historic pine and the modern pine (table 3.6).
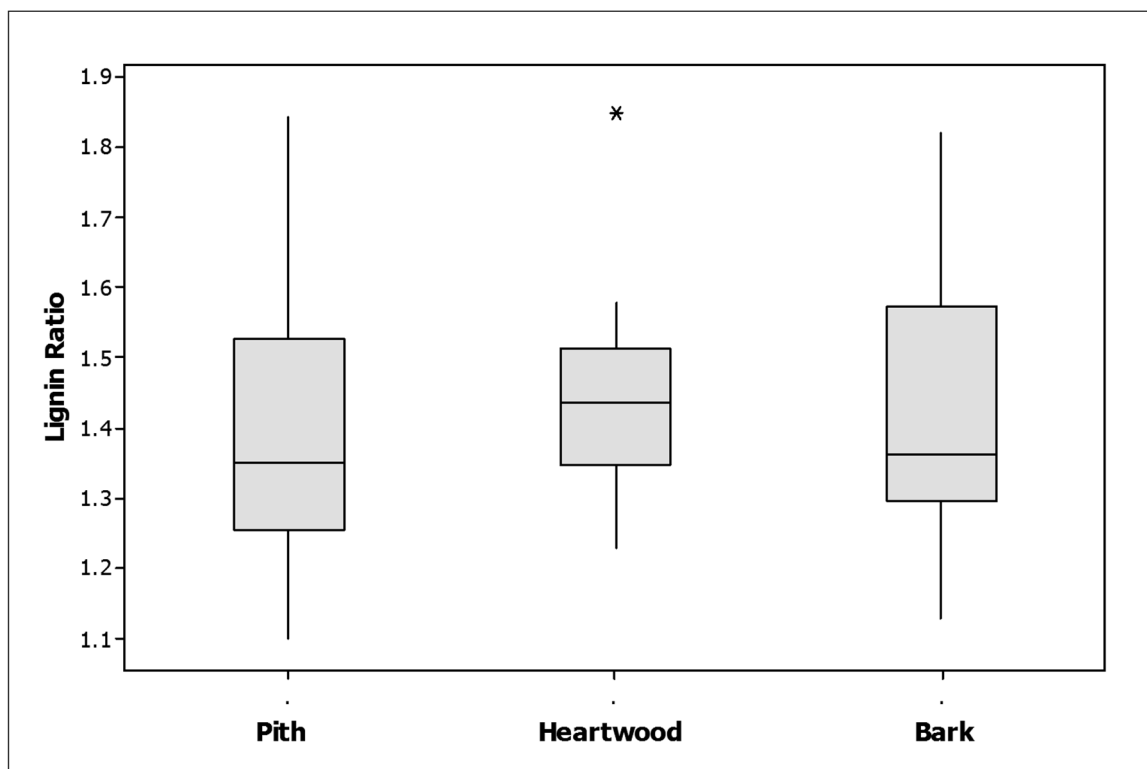
Figure 3.10: The relative lignin content as determined by the lignin ratio, throughout the cross section of the historic Scots pine beams.

	Pith	Heartwood	Bark
Lignin Ratio	1.434	1.426	1.382

Table 3.7: Mean lignin ratio through the cross section of historic pine beams.

There were no significant differences between the means (ANOVA P>0.05).

Here the results (figure 3.10) suggest that the lignin content in pine increased slightly in the heartwood as in the oak samples, but one way analysis of variance confirmed that this effect was not statistically significant and was just due to scatter in the data (table 3.7).

3.4.4 Pine Hemicellulosic Acetate
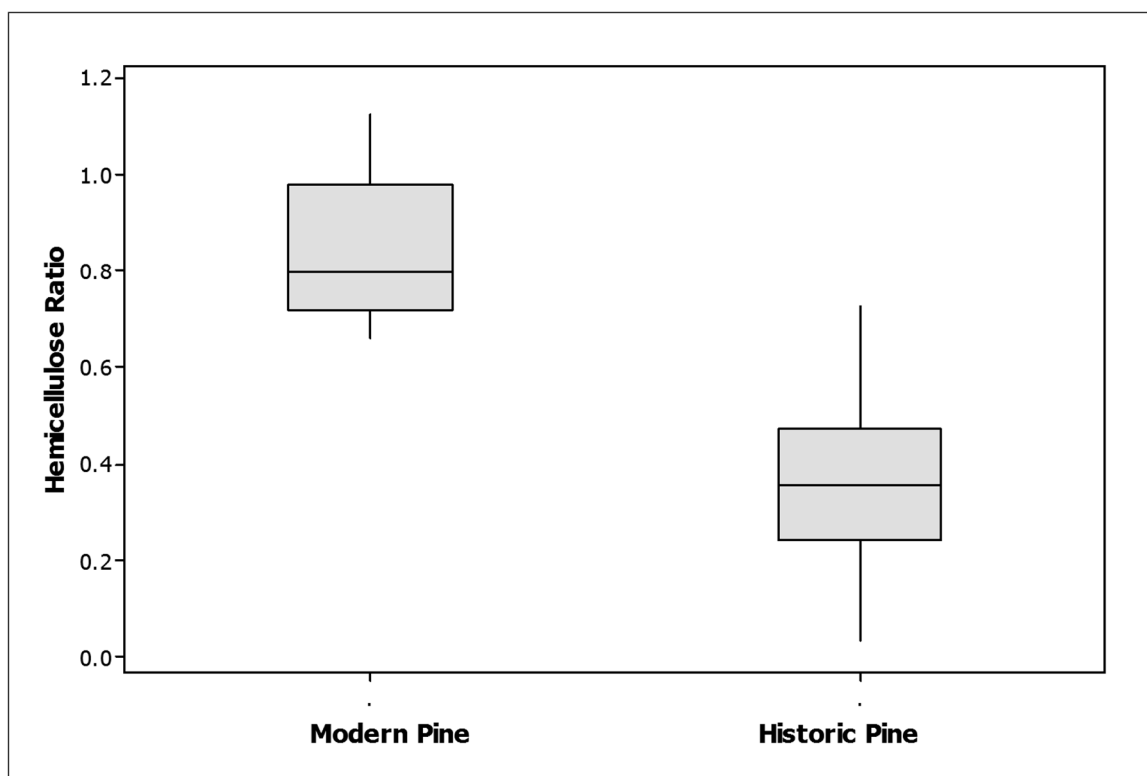
Figure 3.11: The difference in relative hemicellulosic acetyl content as determined by the acetyl ratio, in the different sample ages of Scots pine.

	Modern pine	Historic Pine
Hemicellulosic acetyl Ratio	0.84 a	0.36 b

Table 3.8: Mean hemicellulosic acetyl ratio of pine samples of different ages.

Means followed by the same letter are not significantly different, Fisher LSD (P>0.05).

For Scots pine as for oak it can be seen that acetyl groups have been lost from the wood (figure 3.11), whether these were removed from the hemicellulose polymers or whether the hemicelluloses themselves were being lost.
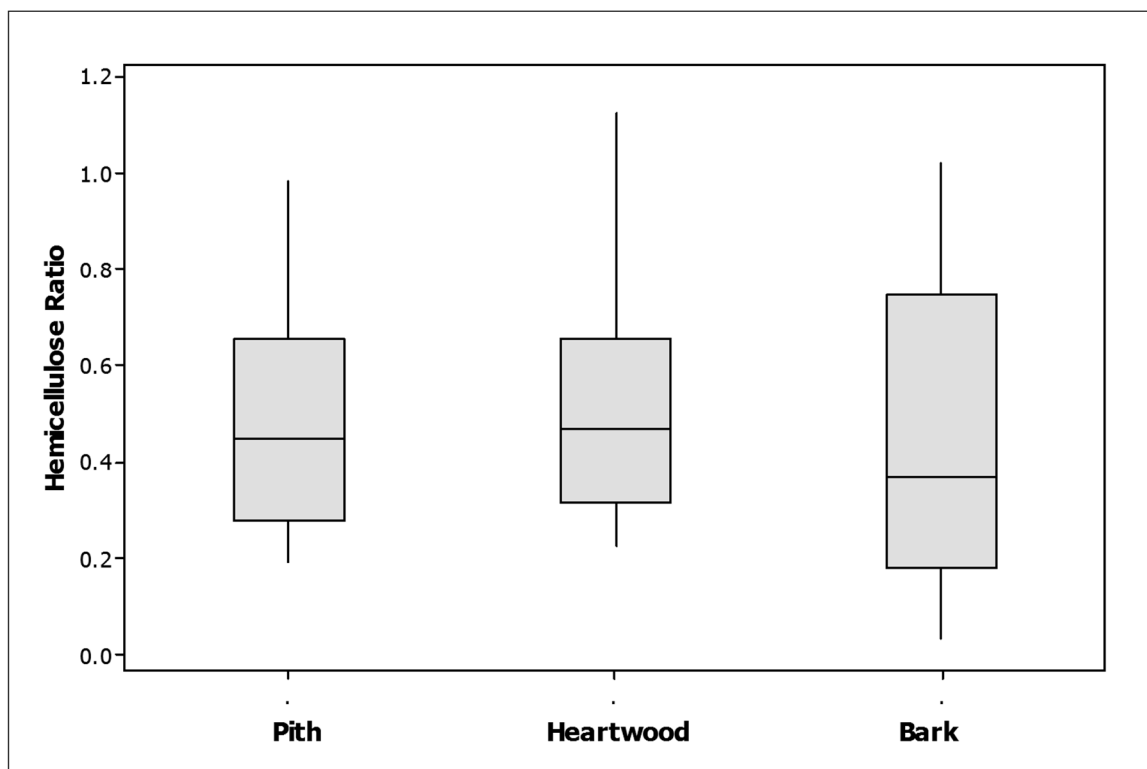
Figure 3.12: The relative hemicellulosic acetyl content as determined by the acetyl ratio, throughout the cross section of the historic Scots pine beams.

	Pith	Heartwood	Bark
Hemicellulose acetyl Ratio	1.455	1.449	1.401

Table 3.9: Mean hemicellulose acetyl ratio through the cross section of historic pine beams.

There were no significant differences between the means (ANOVA P>0.05).

Here the one way analysis of variance showed that the differences due to position were not statistically significant (table 3.9). The loss of acetyl groups was observed all through the wood from the pith to bark (figure 3.12) and is therefore likely to be due directly to aging rather than just to biological attack, which would have been seen more prominently at the bark.

3.5 Discussion

From the results it can be clearly seen that there was a loss of hemicellulosic acetyl groups from the wood cell walls with age, apparently not associated with biological decay. There was no additional loss of peak intensity from hemicellulosic acetyl groups

in either pine or oak at the sapwood end of the samples. They both showed a uniform loss of acetyl throughout, from pith to bark, within the limits of statistical significance. This observation suggests that the loss of acetyl groups was to do with chemical degradation with age. From the spectra alone it is unclear whether this is a loss of acetyl groups from the hemicelluloses or the breakdown of the hemicellulose polymers themselves. In Chapter 4 it is shown that there was an increase in soluble sugars within the historic wood, evidence that the hemicellulose polymer themselves might be breaking down and not just losing the acetyl groups. Loss of acetyl has not been documented before, to the author's knowledge. Previous experiments using FTIR on the chemical composition of older Pine carried out by Esteban et al (2006) have shown little to no chemical change in pine aged 205 years. Esteban et al (2006) used sawdust obtained from historic pine, which pressed in to potassium bromide disks. The FTIR experiments where done to specifically look at the –OH bands of the spectrum. The results showed that the FTIR spectrums were similar for the old and new wood tested (Esteban et al., 2006). The fact this experiment found little to no change in FTIR spectra between old and new wood may be due to the narrower focus on the regions associated with water sorption. But in another paper from Esteban et al (2005) the acetyl peak has been found to disappear completely from the spectra in some cases with buried and waterlogged wood (Esteban et al., 2005).

Some observations have been reported of the hemicellulosic acetyl 1740 cm^{-1} peak when looking at fungal degradation. In these experiments, no real change in this peak could be seen throughout the destruction of the wood by fungal decay (Faix et al., 1991). This implies that the reduced intensity of this peak, observed in this experiment, is more likely due to chemical aging of the wood and not to fungal attack alone. It is still possible that there may have been other fungi, not present in the experiment of Faix et al., (1991), which might take out acetyl groups.

The chemical loss of the acetyl groups randomly from the monosaccharide units would disturb the alternating acetylation pattern that Busse-Wicher et al (2014) have shown to be necessary for ordered binding of hardwood glucuronoxylan to cellulose. The loss of acetylation would be expected to lead to changes in moisture absorption and mechanical properties which might differ between hardwoods and softwoods (Busse-Wicher et al., 2014; Altaner and Jarvis, 2008; Popescu et al., 2006; Erhardt et al., 1996; Chang and Chang, 2002).

In the oak wood there was a slight increase in lignin in the historic wood. This was shown to occur throughout the sample from pith to bark with no significant increase at the sapwood edge. If the increase had been only at the sapwood it would be a sign of biological decay, which would have removed the cellulose leaving the lignin behind

(Fackler and Schwanninger 2012; Yilgor et al., 2013; Faix et al., 1991). The increase in lignin throughout the oak samples, turned out to be due to the way in which the comparison was run against the FTIR intensity in the fingerprint region which contains both cellulose and hemicellulose. When the comparison ratio was re-calculated using the cellulose peak at 1425 cm^{-1} it showed that lignin did not increase with age. Overall, FTIR microscopy is a fantastic tool for conservation. Here it has allowed us to look at sample composition under a microscope, pin-pointing spectral changes across the tree's growth from pith to bark to determine if there were changes in chemical structure and if these could be attributed to age or to fungi. Here it has given us clear evidence that what was occurring was chemical change through age, resulting from this ability to pin-point each growth region and show that the changes were not confined to the sapwood region where biological decay was visible (figure 3.13).

Figure 3.13: Decayed sapwood in historic Scots pine Image: K Hudson-McAulay.

Chapter 4

Water sorption / Relative Humidity (RH) testing

4.1 Introduction

Relative humidity (RH) is of great concern in conservation, making this a key point within the thesis aims in Section 1.13. Every historic object has a set RH range in which it has to be kept for its survival. Traditionally this is a lot lower for metal than for biological objects like wood. Problems can occur in many different ways but the worst is wood picking up enough moisture for fungi and pests to live in and destroy the wood (Gerhards, 1980; Popescu and Hill, 2013; Glass and Zelinka, 2010). There are regulations concerning building materials which specify moisture buffer values for RH, indicating the amount of water vapour that can be transported in or out of the material under varying conditions (Abadie and Mendonce, 2009).

Relative humidity can be very difficult to control in buildings other than museums, as the outside RH can vary from 90 % down to 30% depending on the season and region (Popescu and Hill, 2013). Although we dry wood to a specific moisture content before it is used in construction, it is a hygroscopic material and will always react to the amount of moisture in the air. The moisture content and the effects of relative humidity are extremely important factors in all of wood science as they affect almost everything about wood's behaviour. The most important question in this research is whether new wood would take up more or less moisture than historic wood at the same RH, as differential swelling could cause damage to any splice joint used in the repair of buildings, especially if resins are used in the repairs. Unfortunately there have been very few studies on moisture sorption by historic wood (Esteban et al., 2009).

Bio-deterioration of wood will occur whenever it is exposed to an environment which will encourage the growth of microbes. These are essential for the recycling of wood in a forest but in a building, microbial growth can cause serious weakness and damage to wooden structural elements (Blanchette, 1995). It is often asked how fungal enzymes are able to penetrate the thick dense cell wall to begin the decay process in structural timbers, as in dry wood there are hardly any micro-pores to allow fungal enzymes entry, but it is believed that the swelling caused by water uptake at high RH allows these pores to open and provides the right conditions for the fungus to get a foot-hold and begin decaying the wood (Chirkova et al., 2006). As well as being of concern for fungal growth the moisture content of wood is an important parameter influencing almost all

mechanical properties. It is widely known that the strength properties of wood increase with decreasing moisture content (Hiziroglu, 2009).

When working with wood and wood structures it is generally forgotten that wood comes from trees, and trees did not produce this material to provide humans with a good building material. Wood in its natural state, working for the tree, is a wet material. It grows in a wet state and its main function is the transport of water around the tree. The only reason it is dried out is for human purposes as a building material. We do this because, once wood is dried out, its durability and mechanical properties greatly improve for building and other purposes (Patera et al., 2013; Gerhards, 1980). Freshly cut, non-dried wood is still used in this state and is known as green wood. This is where wood is above the fibre saturation point, at which the mechanical properties cease to be affected by change in moisture (Green, 2001, Engelund et al., 2013, Gerhards, 1980). Green wood contains both free water in the cell lumina, drawn there by capillary action, and bound water which is in direct contact with the polymers of the wood cell wall (Engelund et al., 2013, Williams et al., 2010, p.63).

Fibre saturation point is commonly acknowledged as the point at which there is no free water left in the cell lumen, only water bound to the cell wall polymers (Kolin and Janezic, 1996). It is the cellulose and hemicellulose polymers that are believed to bind most of the water in the cell wall (Zabler et al., 2010; Feilke et al., 2011). Changing RH below the fibre saturation point causes shrinkage of the wood, but when the RH increases, wood keeps taking in moisture and swells until it reaches its fibre saturation point.

As mentioned before there has been little research on historic wood but there has been much done on waterlogged wood. Most archaeological wood has survived through being waterlogged, preventing large scale biological breakdown (Lionetto et al., 2013; Čufar et al., 2014; Klaassen, 2014). Waterlogged wood has the potential of reaching a moisture content of up to 200%. Most of the water is no longer bonded to the polymer fibres in the cell wall but is stored in the cell lumen. Diffusion of oxygen is slow in water so when the cell lumen contains no air and is completely filled with water, fungi cannot grow in the waterlogged wood (Kennedy and Pennington, 2014; Williams et al., 2010, p.27; Babiński et al., 2014; Tamburini et al., 2014). This area of wood conservation has been researched a great deal with large waterlogged ships, like the Tudor warship Mary Rose and the Swedish warship Wasa being brought up from the sea bed (Preston et al., 2014; Giorgi et al., 2005).

When wood is exposed to a normal environment, as in a building, or in a ship which has remained above water, like the HMS Victory (McGowan, 1999, p.1), the moisture

changes in response to the RH, leading to the cell wall matrix swelling and shrinking (Zabler et al., 2010).

Knowing the hygroscopic properties of wood is extremely important in the conservation of historic structures; as timber from different environments will have different responses to any new environment. For example, waterlogged, archaeological and historic wood all react differently to moisture sorption and go through different decay systems (Esteban et al., 2010; Kennedy and Pennington, 2014; Blanchette, 2000; Singh, 2012).

 The sorption properties of timber are controlled by its chemical components and depend greatly on hydrogen bonds from water to cellulose and hemicelluloses. Therefore potentially, the degradation of these polymers over time will influence the sorption properties of wood (Kozlov and Kitsernaya, 2013).

In wood polysaccharides there are two potential sites for the absorption of water, at the hydroxyl groups and at the carboxyl groups of glucuronoxylans (Olsson and Salmen, 2004; Mihranyan et al., 2004).The hydroxyl groups, on hemicelluloses and cellulose, are the most abundant. Hemicelluloses comprise around 30% of the cell wall mass depending on the species (Bikova and Treimanis, 2001; Hosseinaei et al., 2012).Hemicelluloses are thought of as more closely linked to moisture uptake due to their ability to interact with water molecules and become more mobile, even below room temperature, whereas lignin and cellulose stay a lot stiffer (Karenlampi et al., 2003). The extraction of hemicellulose from wood has been shown to reduce the amount of water sorption (Ozdemir et al., 2014; Hosseinaei et al., 2012).

Not all of the hydroxyl groups are accessible to water, due to the way the polymers are arranged in the cell wall. Cellulose forms crystalline regions where the chains are held together by hydrogen bonding between –OH groups, and are too tightly packed to allow water to penetrate between them (Esteban et al., 2006; Engelund et al., 2013; Khali and Rawat, 2000; Esteban et al., 2010). Cellulose microfibril surfaces and hemicelluloses are believed to be the key areas for hydrogen bonding to water (Fernandes et al., 2011). Cellulose microfibrils form aggregated bundles that differ between softwoods and hardwoods (Thomas et al., 2014).

In softwoods these aggregates are around 10-20 ηm across. Inside dry aggregates the microfibrils are held together by disordered hydrogen bonding between the hydroxyl groups on the outside of the microfibrils. Water can penetrate between some of the microfibrils, forming hydrogen bonds to their surface hydroxyl groups, but not all of their surfaces are accessible to moisture (Fernandes et al., 2011). These aggregates and their expansion when water penetrates can be seen using small-angle neutron scattering (SANS) (Fernandes et al., 2011). This sideways expansion does not occur over the full

length of the microfibril aggregate, because if it did, more volume change would be seen on hydration (Fernandes et al., 2011). Other experiments on the sorption of water by softwood polysaccharides have been carried out through the use of FTIR spectroscopy to detect the contribution of water molecules to the spectrum. Results from these experiments show that there is no single location at which water is taken up by the wood cell polymers (Olsson and Salmen, 2004).

Hardwoods also have aggregates of cellulose microfibrils but as mentioned above their structure is not quite the same, and the level of aggregation in hardwoods is not as well documented as softwoods. The aggregation that has been seen in hardwoods has tighter microfibril contact than in softwoods. This results in less access for moisture (Thomas et al., 2014).

Where, inside or on the outside of these aggregates the hemicellulose polymers are positioned, also differs between hardwoods and softwoods in addition to the different types of hemicellulose present, with consequences for their reaction to moisture (Altaner et al., 2014; Akerholm and Salmen, 2004). Within softwoods the hemicellulose polymers are outside the microfibril aggregates (Fernandes et al., 2011). The glucomannan is more closely associated with cellulose and the glucuronoxylan with lignin (Altaner et al., 2010; Akerholm and Salmen, 2004). The wider spacing of the aggregated hardwood microfibrils could mean that they are separated by glucuronoxylan chains (Thomas et al., 2014) or by very tightly bound water molecules resistant to drying (Langan et al., 2014). This causes a difference in swelling between softwoods and hardwoods. Lateral swelling in hardwoods occurs only by the penetration of water between these microfibril aggregates, but in softwoods water can penetrate between the aggregates but also into the aggregates as well. In both hardwoods and softwoods water does not occupy pre-existing pores in the wood but physically bonds to accessible sites, becoming hydrogen bonded to the polymer chains and forcing them apart. Again this shows that a difference in reaction to moisture between hardwoods and softwoods can be expected, and differences in mechanical properties (Thomas et al., 2014; Altaner et al., 2014a; Akerholm and Salmen, 2004).

It has been suggested that the sorption properties of wood are possibly affected in timber of some species by re-bundling of the aggregates or even the rearrangement of the molecules with age, allowing more or less of the –OH groups to become available (Esteban et al., 2006; Esteban et al., 2009).

Relative humidity and the water content of wood have a huge impact on its survival. Allowing wood to reach or exceed its saturation water content encourages the rotting process. Below 18% moisture content fungi and pests are normally dormant (Ashour et al., 2011). As with most problems concerning wood the equilibrium moisture content in

wood at a given relative humidity will depend on the species. It is even possible for its past environment to have some small effects on how it will behave with varying RH (Fielke et al., 2011).

In some cases timber members have undergone chemical treatment at some point in their lifetime, usually to prevent pest infestation. The treatments often contain salts, which alter the sorption properties of the wood (Kozlov and Kitsernaya, 2013). The finishes and coatings conventionally used on wood do not change its sorption capacity but they do affect the rate at which moisture is absorbed and desorbed by the wood (Williams, 2010, p16-6; Gereke et al., 2011). Other finishes tend to protect the direct surface of the wood and can have a more decorative effect as well, such as varnishes, polishes and stains. Good examples of these for wood are; beeswax, one of the oldest known finishes, found on wood discovered in Egyptian tombs (Unger et al., 2001, p.186; Horie, 1987, p.150), and shellac, also known as button polish or French polish, a natural resin traditionally used from the 19th century to seal and polish wooden furniture leaving an attractive finish (Desch and Dinwoodie, 1996, p.287; Unger et al., 2001, p.399; Horie, 1987, p.150). Research into finishes is outside the remit of this project as the wood samples available for testing have not undergone any finishing procedures allowing for this type of testing.

There is a common misconception that once wood has been seasoned from the green state its response to high moisture becomes fixed, but the RH environment will continue to have a great influence on its survival and on the rate at which it can degrade. Wood is a hygroscopic, porous material that absorbs and desorbs moisture depending on its availability in the surrounding atmosphere (Patera et al., 2013; Buck, 1952; Popescu and Hill, 2013). It is constantly struggling to reach equilibrium moisture content with its environment. Equilibrium in reality is probably never reached, as this would take a very long time and conditions are always changing (Engelund et al., 2013; Esteban et al., 2005; Chauhan et al., 2001; Buck, 1952). It has also been suggested that the sorption history of the wood may influence its ability to reach equilibrium (Popescu and Hill, 2013).

When wood is in service it is subject to constant change in environment, causing the wood to swell and shrink. The constant changes in RH cause wood to repeat these swelling and shrinkage cycles. As a result this constant movement can cause damage to wooden objects or structures, or permanent distortion such as sagging of timber structures under their own weight. That is why museums have strict rules on keeping the RH of an area as constant as possible to limit damage (Patera et al., 2013).

There have been very few studies on the hygroscopic nature of historic wood (Esteban et al., 2005; Esteban et al., 2009; Popescu and Hill, 2013; Kozlov and Kitsernaya., 2013;

Buck, 1952) but this is a key feature that needs to be uncovered. If timber components with different sorption properties are fixed together it could have disastrous effects on the wood dimensional stability (Esteban et al., 2005; Esteban et al., 2009). There are a few different ways in which dimensional changes could cause problems after traditional 'like for like' repair. Problems could be caused by the different amounts of water absorbed by the two separate pieces, or by them swelling to different extents or in different directions at the same moisture content. Differential swelling is likely to occur with difference in MFA, which is highly possible as modern softwoods tend to have a higher MFA than historic wood due to the way in which they were grown (See Chapter 6 for more detail on MFA). Trying to understand sorption behaviour will also be the key to understanding the degradation of wood (Popescu and Hill 2013). In conservation of any historic wood it needs to be clear how the wood will react to the surrounding environment (Buck, 1952).

This chapter discusses how sorption of water by oak and Scots pine changes as the wood ages.

4.2 Experiment

The samples were produced from both new and historic timber. 5mm cubes were cut along a line from pith to bark cut using a single edged razor blade, so that as little material as possible was lost between each pair of samples, giving a accurate pith to bark profile of each timber.

The RH Chamber was set up as shown in figure 4.1. Boiling water was placed in the bottom of the container and the samples were then placed on a perforated shelf above the water. The RH sensor was placed inside and the lid was sealed (figure 4.2). The RH sensor recorded the RH in the container every hour. The results from the sensor showed that the RH remained stable around 95-98% RH throughout the 24 hour testing time. The samples were weighed before they went into the chamber, then again after 24 hours in the chamber to obtain the amount of water absorbed by the sample blocks.
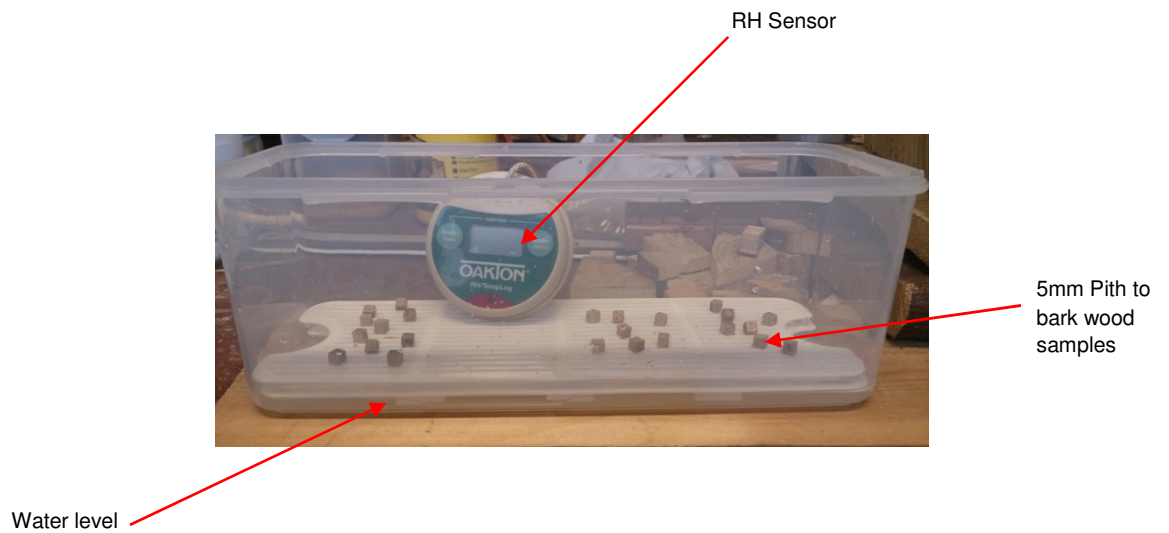
Figure 4.1: The environmental chamber set up with samples Image: K Hudson-McAulay.

Figure 4.2: Overhead view of the samples in the environmental chamber. Image: K Hudson-McAulay.

4.3 Results

4.3.1 Oak
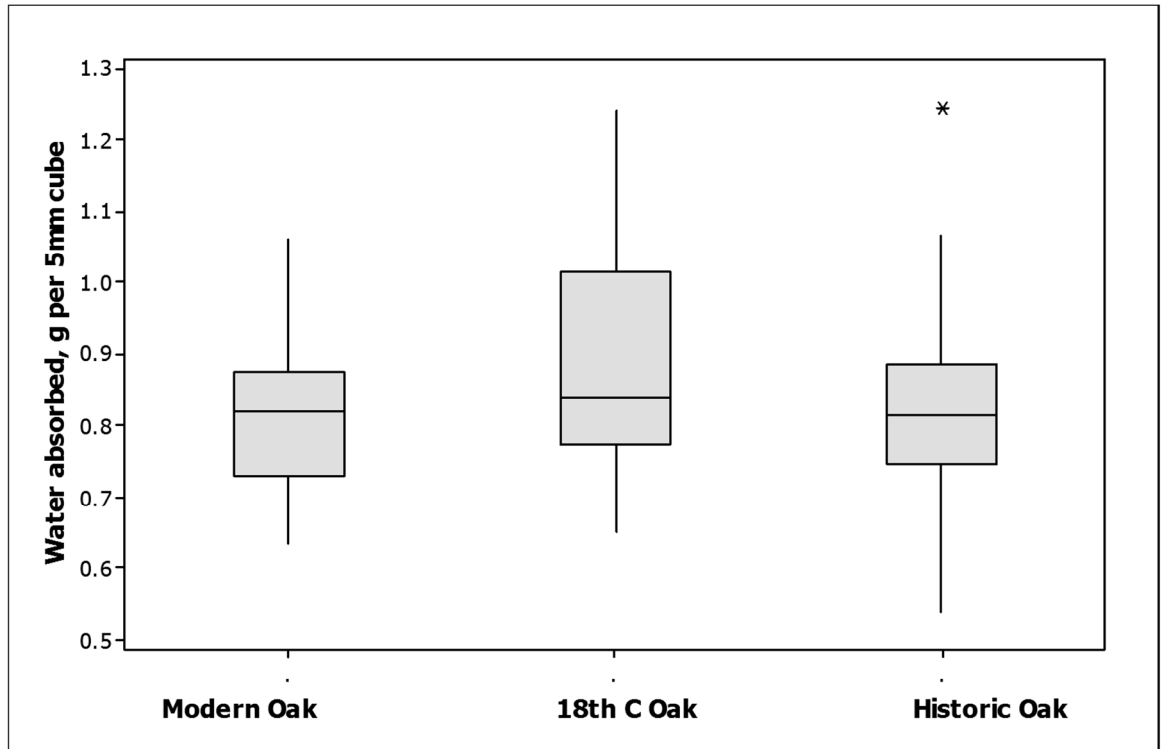
Figure 4.3: Moisture sorption by modern, 1800's and Historic Oak. One-way ANOVA gave a P Value of <0.001 showing that moisture sorption by wood of different ages was significantly different.
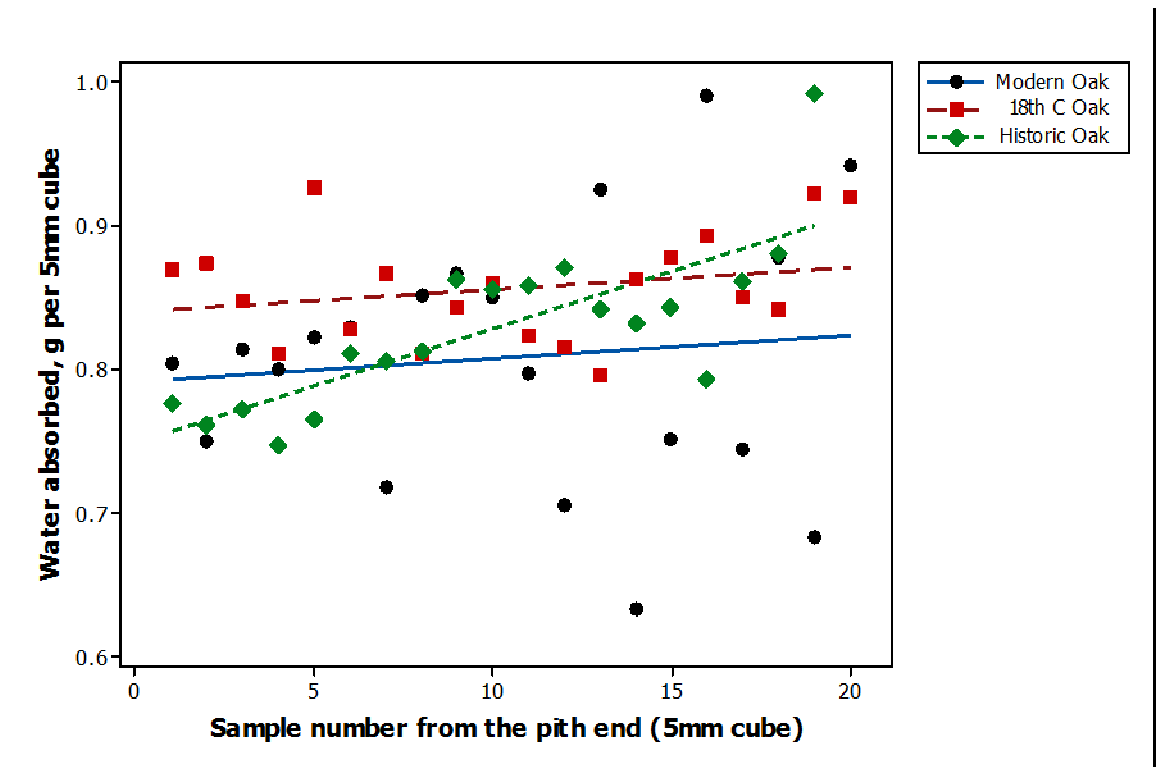
Figure 4.4: Variation in moisture sorption in oak from pith to bark for the different age categories.

	Modern Oak	18[Th] C Oak	Historic Oak
Moisture sorption (%)	80.9% b	88.7% a	82.4% b

Table 4.1: Mean moisture sorption (% of dry mass) of oak samples of different ages.

Means followed by the same letter are not significantly different, Fisher LSD (P>0.05).

4.3.2 Pine

Figure 4.5: Moisture sorption by modern and Historic Pine. A *t*-test for the difference between ages gave a P Value of <0.001.

	Modern Pine	Historic Pine
Moister sorption (%)	80.9% a	88.7% b

Table 4.2: Mean moisture sorption (% of dry mass) of pine samples of different ages.

Means followed by the same letter are not significantly different, Fisher LSD (P>0.05).
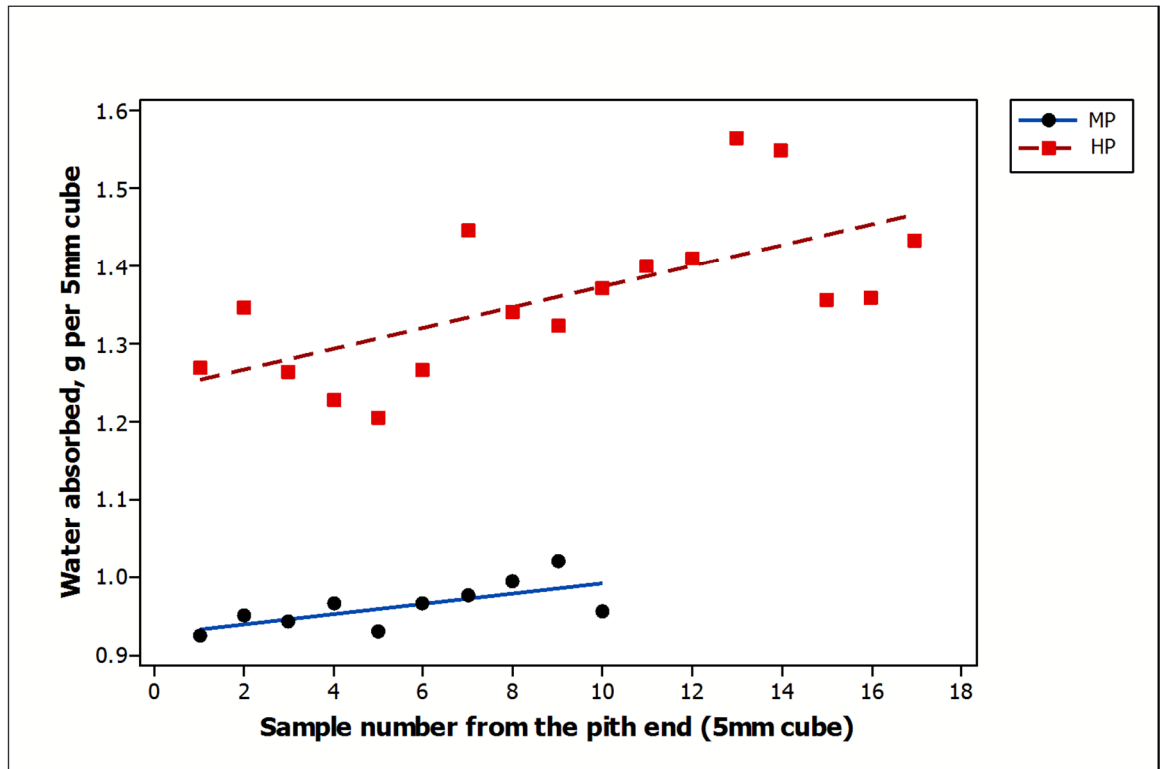
Figure 4.6: Variation in moisture sorption in Pine from pith to bark with the different age categories.

Firstly the moisture contents of the pine samples were subjected to a *t*-test which gave a P Value of <0.001, showing that the difference between the modern and historic samples was statistically highly significant (table 4.2). The pine samples were not only different with age (figure 4.5) but the historic pine samples showed a much larger sorption of water than was seen in any of the oak samples (figure 4.6). As there was more than one comparison to make with the oak samples these were run through a one way analysis of variance to see if the difference between the ages (figure 4.3) would be statistically significant. The ANOVA had a highly significant P value of <0.001. To see which oak samples differed significantly a Fisher Least Significant Difference test at 95% confidence was then calculated (table 4.1). This showed that modern and historic oak were significantly different from the 18th C oak (Fisher LSD P<0.05), but not different from one another.

From the data it can be clearly seen that Scots pine had a very different reaction to sorption with age compared with the oak. The historic pine wood picked up over double the amount of moisture compared with the modern pine, whereas differences in historic oak are small. Tests have been published on the sorption of water by oak showing that historic oak picks up less moisture than recently felled oaks (Esteban et al., 2010).

The pith to bark variation showed that the pine wood was picking up excess water throughout, whereas oak seems to pick up more moisture towards the sapwood (figure

4.4). This is most likely due to biological damage to the cells. Usually pine will have more mass of wood per 5 mm cube close to the bark as it increases in density. This would also increase its potential intake of moisture as there would be more available hydroxyl groups. But within the historic sample the polymer mass per 5 mm cube may have been reduced at the sap edge due to loss of material from biological attack.The uniformly high moisture uptake from pith to bark tends to imply chemical aging rather than effects of biological attack.

The results show a great difference between the two species suggesting that the chemical breakdown is different. This could be a difference between hardwoods and softwoods or just between these two particular species.

Results from the chemical analysis of the two species in Chapter 3 show the loss of the acetyl groups from the hemicellulose polymer, which could be causing this difference between oak and pine. Another possibility is that over time cellulose or hemicellulose molecules may be degrading to water soluble products such as sugars and organic acids (Kozlov and Kitsernaya, 2013). The experiment below was done to determine if there was more soluble sugar found in the historic pine than in its modern counterpart.

4.4 Chemical analysis of soluble sugars

As discussed in the previous section of this chapter, historic pine wood absorbed 30-50% more moisture than the modern pine samples. This is unique to the historic Scots pine as within the historic oak there was no consistent change with age. It was thought that this difference in water sorption by historic pine might be the result of an excess of soluble sugars in the wood cell as a result of the breakdown of the hemicellulose polymers (figure 4.7), (Kisternaya and Kozlov, 2007).

In this section we aim to find out if soluble sugars are partly the cause of this strange phenomenon. The method for determining the amount of soluble sugars present in the historic wood samples was the dinitrosalicylate (DNS) reducing sugar method developed by Miller (1959).

The DNS method has been used in carbohydrate science to detect soluble sugars ever since it was re-developed by Miller and has been used with good success to determine sugars such as xylose, glucose and mannose (Bailey et al., 1992; Khan, 1986; Beck and Strickland, 1984). These are the sugars that make up the main body of the hemicellulose polymers in softwoods.
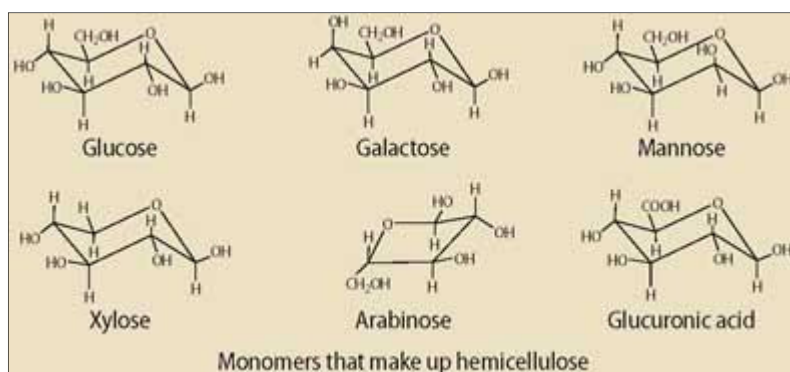
Figure 4.7: The different sugars that make up wood polysaccharides (Gross, 2010).

The Miller DNS method has been shown to be sensitive to these monosaccharides and is often used to measure the activity of enzymes that break down lignocelluloses (Breuil and Saddler, 1985). This is of great interest when looking into the effects of biological attack by fungi such as brown and white rots, and in the biofuel industries where the wish is to separate and depolymerise the wood polymers (Ferraz et al., 2003).

4.4.1 Sample preparation:

Samples were prepared from both historic and modern pine. Unfortunately due to the high level of tannins in the oak samples it was not possible to test these. Tannins affect colour formation in the Miller reaction leading to artificially high absorbance readings. The samples were soaked overnight in water to dissolve the soluble sugars out of the samples. The pine samples, both modern and historic were cut from pith to bark into 5mm cubes to give a higher surface area allowing the water to dissolve out as much of the soluble sugar present as possible. Approximately 20 ml of water was added to 10 of the 5 mm cubes from each of the wood beams tested. This water was then collected and used to determine how much if any soluble sugar was present.

4.4.2 Determination of reducing sugars by the Miller method

The main reagent of the experiment is made up freshly from two components, the main DNS solution and a second sodium sulfite solution. These are mixed together to produce the full reagent in small quantities when it is needed as the combined solution cannot be kept overnight (Lee et al., 2008; Yu et al., 1982; Kong et al., 1992).

The two components were made up as follows:

DNS reagent – main component:

- *3g Sodium Hydroxide*

- *0.6g Phenol*

- *3g Dinitrosalicylic Acid*

Firstly the sodium hydroxide was dissolved in water using a magnetic stirrer to ensure it was thoroughly mixed. After this had completely dissolved, the phenol and dinitrosalicylic acid were added, adding as little water as possible to allow the stirrer to dissolve them. Once the solid reagents had been fully dissolved more water was added to make up a solution volume of 250ml.

DNS reagent – sodium sulfite component:

- *0.15g Sodium Sulfite*

To make up the second component 0.15g sodium sulfite was dissolved in as little water as possible until the solution was clear. Once it had been fully dissolved, water was added to make the solution up to 50ml.

Potassium sodium tartrate reagent:

- *40g Potassium sodium tartrate*

The potassium sodium tartrate solution is a colour stabiliser and is made up in the same way by adding 40g of potassium sodium tartrate to as little water as possible until it was fully dissolved and then adding enough water to the solution to make it up to 100 ml.

4.4.3 Experimental Procedure.

Before any of the historic samples could be tested sugar standards needed to be set up to determine whether the method would work successfully and to produce a calibration graph to quantify any results gathered from the historic material.
The calibration set was made from stock solutions of glucose, mannose and xylose, the three main sugars associated with the hemicellulose polymers in softwoods. The galacto-glucomannan comprises 60% of the hemicellulose fraction whereas the arabino-4-0-methylglucuronoxylan comprises about 40% of the hemicelluloses (Curling et al., 2001). The stock solutions were made up as 1mg per 1 ml solutions of each of the sugars in water.

Once the stock solution had been made up a 0.1mg to 1.0mg calibration series, with a blank of 1.5ml water, (Nagpure et al., 2014) was prepared. The process involves adjusting the levels of stock solution to water in each test tube, slowly increasing the amount of the stock solution. The first tube contained 0.1ml of the stock solution with 1.4 ml of water to make 1.5 ml of solution containing 0.1 mg of the sugar. Each test tube is then filled with 0.1 ml more of the stock solution and 0.1 ml less of water until the last contains 1.0 ml of stock to 0.5 ml of water.

Now the DNS reagent needs to be added to the stock solution. 5 ml of the sodium sulphite component was mixed with 25 ml of the main component, giving 30 ml of the final DNS reagent, enough for around 20 tests. As said before mixing the DNS reagent in these smaller quantities will prevent the mixture going off before it is used.

1.5 ml of the mixed DNS reagent was added to each sugar solution in an 18 mm test tube. This was then mixed thoroughly before the tubes were put in a boiling water bath for 5 minutes. After this the samples were removed from the water bath and cooled using a water bath of cool water. Once the samples were cool 0.5 ml of the potassium sodium tartrate solution was added to each one and mixed in order to keep the colour of the regent stable.

The samples were then transferred to a polystyrene 1 cm cuvette and the absorbance was measured at a wavelength of 575 nm in a Hitachi U-1500 spectrophotometer to record the colour produced, which depends on the amount of sugar present.

The calibration graphs of absorbance against mass of sugar are shown below:

Calibration graphs

The calibration graphs in figure 4.8 follow the same pattern as seen in the original description of the method (Miller, 1959) but some of the absorbances were above 1, which is considered to be too high for accurate measurement by the spectrophotometer. The experiment was re-run with a lower concentration, as it was expected that the historic sample would not have as much soluble sugar and the lower standard concentrations would give a more precise calibration graph.
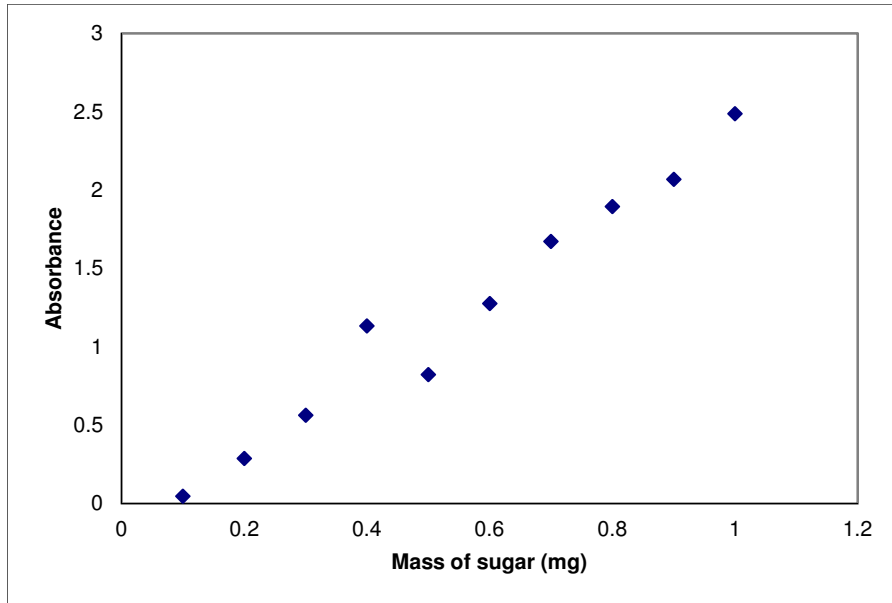
Figure 4.8: Calibration graph for Glucose.

Dilution calibration graph

The experiment was re-run in exactly the same manner as before except that the stock solutions were of mannose and xylose and were diluted x5 in order to give a better calibration graph. The results of this are shown below in figure 4.9 and 4.10.
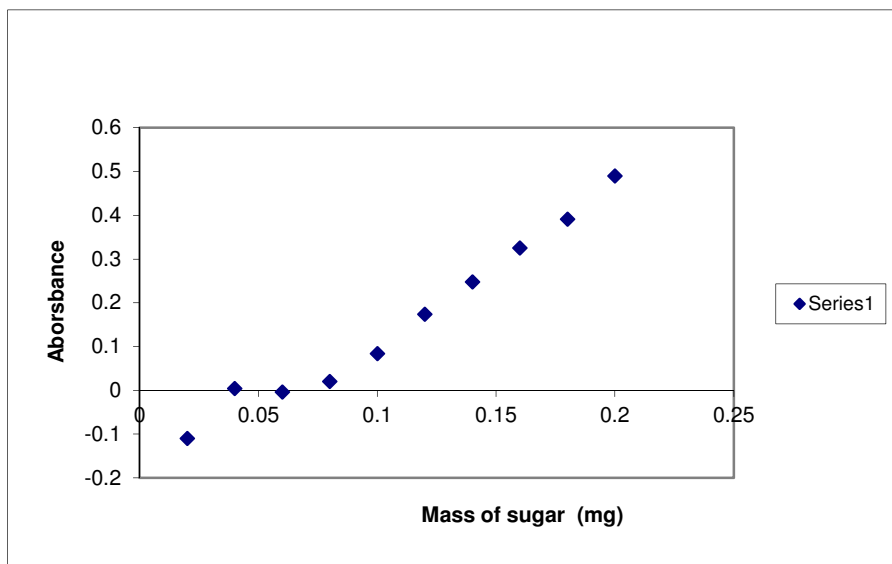
Figure 4.9: Calibration graph for dilute Xylose.
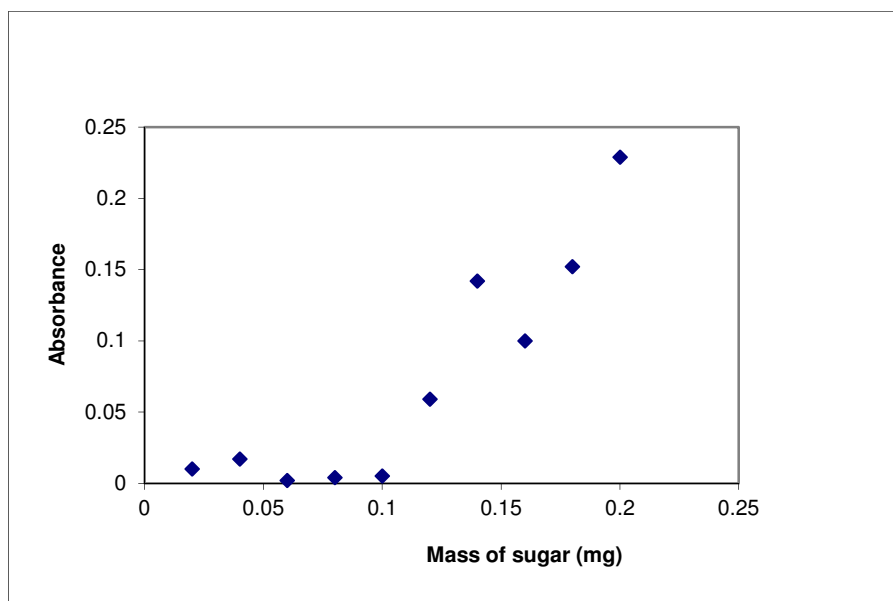
Figure 4.10: Calibration graph for dilute Mannose.

The negative intercept on the calibration graph (figure 4.11) is normal for this method, although generally in colorimetry negative intercepts are uncommon. It is thought to be due to the effect of dissolved oxygen destroying the pigment produced by low levels of sugar; therefore it is important to make sure that at least 0.1 mg of sugar is present in the analysis. If not, the only result that can be deduced is that less than 0.1 mg was present.

As it was not known which of these soluble sugars, or a possible mixture of them, had been extracted from the historic sample, the calibration graph below for glucose was chosen as it fitted well with what was expected from the literature (Miller, 1959) and because glucose is widely used as a standard for this method (Vats and Banerjee, 2002). Other issues could cause error in the interpretation of the breakdown of the hemicellulose polymer within the historic samples. It will be unclear if they have broken down to monosaccharides, as they may remain as disaccharides or oligosaccharides which have only one reducing sugar end. One molecule of each oligosaccharide should give approximately the same colour as one molecule of monosaccharide. As the DNS method measures the total number of monosaccharides and disaccharide molecules released, this is the equivalent to the number of bonds broken within the polymers. Therefore there may be more breakdown of the hemicellulose polymers than is apparent from the DNS results when calibrated with glucose.
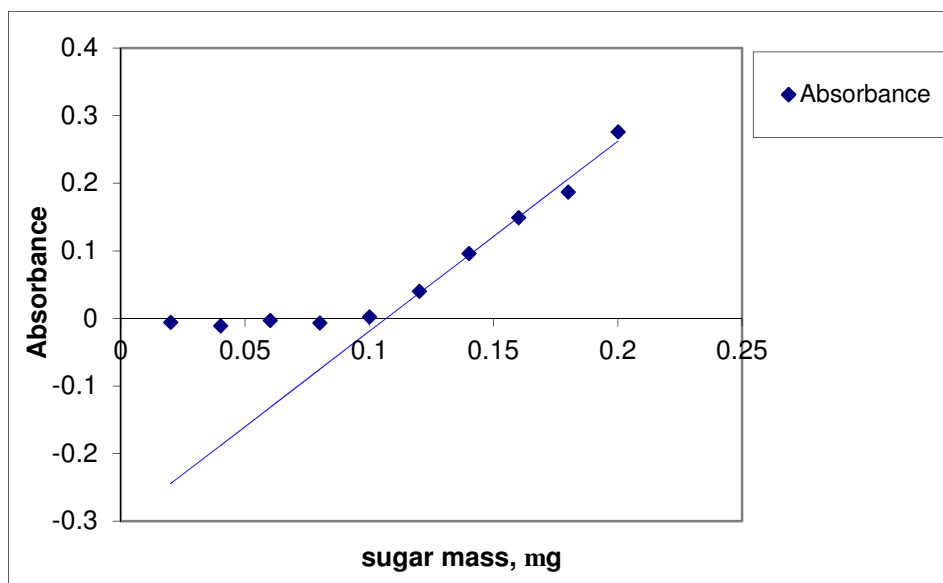
Figure 4.11: Calibration graph for diluted glucose.

4.4.4 Testing of the historic samples

The historic samples were tested by adding 1.5ml of the solution that had been equilibrated with each historic sample to 1.5ml of the DNS reagent. Four 1.5 ml samples were taken from the 20ml solution obtained from each of the historic pine samples and were carried through the DNS analysis. As well as the samples made up with the DNS solution a blank for each historic sample was made up containing 1.5ml of the historic sample and 1.5ml of water, and run through the same treatment to subtract any colour which may be coming from the sample itself in the absence of the colorimetric reagents. The samples were then all put in the hot water bath for 5 min and cooled afterwards in the cold water bath, after which 0.5 ml of the potassium sodium tartrate solution was added to stabilise the colour and the absorbance was measured at the same wavelength of 575nm.

A cell containing water was used to zero the spectrometer before testing the sample blank to see how much colour absorbance was recorded from the sample itself without the colorimetric reagents. A cell containing 1.5 ml water and 1.5 ml DNS reagent was used to zero the rest of the samples to remove the absorbance of the colorimetric reagent itself.

4.5 Results

Firstly the blank absorbance for each sample was subtracted from the absorbance recorded from the sample and DNS reagent, to remove the minor interference caused

by the original colour of the samples. Then the four replicate absorbances were averaged to give one reading for each of the historic pine beam ends tested. With this averaged absorbance it was possible, using the calibration graph for glucose, to calculate the concentration of sugar detected in the historic samples. This was done using the following equation:

$$X = (Y - C) / M$$

Where X is the glucose equivalent concentration, Y is the absorbance of the historic sample, C is the (negative) intercept of the calibration graph and M is the slope of the calibration graph.

Table 4.3 shows the glucose equivalent concentrations calculated using the above equation for the historic samples.

Table 4.3: Sugar concentrations released by modern and historic Scots pine.

Sample	Concentration (mg/ml)
Historic Pine – 1500-1	0.144
Historic Pine – 1500-2	0.151
Historic Pine – 1500-3	0.127
Historic Pine – 1500-4	0.577
Historic Pine – 1500-5	0.121
Historic Pine – 1500-6	0.131
Modern Pine - 1	0.108
Modern Pine - 2	0.108

From the concentration of sugar in the solutions it was then possible to work out how much sugar was released per 1 mg of wood. This was done using the calculation below:

$$(X \times V) / W$$

Where X is the concentration, V is the volume of water collected from the original historic sample and W is the oven dry weight of the wood samples used. The results in the table 4.4 show how much of the soluble sugar would be found in 1 mg of the wood samples.

Table 4.4: showing the final sugar/wood content.

Sample	Volume (ml)	Weight (g)	Concentration (mg/ml)	Sugar released (mg/g)
Historic Pine – 1500-1	16.3	0.5047	0.144	4.6
Historic Pine – 1500 -2	15.8	0.7656	0.151	3.1
Historic Pine – 1500-3	14.9	0.7668	0.127	2.4
Historic Pine – 1500-4	12.1	0.5972	0.577	11.7
Historic Pine – 1500-5	22.4	0.5691	0.121	4.7
Historic Pine – 1500-6	13.2	0.5299	0.131	3.2
Modern Pine - 1	14.2	0.5635	0.108	2.7
Modern Pine - 2	14.1	0.5744	0.108	2.6

From table 4.4 it can be seen that more soluble sugar per g of wood was present in the majority of the historic samples.

4.6 Discussion

This increase in soluble sugar content supports the argument presented in Chapter 3 where the hemicelluloses were considered to be breaking down. This experiment also supports the theory that the hemicellulose polymer chains were breaking down into monosaccharides or oligosaccharides, and not just losing acetyl groups. This seems to be affecting the pine and the oak very differently, although the oak was not tested through the DNS method due to the effect of tannins on the colour. The historic pine seemed to be producing more soluble sugars than the modern pine. On average the amount of soluble sugar released from the historic pine was 5 mg/g. Initially there would have been 200 mg/g of hemicelluloses as hemicellulose is on average around 20% of softwoods content (Schädel et al., 2010).

In their natural state hemicellulose chains are from 30 to several hundred monomer units in length. If hemicelluloses are broken down to chains only 7-8 monomers long

they are more soluble. When this occurs the wood can no longer swell as much as the loss of hemicelluloses forces the cellulose microfibrils to stick together (Bromley et al., 2013; Sedighi-Gilani and Navi, 2007). Therefore it is possible there was much more breakdown of the hemicellulose than could be calculated by the DNS method as some may have remained insoluble. Alternatively, due to the presence of decay in the sapwood samples the sugars may have been consumed by fungi. It is possible that both of these mechanisms occurred.

These free sugars are soluble and can attract water in the way that is characteristic of solutes, and is independent of the normal interaction of water with the insoluble polymers of wood. The attraction of water by soluble sugars can in theory be represented by the Van't Hoff equation (Bhadusha and Ananthabaskaran, 2011). As an example of the theory one hemicellulose chain in solution, if broken down to 40 individual sugars, would be 40 times as capable of absorbing water. This could be a major factor in why the historic pine wood took up 30-50% more moisture than the modern pine wood and the oak samples. The acetic acid released by hydrolysis of the acetyl groups maybe led to breakdown of the hemicellulose polymer chains as the resulting acid conditions can provide catalysis for depolymerisation (Hosseinaei et al., 2012). What the DNS measurement cannot do is to reveal whether it was sugar monomers reacting with the DNS or longer broken chains of hemicellulose, as each hemicellulose molecule only has one reducing end that will react with the DNS. The reaction with DNS implies breakdown of the polymer but does not identify the chain length of the breakdown products (Gabrielii et al., 2000; Sun et al., 2001). Chemical depolymerisation by acid catalysis would be at random points in the chain and would therefore initially release large fragments. The way in which fungal enzyme mixtures break down hemicelluloses is more consistent with the release of monomers from the hemicellulose chains (Srivilai et al., 2013; Enoki et al., 1989; Pérez et al., 2002; Szabo, 2015).

Chapter 5

Wood Shrinkage

The manner in which wood swells and shrinks is a complicated function of its anisotropic properties and, as a result, of its anatomy. Due to this anisotropic behaviour, wood shrinks unevenly in its different planes (Barber and Meylan, 1964). Shrinkage is a widely studied area of research today, due to the implications that it has for the quality of wood from the forest and the sale of timber. Shrinkage is therefore one of the most important concerns for these industries (Badel at el., 2006, Perré and Huber, 2007, Burgert and Fratzl, 2009).

Wood, being a natural material, grows in a wet condition where shrinkage rarely occurs. When it does occur it leads to growth cracking or checking, where the standing trees have dried out enough to actually crack. This usually occurs in a period of drought (Mattheck et al., 1995). It is only once wood is dried out for human utilisation that warping and twist occur (Patera et al., 2013). The initial shrinkage of wood, from the green state, occurs at fibre saturation point after all the free water in the cell lumen is lost. The moisture content at this stage is usually round 24-30%. As the wood begins to equilibrate with a drier environment and dries out further, water is lost from the cell walls themselves and the wood becomes dimensionally unstable (Rosner et al., 2009, Buck, 1952). Drying of wood in kilns forces distortion to happen. Unrestrained softwood can warp and twist badly during drying (Kifetew et al., 1998). Wood is generally dried down to 12% moisture (Koponen and Virta, 2004) on the Continent, but in the UK it is dried to 20%. This can lead to issues where the wood will continue to dry and distort once it is placed in a building with central heating.

Wood changes its dimensions in reaction to the surrounding Relative Humidity (RH) (Popescu and Hill, 2013), and will vary in how it reacts to RH depending on the species, as with all issues related to shrinkage. The influence of the direction of shrinkage, radial or tangential, can again be different between species (Silva et al., 2014a, Williams, 2010, Badel at el., 2006). The effects and control of moisture in wood are discussed further in Chapter 4.

Distortion is a conservation problem in buildings which do not have a well controlled RH environment.The swelling and shrinking of wood will also have a bad effect on wood panelling, wood paintings and polychrome sculptures, as movement can cause the paint layer to flake off the wood surface as well as causing micro-cracking or craquelure (Mazzanti, 2012, Buck, 1952, Gereke et al., 2011). If repair work on wood with new

wood causes more difference in shrinkage, the wood species needs to be taken into account when areas of wood are replaced, especially with wooden art panels. Understanding shrinkage comes from understanding the structure of the wood itself (Badel at el., 2006). One of the controlling forces behind shrinkage is the microfibril angle (MFA). The measurement of the MFA is discussed in detail in Chapter 6. But it is not the microfibrils themselves that absorb the water which causes swelling and shrinkage. The microfibrils act as a semi-crystalline skeleton holding the matrix material between them in place (Yamamoto et al., 2001). The matrix polymers between the microfibrils are believed to cause the shrinkage forces, but these do not have a uniform direction as water is removed and it is the direction of the constraint from the microfibrils that causes the differential pattern of shrinkage in wood (Yamamoto et al., 2001).

Shrinkage is known to be uneven for the different wood directions. Typical shrinkage levels from green to dry are generally believed to the about 0.5% longitudinally, 4% radially and 6% tangentially. Much research has gone into why shrinkage in the radial and tangential directions are so different but the reason is still unclear today (Patera et al., 2013, Leonardon et al., 2009, Babinski, 2011, Kifetew et al., 1998).

The cellulose microfibrils restrict how much the wood can shrink (Cown et al., 2005, Harris and Meylan, 1965, Treacy et al., 2000, Tabet and Aziz, 2013). For example longitudinal shrinkage decreases with decreasing MFA. But tangential shrinkage increases as the MFA lowers (Donaldson, 2008, Treacy et al., 2000, Verrill and Kretchmann, 2011, Leonardon et al., 2009). Figure 5.1 gives a clearer idea of this. Although the MFA does affect the longitudinal shrinkage, wood still shrinks less longitudinally than in either of the transverse directions, as it is always fairly constricted by the cellulose microfibrils running in this direction.

Higher MFA restrains the cell walls across the grain and decreases shrinkage in the transverse direction

Lower MFA restrains the cell walls along the grain and decreases shrinkage in the longitudinal direction
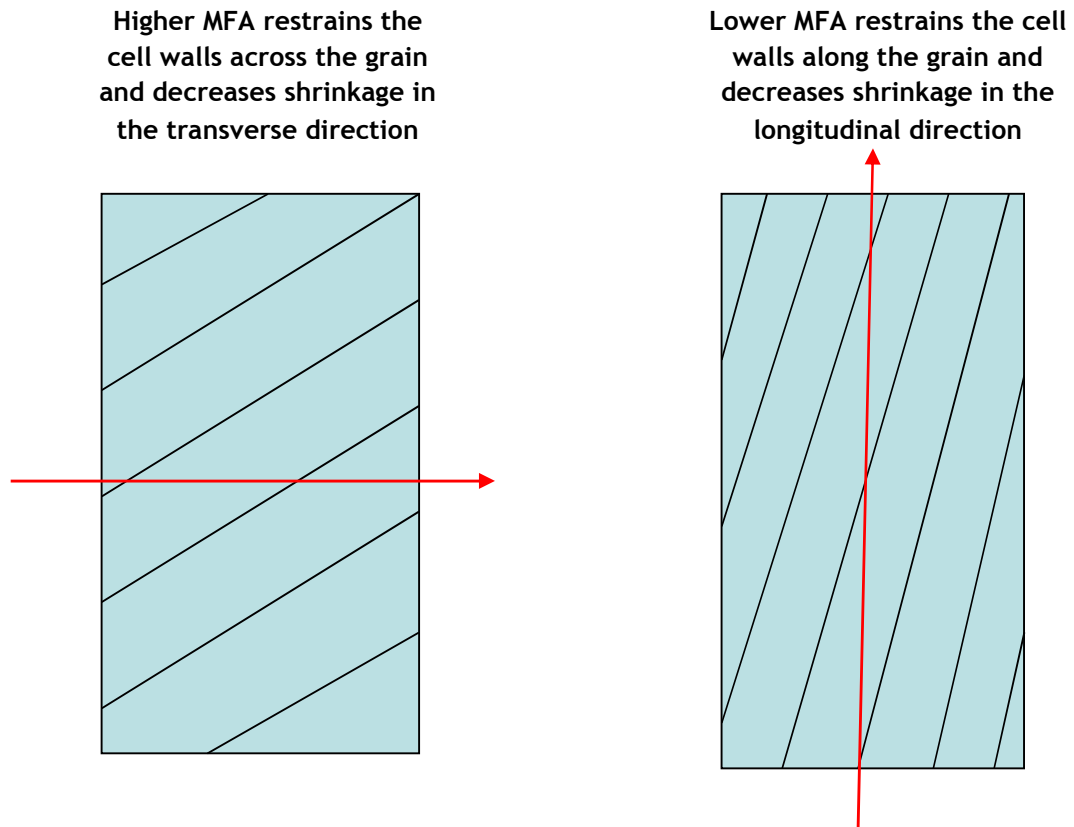
Figure 5.1: Relationship of MFA to longitudinal and transverse shrinkage of wood.The grain direction is vertical in both diagrams. Longitudinal (vertical) and transverse (horizontal) shrinkage directions are represented by the red lines. The cellulose microfibrils, whose orientation (MFA) is represented by the diagonal black lines, have a restrictive effect on shrinkage. Image: K Hudson-McAulay

The relationship between MFA and radial shrinkage is less obvious, as radial shrinkage is less then tangential. If it was simply to do with the MFA, there logically should not be this difference. Other factors may influence shrinkage in this direction, including anatomical features like the ray cells and pits (Harris and Meylan, 1965, Treacy et al., 2000, Patera et al., 2013). The reduced level of radial shrinkage has been suggested to result from the constriction provided by the ray cells or by pit fields where the MFA is higher. These pit fields form between a ray cell and the adjoining tracheids (Barber and Meylan, 1964, Patera et al., 2013). It has also been suggested that there are swelling differences between the early- and latewood cells in softwoods. Latewood contains a much larger volume of tangential cell walls than earlywood (Engelund et al., 2013, Koponen et al., 1989, Harris and Meylan, 1965). None of the possible given reasons for the different shrinkage between the radial and tangential directions are proven, and no single one really gives a convincing argument for this occurrence.

Shrinkage is also different between hardwoods and softwoods. One of the biggest problems in oak is known as shake. Shakes are large cracks or splits that can occur in oak longitudinally up the stem of the tree. Shake is thought to be due to a combination

of large earlywood vessels (Mather et al., 1993, Mather and Savill, 1994) and the difference between the longitudinal and radial shrinkage. The difference between these two shrinkage directions causes tangential stress on the drying wood causing it to split (Badel and Perré, 2002, Yang and Normand, 2012). Great effort goes in the breeding of oak to reduce shake by selecting for small vessel cells in the early wood (Mather et al., 1993, Mather and Savill, 1994). Oak also has superior radial strength compared to softwoods due to the larger volume of rays (Bjurhager et al., 2010). This may constrain swelling and shrinkage in the radial direction in oak.

Softwoods have been shown to shrink less than hardwoods (Barber and Meylan, 1962). They also do not suffer from shake as readily as oak due to the lack of vessel cells (Babinski, 2011). However compression wood in softwoods shows more longitudinal shrinkage, which can lead to curvature (Leonardon et al., 2009)

Density of wood is also something which affects the shrinkage and swelling of wood. The more dense the wood is, the slower water penetrates into the wood and the more slowly it swells (Alteyrac et al., 2006, Treacy et al., 2000).

It is the availability of hydroxyl groups that causes the swelling and shrinkage of wood (Patera et al., 2013, Engelund et al., 2013). As the cellulose hydroxyl groups are only accessible on the outside of some of the microfibrils, water does not penetrate between the crystal planes (Fernandes et al., 2011). Therefore the cellulose microfibrils do not swell themselves, and access for water is limited to the matrix material between them.Binding sites for waterare generally provided in the matrix by the hemicellulose polymers (Leonardon et al., 2009, Hein et al., 2013). The hemicelluloses are probably located largely between the microfibril bundles so that swelling between the bundles forces them apart, as well as swelling between the microfibrils in each bundle (Thomas et al., 2014). The deformation seen when wood is dried is due to the loss of water from the matrix material, which then shrinks (Barber and Meylan, 1964).

The swelling and shrinkage is dominated by the movement of water in and out of the thickest S2 layer of the wood cell wall. But it is believed that swelling from moisture uptake is not only controlled by the MFA of the S2 layer but by the S1 and S3 layers of the cell wall, thus preventing the cell walls from excessive swelling in thickness that might lead to the cell bursting (Patera et al., 2013, Kifetew et al.,1998, Meylan, 1972). The restraint by the S1 and S3 layers is believed to have a greater effect in the earlywood than the latewood and also more effect on the juvenile than the mature wood (Harris and Meylan, 1965), leading to yet more heterogeneous shrinkage within the wood.

Although much has been discovered about shrinkage not all of the relationships are fully understood, especially the difference between radial and tangential shrinkage

(Hittmeier, 1967, Barber and Meylan, 1964). Much applied research still goes into this area to reduce loss of revenue from timber that warps and twists during the drying process, making it unable to be sold into the building trade. When wood swells as a result of raised RH in a building it is subject to restraint from the frame it is placed in (Ispas, 2013). Differential shrinkage between old and new timber in sensitive areas could cause damage to the building structure. There is a separate problem with differential shrinkage in heritage items, which is not caused by the anatomy of the wood but is due to coatings, paint and other finishes which are known to cause differential shrinkage of panels when moisture can only get to the panels from one side, causing them to warp (Gereke et al., 2011, Buck, 1952, Chauhan et al., 2001).This problem is outside the remit of this project.

5.1 Experiment

5.1.1 Sample preparation

5mm cubes were cut from pith to bark from each of the beam ends using razor blades in order not to lose too much of the original material.The intention was to obtain a detailed assessment of how shrinkage changes throughout each beam end and to allow comparison with the modern samples.

5.1.2 Procedure

The samples were first fully saturated to above fibre saturation point. Then they were measured longitudinally, tangentially and radially with digital callipers (Powerfix Profi +) reading to 0.01 mm. Once this first measurement was complete the cubes were oven dried at 108°C for 6 hours to drive out all moisture. To assess shrinkage, they were then measured again with digital callipers longitudinally, tangentially and radially.

5.2 Data analysis and results

To calculate shrinkage in each direction the fractional change in that dimension was calculated by the equation below:

$$\text{Fractional Shrinkage} = (SW\text{-}OD)/OD$$

Where SW is dimension of the saturated wood and OD is the dimension of the oven dried wood.

5.2.1 Oak
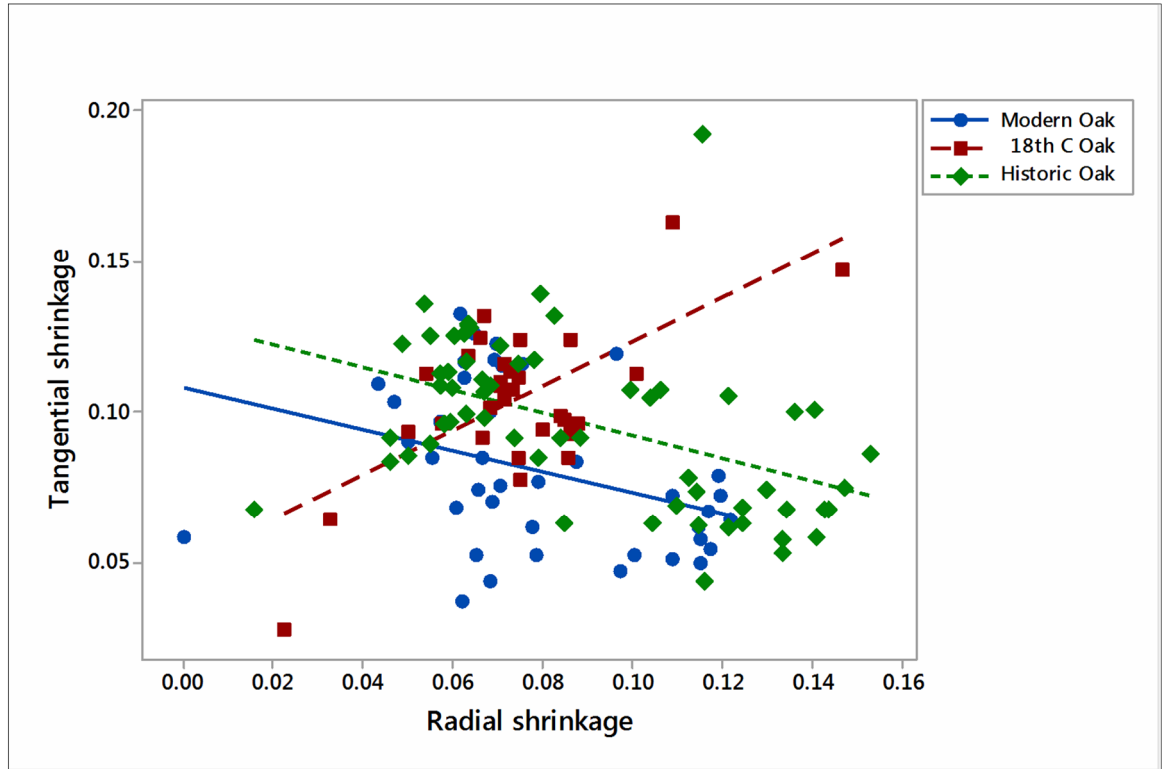
Figure 5.2: The relationship between tangential and radial shrinkage in all of the oak samples. The r value of the correlation for the modern oak was -0.345, the 18th C oak had an r value value of 0.658 and the historic oak had an r value of -0.465.

From the results seen in figure 5.2 there seems to be a very weak relationship between the radial and tangential shrinkage of oak samples. This is unexpected, as due to influence of microfibril angle (MFA) on shrinkage in both transverse directions they might be expected to have a much stronger positive relationship (Yamashita et al., 2009, Yao, 1969). The reason for this is outside the limits of this research, but that is why the shrinkage directions are looked at separately.

5.2.2 Tangential shrinkage of oak.
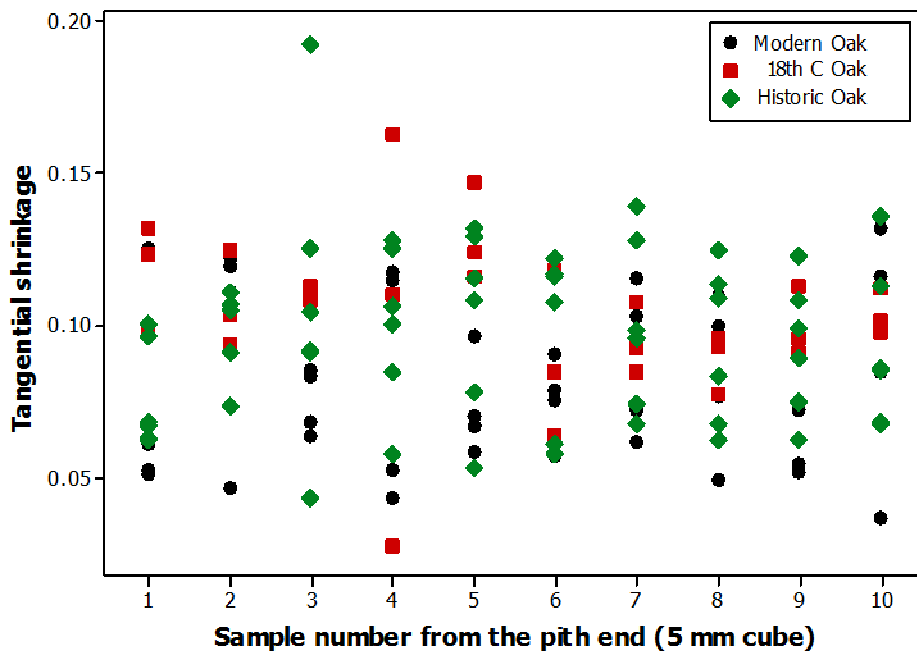
Figure 5.3: The pith to bark variation in tangential shrinkage of oak in the different age ranges.

Figure 5.3 plotting tangential shrinkage against distance from the pith shows a slight difference between the age groups of oak tested. One way variance of analysis (table 5.1) showed this difference to be highly significant with P <0.001, but there is still a great deal of scatter. The Fisher test showed that shrinkage was lower in the modern samples compared to both the 18[th]C and historic oak (Fisher P<0.05) but the 18th century and historic oak samples were not significantly different from each other.

	Modern Oak	18[Th] C Oak	Historic Oak
Tangential Shrinkage	0.080 a	0.104 b	0.095 b

Table 5.1: Mean tangential shrinkage of oak samples of different ages.

Means followed by the same letter are not significantly different, Fisher LSD (P>0.05)

To eliminate the possibility that the different shrinkage was just due to the decay of the sapwood, the heartwood samples alone were run through a one way analysis of variance (table 5.1), showing that there was a difference between the heartwood shrinkage in the different ages of oak with a significant P value of <0.05. A further

Fisher test revealed that this difference was between the modern and historic oak (Fisher LSD P<0.05). There was no significant difference between the historic and 18thC oak (table 5.2).

	Modern Oak	18Th C Oak	Historic Oak
Tangential Shrinkage (heartwood)	0.083 a	0.093 ab	0.098 b

Table 5.2: Mean tangential shrinkageof oak heartwood at different ages.

Means followed by the same letter are not significantly different, Fisher LSD (P>0.05)

5.2.3 Radial shrinkage of oak
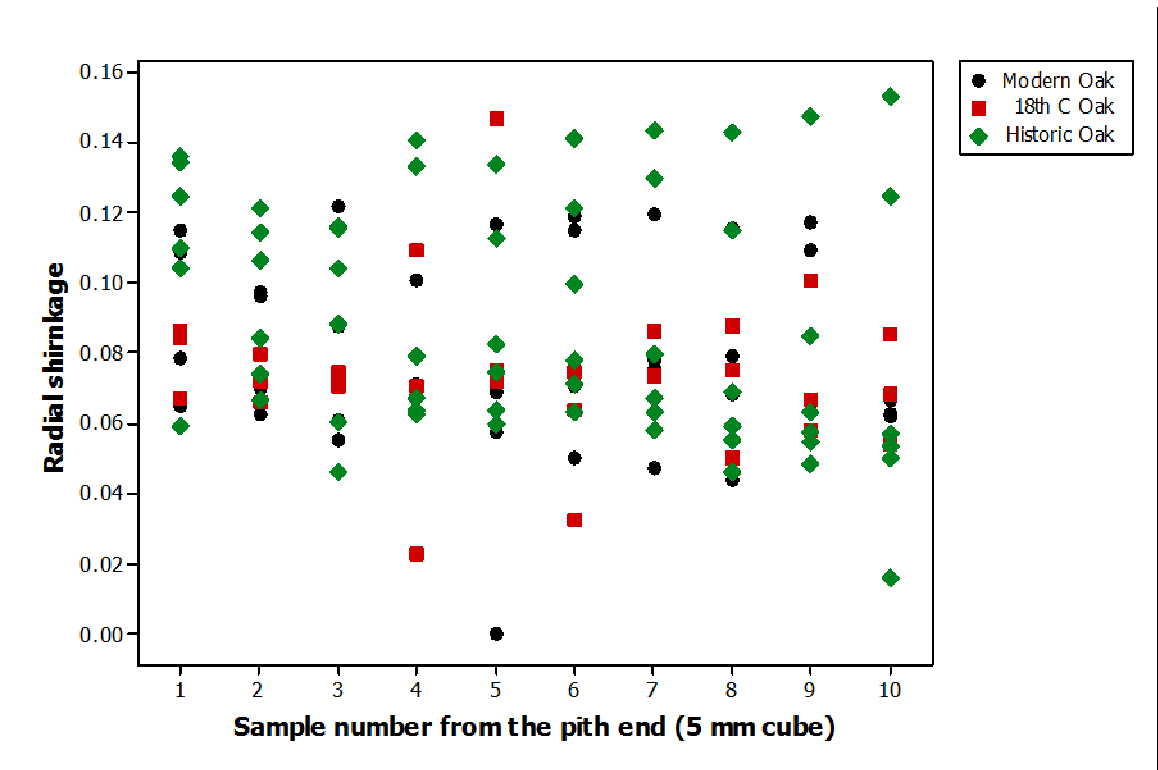
 Figure 5.4: The pith to bark variation in radial shrinkage of oak in different age ranges. None of the differences between different ages of oak samples were significant (P >0.05)

Figure 5.4 shows that shrinkage in the radial direction was fairly constant from pith to bark with a very slight decrease at the bark. The difference between the different age ranges of oak was not significant (table 5.3), as can be seen in the P value of >0.05.

	Modern Oak	18Th C Oak	Historic Oak
Radial Shrinkage	0.078	0.074	0.089

Table 5.3: Mean radial shrinkage of oak samples of different ages.

There were no significant differences between the means (ANOVA P>0.05)

The heartwood samples alone were run through one way anaylsis of variance which showed no significant difference in radial shrinkage between the different ages of oak (table 5.4).

	Modern Oak	18Th C Oak	Historic Oak
Radial Shrinkage (heartwood)	0.07	0.08	0.076

Table 5.4: Mean radial shrinkage of oak heartwood at different ages.

There were no significant differences between the means (ANOVA P>0.05)

	Sample	Tangential	Radial	T/R Ratio means
Historic oak	HO-15-01	0.073	0.073	1.06
	HO-15-02	0.079	0.09	1.3
	HO-15-03	0.072	0.068	1.17
	HO-15-04	0.097	0.083	0.99
	HO-15-05	0.105	0.082	0.77
18th C oak	HO-18-01	0.089	0.069	0.78
	HO-18-02	0.116	0.07	0.6
	HO-18-03	0.096	0.075	0.66
Modern oak	MO-01	0.117	0.078	1.55
	MO-02	0.101	0.067	0.65
	MO-03	0.128	0.067	2.01

Table 5.5: Tangential (T) and Radial (R) fractional shrinkage and T/R Ratios: means for each Oak sample.

Wood in general shrinks more in the tangential direction than in the radial direction (Perré and Huber, 2007, Lionetto et al., 2013). The oak samples in this experiment show

this effect (figure 5.2). We also wanted to find out if the size of the effect was different between the historic and modern oak. Firstly the ratio T/R was calculated between tangential and radial shrinkage.

Ratio T/R = (Mean Tangential Shrinkage) / (Mean Radial Shrinkage)

This ratio was transformed to its natural logarithm in Microsoft Excel. An ANOVA then showed a significant difference in the T/R ratio between the age ranges with a highly significant P value of <0.001. Figure 5.5 above shows the overall difference in the T/R ratio in the oak age ranges.

The Fisher test showed that the 18thC oak had a significantly lower T/R ratio than both modern and historic oak (Fisher LSD, P<0.05) but there was no significant difference between the historic and modern oak (table 5.6).

	Modern Oak	18Th C Oak	Historic Oak
T/R Ratio	1.236 a	0.696 b	1.034 a

Table 5.6: Mean T/R ratio for shrinkage of oak samples of different ages. Means followed by the same letter are not significantly different, Fisher LSD (P>0.05)
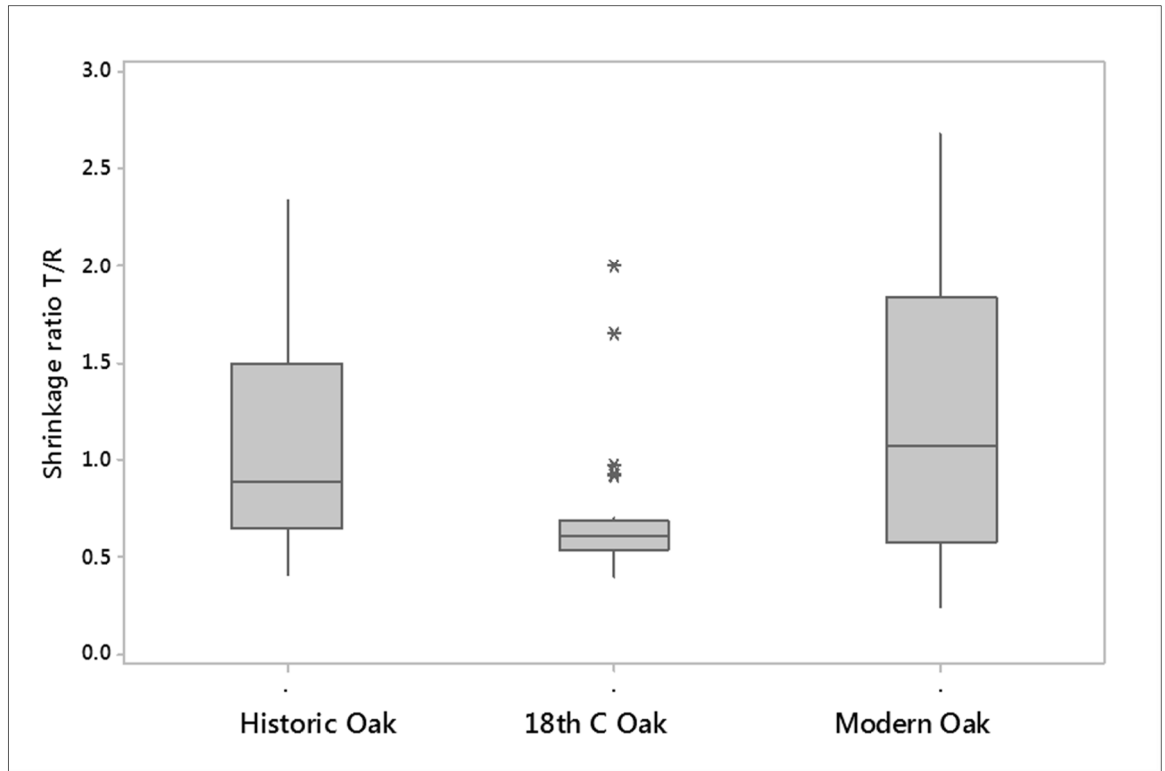
Figure 5.5: The shrinkage Ratio T/R between tangential and radial shrinkage in the historic, 18th Century and modern oak.

5.2.4 Pine
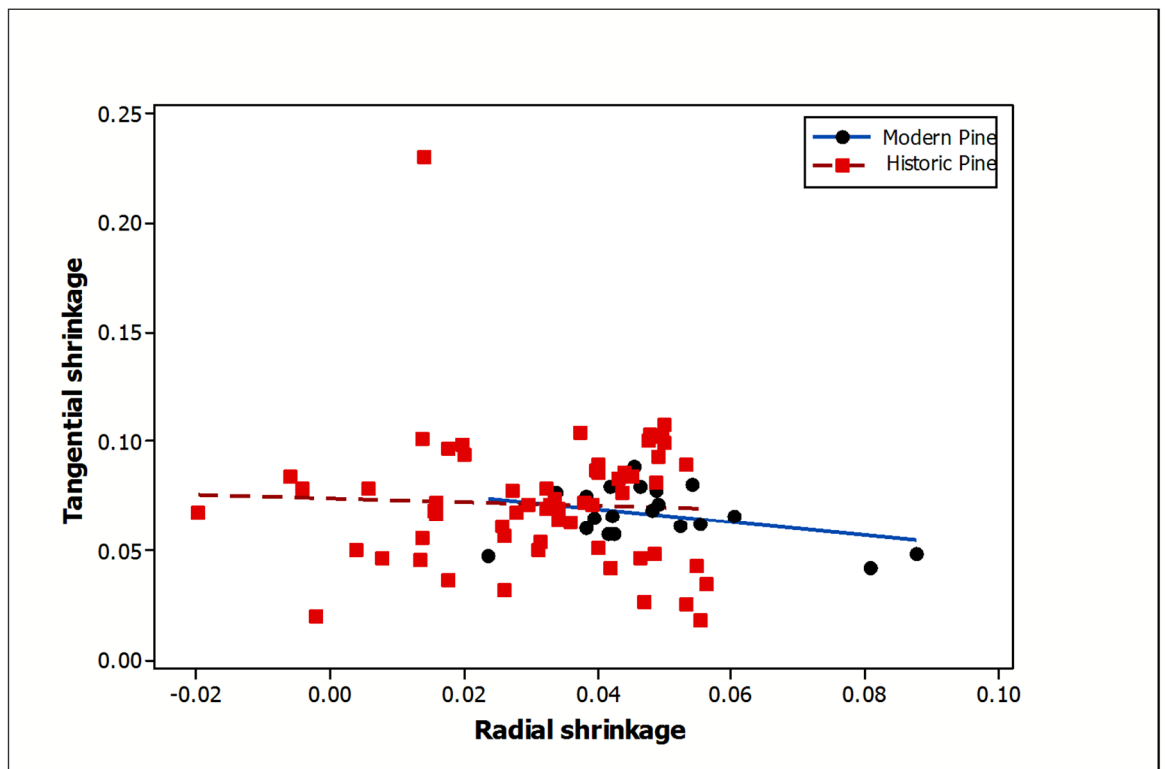
Figure 5.6: The relationship between tangential and radial shrinkage in all of the pine wood samples. The correlation line for the modern pine has an r value of -0.359, and the historic pine has an r value of -0.042

From figure 5.6, tangential and radial shrinkage in Scots pine were as weakly correlated as in oak.

5.2.5 Tangential shrinkage of pine
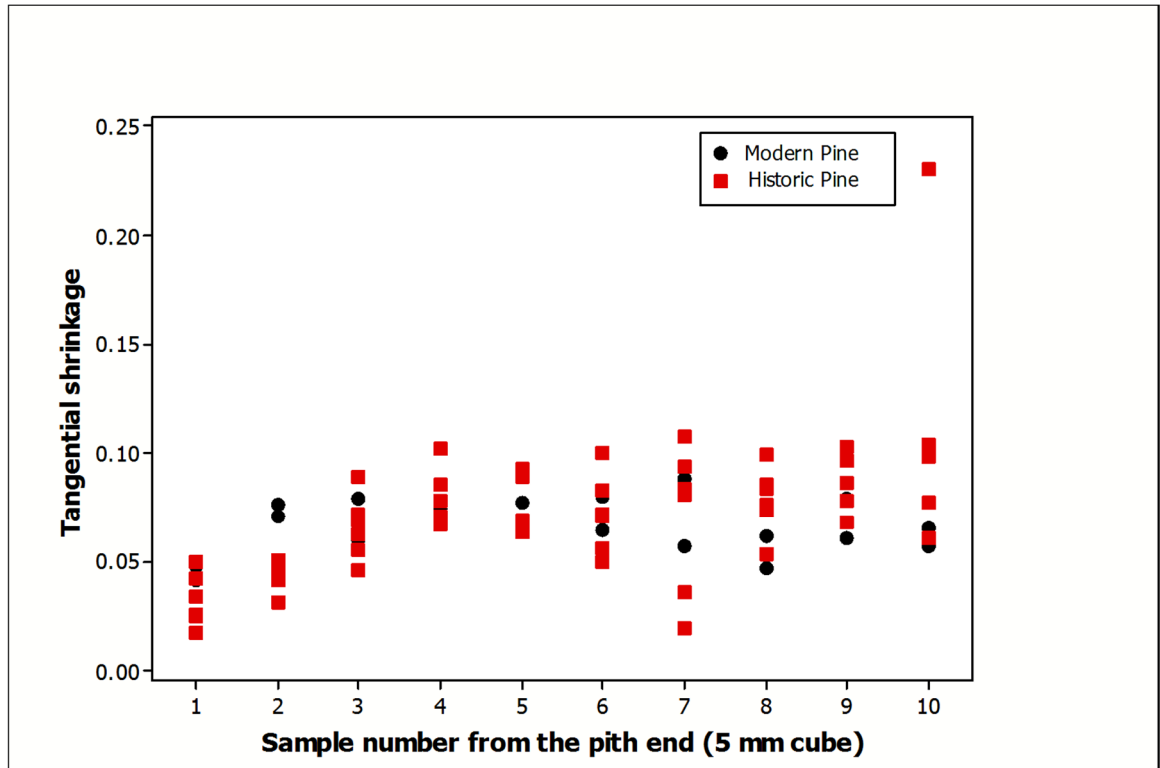
Figure 5.7: The pith to bark variation in tangential shrinkage of pine for the different age ranges.

From the scatter graph (figure 5.7) of tangential shrinkage against distance from the pith, there was little difference in the shrinkage pattern between the historic and modern samples. Both increased in shrinkage for a short distance away from the pith. Linear regression is a poor model for this behaviour but the regression statistics for the historic pith to bark samples gave a highly significant P value of <0.001 whereas the modern samples gave no significant increase. The tangential shrinkage matched what is normally seen in softwoods where shrinkage increases outward with decreasing MFA, which levels off close to the bark (Leonardon et al., 2009).

	Modern pine	Historic pine
Tangential Shrinkage	0.066	0.071

Table 5.7: Mean Tangential shrinkage of pine at different ages.

There was no significant difference between the means (ANOVA P>0.05)

One way analysis of variance shows that there were no statistically significant differences between the age groups as in Scots pine, but figure 5.7 clearly shows the pattern from pith to bark.

A second one way analysis of variance on just the heartwood showed that there was a difference with a very significant P value of <0.01 between the tangential shrinkage in the heartwood of the modern and the historic wood.

	Modern pine	Historic Pine
Tangential Shrinkage (heartwood)	0.067 a	0.027 b

Table 5.8: Mean tangential shrinkage of pine heartwood at different ages.

Means followed by the same letter are not significantly different, Fisher LSD (P>0.05)

5.2.6 Radial Shrinkage of pine
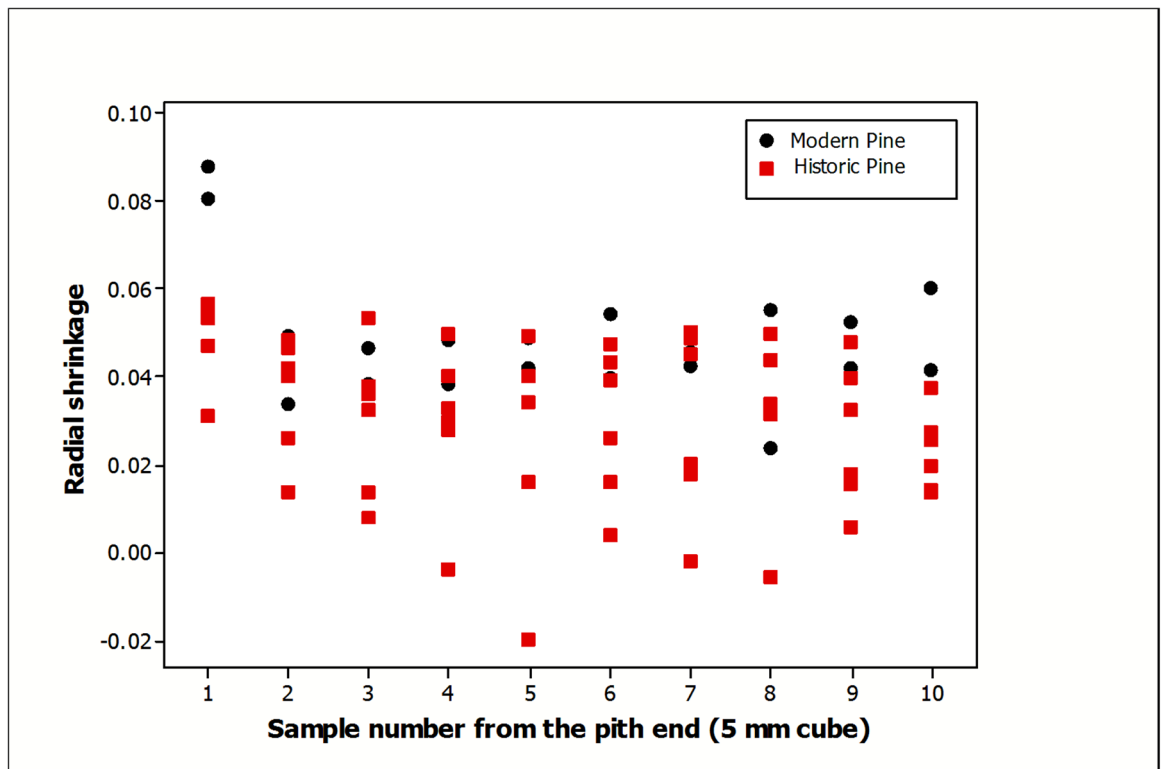
Figure 5.8: The pith to bark radial shrinkage of pine for the different ages of samples tested.

Figure 5.8, radial shrinkage from pith to bark shows a different pattern from oak and from the tangential shrinkage. The one way analysis of variance showed that in the radial direction there was more shrinkage in the modern wood than the historic. Radial shrinkage in the historic samples decreased from pith to bark with a significant P value

of 0.05 and an R^2 value of 0.084. The difference for modern pine was non-significant. From figure 5.8 it can be seen that the historic pine appears in general to shrink less in this direction than the modern samples. This can be seen in the ANOVA in table 5.9.

	Modern pine	Historic Pine
Radial Shrinkage	0.048 a	0.031 b

Table 5.9: Mean radial shrinkage of pine at different ages.

Means followed by the same letter are not significantly different, Fisher LSD (P>0.05)

The pine samples showed more tangential shrinkage than radial shrinkage (figure 5.6). The ratio T/R between tangential and radial shrinkage was calculated.

Ratio = (Mean Tangential Shrinkage) / (Mean Radial Shrinkage)

The ratio was transformed to its natural logarithm using Microsoft Excel. ANOVA on the transformed data showed that modern pine and historic pine differed with a significant P value of <0.05. After running only the heartwood samples through ANOVA there was again a significant difference in shrinkage ratio between the historic and modern samples, so this was not just caused by the decay in the sapwood. Figure 5.9 shows this.
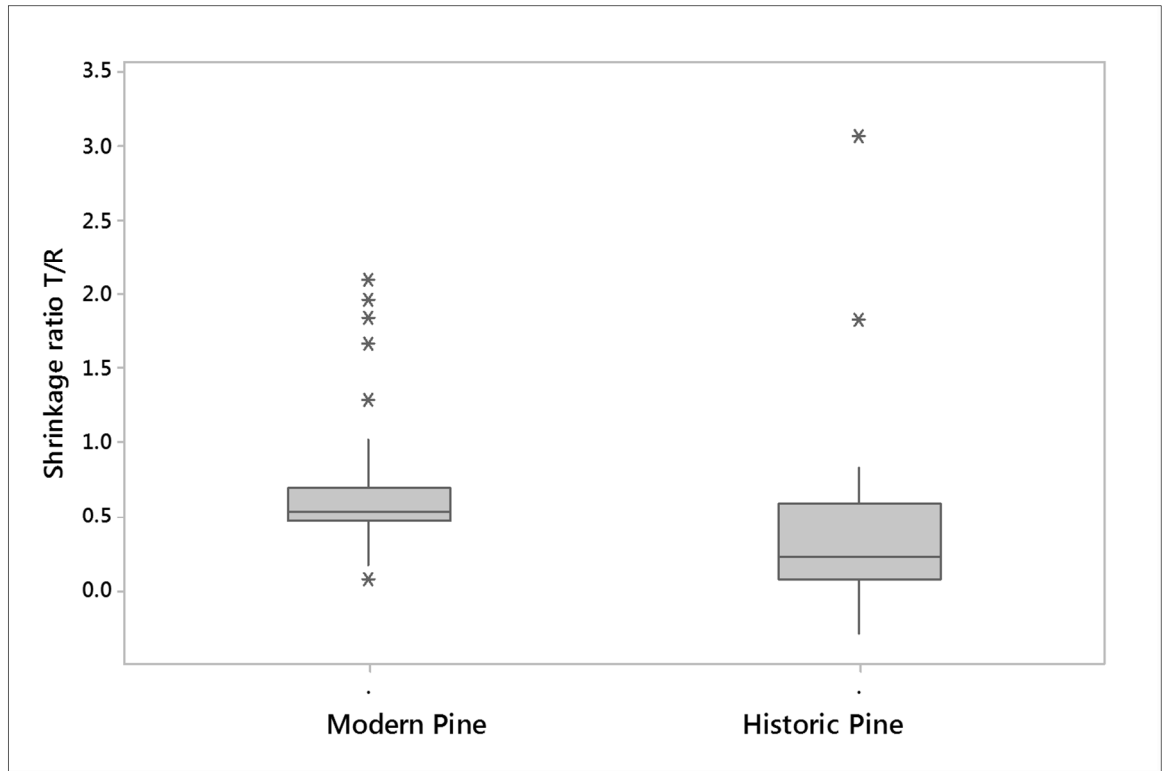
Figure 5.9: The shrinkage ratio T/R between tangential and radial shrinkage in the historic and modern pine.

	Sample	Tangental	Radial	T/R Ratio means
Historic pine	HP-15-01	0.057	0.025	0.62
	HP-15-02	0.062	0.051	0.46
	HP-15-03	0.07	0.045	0.85
	HP-15-04	0.087	0.048	0.7
	HP-15-05	0.075	0.036	0.5
Modern pine	MP-01	0.069	0.013	0.52
	MP-02	0.069	0.025	0.45

Table 5.10: Tangential (T) and Radial (R) fractional shrinkage and T/R Ratios: means for each pine sample.

5.3 Discussion

The swelling and shrinkage of wood is still a highly researched topic and is not fully understood. It is complicated due to the anisotropy and anatomical structure of wood cells. Because wood is an anisotropic material, shrinkage is different in the three

different directions (Piazza and Riggio, 2008, Barber and Meylan, 1964, Patera et al., 2013, Harris and Meylan, 1965). In this chapter we tested both historic and modern wood in the different planes to see if there was any effect of aging on shrinkage.

The results showed that in pine there was a difference in shrinkage with age. The historic pine shrank more in the tangential direction, as the samples got closer to the bark, than the modern pine. But the real difference between the two wood species appeared in the radial direction where there was a significant difference between the two wood ages, with the historic pine shrinking less than the modern. The ratio T/R between tangential and radial shrinkage was also different between the two age groups and this ratio was higher in the modern pine.

From the results for the pine wood it can be seen that modern and historic pine shrink differently. This could be damaging when the two are used together in traditional repairs. If the RH environment is not controlled, it is possible for fluctuating RH to cause serious damage.

Comparing only the shrinkage of the heartwood samples of the historic and modern pine wood, the difference was not just due to changes with age but also the damaging effects of biological attack making the shrinkage response worse.

The results for the oak samples also showed a difference in shrinkage with age, although there is a lot of scatter. Statistical analysis showed that modern oak shrank less, in the tangential direction, than either the 18th C or the historic oak samples. In contrast to pine, oak did not show significantly different shrinkage in the radial direction with age. There was no noticeable increase at the sap edges of the oak, unlike pine. This may be due to oak being more resilient to biological attack (Carvalho et al., 2009, Clausen, 2010). The T/R ratio was significantly different in oak but after running the Tukey and Fisher tests this difference was significant only for the 18th C oak, which may be just down to this age range having a smaller range of samples.

The anatomical structure of wood controls its shrinkage capabilities. Different cell types have a different role in each different dimension. It has been observed that the length of the cells (Perré and Huber, 2007) as well as the density and the microfibril angle (Alteyrac et al., 2006) influence shrinkage. Therefore it might be suggested that the loss of density and its influence on the mean MFA of the residual cell wall, after biological attack (Faix et al., 1991, Hastrup et al., 2012, Harris and Meylan, 1965), might influence shrinkage.

Ray cells and tracheids have similar cell structure but they differ in the orientation in which they are laid down within the xylem. Trachieds are vertical whereas rays are laid down horizontally, resulting in a different shrinkage pattern. The radial shrinkage in both pine and oak decreased towards the bark. This was more prominent in the historic

pine. Radial shrinkage is controlled by wood anatomy but particularly by the ray cells which may not be as damaged by biological attack as the tracheids (Patera et al., 2013, Harris and Meylan, 1965, Leonardon et al., 2009), resulting in a less dramatic change in shrinkage between the old and modern samples.

No swelling and shrinkage can happen without the influence of moisture moving in and out of the wood polymer structure. This is what causes the dimensional changes in wood (Schniewind and Cal, 1968). Decay from biological attack might cause the wood to become more porous as the fungi and pests have eaten through the S2 layer of the walls leaving cavities where more water can collect. Pests also destroy the microfibrils (Engelund et al., 2013, Tabet and Aziz, 2013), which can have a huge effect as the microfibrils are the skeleton of the cells, controlling how far they can swell. From the results above in figure 5.2 it can be seen that at the sap edge, where there is evidence of pest attack, there is more shrinkage which is likely due to loss of cellulose microfibrils.

The shrinkage forces acting on the wood also need to be taken into account. The outside of a beam equilibrates to atmospheric moisture at a different rate from the middle of the beam, which will shrink eventually but will take longer for equilibration, resulting in minor tensile forces from the swollen wood acting on the dry interior (Hittmeier, 1967). This might be made worse by the extra swelling in the historic wood. Skilled carpenters and cabinet restorers already understand that wood is a material which changes dimensionally under the effect of moisture. Many will seek out seasoned or even historic wood to repair delicate areas, trying to avoid damage from differential shrinkage (Mansfield et al., 2009, Buck, 1952). Careful selection of timber with a MFA closer to that of the historic wood would control the amount of differential shrinkage within the repair (Treacy et al., 2000) especially when looking to repair Scots pine where the matching could be essential to the repair's success. This is a process which should be under consideration for traditional repairs to beams although it is unrealistic to get pieces of historic timber in the size often needed for these repairs; therefore careful consideration of new wood replacement pieces is needed to prevent differential shrinkage which, as seen in the results here, needs more careful selection between historic and modern Scots pine than in oak. It must always be remembered that even though the wood is hundreds of years old it still has the ability to change in dimensions.

Chapter 6

Microfibril Angle (MFA)

Density was once considered the most important factor in wood quality but it is not the only wood property that needs to be taken into account. The microfibril angle controls the mechanical and shrinkage properties of the wood cell walls, specifically those of the S2 layer which is known to determine the wood stiffness (Alteyrac et al., 2006; Krauss et al., 2011; Evans and Ilic, 2001; Chaffey, 2000; Burgert, and Fratzl, 2009; Paris et al., 2010; Verrill and Kretschmann, 2011; Bjurhager et al., 2012; Stevanic and Salmén, 2009). Both density and MFA need to be considered carefully when trying to carry out traditional, "like for like", repairs on historic structures.

Microfibril angle, like other wood features, differs between softwoods and hardwoods due to their different anatomy. In softwoods the MFA shows wide variation, usually with a larger MFA at the pith and smaller towards the outside of the tree (mature wood) (figure 6.1). Although the MFA is larger at the pith of hardwoods there is much less variation (Donaldson, 2008). Work on Scots pine has shown that the variation in MFA from earlywood to latewood is more prominent in the mature wood of the tree (Auty et al., 2013).
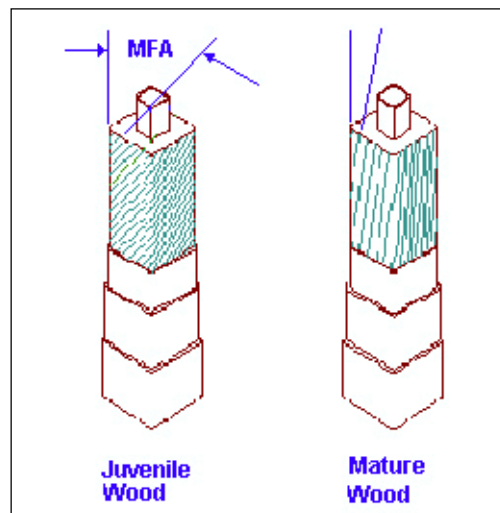
Figure 6.1: The meaning of microfibril angle
(Logan, 2013).

More extensive studies have shown that MFA in conifer (softwood) trees is higher at the base and decreases up the tree. Unfortunately hardwoods have not been studied as thoroughly as softwoods. The studies that have been done show a much lower variation in MFA within the tree. In the few studies on hardwood species oak has been shown to

generally have MFA below 20° (Donaldson, 2008; Tabet and Aziz, 2013; Treacy et al., 2000).

Studies on the variation of MFA from latewood to earlywood have also shown a difference between hardwoods and softwoods. Some softwood species, such as lodgepole pine, show a slow decline of MFA in earlywood and steeper in latewood with maturity, whereas spruces and hardwoods show a similar trend but much less variation (Tabet and Aziz, 2013; Donaldson, 2008; Treacy et al., 2000; Mansfield et al., 2009). Some studies have even shown variation of MFA in one tracheid (Krauss et al., 2011; Khalili et al., 2001).

All structural properties of wood are tied together in influencing the responses of many mechanical properties. MFA is inversely related to the longitudinal stiffness or modulus of elasticity (MOE) of wood (Donaldson, 2008; Ricardo et al., 2011). MFA also is said to be one of the controlling factors in the shrinkage of wood (Ricardo et al., 2011). Again this is one of the qualities which determine the value of wood for the timber industry. Wood cells are normally rectangular in shape although some may appear to be more hexagonal. The typical diameter of the whole wood cell is usually 20-80 μm (De Borst et al., 2013).

The microfibril angle varies within each tree due to a number of factors such as cambial age, growth rate and the height to which the tree grows to, as well as genetic characteristics (Rusinb and Tulika, 2005; Treacy et al., 2000).

Forestry can also influence wood properties such as MFA, which can potentially affect the wood's value. The art of forestry, or silviculture, involves planting and in some cases thinning to provide the correct amount of space for each tree to get the required sunlight and nutrients needed for strong growth, as competition between trees can affect their growth (Adams, 2014, p. 27; Berges et al., 2008). Some experiments have shown that planting trees in close stands significantly reduced the microfibril angle (Lasserrea et al., 2009).

Climate also has a strong impact on tree growth. Wind, precipitation and soil type can affect wood quality, although temperature has been suggested to affect MFA most (Kostiainen et al., 2009; Adams, 2014, p. 28).

Radial growth is affected by the same ecological factors (Berges et al., 2008; Mäkinen et al., 2003; Čejková and Kolář, 2009), and there is a tendency for high MFA to correlate with high growth rate as well as cambial age (Moore et al., 2014; Auty et al., 2012). Moore et al (2014) have found that 68% of the variation found in MFA could be predicted from the radial growth (ring width) variation between different trees (Moore et al., 2014). This radial variation needs to be taken into account when comparing MFA between the historic and modern samples examined in this chapter.

As MFA is a very variable quality within just one single tree (Treacy et al., 2000; Moore et al., 2014), it is essential to understand which part of the tree has been used when part of a historic structure has to be replaced, and to try and make up the new piece of timber with mechanical properties similar to the old.

This chapter aims to measure the MFA for the historic wood using a new quantitative technique derived from polarised FTIR microscopy. Most MFA testing techniques require extensive sample preparation and most of the instruments used are very sophisticated or expensive, making MFA a difficult wood property to measure (Long et al., 1999). This method was developed for this project to allow the MFA of the historic Scots pine and the modern pine to be measured, so that its contribution to the mechanical properties determined in Chapters 8 and 9 could be accounted for and to see if any difference could be detected between wood from silviculture today and wood from historic forests.

6.1 Currently used methods

There are a number of different methods for measuring the MFA of wood. Some are more commonly used than others; these are X-ray diffraction and microscopic methods such as polarized light or direct and indirect light microscopy (Khalili et al., 2001; Tabet and Aziz, 2013; Ricardo et al., 2011; Barnett and Bonham, 2004).

These methods can also be separated into groups according to how the samples are processed. The first group requires a single cell for measurement and the second is done by bulk measurements (Donaldson, 2008).

6.1.1 Microscopy methods

Under the classification of microscopy there are two main techniques used. One includes various methods of microscopy to visually see the MFA and record it. The other is polarised light microscopy (Khalili et al., 2001; Donaldson, 2008; Long et al., 1999).

Light microscopy

There are a number of different light microscopy methods for determining the MFA of wood cells. These are considered to be labor intensive techniques due to the sample preparation needed for light microscopy. Usually microtome thin sections around 20 μm (Roszyk et al., 2010) are needed for microscopy of this kind on wood. It takes skill with the microtome to be able to produce thin enough sections for the work required. Depending on the need for accuracy, the MFA can be seen by a technique called fracturing where the individual microfibrils themselves are not visible, but a cluster at a

fracture zone can be seen under the light microscope, as if it were the grain of the cell indicating the MFA (Khalili et al., 2001; Donaldson, 2008). Images for better accuracy in determining MFA can be obtained by confocal microscopy or scanning electron microscopy at high magnification which can reveal the microfibril bundles and make it possible to measure the MFA (Treacy et al., 2000; Donaldson, 2008).

The use of both these forms of microscopy takes further sample preparation. For MFA measurement by confocal microscopy the samples need to be first subjected to iodine precipitation. The iodine crystals collect within cavities in the cell wall. This technique can be unreliable as not all samples react in the same way, making the crystal pattern patchy or preventing it from appearing at all (Donaldson, 2008; Khalili et al., 2001). Fluorescence microscopy techniques rely on the use of a dye such as Congo red or Acridine orange, as these dyes tend to become oriented with the fibrils after they have been absorbed. These dyes are di-fluorescent so that the direction of polarisation is related to the alignment of the dye (Long et al., 1999; Donaldson, 2008).

Bordered pits

One method to determine the MFA is from the angle of the elongated axis of the pits on the radial cell walls (Lehringer et al., 2009). This method is generally used under a light microscope and in some cases the use of computer image analysis can help to quantify the MFA (Roszyk et al., 2010). In some cases for studying the MFA, the cell walls have been delignified first and then rinsed before being separated onto a microscope slide for the analysis (Treacy et al., 2000). The use of pit apertures is considered to be a semi direct method of obtaining the MFA as the measurements taken from it might not refer to the average MFA, because inside the pit fields the MFA tends to be higher than outside (Khalili et al., 2001; Long et al., 1999).

Soft rot

Soft rot cavities have been used to get a better view of the MFA. Soft rot cavities are aligned along the S2 secondary wall layer (figure 6.2). The technique relies on this association. If the rot is left too long the cavities form larger voids in the cell wall. These are useless for the measurement of MFA so careful control is needed (Khalili et al., 2001; Blanchette, 1995). When using the cavity method more cavities are found in the latewood cell walls (Khalili et al., 2001).
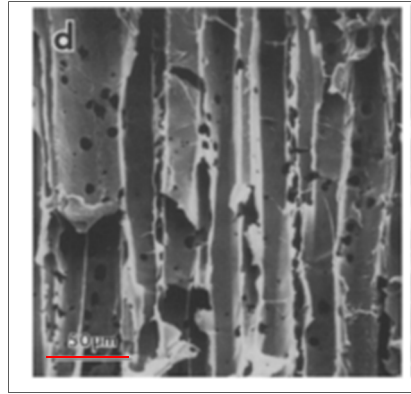
Figure 6.2: SEM view of cavities in wood cell walls caused by rot (Blanchette et al., 1985).

One of the main problems with this technique is uncertainty about how closely the fungal hyphae follow the MFA. Another problem is that it takes much longer to prepare the samples, as it can take up to 14 weeks for the fungi to grow and create the cavities needed (Donaldson, 2008). This technique can be considered as more of a sample preparation to make the cavities expose the MFA, making it easier to analyse. The actual measurement of the MFA is usually done in conjunction with polarised light microscopy, which is discussed further below (Bergander et al., 2002; Khalili et al., 2001).

Polarised light microscopy

Using polarised light to assess the MFA is one of the earliest techniques. Birefringence is produced from the parallel crystalline cellulose fibrils, and can be seen by changing between two polarising angles (Palviainen et al., 2004; Donaldson, 2008; Page, 1969). In some cases this method is also used with visual assistance from image analysis and video or CCD camera imaging as with light microscopy (Ye et al., 1994).

Polarised light microscopy takes advantage of the natural birefringence of cellulose through which cellulose fibrils of a given orientation transmit more intense light when the direction of the polarised light is aligned with them. To measure MFA with this technique a single cell wall needs to be isolated, because if the light passes through the opposite wall of the cell, this will cancel out the polarisation effect from the first. It takes careful sample preparation to remove one half of the cell, usually with skilled use of a microtome (Palviainen et al., 2004; Long et al., 1999; Donaldson, 2008; Leney, 1981). Some older measurements were done by filling the cell lumen with mercury so that the incident light would only pass through the upper cell wall and would be reflected back by the mercury to give the MFA reading (Page, 1969).

Once prepared the sample is illuminated using polarised light. The transmitted light is passed through an analyser crossed in orientation with the polarisation direction of the incident light. The fibre is rotated until the light is extinguished. The angle of the fibre axis at maximum extinction of the polariser is considered to be the MFA (Long et al., 1999; Donaldson, 2008; El-Hosseinu and Page, 1973).

There are other methods of polarised microscopy which do not require the hard task of singling out one fibre, but they do not take into account the effect of the S1 and S3 layers on the final result. But all polarised microscopy needs to be done with care as the error from these S1 and S3 layers can lead to misinterpretation of the end result (El-Hosseinu and Page, 1973).

6.1.2 Wide angle X-ray scattering (WAXS)

Wide angle X-ray scattering, carried out using an X-ray diffractometer (figure 6.3), has been commonly used to determine both MFA and the crystallinity of cellulose fibrils, and even in some cases to find out the shape of a cell (Bjurhager et al., 2010; Hastrup et al., 2012; Park et at., 2010; Sarén and Serimaa, 2006). It has been used on historic samples. The oak from the Vasa ship has been analysed using this method (Svedström et al., 2012).

This method has the benefit of being able to measure larger samples, making sample preparation less labour intensive (Donaldson, 2008). It is also a very fast technique allowing the whole process of determining MFA to be much quicker. The major time is then spent in the interpretation of the data itself (Treacy et al., 2000). As well as being rapid due to the ability to use larger samples it is possible to test the MFA from the pith to bark on a sample strip of the wood provided that the samples have been cut in that manner (Fernandes et al., 2011; Tabet and Aziz, 2013).

WAXS is not a direct method as the process leads to an indirect MFA from which an estimate of the MFA can be given with appropriate interpretation of the data (Treacy et al., 2000; Evans et al., 2000). The data collected by WAXS is the distribution of the microfibril orientation in all the cell wall layers, not an average as used in spectroscopy. Appropriate analysis of the data gives the MFA of the S2 layer.

Figure 6.4: Basic view of how the X-ray beam records the MFA of the wood fibrils through diffraction (Burgert, 2006).

Figure 6.3: Photograph of a XRD machine.

Samples still need to be made up correctly for this method to work, but the procedure can be less intensive than trying to cut thin sections or isolate a single fibre cell wall. WAXS samples are usually prepared in strips along the radius of the tree. It is essential that the samples are not tilted in any way during the process as this could alter the result by over estimating the MFA (Evans et al., 2000; Tabet and Aziz, 2013).

The X-ray diffraction method works by firing a monochromatic X-ray beam through the sample, perpendicular to the grain (figure 6.4). A diffraction pattern, oriented identically with the crystal structure of the cellulose, is created when the X-ray beam interacts with a microfibril, (Evans et al., 2000) and is then recorded by an electronic detector (Tabet and Aziz, 2013; Burgert, 2006).

This method requires a type of X-ray diffractometer which is set up to use single-crystal not powder samples. Ideally it should have an image plate detector so that an image is produced directly, not reconstructed by rotating the sample. WAXS requires a great deal of experience for use on wood. In the UK we initially had access to one of these machines at the University of Bath but it unfortunately broke down, which led to the development of the polarised FTIR method used in this project.

6.1.3 Silviscan

The Silviscan X-ray diffractometer/densitometer is a desirable instrument for obtaining MFA as it not only measures this but can also record other information such as density,

and can put density and MFA together to calculate MOE (Donaldson, 2008; Downes et al 2002). The problem with the Silviscan is there are only three in the world, as each instrument costs over a million pounds. The cost of getting samples run on a Silviscan can be tens of thousands of pounds depending on sample numbers. This amount of money is out of reach for many research projects.

Apart from the amount of information that can be obtained from Silviscan measurements it is useful that, as with other X-ray techniques, the measurements can be carried out on larger samples with limited sample preparation. The sample required is a small strip cut tangentially to very precise dimensions, usually 2 mm thick and cut from pith to bark of the tree to get as much information as possible (Evans and Ilic, 2001; Long et al., 1999; Bjurhager et al 2012).
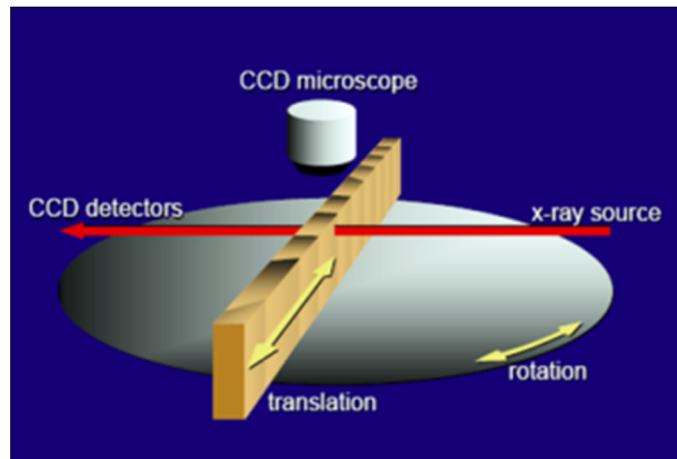
Figure 6.5: The Silviscan X-ray beam path through the sample. (Auty, 2011)

To obtain information on MFA takes around 7 seconds for a reading at one point on the sample strip. The machine is able to calculate the MFA from the diffraction pattern while moving on to collect the next diffraction pattern so it is a much quicker process than other X-ray methods (figure 6.5),(Evans and Ilic, 2001; Lachenbruch et al., 2010). The diffraction pattern recorded is analysed with software which is purposely designed for the Silviscan (Bjurhager et al., 2012).

As with the other techniques for measuring MFA the Silviscan does have disadvantages. It can have less precision when measuring higher MFAs, due to weaker diffraction at high angles (Donaldson, 2008; Long et al., 1999). This can make its use on hardwoods such as oak a little less reliable than on softwoods. But on the whole the speed and overall accuracy make this a favoured technique in acquiring MFA data (Ricardo et al., 2011; Evans et al., 2000; Alteyrac et al., 2006).

6.1.4 Spectroscopy Methods

The method used here to obtain MFA data is through polarised FTIR microscopy, but other forms of spectroscopy have also been used to obtain MFA. Raman and Near Infrared are the main two (Ji et al., 2013; Long et al., 1999; Schimleck et al., 2005; So et al., 2013).

In Raman and FTIR spectroscopy, characteristic peaks appear in the spectrum caused by the absorption of infrared light by vibrating covalent bonds (Stevanic and Salmén, 2009; Fackler and Schwanninger, 2012; Long et al., 1999).The greatest absorption of the polarised IR beam is when its polarisation direction is geometrically parallel to the vibration of the bond (Altaner et al., 2014b). The peak that is most useful in the FTIR spectrum is at about 1160 cm^{-1}, and is associated with the stretching of the glycosidic C-O-C linkage between successive glucose units in the cellulose chain (Ji et al., 2013; Simonović et al., 2011; Chang et al., 2014; Long et al., 1999). This is the peak that changes most in intensity with the orientation of the cellulose. The 1120cm^{-1} peak is considered to be less connected with orientation so that a ratio between the intensities of these peaks can be used to correct for variation in sample thickness.

As well as the orientation of cellulose, polarised FTIR has been used to assess the orientation of the other wood polymers in relation to the cellulose microfibrils and the cell axis. It was discovered that in softwoods the hemicellulose chains, especially glucomannans, have a close link to cellulose (Simonović et al., 2011; Stevanic and Salmén, 2009). This is different from hardwoods as these do not contain much glucomannan, but they have been studied very little in comparison to softwoods (Donaldson, 2008). Lignin is different in many ways but was still suggested by Simonović t al., (2011) and Stevanic and Salmén, (2009) to have a similar orientation to the cell axis (Simonović et al., 2011; Stevanic and Salmén, 2009).

Determining MFA by use of NIR, on the other hand, is claimed to work by using a correlation with the air dry density of the wood to determine MFA (So et al., 2013, Schimleck et al, 2005). They again use bulk wood samples so less precision and labour is need in preparing samples, using the radial- longitudinal face of the wood strips (So et al., 2013, Schimleck et al, 2007, Schimleck et al, 2005).

There are disadvantages with both NIR and Raman. They are both relatively new techniques for determining MFA, and with NIR in particular the underlying fundamentals of each process have still to be found out, even whether it is in fact MFA that is being analysed (Schimleck et al, 2007; Schimleck et al, 2005). For Raman the sample preparation can be limiting, because the sample needs to be de-lignified before use to

prevent lignin fluorescence from interfering with the spectra (Ji et al., 2013; Long et al., 1999).

6.2 Methods

6.2.1 Polarised FTIR microscopy

The currently preferred methods of determining MFA are through either the Silviscan or solid state XRD. Both also have a range of problems making them inaccessible to some research groups in the wood science field. Due to these problems the decision was made to develop the use of polarised FTIR microscopy to determine MFA. This method has been used before to determine MFA but only qualitatively (Fackler and Schwanninger, 2012; Simonović et al., 2011; Stevanic and Salmén, 2009). In this chapter a way to calibrate and quantify the FTIR procedure was achieved and applied to historic timber. By comparison with Silviscan data for Scots pine it was then possible to calibrate the FTIR and gain quantitative MFA results.

The spectra were collected using a Nicolet Nexus FTIR spectrometer attached to a Nicolet Continuum Microscope with an MCT detector which is cooled using liquid nitrogen. The Nicolet Omnic version 7,2a software was used both to control the spectrometer and to process the spectra. The spectrometer was set to scan 32 times per spectrum, with a spectral range of 800cm^{-1} – 4000cm^{-1} and spectral resolution of 2 cm^{-1}. Spectra were recorded through a window set at 100 µm square. The spectra were saved in their raw .CSV form and then further processed in Microsoft Excel. A Continuum ZnSe IR polariser 0045-347 was added which needed to be changed between 45° and 135° manually to give the parallel and perpendicular polarisation angles. Spectra were recorded with the infrared beam passing through the polariser at two different angles, one parallel to the grain (Longitudinal or L) and one perpendicular to the grain (Transverse or T). Due to the angle at which the polariser sits in the FTIR microscope used, these angles were 45° and 135°. One of the angles will have a greater absorbance than the other due to the alignment of the C-O-C glycosidic bonds with the plane of polarisation of the IR beam. The ratio is then obtained between the two absorbance figures. This ratio L/T depends on the MFA and is known as the dichroic ratio (Marchessault, 1962; Stevanic and Salmén, 2009). The 1160cm^{-1} peak has the highest dichroic ratio in the spectrum (Simonović et al., 2011; Stevanic and Salmén, 2009; Chang et al., 2014).

During this process the transmitted infrared beam passes through both front and back walls of each cell, as well as the side walls which are parallel to the beam's path. Each

layer of the cell wall that the beam passes through contributes to the MFA. A calibration is then needed to calculate the MFA from the dichroic ratio.

6.2.2 Sample preparation: Silviscan samples for calibration

For this MFA experiment to work a calibration needed to be made using a sample set of Scots pine for which the MFA was already known. A set of Scots pine samples which had been previously analysed using the Silviscan (Auty et al., 2013) was kindly donated by Dr David Auty. With his permission, access was allowed to his samples to re-use them for our calibration.

The Silviscan samples are prepared in a different way from those required for FTIR. They are strips 2mm in thickness cut longitudinally on the radial plane from pith to bark using precision sawing with twin circular saws. The samples were then soaked in acetone, three times for 24 hours to remove the extractives, and any bark was removed. Before use in the Silviscan the samples were conditioned to 7.8% moisture content by keeping them at 22°C and 40% relative humidity (RH) for 24 hours (Auty, 2011).

As 2 mm thickness is far too thick for use on the FTIR microscope (Evans and Ilic, 2001; Long et al., 1999; Bjurhager et al., 2012), the samples had to be re worked.

Firstly the Silviscan sample was cut in half lengthwise to preserve part of the sample for the original Silviscan collection. As this half was then too long to be safely cut in the microtome, it was divided into 2.5cm sections that would fit in the microtome clamp giving good contact with the steel blade. This was done using a flat edge razor to avoid losing any of the material, as ring number is essential for the calibration to work correctly. Each sample was marked in order to keep it in the correct orientation from pith to bark. As the samples are only 2 mm in thickness they needed to be attached to bigger blocks of wood in ordered to be safely clamped in the microtome. These blocks were cut to 3 cm by 0.5 cm (figure 6.6). To allow for a good bond between the support blocks and the samples they were firstly oven dried to remove any moisture, then the Scots pine samples were bonded to the surface using Araldite epoxy resin at a hardener to resin ratio of 1/1.

Silviscan strip.

Silviscan strip cut in two.

Strip cut into sections and attached to block to safely fit in the microtome.

Microtomed thin section for polarised FTIR microscope.
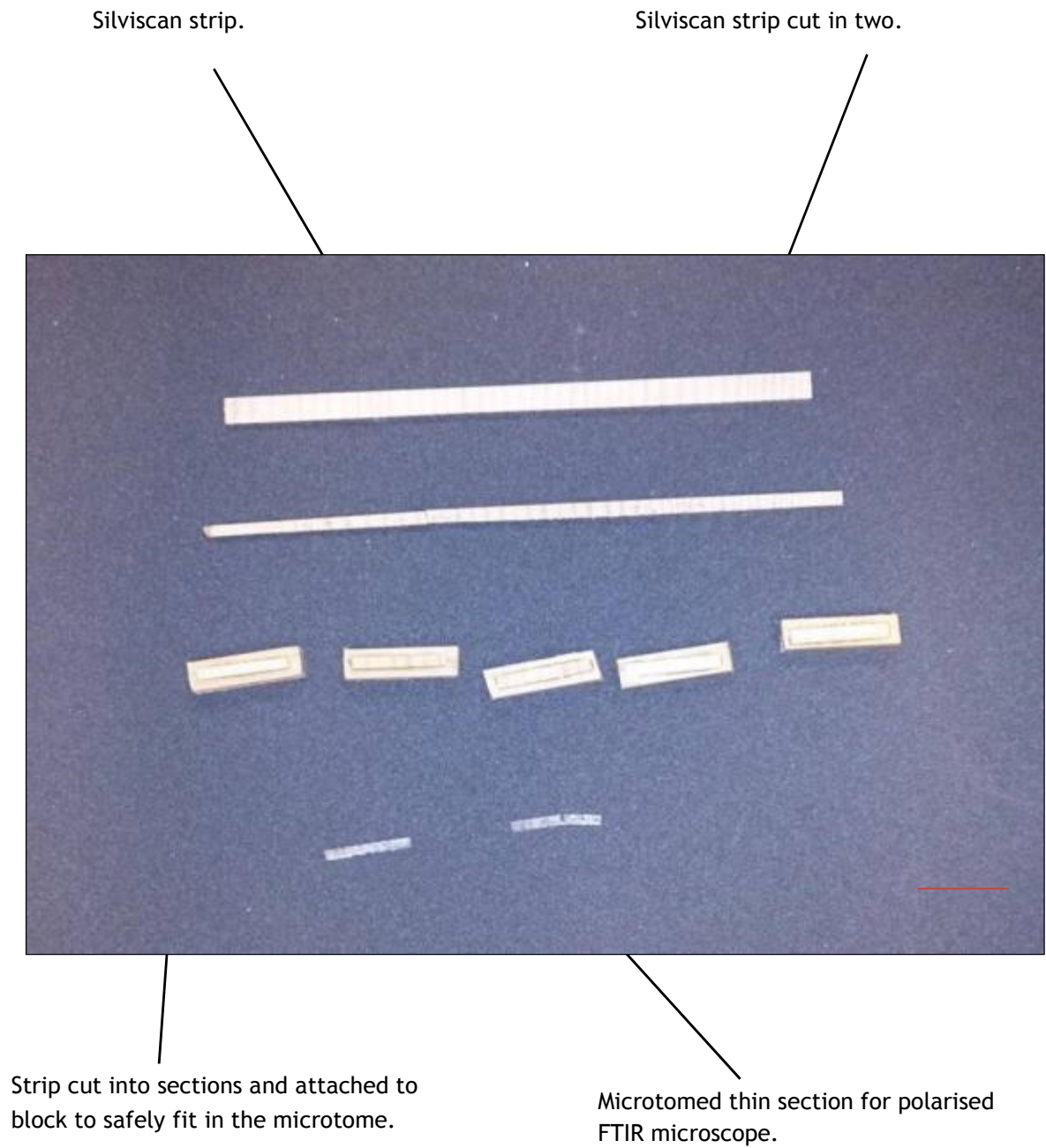
Figure 6.6: Preparation of Silviscan samples for polarised FTIR. Scale bar 3 cm. Image: K Hudson-McAulay.

Once the resin had hardened the samples were cut on a Leica RM2255 microtome fitted with a solid steel blade, as the thickness of the sample must be tightly controlled (figure 6.7). When using wood samples on an FTIR microscope they need to be around half a cell thick (Roszyk et al., 2010) to obtain useable spectral data. The microtome was set to cut sections of 19 μm thickness, (Faix and Böttcher, 1992; Gruchow et al., 2009; Krauss et al., 2011). With thicker samples saturation of the 1160 cm^{-1}peak occurs causing the dichroic ratio to be inaccurately measured. It is still possible to find spectra from latewood with too high an absorbance (above 1). Such spectra were removed before averaging. In the light of this the sample needs to be thin enough or the data produced will be unusable. Five sections from each sample were taken in case of uneven thickness or loss.
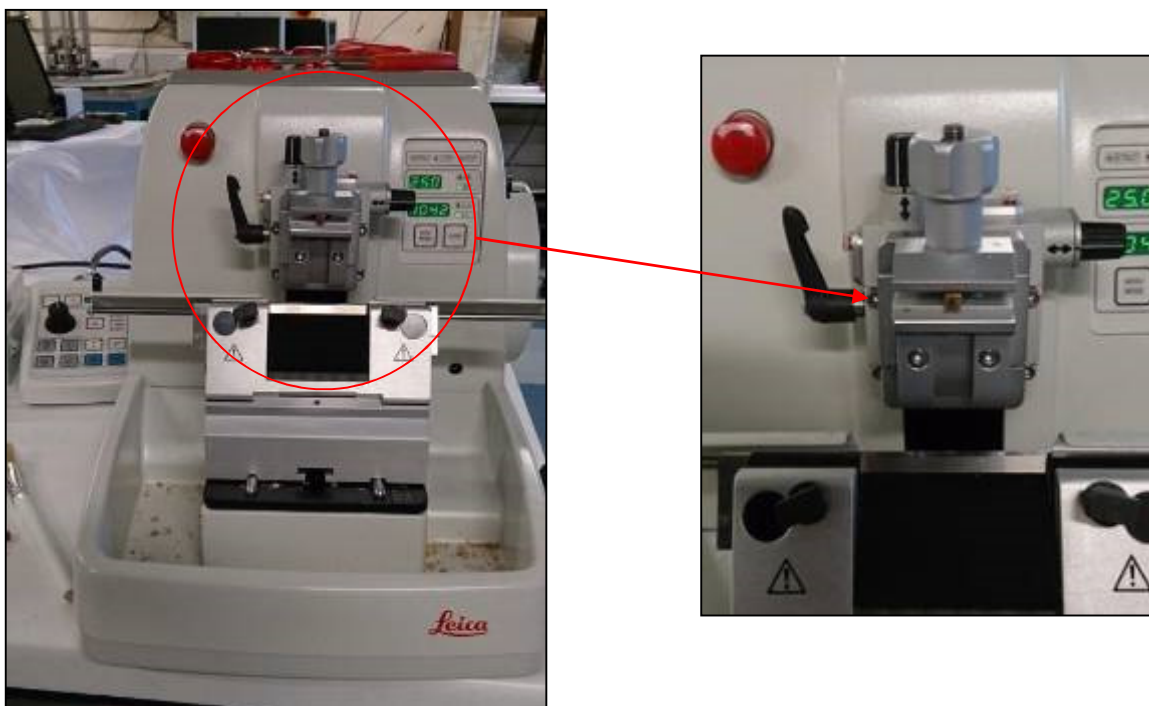
Figure 6.7: The Leica microtome used. The close up image shows a historic sample in the vice. Image: K Hudson-McAulay.

6.2.3 Sample preparation: historic samples

Samples for this experiment needed to be carefully prepared in order to gain correct results. Firstly samples were taken from each of the timber beam ends using scalpels in order to not lose too much of the material. One 5mm by 5mm cube was made from the pith, one from the heartwood and one from the sapwood. As the samples for FTIR need to be no bigger than half a cell thick for the data to be useable, samples were taken from this block using a microtome. The sample had to be cut along the longitudinal

radial plane of the wood in order to get a clear MFA from the wood cells. The microtome was set up to take 19μm sections from the original block, as for the calibration set. Five sections of each block were taken (figure 6.8).

Figure 6.8: Thin sections cut from the 5mm block of historic wood for use on the FTIR microscope Image: K Hudson-McAulay.

6.3 Calibration procedure

With the use of polarised FTIR microscopy (figure 6.9) is it possible to measure differences on a chemical level, giving a good idea of the relative abundance of the wood polymers as well as their orientation within the cell wall (Chang et al., 2014). The calibration Scots pine samples were measured from pith to bark making sure that each ring was accounted for. To enable good coverage of each sample a spectrum was taken every 0.5 mm. This spacing was measured using a vernier scale on the microscope stage. Three spectra were taken at each 0.5 mm point: one in normal light, one in polarised light at 45° and one at 135° throughout the entire length of the sample. Each sample was measured four times on different paths along its length to produce the large data set needed for a calibration.

Each time a spectrum was taken it had to be made sure that the sample was in the correct position in order to get an accurate measurement of the MFA. The cells must be correctly aligned before taking the spectra so the reading taken will be true to the MFA, not affected by misalignment of the cells.
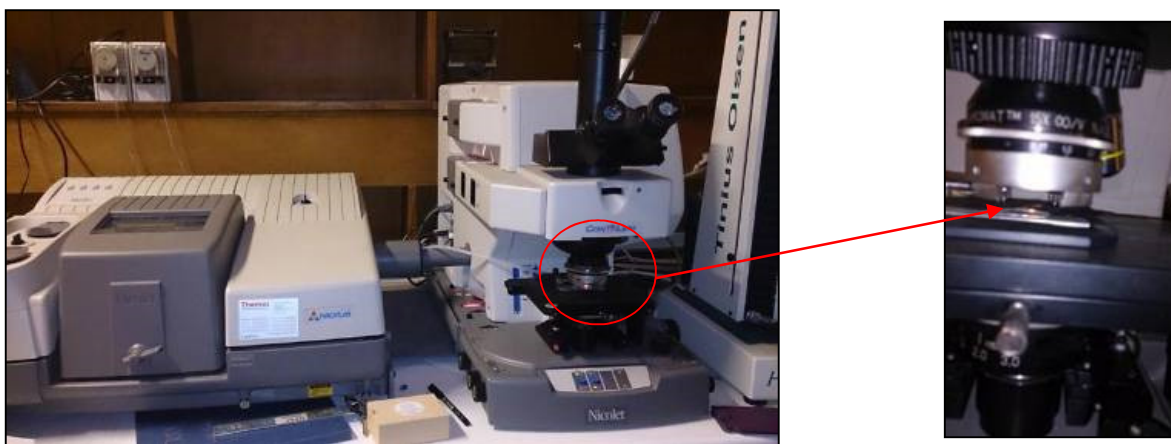
Figure 6.9: The FTIR microscope Image: K Hudson-McAulay.

A total of approximately 4000 FTIR spectra were taken in non polarised, 45 °and 135° polarised light. The spectra were processed in Microsoft Excel where they were baseline corrected. This was done in Excel rather than using the Omnic software due to the large volume of spectra needing to be processed in exactly the same way. Full details of how the baseline correction was done and the equation itself can be seen in Chapter 3. After baseline correction, the spectra that were unclear due to the samples being too thick and their absorbance too high were identified using a correlation coefficient to compare each individual spectrum to the average of the spectra. If the correlation coefficient was lower than 0.95 the spectrum in question was regarded as being different from the rest of the results and was removed.
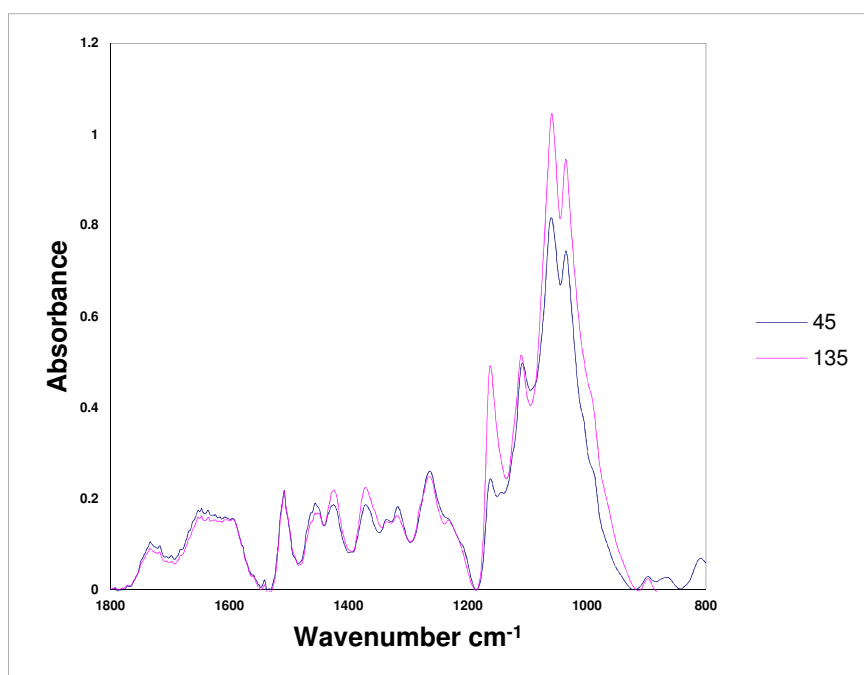
Figure 6.10: The fingerprint region of the spectrum and the difference in absorbance of the 1160 cm^{-1} peak between parallel and perpendicular polarisation. This give the MFA ratio.

The MFA ratio was defined as the dichroic ratio L/T for the key 1160cm^{-1} cellulose peak (figure 6.10). In both the 45° and 135° spectra the average absorbance was taken from 1153 cm^{-1} to 1169 cm^{-1} using Excel.

Once the average absorbances had been obtained for the 1160cm^{-1} peak range in both the 45° and 135° spectra, these were used to produce the MFA ratio using Equation 6.1:

Equation 6.1

MFA Ratio = (A45/A135)

Where A45 is the average for the 1160 peak range in the 45° spectra and A135 is the average in the 135° spectra.

The MFA ratios at 0.5 mm spacing from the pith to the bark were then put in order for the four separate runs for each sample. From this data set it is then possible to separate the measured spectra according to which came from each separate annual ring, corresponding to the data from the Silviscan.

Once the spectral data set from each sample had been separated into rings, the data for each ring was averaged across the four replicate measurements to give a MFA value for that ring. These averages where then taken and plotted against the MFA for each ring from the Silviscan data (Auty et al., 2013).

By a linear fit to the calibration graph produced in this way it was possible to develop the calibration equation to obtain the MFA of the historic Pine (figure 6.11).
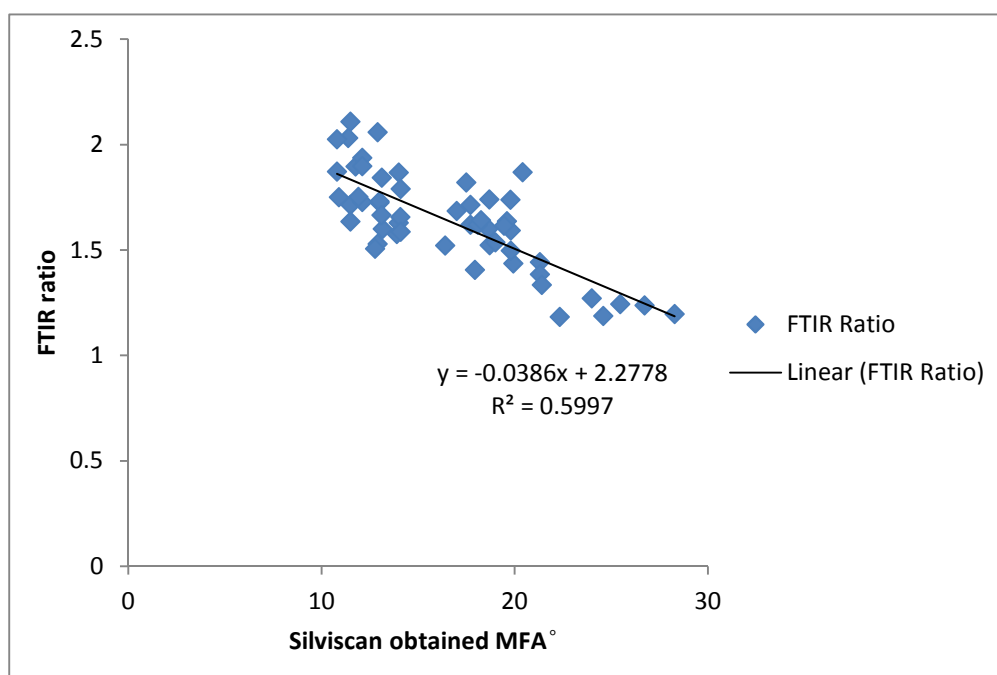
Figure 6.11: The dichroic ratios obtained with the FTIR microscope against the MFA obtained by the Silviscan.

Equation 6.2

FTIR ratio y = 2.2778 – 0.0386x

Where x = MFA from Silviscan

Therefore rearranging this equation

MFA = (2.2778 – FTIR ratio)/0.0386

6.4 Testing Historic Material

With the calibration being successful it was then possible to obtain a semi-quantitative MFA from FTIR microscopy of the historic Scots pine samples. Microtome samples were taken from three of the 5 mm cubes one from the pith, one from the heartwood and one for the sapwood. They were then run through the same procedure as the calibration standards, taking a spectrum in un-polarised mode and with 45° and 135° polarisation every 0.5 mm along each 5 mm thin section with four replicate paths. Each path was covering a new section of the sample allowing for good coverage of the cells. Each run was averaged separately and this average was then used with the average from the other 3 runs on the same sample to produce an overall average for the whole sample which was then used to calculate the final average dichroic ratio and produce the MFA.

6.5 MFA determined from the dichroic ratios for Scots Pine

The spectra were then processed in the same manner as for the calibration samples. The dichroic ratios were inserted into the calibration equation to give the estimated microfibril angle.
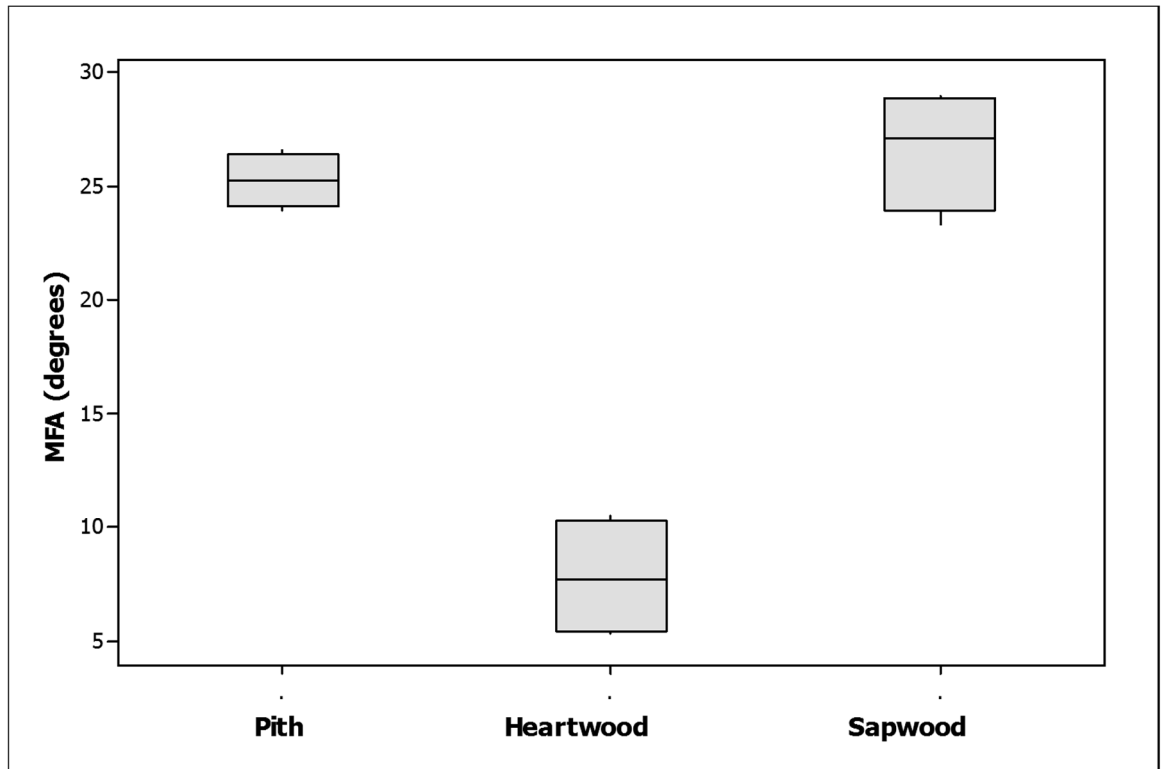
Figure 6.12: MFA in Historic pine sample HP-1500-1. The one way ANOVA shows that differences between radial positions are significant with a P value of <0.001. The Fisher test showed that all three positions were significantly different from each other.
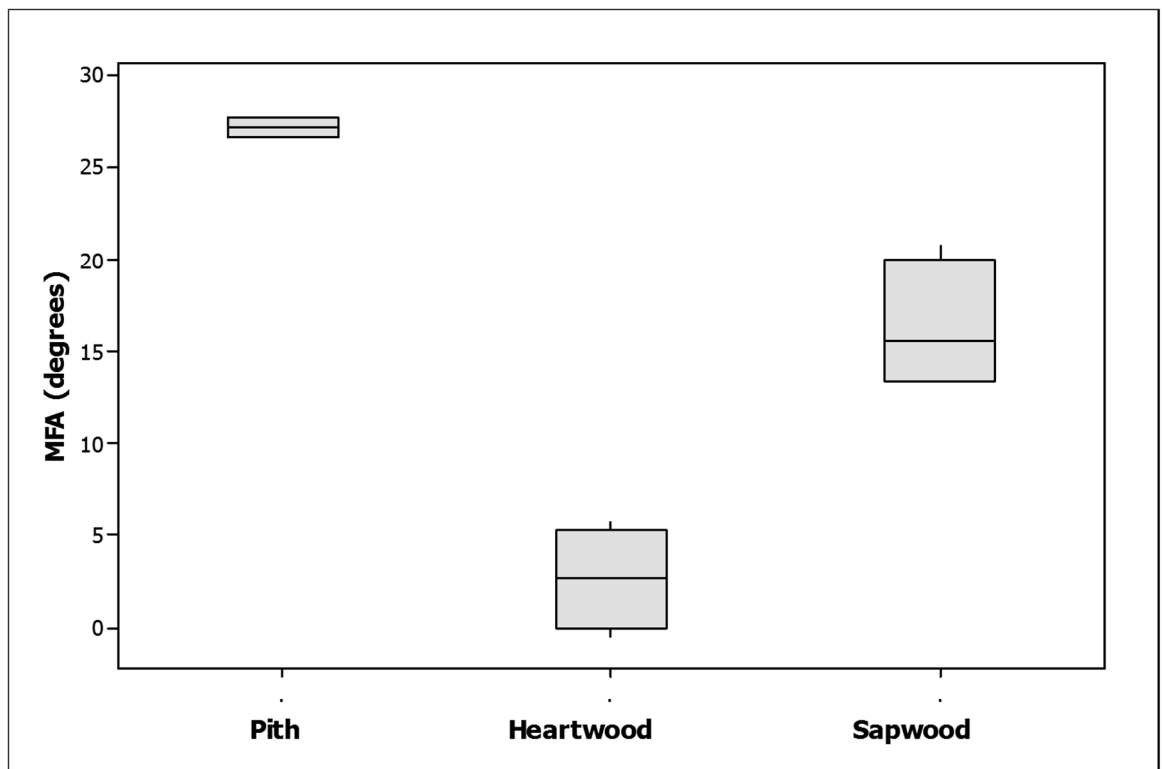
Figure 6.13: MFA in Historic pine sample HP-1500-2. The one way ANOVA shows that differences between radial positions are significant with a P value of <0.001. The Fisher test showed that all three positions were significantly different from each other.
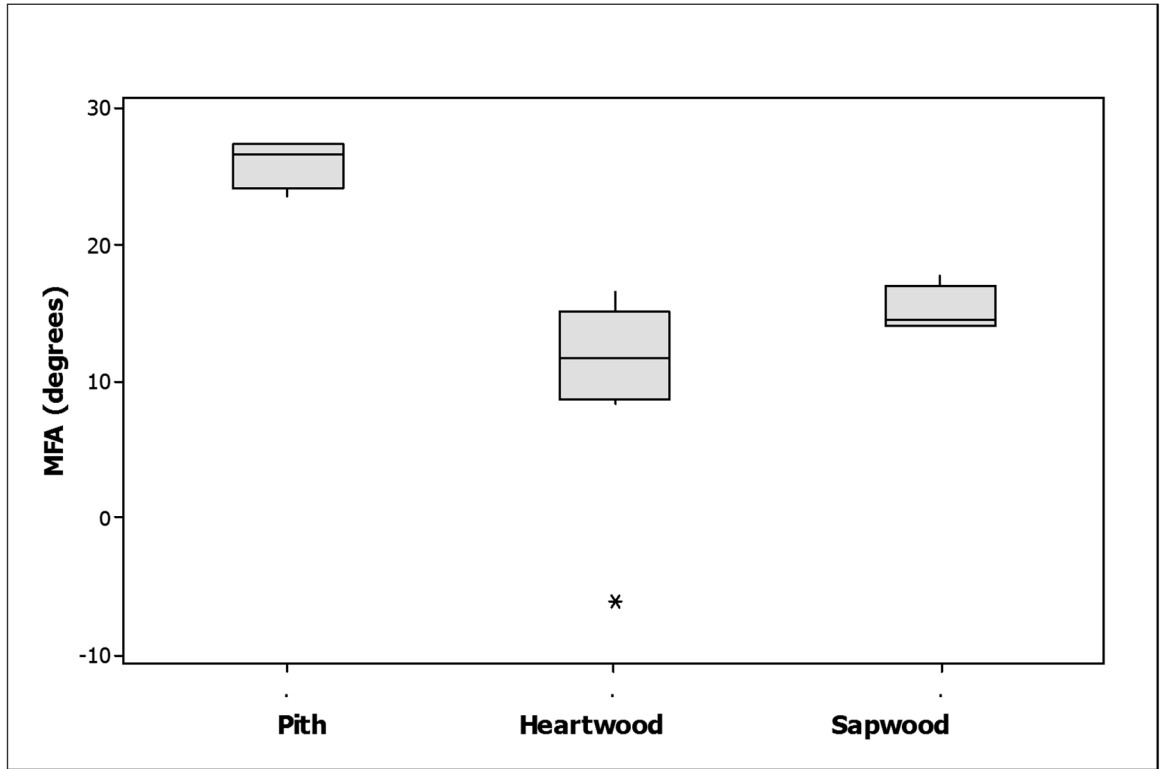
Figure 6.14: MFA in Historic pine sample HP-1500-3. The one way ANOVA shows that differences between radial positions are significant with a P value of <0.001. The Fisher test showed that all three positions were significantly different from each other.
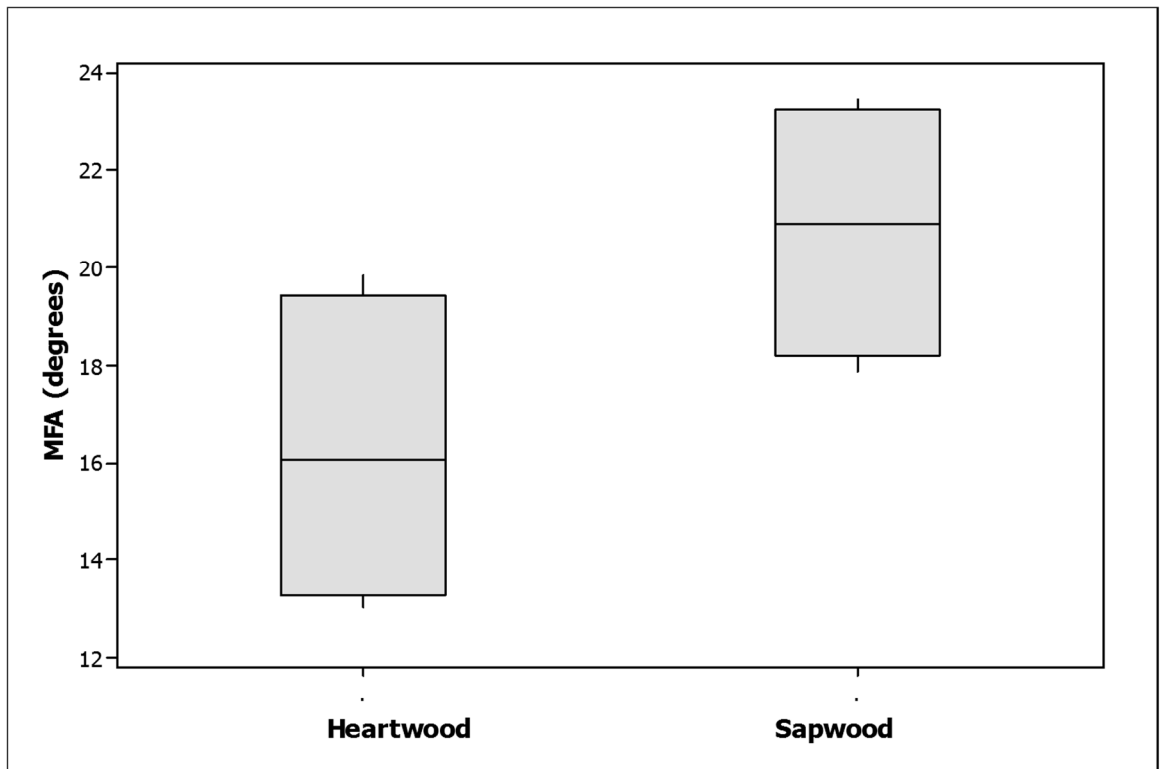
Figure 6.15: MFA in Historic pine sample HP-1500-4. The one way analysis of variance showed that the differences between the radial positions were not statistically significant in this case.
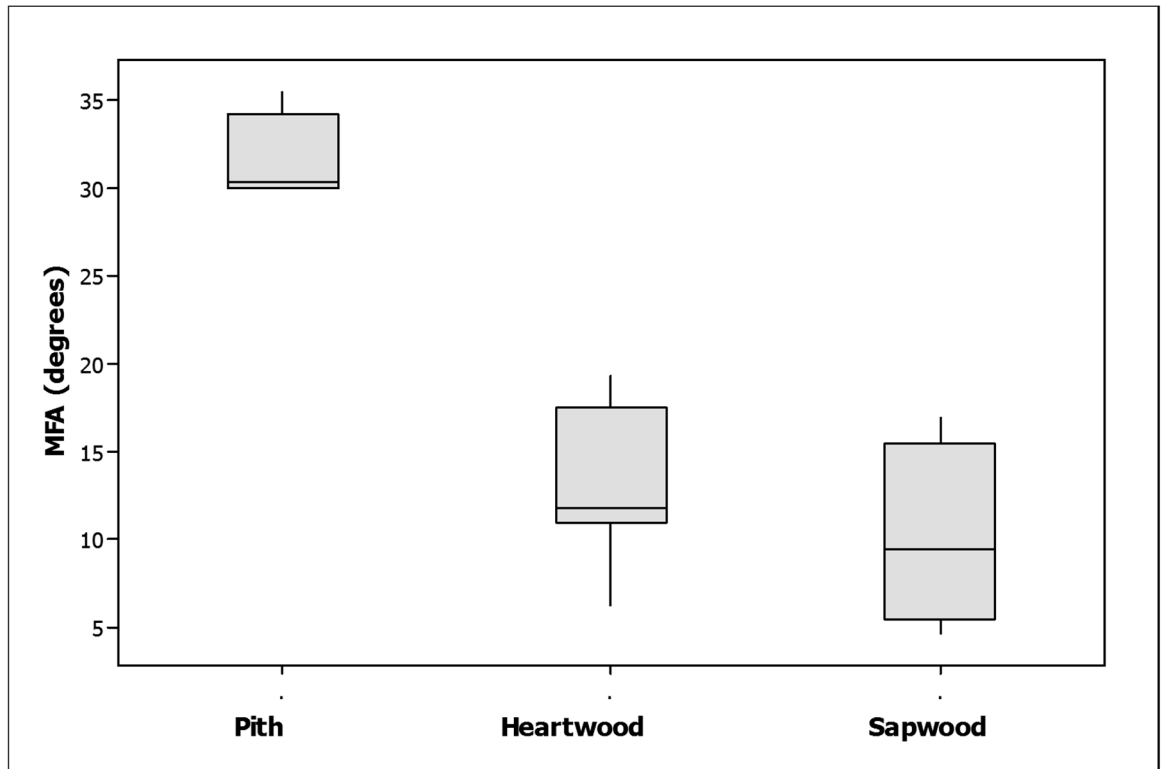
Figure 6.16: MFA in Historic pine sample HP-1500-5. The one way ANOVA shows that differences between radial positions are significant with a P value of <0.001. The Fisher test showed that the pith was significantly different (P < 0.05) from the heartwood and sapwood, but there was no significant difference between the heartwood and sapwood
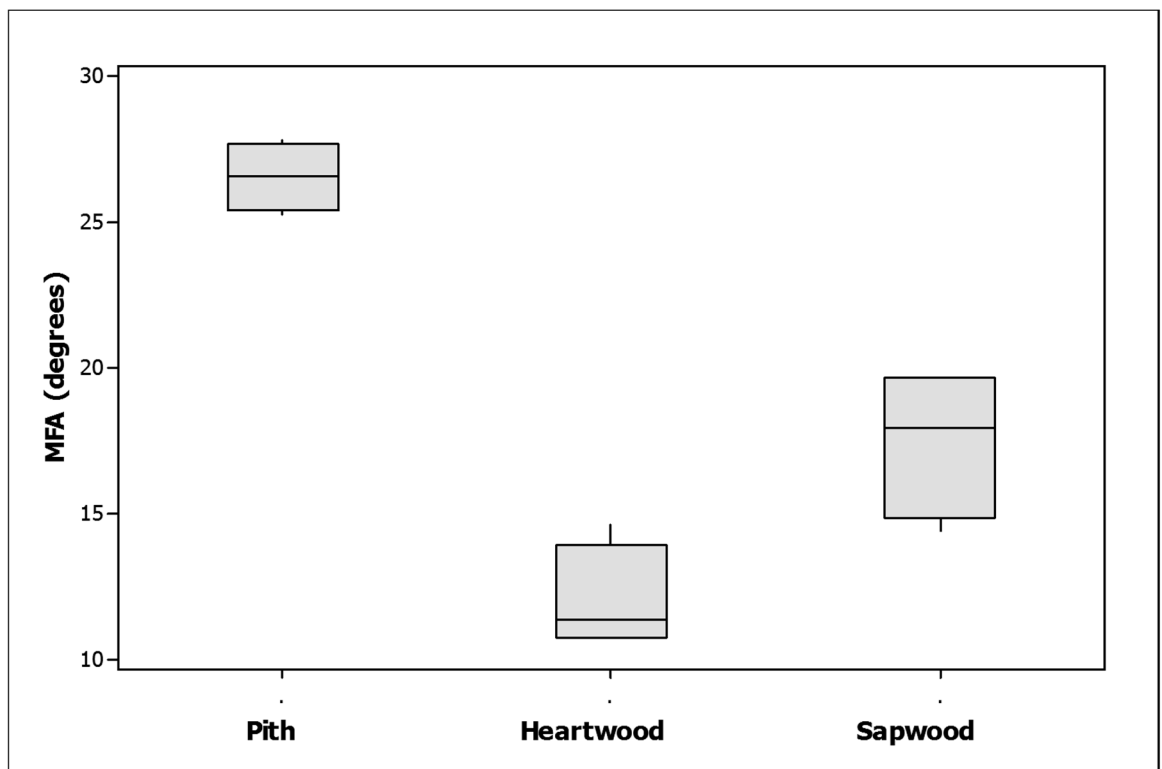
Figure 6.17: MFA in Historic pine sample HP-1500-6. The one way ANOVA shows that differences between radial positions are significant with a P value of <0.001. The Fisher test showed that all three positions were significantly different from each other.

146

MFA (degrees)	Pith	Heartwood		Bark
HP-1500-1	25.2 a	7.7	b	26.5 c
HP-1500-2	27.1 a	2.6	b	16.3 c
HP-1500-3	26. a	10.1	b	15.1 c
HP-1500-4	16.2 a	20.8	a	
HP-1500-5	31.5 a	12.9	b	10.1 b
HP-1500-6	26.5 a	11.9	b	17.4 c

Table 6.1: MFA of historic Scots pine in different radial positions.

In each row, means followed by the same letter are not significantly different, Fisher LSD (P>0.05).
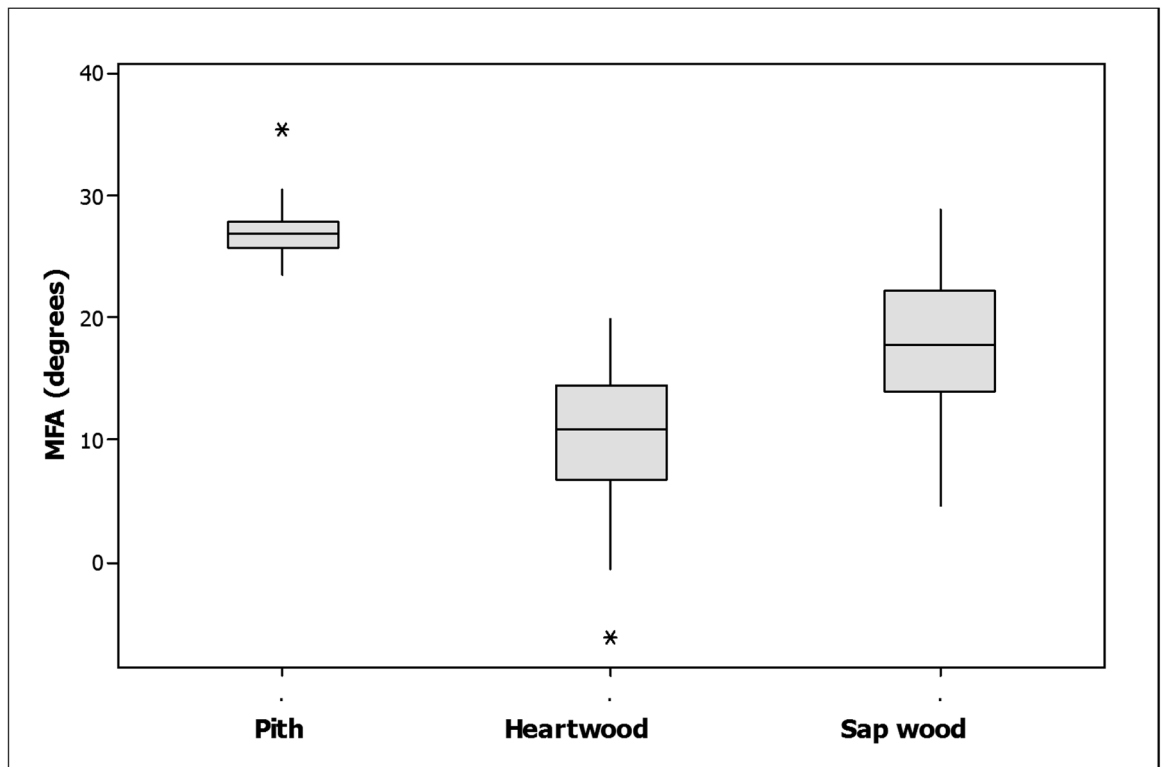
Figure 6.18: The trend of MFA from pith to bark averaged for the collective historic Scots pine samples.

_____

	Pith	Heartwood	Sapwood
MFA	27.3 a	10.6 b	17.7 c

_____

Table 6.2: Mean MFA of historic Scots pine in different radial positions.

Means followed by the same letter are not significantly different, Fisher LSD (P>0.05).
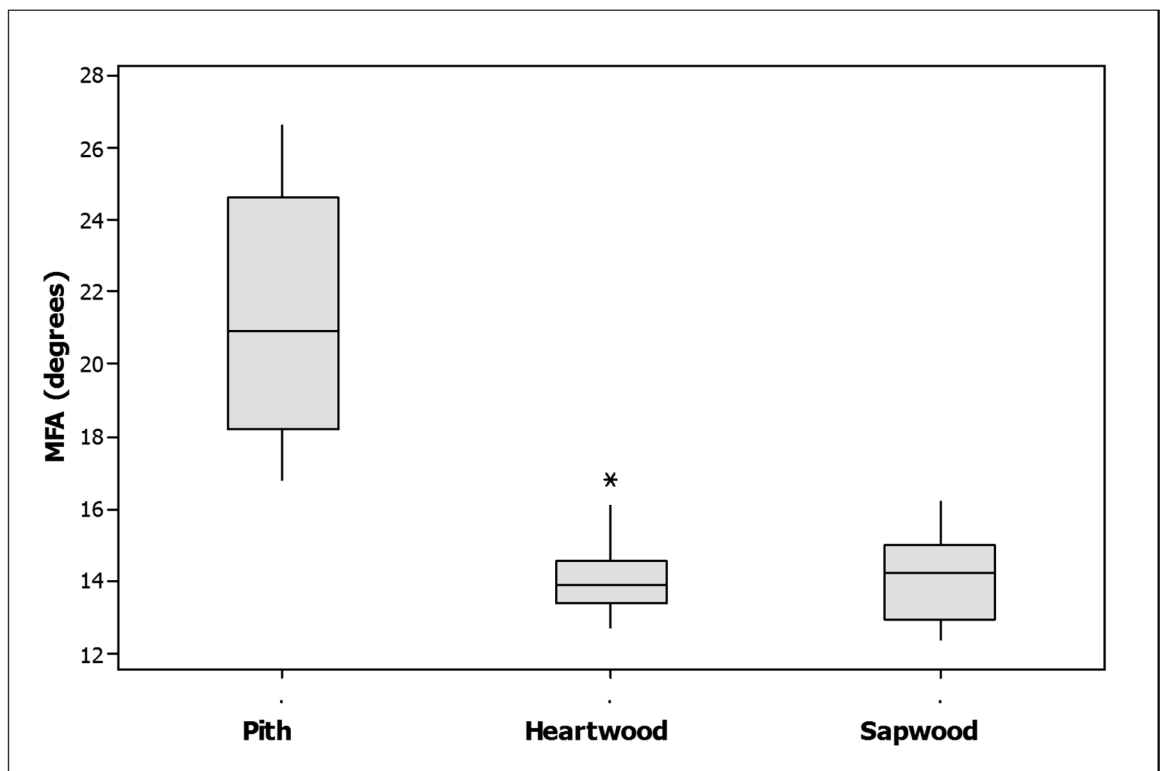
Figure 6.19: The trend of MFA from pith to bark in the modern Scots pine samples, obtained from the Silviscan data.

_____

	Pith	Heartwood	Sapwood
MFA	21.4 a	14.1 b	14.0 b

_____

Table 6.3: Mean MFA of modern Scots pine in different radial positions.

Means followed by the same letter are not significantly different, Fisher LSD (P>0.05).

Figure 6.18 shows the variation in the MFA from pith to bark in the historic wood, with all historic samples combined (figures 6.12-17). The highest MFA was at the pith as in the modern pine samples but, compared to the heartwood, there was an increase in MFA at the sapwood in historic pine (table 6.1). One way analysis of variance shows that the difference with radial position was significant. Least significant difference Fisher criteria (LSD with $p<0.05$) showed that each radial position was significantly different from the others.

This did not occur in the modern pine (figure 6.19). One way analysis of variance showed there was a highly significant difference with tree age but the Fisher test showed that the significant difference was between the pith and the heartwood (Fisher LSD $P<0.05$) and there was no significant difference between the heartwood and sapwood in the modern samples (table 6.3).

The literature states that most commonly in softwoods the MFA will decrease from pith to bark (Evans et al., 2000; Tabet and Aziz, 2013; Moore et al., 2014). Scots pine in particular follows this rule (Auty et al., 2013). It can be seen in figure 6.19 that the results from the modern Scots pine samples also follow the changes in MFA with the known growth pattern.

The results from the MFA testing of the historic wood seem to be following this trend until the sapwood, where the MFA greatly increased. Statistical analysis through one way analysis of variance and Fisher test (table 6.2) showed that this increase in MFA in the sapwood was statistically significant (Fisher $P<0.05$). This increase is not paralleled in the literature on modern pine.

There are natural variations in tree growth that cause variation in MFA (Kostiainen et al., 2009, Adams, 2014 Berges et al., 2008, Mäkinen et al., 2003), and forest management techniques such as thinning have been shown to cause an increase in the MFA (Ulvcrona and Ulvcrona, 2011), but these increases are only a temporary (Moore, 2011; Moore et al., 2009a) unlike the observations on the historic samples.

This increase in MFA at the sapwood could be explained by the biological decay of the S2 cell wall layer by fungi. Evidence of biological attack can be seen in figure 6.20 and in more detail in the microscopy images in figure 6.21.

Figure 6.20: The decayed sapwood of the historic Scots pine Image: K Hudson-McAulay.

6.5.1 Light microscopy analysis of Scots pine samples

A Leica ATC 2000 light microscope was used with objective magnification up to 100x. The microscope was fitted with a Nikon Coolpix 990 3.34 megapixel camera to provide images of the wood sections. Light microscopy can show early cell damage from biological decay (Anagnost, 1998).Thin sections from Chapter 2 were examined by light microscopy, to see if visible biological damage was present (figures 6.22-27).
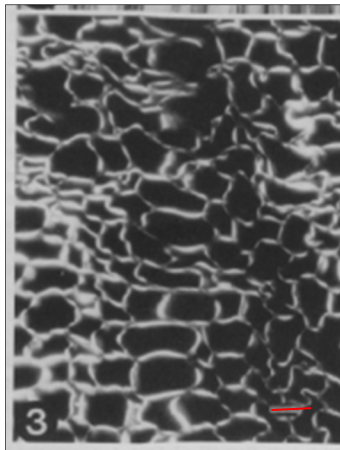
Figure 6.21: Published image of brown rot damage to wood cells. Scale bar 25 μm (Anagnost, 1998).

Figure 6.22: Sample HP-1500-01, showing damage from fungus. 1 mm scale bar. Image: K Hudson-McAulay.
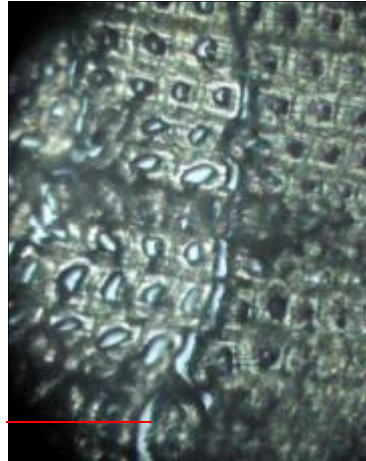
Figure 6.23: Sample HP-1500-02, showing damage from fungus. Scale bar 0.5mm. Image: K Hudson-McAulay.
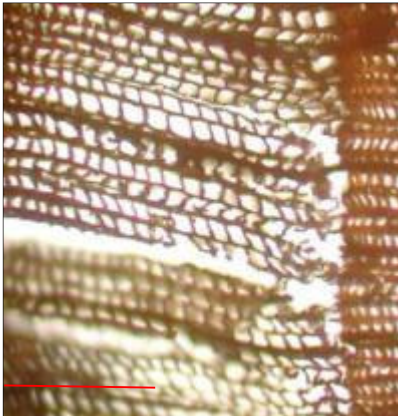
Figure 6.24: Sample HP-1500-03, showing damage from fungus. Scale bar 1 mm. Image: K Hudson-McAulay.

Figure 6.25: Sample HP-1500-04, showing damage from fungus scale bar 1 mm. Image: K Hudson-McAulay.
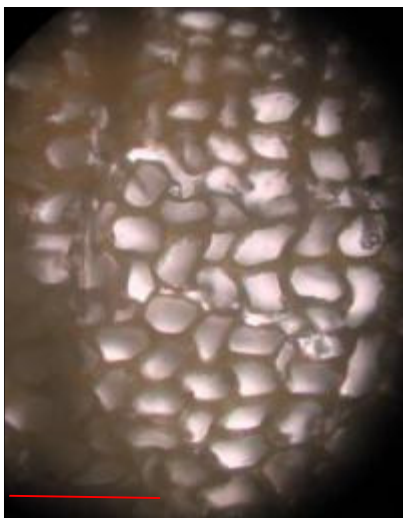
Figure 6.26: Sample HP-1500-05, showing damage from fungus. Scale bar 0.5 mm. Image: K Hudson-McAulay.
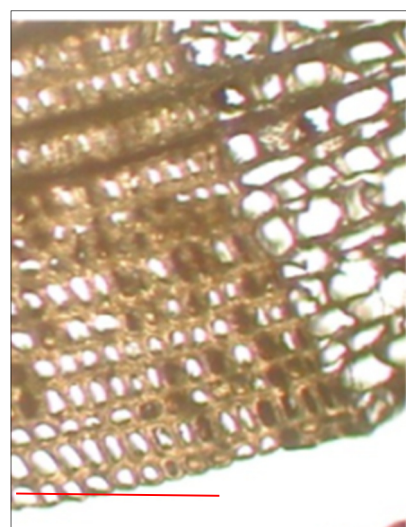
Figure 6.27: Sample HP-1500-6, showing damage from fungus. Scale bar 0.5 mm. Image: K Hudson-McAulay.

Brown rots are well known to cause thinning of the cell wall, starting from the S2 layer and working towards the middle lamella (Blanchette et al., 1985). There can be different patterns of cell thinning depending on the fungal species. One is known as general erosion where the hyphae of the fungus grow through the lumen. The other is known as local degradation where damage seems to be more localised to a certain spot in the cell wall and middle lamella (Yilgor et al., 2013).

If the S2 layer is depleted, the FTIR spectra may be derived principally from the S1 layer and the compound middle lamella, as these have much higher lignin content than the S2 layer and therefore stand up better to biological attack, especially from brown rots (Curling et al., 2001). The Scanning Electron Microscope image in figure 6.24 (Blanchette et al., 1985) shows the fungus preferentially attacking the S2 wall layer, at higher resolution than is possible by light microscopy.
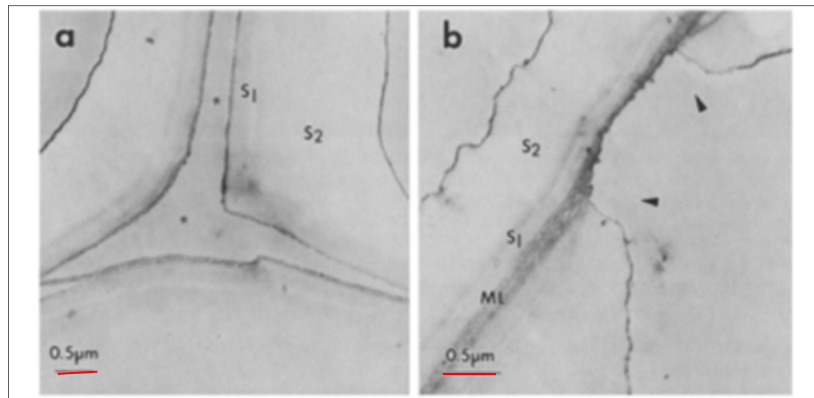
Figure 6.28: SEM image of the S2 layer being destroyed by fungus (Blanchette et al., 1985).

With the evidence from the results of the MFA experiment and the images from the microscope and the literature (figure 6.28), (Yilgor et al., 2013; Blanchette et al., 1985; Curling et al., 2001), it can be said that the increased MFA seen in the historic samples is most likely due to the degradation of the S2 layer, causing the FTIR results to be influenced by the more disorganised microfibril orientation in the S1 and primary wall layers. The increase in MFA appears to be unique to historic pine sapwood as a result of biological decay, since it is not paralleled in modern softwoods (Evans et al., 2000; Auty et al., 2012; Moore et al., 2014).

From the data in figure 6.18 and 6.19 it can be seen that generally the historic Scots pine had lower MFA than the modern Scots pine. This was to be expected as the historic samples date from the 15-1600's. At this time pine used in construction was taken directly from historic forests that had been subjected to a different climate and different management factors. Scotland's historic pine forests are considered to be semi-natural and were mostly managed for the casual extraction of timber, rather than

for commercial forestry as in modern times (Edwards and Mason, 2006; Mills and Crone, 2012). Scotland also began in import wood from Scandinavia and the Baltic regions long before England, and the dendrochronological data from the historic timbers tested here is consistent with Baltic sources as discussed in Chapter 2. In the Baltic states large forest areas went without much management, allowing the trees to grow to much older ages, producing slower grown wood of large diameter and high quality (Kisternaya and Kozlov, 2006; Tabet and Aziz, 2013). Although the samples tested here showed the modern heartwood MFA to be higher than the MFA of the historic pine, it is not difficult to get modern Scots pine with an MFA between 10° and 15° (Auty et al., 2013), so that with careful selection of timber, problems caused by differences in MFA could be avoided.

6.6 MFA determined from the dichroic ratios for Oak.
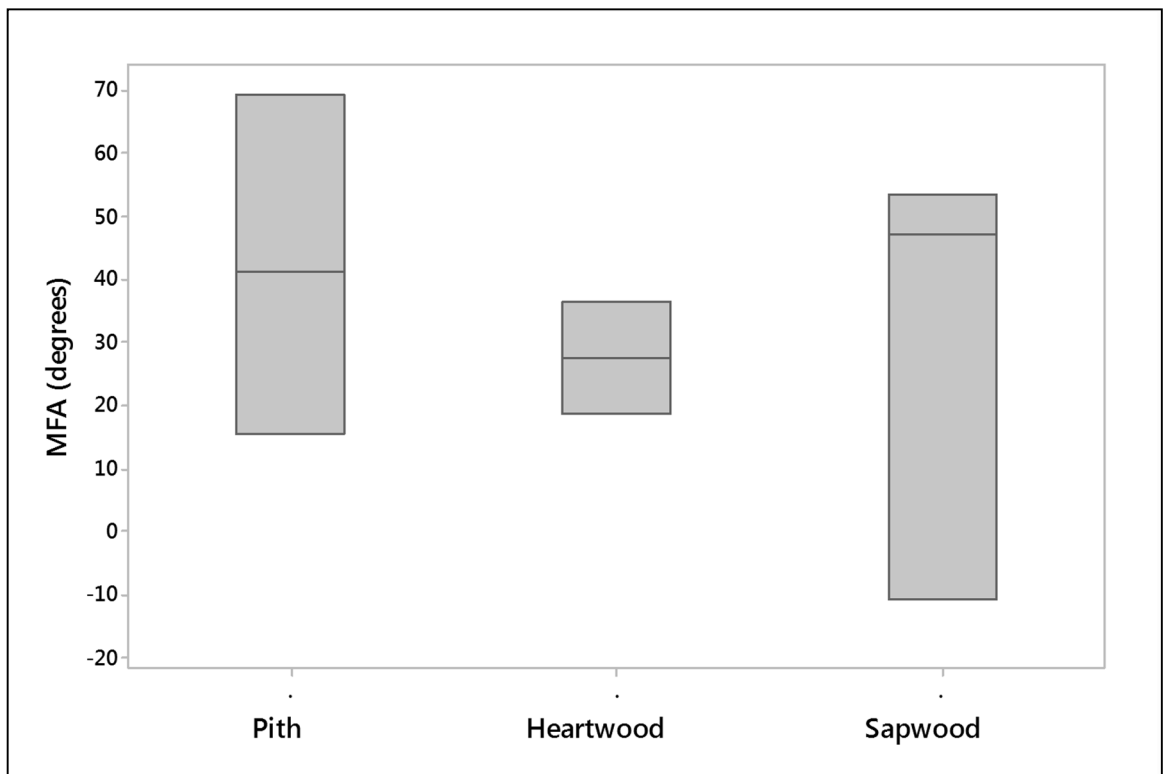
Figure 6.29: The variation in MFA with radial position in Historic Oak sample HO-1500-1. The one way analysis of variance shows that there is no significant difference in MFA between the radial positions.
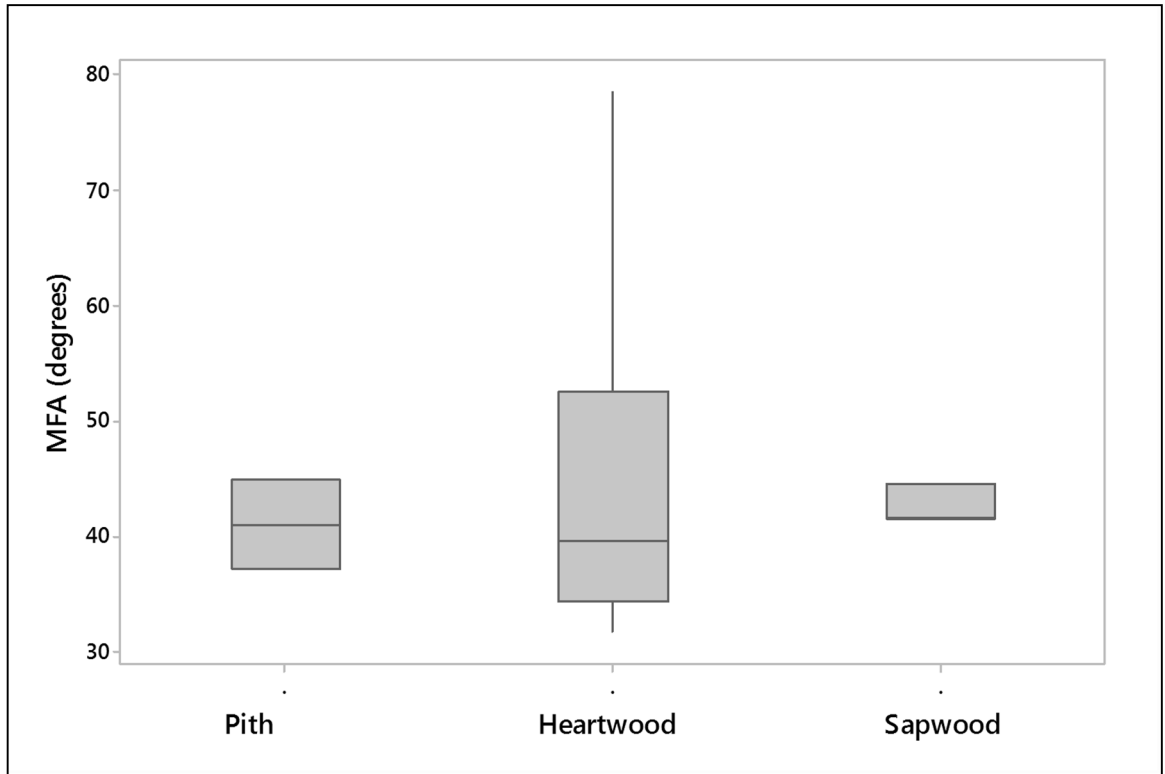
Figure 6.30: The variation in MFA with radial position in Historic Oak sample HO-1500-2. The one way analysis of variance shows that there is no significant difference in MFA between the radial positions.
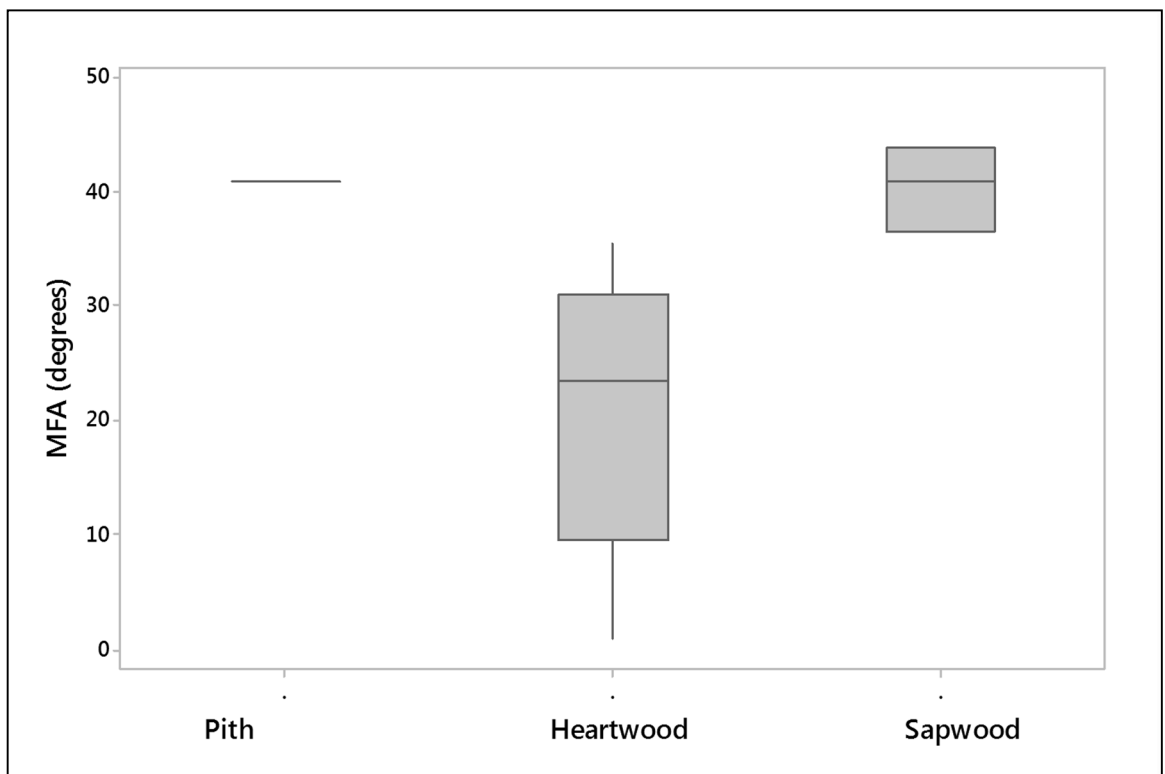
Figure 6.31: The variation in MFA with radial position in Historic Oak sample HO-1500-3. The one way analysis of variance shows that there is no significant difference in MFA between the radial positions.
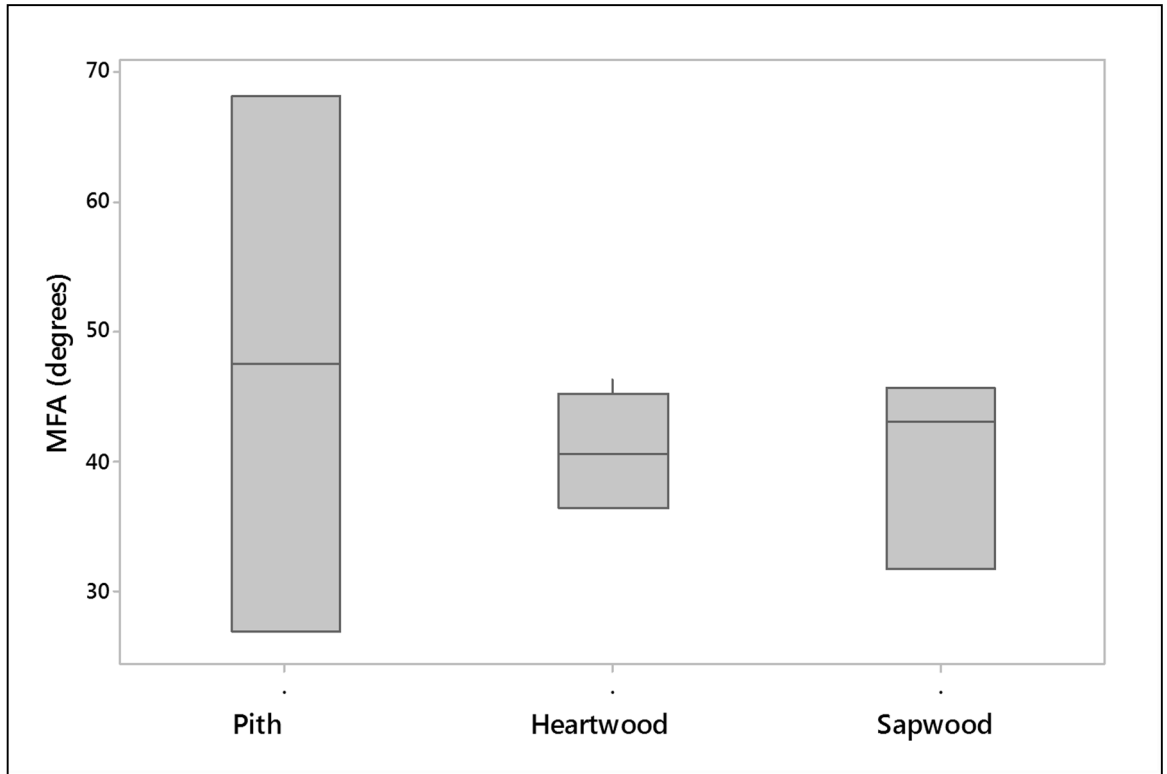
Figure 6.32: The variation in MFA with radial position in Historic Oak sample HO-1500-4. The one way analysis of variance shows that there is no significant difference in MFA between the radial positions.
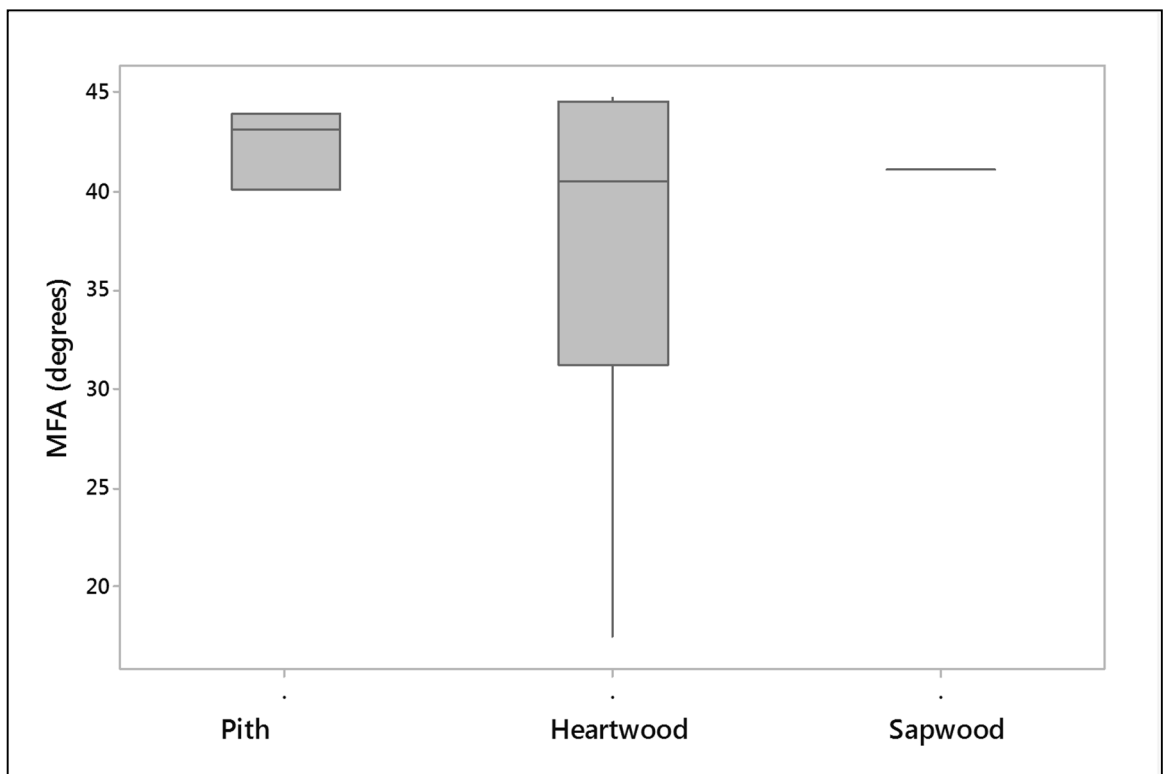
Figure 6.33: The variation in MFA with radial position in Historic Oak sample HO-1500-5. The one way analysis of variance shows that there is no significant difference in MFA between the radial positions.
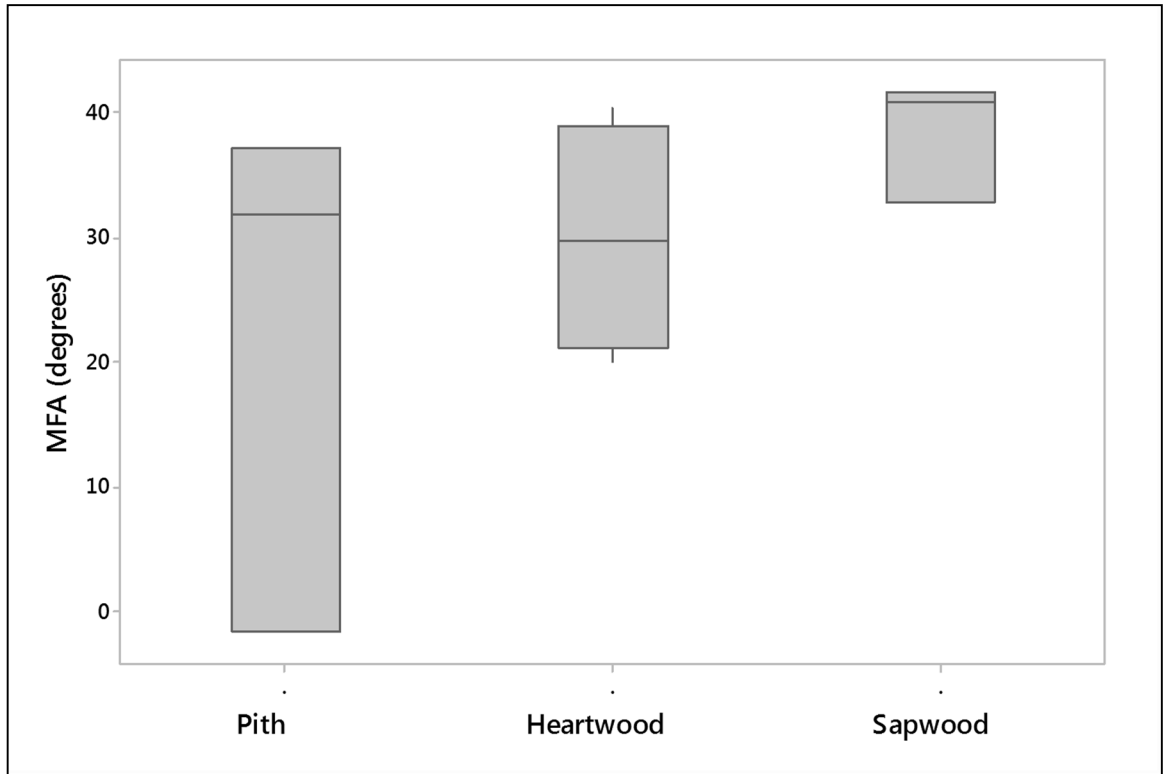
Figure 6.34: The variation in MFA with radial position in Historic Oak sample HO-1500-6. The one way analysis of variance shows that there is no significant difference in MFA between the radial positions.

MFA (degrees)	Pith	Heartwood	Bark
HO-1500-1	42	27.4	29.8
HO-1500-2	40.9	44.7	42.5
HO-1500-3	40.8	20.8	40.4
HO-1500-4	47.4	40.8	40
HO-1500-5	42.3	41.1	37.2
HO-1500-6	38.5	29.9	22.5

Table 6.4: MFA of historic oak in different radial positions.

There were no significant differences between the radial positions for any of the oak samples (ANOVA P>0.05).
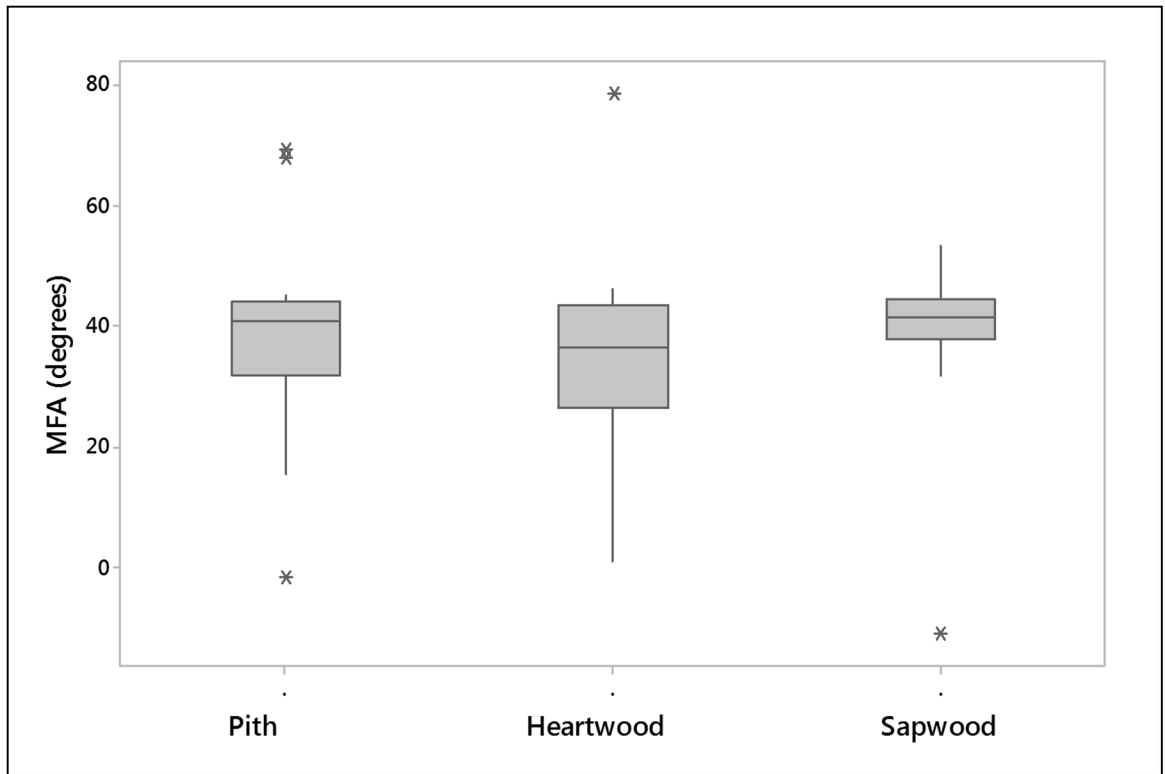
Figure 6.35: The MFA at different radial positions in Oak, averaged across the historic samples. One way analysis of variance showed that there was no significant difference in MFA between pith, heartwood and sapwood.

	Pith	Heartwood	Sapwood
MFA	38.6	34.5	38.4

Table 6.5: Mean MFA of historic oak in different radial positions.

There were no significant differences between the means (ANOVA P>0.05).

Figure 6.35 shows that there was no significant variation in the MFA of oak with radial position (table 6.4). Although the normal tendency in oak is towards little variation in MFA with radial position, it is usually slightly higher at the pith (table 6.5).

Due to the calibration being set for using Scots pine, its use with oak was only semi quantitative. As mentioned before hardwoods have not been as widely studied as softwoods (Donaldson, 2008) so it was not possible to obtain any Silviscan samples that

could be used, destructively, for FTIR calibration. Although the calibration was only semi quantitative and the measured dichroic ratios are a little high, the results fit with the literature in showing that there was very little pith to bark variation of MFA in oak (Tabet and Aziz, 2013; Donaldson, 2008; Treacy et al., 2000; Mansfield et al., 2009). Unlike the historic pine sample the historic oak sample showed no significant increase of the MFA at the sap edge (figures 6.29-34), showing that the biological decay of the historic oak was not as severe. Oak is known to have better defences against biological attack due to increased level of extractives (Bader et al., 2012; Ridout, 2000, p.15). The MFA results published on oak are not without problems, due to the fact that most have been taken from the Vasa ship and the polyethylene glycol (PEG) treatment previously carried out on the wood had to be reversed before the samples were run on the Silviscan, so some interference from this treatment may still be present in the wood samples (Bjurhager et al., 2010).

Microfibril angle, like other wood features, differs between softwood and hardwoods due to their different anatomy. In softwoods the MFA has wide variation with usually a larger MFA at the pith and smaller in the heartwood (mature wood) whereas even though the MFA is larger at the pith of hardwoods there is much less variation (Donaldson, 2008). This can be seen clearly form the results obtained (figure 6.31) from the wood tested in this experiment.

6.8 Discussion

From the MFA experiment done within this research, there was a difference in MFA between historic and modern pine. This had nothing to do with the age of the samples, but was partly the result of how the trees were grown and partly due to decay.

MFA is of importance to the timber industry as it is a factor in wood quality. This topic has been well investigated for softwoods but little work has been done at that level on hardwoods (Donaldson, 2008). There is very little literature on MFA of historic oak except what was once part of the Vasa ship with the added issue of the influence of the PEG treatment. The limited variation within the tree found in this research matches what is known about hardwoods (Tabet and Aziz, 2013; Donaldson, 2008; Treacy et al., 2000; Mansfield et al., 2009). There seemed to be little difference between the modern and historic oak. This may be due to the calibration being artificially high so that the difference may not be as clearly seen. The increased MFA in the historic pine sapwood is unlike the modern pine where the MFA in higher at the pith then falls in mature wood (Evans et al., 2000; Auty et al., 2012). The increased MFA observed in the sapwood is believed to be a result of biological decay, from the evidence in the literature of the

preferred fungal decay of the S2 layer (Yilgor et al., 2013; Blanchette et al., 1985; Curling et al., 2001).

All wood properties are interlinked and MFA, in sound wood, can be a good indicator of not only stiffness but also shrinkage (Treacy et al., 2000). This quality has been previously discussed in Chapter 4. The modulus of elasticity (MOE) and MFA are also strongly linked which can make it possible to predict the MOE from the MFA and density, as in the Silviscan analysis (Alteyrac et al., 2006).

MFA is an important factor in the use of wood for a variety of reasons and should be considered prior to timber repairs in the conservation world, although at present testing for MFA is not possible *in situ*. Only a small sample is needed but sampling is necessarily destructive. It is a key principle for the success of any repairs to wood, whether a beam, picture frame or sculpture, that the MFA should be matched to the original wood by one means or another. This will be discussed further in Chapters 12 and 13.

Chapter 7

Density

Density of conventional solids is mass per unit volume (Unger et al., 2001, p.32; Decoux et al., 2004). In this thesis density is referred to as the mass at a given moisture content / volume at the same moisture content. Normally density is considered to be the oven-dry mass / volume at current moisture content and basic density refers to the oven-dry mass / green volume, this being the volume above the fibre saturation point. The density of wood depends on the mass of the cell walls and the middle lamella, and will therefore depend on the thickness of the cell walls and the size and shape of the wood cells (Roszyk et al., 2010; Decoux et al., 2004; Vavrčík et al., 2009; Leal et al., 2011).

As density is a key property influencing the mechanical performance of wood it is important that the density for the samples used here was measured, not only to assess if there were changes in density with age, but also to account for density when assessing other properties as it will have an impact on how these are calculated (Evans and Ilic, 2001; Müller et al., 2002; Anjos et al., 2008). Density can also be used to predict some wood properties such as strength (Aydin, 2007).

The density of wood and biomass is not just important to the heritage and construction world but it is also key in the biofuel, paper and wood fibre industries. As a result wood density has been heavily researched as it affects the final product quality produced from these industries (Auty et al., 2014; Repola 2006; Hannrup et al., 1998; Machado et al., 2014; Roszyk et al., 2010).

Variation in density has an impact on the mechanical properties of each piece of wood and has a direct, linear effect on modulus of elasticity (MOE). Therefore density should always been taken in account when trying to determine the MOE of wood, as well as the MFA. The two together control wood stiffness. Density and MFA are determined at the same time by the Silviscan instrument, which uses both measurements to predict the MOE (Evans and Ilic, 2001; Auty et al., 2014; Machado et al., 2014; Hein et al., 2013).

The tensile strength of wood has been commonly predicted as a combination of these two properties and the analysis has shown that these vary between early and latewood. Earlywood is laid down during fast growth in spring; therefore the cells have a wider lumen and less cell wall material making them less dense, whereas latewood has a smaller lumen and thicker cell walls making this denser (Taylor and Franklin, 2014).

Wood density and all other wood properties are interlinked and density is one of the most important wood properties for the correct utilisation of timber (Vavrčík et al., 2009; Auty et al., 2014; Farruggia and Perré, 2000). That is why this chapter is concerned with finding out the density of historic wood in relation to modern wood to see if, and how, this property is affected by age.

7.1 Experiment

7.1.1 Sample preparation

The samples were produced from the beam ends described in Chapter 2. To get representative data for the density throughout the beam ends 5mm cubes were cut from pith to bark using a single edged razor blade to avoid losing too much material between the cubes. This allowed accurate determination of how density changes throughout each beam end; as well as allowing good comparison to the modern samples.

7.1.2 Procedure

There are different ways to measure wood density. One of the most accurate is the Silviscan which uses x-ray densitometry to gauge the density of each ring (Bergsten et al., 2001; Knapic et al., 2007; Mansfield et al., 2009; Rinn et al., 1996). This technique is very expensive and due to this is out of reach for many researchers. Another method is the use of the Itrax wood scanner which also works using x-ray densitometry. As with the Silviscan, the Itrax requires a very strictly dimensioned 2mm thick sample strip to be prepared and this was not possible on the historic material. The most common way to measure density, and the one used here in this chapter, is by measuring mass and volume on small cubes of oven dried wood (Unger et al., 2001, p. 33; Buck, 1952; Korkut and Guller, 2008). This is the most appropriate estimate of the true density of wood and is used to calibrate x-ray methods (Decoux et al., 2004; Unger et al., 2001, p.157; Hannrup et al., 1998).

The oven-dry density was measured by placing the cut samples into a fan oven at $110\,^{\circ}C$ and leaving them to dry for 4 hours. Once all the moisture was driven from the samples they were taken out of the oven and put directly into a dry, sealed environment chamber containing silica gel to prevent them from picking up any moisture from the atmosphere. As they are small samples moisture uptake would have occurred rapidly without this step.

Each sample was then weighed on a four-figure balance to 0.1 mg accuracy and was measured using digital callipers reading to 0.01 mm to determine the oven dried volume of each cube.

7.2 Results

Once the samples were weighed and measured, the oven dried density was obtained using equation 7.1 to get the oven dried volume:

Equation 7.1

V=H*W*D

Where V is volume (mm^3), H is the height (mm) of the sample, W the width (mm) and D the depth (mm).

This was then used in the equation 7.2 below to obtain the oven dried density of the samples.

Equation 7.2

ρ = (W/ (V/1000))

Where ρ is the density (mg/mm^3), W is the oven dried weight (mg) of the sample and V is the volume (cm^3) of the samples.

Once the density of the samples is known it can be used to compare the historic wood samples to their modern counterparts.

7.2.1 Oak
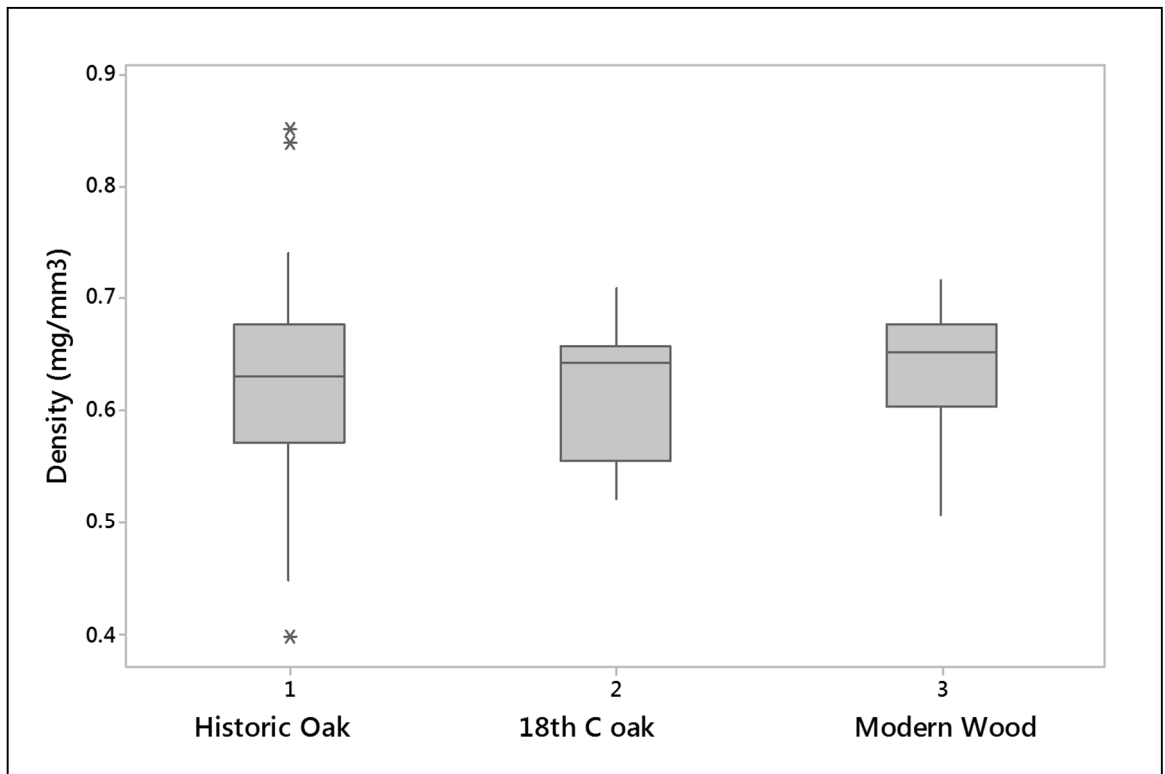
Figure 7.1: Mean density of the different ages of the oak samples.
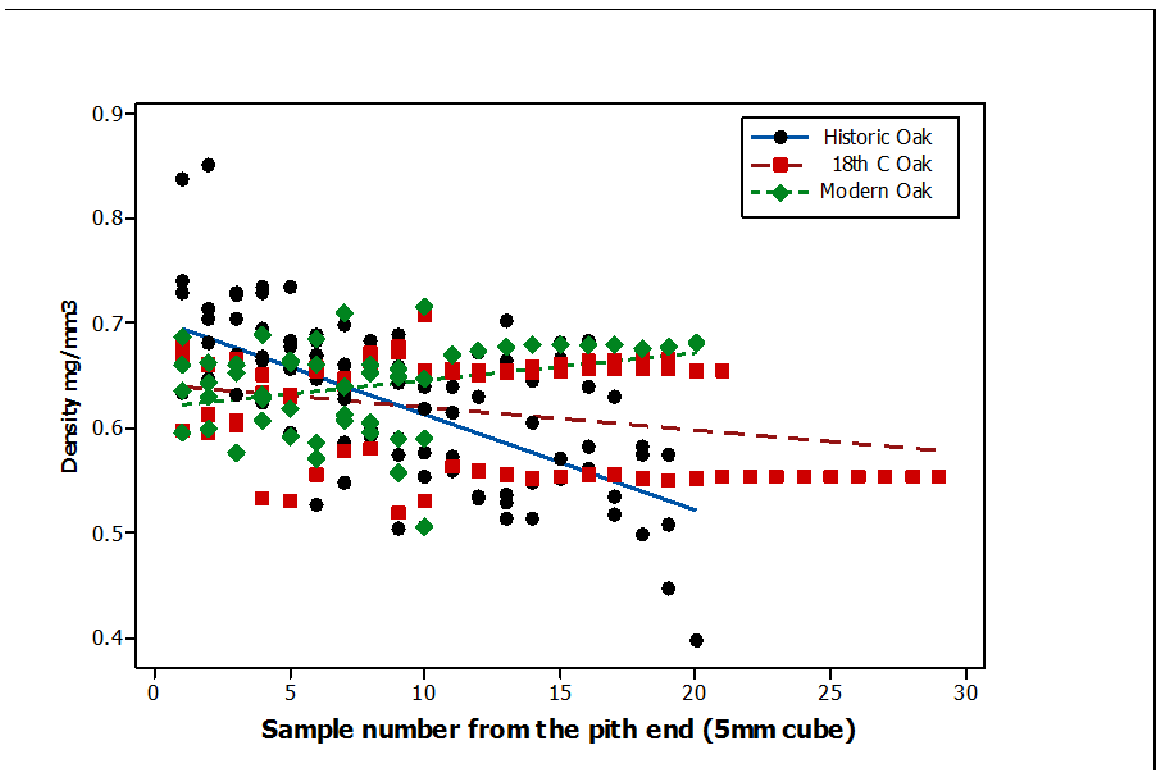
Figure 7.2: Variation in density from pith to bark of the different ages of oak.

	Historic Oak	18th C Oak	Modern Oak
Denisty	0.622	0.614	0.639

Table 7.1: Mean density of oak samples of different ages.

There were no significant differences between the means (ANOVA P>0.05).

The density results were run through a one way analysis of variance (table 7.1). This showed that there was no statistically significant difference between the different ages of oak tested, as can be seen in figure 7.1 above. These results were then put into a regression model which showed that in the 15th Century and 18th Century oak samples, densities are higher at the pith and get lower towards the sapwood (figure 7.2). Oak is known to decrease in density towards the sapwood but there can also be naturally varying density within each tree (Knapic et al., 2007). The regression model does not fit perfectly due to the data showing a kinked line, but the P value for the slope of the regression line for the historic oak is highly significant at <0.001 which means that density decreased with maturity. Many of the historic oak samples dropped in density at the bark edge. This was most likely due to loss of mass through pest infestation. The slope of the regression line for the 18th C oak has a significant P value of <0.05, but this may be just the density levelling out from the high values at the pith. The modern counterpart has a fairly even density throughout as it has not suffered any damage through biological attack. The slope of the regression is significant (P = <0.05) due to the slightly increased density in the mature wood.

Generally the biological decay of wood is confined to the bark and sapwood. This can been seen clearly in figure 7.3 below, which shows the sudden drop in density at the outer end where mass loss has occurred due to biological attack. Pest infestation is easily observed but the extent of damage caused by fungi is not, due to their ability to selectively break down wood polymers in the S2 cell wall layer through the use of enzymes.
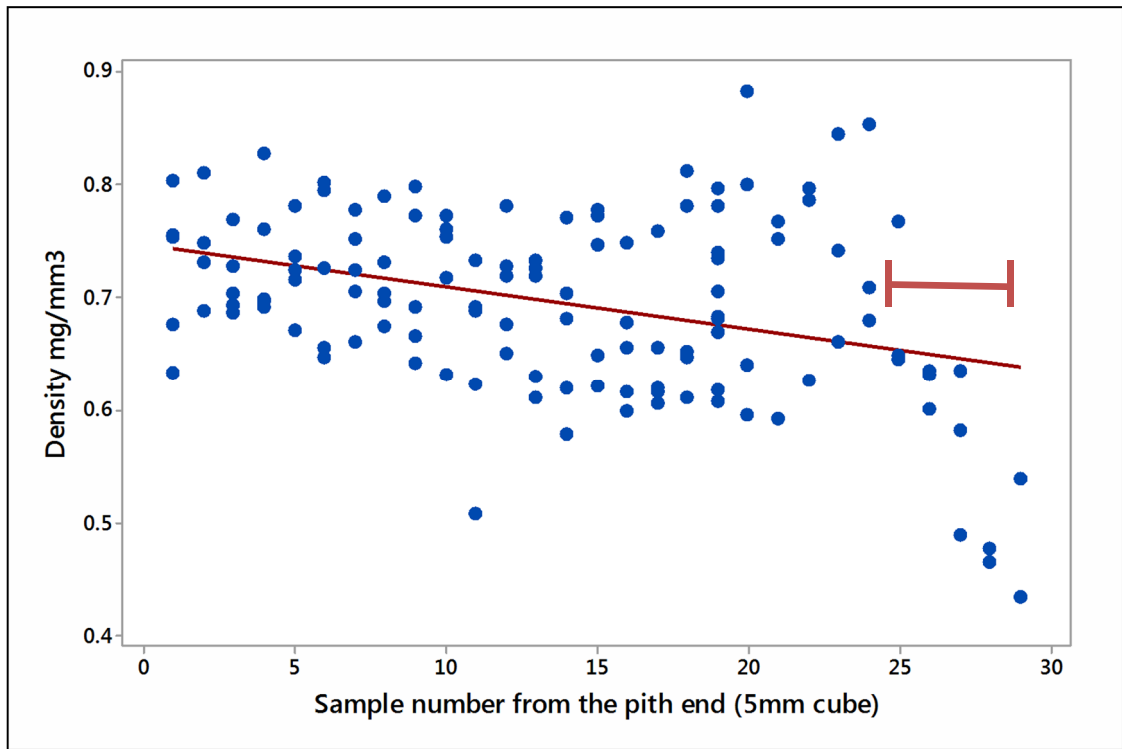
Figure 7.3: Variation in the density of historic oak from pith to bark.

	Heartwood	Sapwood
Density	0.713 a	0.617 b

Table 7.2: Difference of mean densitybetween the heartwood and sapwood.

Means followed by the same letter are not significantly different, Fisher LSD (P>0.05).

A *t*-test was then run to compare the density of the heartwood and the sapwood, as figure 7.3 shows a drop in density in the sapwood, attributed to pest action. The *t*-test showed that the difference had a highly significant P value of <0.001.

7.2.2 Pine
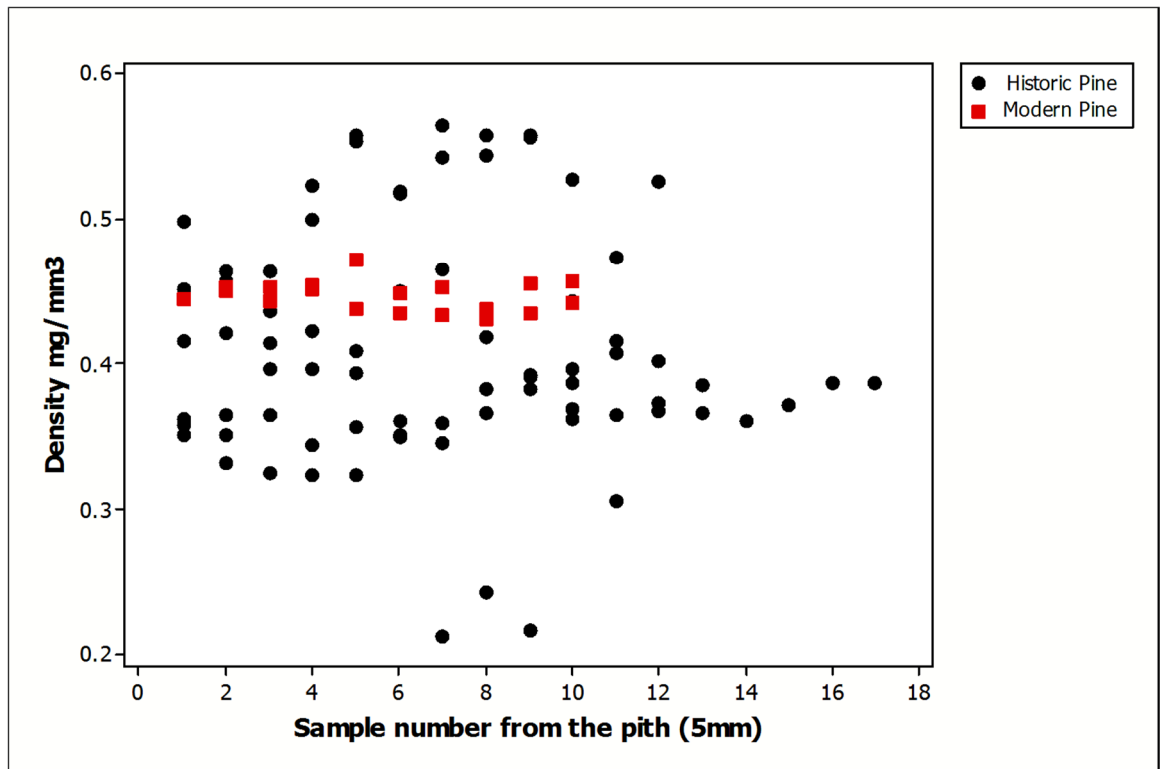
Figure 7.4: Variation in density from pith to bark of the different ages of Scots pine.

	Historic Pine	Modern pine
Density	0.41 a	0.44 b

Table 7.3: Mean density of pine samples of different ages.

Means followed by the same letter are not significantly different, Fisher LSD (P>0.05).

The density data from the historic and modern pine samples were compared in a *t*-test giving a higly significant P value of <0.001. This shows a more significant difference in density between the modern and historic pine than between modern and historic oak (table 7.3). Plotting the density from pith to bark in figure 7.4, it appears that the density of the historic pine gets slightly lower towards the bark. The P value from this regression line shows that this trend was not significant in either the historic or the modern samples. As linear regression does not detect slopes if the trend line has a kink like the one at the end of this graph, the test is not rigorous. The graph does show that the modern samples have more uniform density, which is generally higher than in the majority of the historic pine samples. A second *t*-test on the heartwood samples alone showed that there was no significant difference between the historic and modern

samples (table 7.4). Therefore the difference is most likely due to the mass loss from the pest infestation seen at the bark end in the historic Scots pine. All the modern pine samples were slightly higher in density than the historic pine samples but there was considerable tree to tree variation in the historic samples.

	Heartwood	Sapwood
Density	0.713	0.617

Table 7.4: Mean density of pine heartwood and sapwood.

There was no significant difference between the means (ANOVA P>0.05).

7.3 Using density to reveal decay.

Pest damage on the historic sample can be easily detected visually. The tunnels left by the pest will obviously reduce the density of the sample. Discovering fungal decay within a historic building is extremely difficult without seeing visual signs of the fruiting bodies of the fungus, but by that time the wood will have been severely weakened (Unger et al., 2001, p. 150; Ridout, 2000, p. 90; Desch and Dinwoodie, 1996, p. 238). Only under laboratory conditions can incipient decay be discovered. Traditionally this is done using density, as biological decay causes mass loss (Bader et al., 2012; Brites et al., 2013; Curling et al., 2001). Microscopy is also commonly used to detect fungi but this is unreliable for accurate detection of decay as it only gives a qualitative pattern rather than any form of quantitative measurement (Gelbrich et al., 2008; Clausen, 2010; Pandey and Pitman, 2003 ; Gelbrich et al., 2012).

7.3.1 Pine
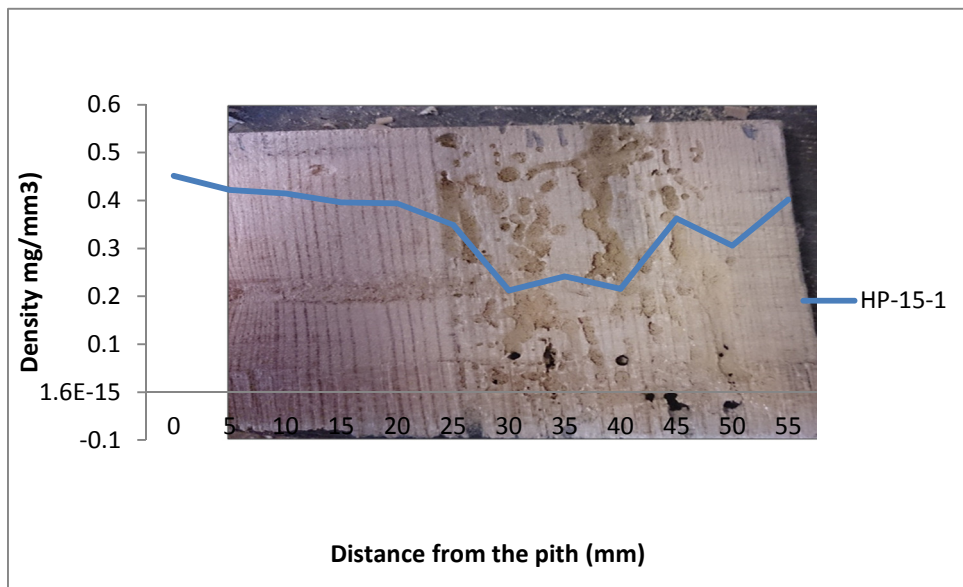
Figure 7.5: The loss in density of HP-15-1 matching the image of the biological decay.
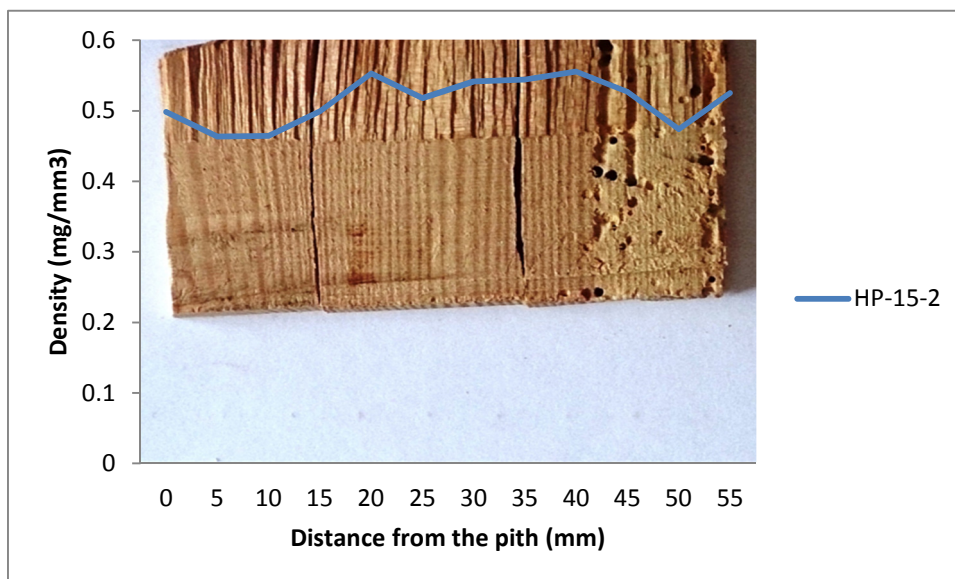
Figure 7.6: The loss in density of HP-15-2 matching the image of the biological decay.
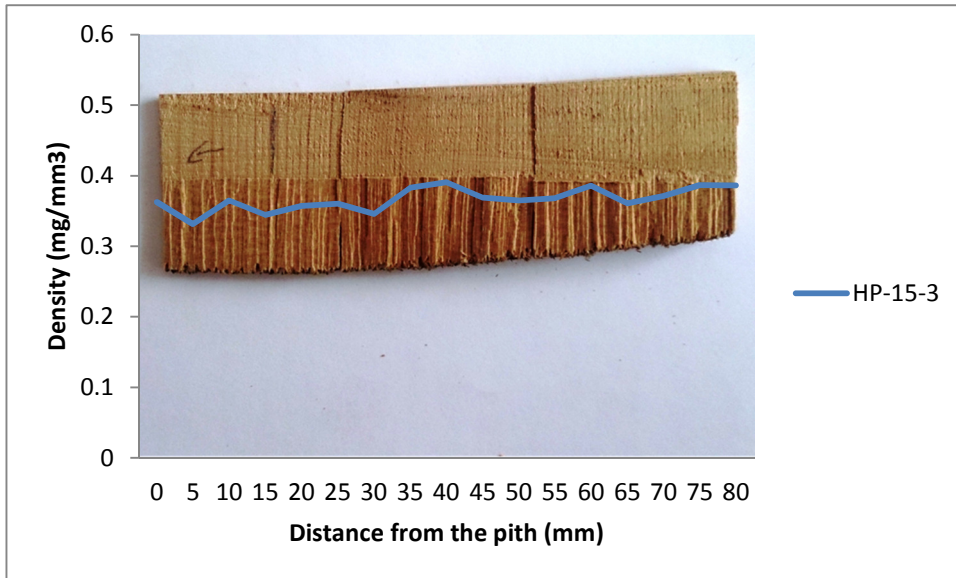
Figure 7.7: The loss in density of HP-15-3 in some areas without visible sign of biological decay.
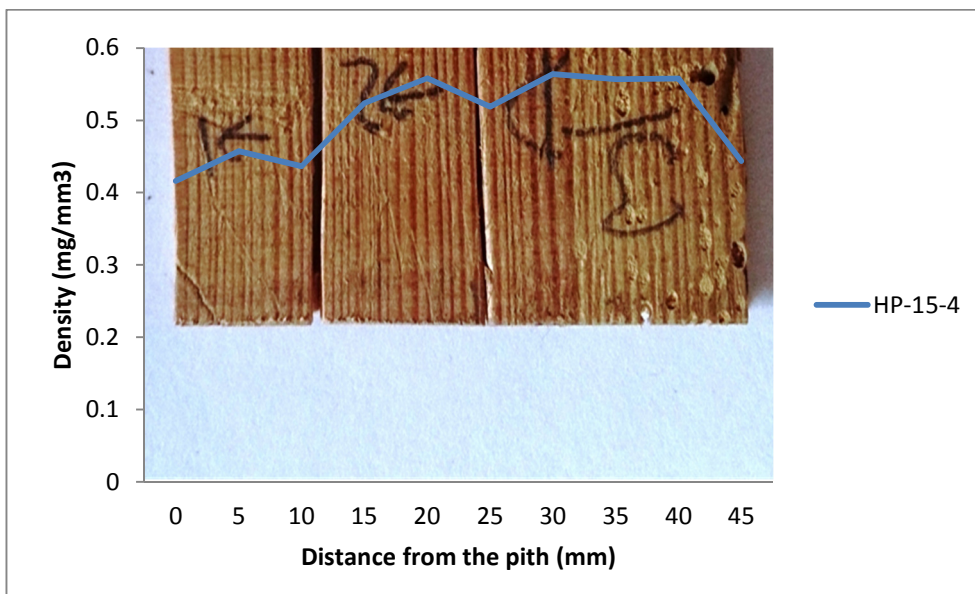
Figure 7.8: The loss in density of HP-15-4 matching the image of the biological decay.
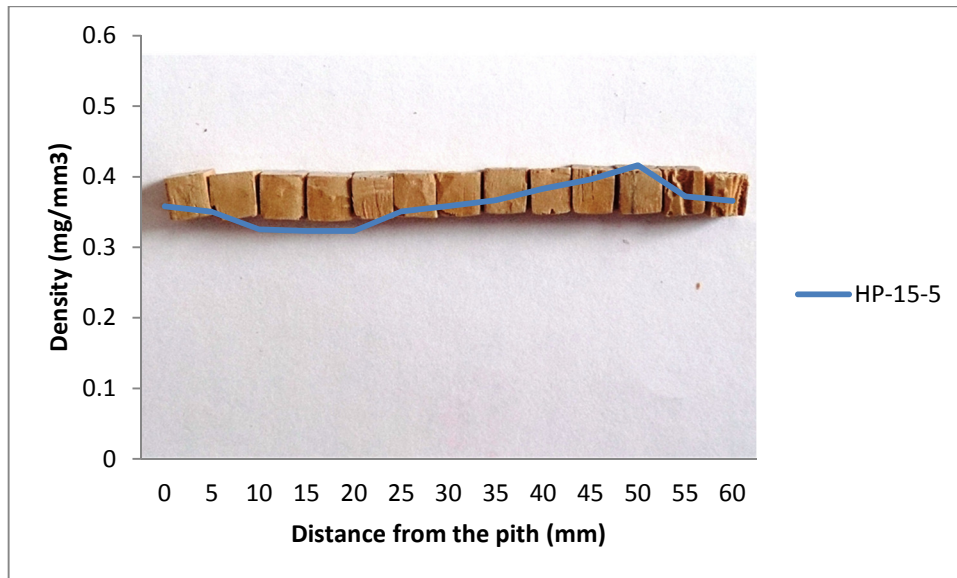
Figure 7.9: The loss in density of HP-15-5 matching the image of the biological decay.

7.3.2 Oak
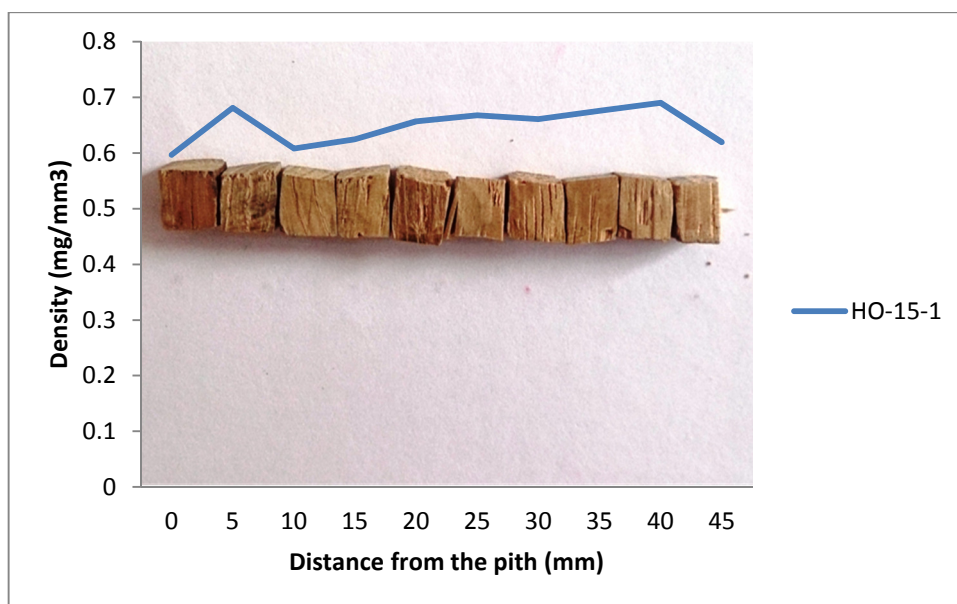
Figure 7.10: The loss in density of HO-15-1, without visible sign of biological decay.
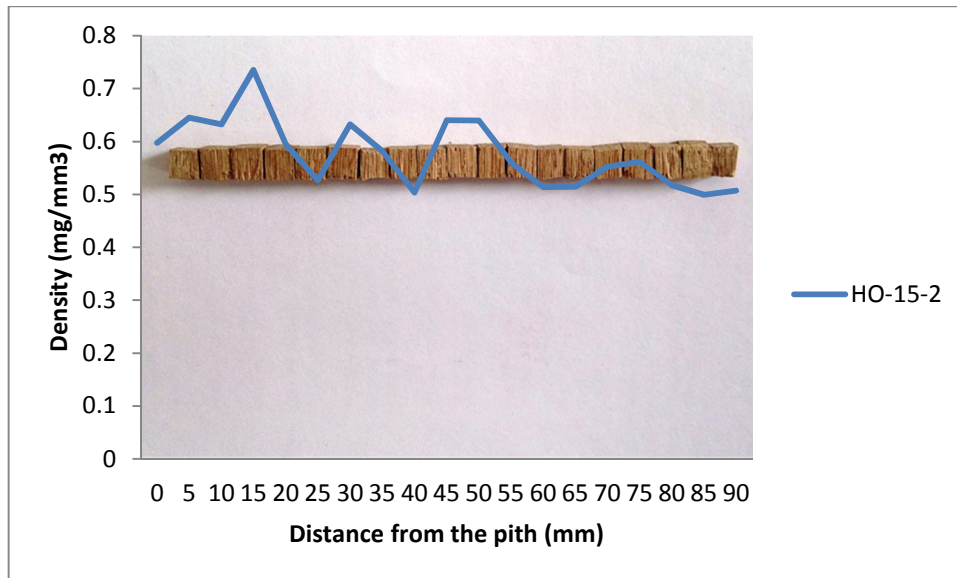
Figure 7.11: The loss in density of HO-15-2, without visible sign of biological decay.
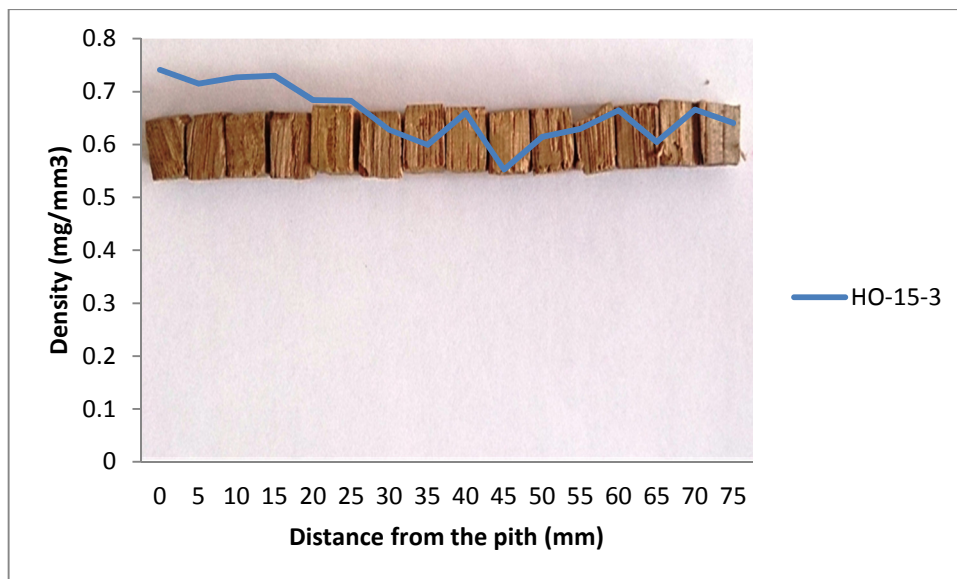
Figure 7.12: The loss in density of HO-15-3, without visible sign of biological decay.
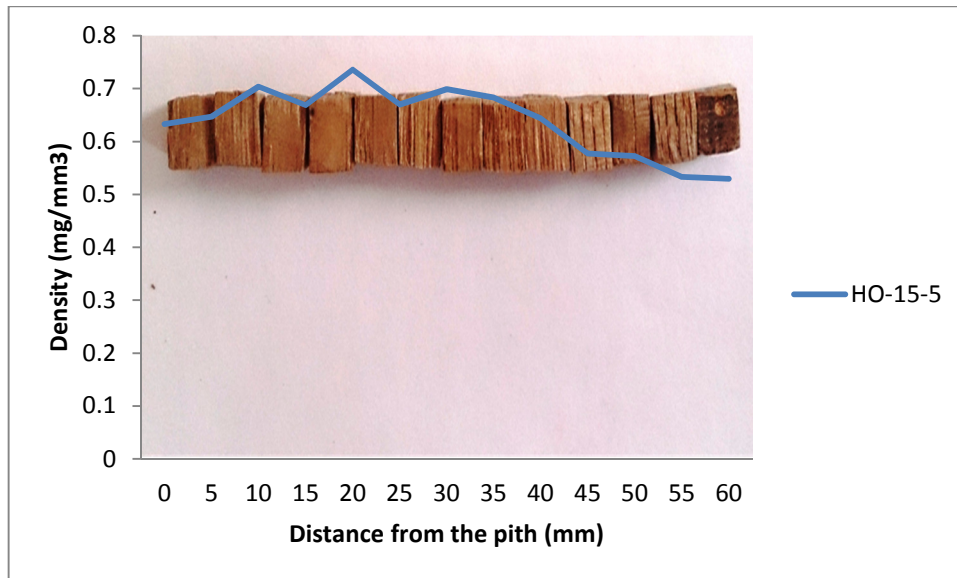
Figure 7.13: The loss in density of HO-15-4, the only historic oak sample containing visible pest decay.
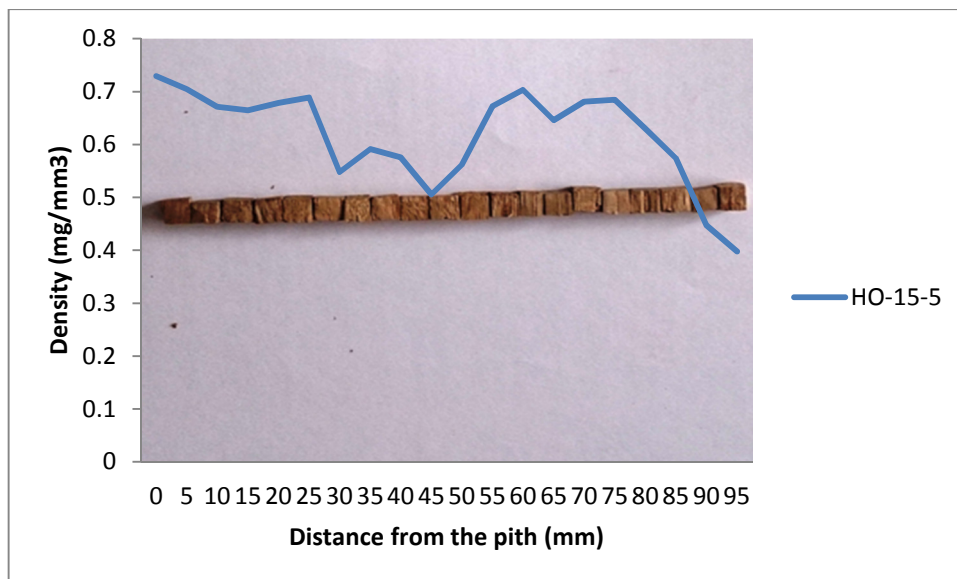
Figure 7.14: The loss in density of HO-15-4, without visible sign of biological decay.

Although the results from the density show mass loss in both the historic pine (figures 7.5-9) and oak (figure 10-14), associated with both visible pest infestation and non visible fungal decay, mass loss is considered to be an inefficient way to detect incipient decay. Once mass loss has occurred significant loss of strength has already occurred (Bader et al., 2012; Brites et al., 2013; Curling et al., 2001). This can be seen in figure 8.4 where the loss in MOE is occurring well before loss of density can be seen in figure 7.3. There are currently more accurate methods for detecting the first signs of decay, one of which is with the use of ultrasonics in which differences in wave speed can be

used for the early detection of loss in stiffness due to decay (Reinprecht and Hibký, 2011; Ross and Pellerin, 1993).

7.4 Using Density and MFA to estimate the MOE of Scots pine

As the major properties of wood are interlinked it should be possible to calculate the modulus of elasticity (MOE) of a wood sample from its density and microfibril angle (MFA), if both are obtainable. Both density and MFA in their own right influence the mechanical properties of wood. Together they comprise most of the information necessary to predict wood stiffness (Hein and Lima, 2012).

The direction of the microfibrils strongly influences the stiffness of the cell wall, in particular the S2 layer which contains most of the cell-wall mass and where the microfibril angle (MFA) is defined (Cave and Hutt, 1968; Roszyk et al., 2010). The stiffness along the microfibrils of the cell wall is closely related to the stiffness of cellulose itself (Barnett and Bonham, 2004). When the microfibrils are at an angle (the MFA) to the grain and the stress, however, the stiffness of the wood is more complex than would be simply calculated by geometry (Wagner et al., 2013; Tabet and Aziz, 2013; Cave and Hutt, 1968).

The density has a simpler relationship to stiffness as it specifies how much cell wall mass there is within a volume of wood (Unger et al., 2001, p. 37; Decoux et al., 2004; Vavrčík et al., 2009). The natural variation in both density and MFA within the cell wall is inconsistent as the tree grows. There is no strong correlation between density and MFA (Yang and Evans, 2003; Treacy et al., 2000; Roszyk et al., 2010).

MOE is routinely determined by the Silviscan wood scanner (McLean et al., 2010; Cown et al., 2005; Downes et al., 2002) but this is done directly from the X-ray diffraction patterns, not by the use of density and MFA, although these are calculated separately from the same diffraction patterns (Alteyrac et al., 2006; Hein et al., 2012; Evans and Ilic, 2001; McLean et al., 2010). A number of different equations have been described to utilize the data the Silviscan obtains, although the exact calculations used by the Silviscan in routine commercial operation are not published. Silviscan data were used here to help calibrate the estimation of the MOE of Scots pine from density and MFA. The data set used for this calibration was the same data set as was used in the original MFA calibration in Chapter 6, and was kindly provided by Dr David Auty.

7.4.1 Calibration

There are a few different equations in the literature for determining the MOE from Silviscan data (Evans and Ilic, 2001; McLean et al., 2010), but these would have required

data measured directly on historic samples with the Silviscan rather than modern Scots pine, and these data could not be obtained for this project.

Equation 1 was taken from a D/MFA graph published by Hein, et al (2013). Their data were for Eucalyptus, therefore the Slope (0.20) and the Intercept (0.43) would be incorrect for Scots pine.

<div align="center">

Equation 1

</div>

$$E_L \text{ (GPa)} = 0.20 * \rho/MFA + 0.43$$

In the notation of Hein et al (2013). E_L is equal to the MOE and ρ is the universal symbol for density.

Equation 1 works on the principle that stiffness is directly proportional to density, as would be expected and that it is also inversely proportional to MFA. Thus a linear relationship with D/MFA is expected

This can be set out as in Equation 2 below, where the notation has been changed to be in keeping with the rest of this thesis.

<div align="center">

Equation 2

</div>

$$MOE = k_1 D/MFA + k_2$$

Where k_1 and k_2 are constants and D is density.

To adapt Equation 2 to work for Scots pine the slope k_1 and the intercept k_2 of the relationship between MOE and D/MFA need to be determined. This was done using the Silviscan data for modern Scots pine samples for density, MFA and MOE; available from the data given by Dr David Auty which can be found in Auty (2013). This can then be used to construct Equation 3 and applied to the historic samples.

The Silviscan data is plotted in figure 7.15 below:
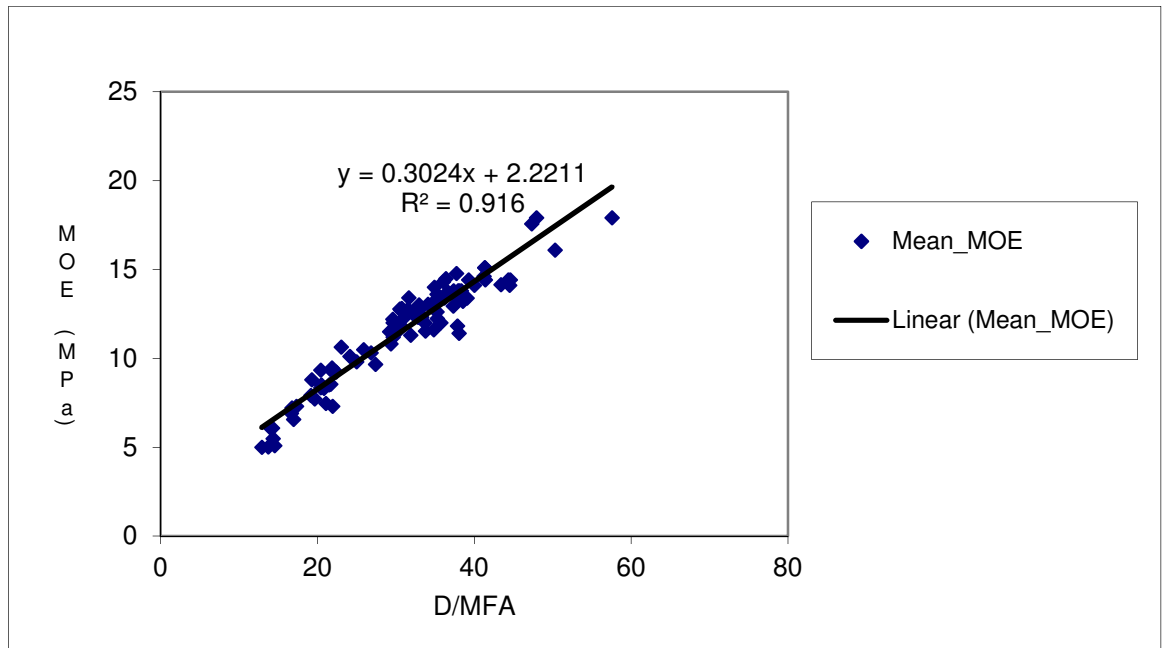
Figure 7.15: The relationship between MOE and D/MFA for the Scots pine samples measured by Silviscan.

Equation 3

MOE= 0.3 * D/MFA + 2.2

Where MOE is the modulus of elasticity, 0.3 is the slope k_1 taken from figure 7.15, D is the density, MFA is the microfibril angle and 2.2 is the intercept k_2 again taken from figure 7.15. This equation was then used on the historic samples, taking the density and MFA from the measurements on the historic samples and using the slope and intercept from the Silviscan calibration.

7.4.2 Results

The results below show the variation in predicted MOE for each of the historic samples from pith to sapwood.
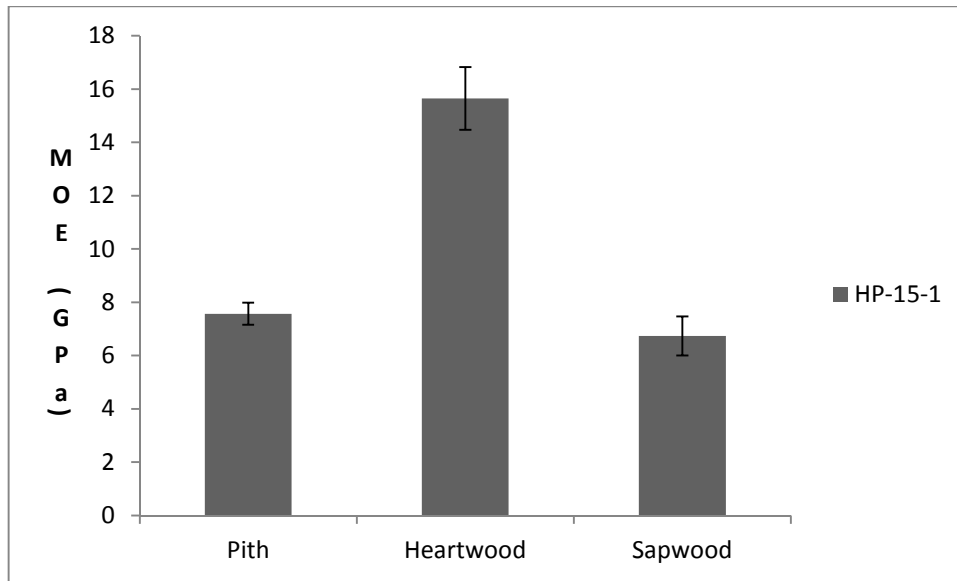
Figure 7.16: The MOE at different radial positions in historic Scots pine sample 1500-1.
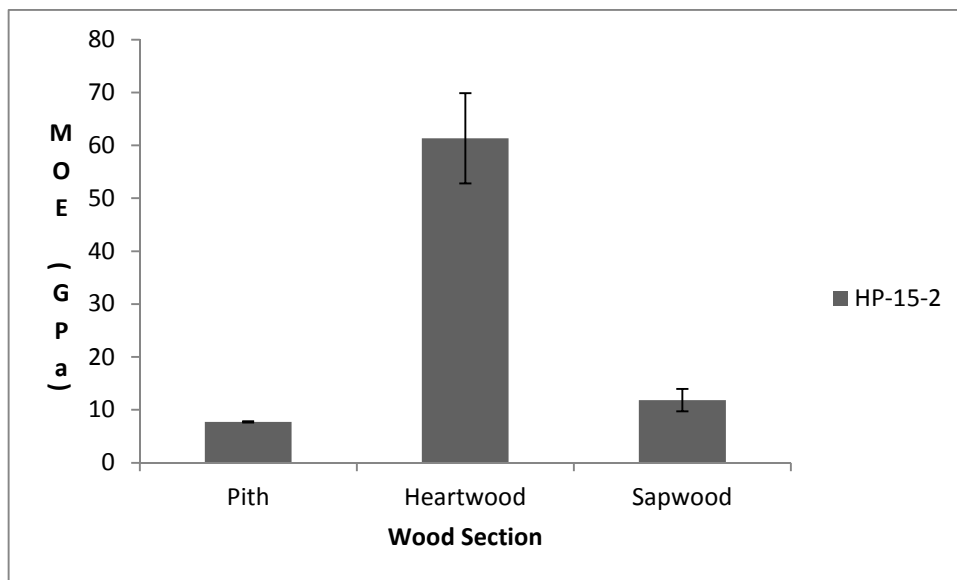
Figure 7.17: The MOE at different radial positions in historic Scots pine sample 1500-2.
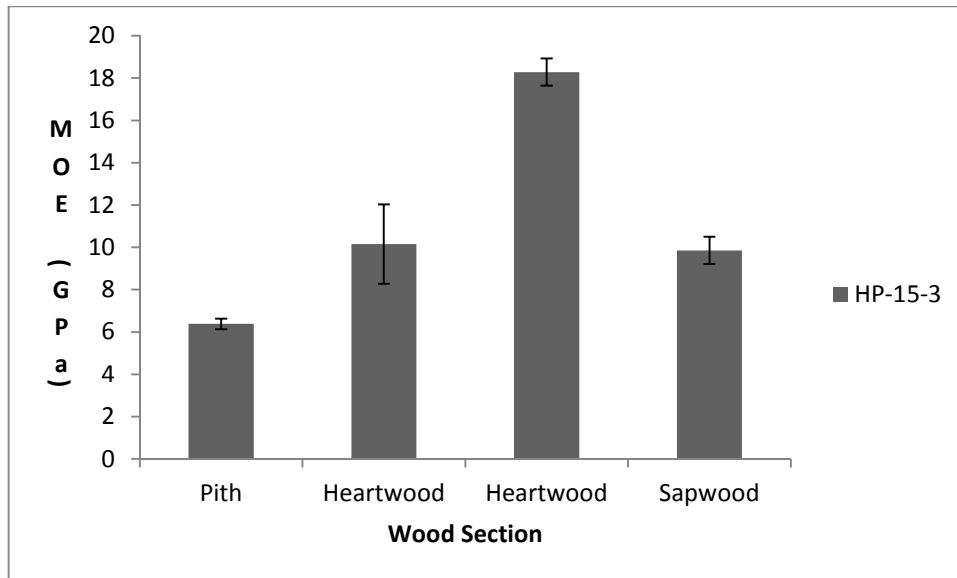
Figure 7.18: The MOE at different radial positions in historic Scots pine sample 1500-3.

Figure 7.19: The MOE at different radial positions in historic Scots pine sample 1500-4.
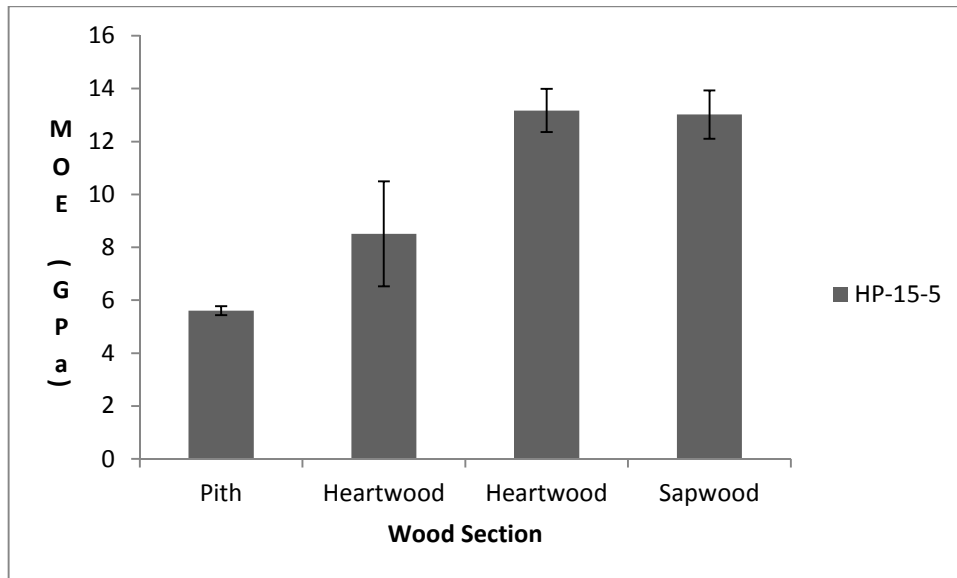
Figure 7.20: The MOE at different radial positions in historic Scots pine sample 1500-5.

Figure 7.21: The MOE at different radial positions in historic Scots pine sample 1500-6.

From figure 7.16 to 7.21, the MOE for the pith and heartwood of most of the historic pine samples are within the range of MOE seen in good quality modern Scots pine. This excludes sample HP-15-2 which has a recorded MOE that is exceptionally high (figure 7.17). This is due to the very low measurement for the MFA for this sample, which was beyond the range of the Silviscan calibration. This may have caused the MOE for this sample to be overestimated, as going beyond the calibration range can introduce considerable uncertainties. The uncertainties are due to there being no assurance that beyond the range of the calibration the relationship is still a straight line. If it curves, this will result in over-estimation of the MOE.

The historic Scots pine also, in general, shows a lower MOE at the pith than in the heartwood, as is found in modern Scots pine. As can be seen from figure 7.16, 7.17, 7.18, 7.19 and 7.21 (figure 7.20 is the exception), the majority of the historic Scots pine samples have been predicted to drop in MOE at the sapwood.

The drop in the MOE of the historic pine sapwood is not normally seen in modern Scots pine, which in general increases in MOE towards the bark edge (Wagner et al., 2013; Auty et al., 2012; McLean et al., 2010; Moore et al., 2009b; Cowdrey and Preston, 1966). This difference may correspond to fungal damage in the sapwood which has caused the predicted MFA to increase through loss of the S2 cell wall layer as described in Chapter 6. The MFA used is being obtained from other cell wall layers which have a more disordered microfibril orientation and may be having a much smaller effect on the longitudinal stiffness.

The calculation of the MOE as described here is certainly not enough for the accurate prediction of MOE for historic Scots pine. Lower MOE is expected in decayed timber, but although Sample 1500-5 (figure 7.20), suffered from decay through pest infestation which is clearly visible in figure 7.22, a drop in MOE was not detected using this method of obtaining MOE. Also the MOE given for the sample 1500-06 in figure 21 is much higher than would be expected with the level of pest infestation seen in the sapwood of this beam end in figure 7.22. The presence of pest holes is erratic and if they are distributed over the sample they could induce large random errors in the measurement of density and the calculation of MOE. This is consistent with the theory that while fungal decay destroys the S2 layer affecting the average MFA, pests leave nothing behind so that the MFA recorded is from unaffected neighbouring cells. Figure 7.23 shows no apparent decay by pests, yet figure 7.21 has the same drop in MOE at the sapwood showing that even though fungal decay may not be visible it can still be doing considerable damage to the sapwood.

Figure 7.22: Image of pest infestation on sample 1500-05 Image: K Hudson-McAulay.

Figure 7.23: Image of sample 1500-06 with no pest infestation present Image: K Hudson-McAulay.

7.5 Discussion

From the results it can be seen that in both historic pine and oak there was a decrease in density towards the bark. Although a decrease in density towards the bark is usually seen in oak, due to it being a ring porous hardwood, it is not normally as steep and, in this case, can to some extent be accounted for by mass loss due to biological attack (Unger et al., 2001, p. 157; Sousa et al., 2014).

Pest infestation will cause other forms of weakness in the mechanical properties of wood and there have been reports of loss of strength towards the outside of the beam where biological attack has taken place (Grabner and Kotlinova, 2008). The mechanical properties of timber may change with age and in addition, how loss of density due to pest infestation weakens timber will be discussed further in Chapter 11. But further damage from fungal attack could weaken the wood and be less easily visible through loss of density. Fungal enzymes cutting the cellulose chains may degrade mechanical properties but this will not be as easily seen on the surface, as is discussed further in Chapter 11.

Although the results show that both species of historic wood decreased in density from pith to bark, the significance of the difference with age was not as strong in oak. This may be due to the large variation in density naturally found within each tree, and the quality of the wood, especially the latewood, of each tree (Machado et al., 2014; Dutilleul et al, 1998; Vavrčík et al., 2009; Zhang 1993; Krauss et at., 2011). Density depends largely on how the trees were grown, their genetics and their ages. The historic wooden beams came from trees that were grown in historic forests, grew slower and were felled at a much greater age, whereas today trees are produced by careful silviculture to maximise wood yields (Cown et al., 2005; Gryc et al., 2011; Gapare et al., 2012; Guilley et al., 2004; Hannrup et al., 1998; Berges et al., 2008; Mather and Savill, 1994).

Many things in a tree's growth can also affect its density, such as the ratio of juvenile to mature wood and the frequency of knots. This again emphasises the need for careful selection of wood for repair work to historic timbers (Beaulieu et al., 2006; Lasserre et al., 2009). In the case of some wood species such as beech, density and other quality characteristics have not been studied as closely and need to be more carefully considered when sourcing replacement material for traditional repairs (Bouriaud t al., 2003).

The aim of this chapter was not only to compare the density of the historic and modern wood but also to look at density as a key factor influencing many other properties (Knapic et al., 2007; Vavrčík et al., 2009; Korkut and Guller, 2008). It is already well

known that density alone cannot explain the mechanical behaviour of wood (Hein et al., 2013), but it works in conjunction with the microfibril angle of the cellulose fibres to give the wood its stiffness (Treacy et al., 2000). Therefore density will also be important for correctly determining many of the other wood properties throughout this research.

The methods used here for measuring both density and MFA are destructive. However in some cases it may be worth sacrificing the small amount of historic timber needed for the test to provide a more accurate match between new and old wood in traditional repairs. This would be unnecessary for every timber but for the main structural beams, the closer it is possible to match the current timber the more success the repair will have in prolonging the life of the building.

Chapter 8

3-point Bend Testing

Longitudinal stiffness, more accurately described as the longitudinal modulus of elasticity (MOE), is one of the most important qualities of wood and is greatly desired for wood in modern buildings. The longitudinal MOE (longitudinal Young's modulus) is important for wood in historic buildings to continue to meet the building regulations in place to determine their safety, because it is required for all calculations of load-bearing capacity in structural members.

Longitudinal stiffness is controlled by a combination of density and microfibril angle (MFA) (Evans and Ilic, 2001; Koponen and Virta, 2004; Bjurhager et al., 2012). Bending tests actually expose the beam at the same time to different types of stress, which all contribute to its MOE. With a downward load, the top part of a beam is under compression stress whereas the bottom part is under tensile stress. These tensile and compressive stresses cause a band of shear stress running through the middle of the beam. Shear stress running parallel to the grain, such as this, is known as horizontal shear (Varner et al., 2012). The structural characteristics of the wood affect its longitudinal bending stiffness just as they affect the other mechanical properties of wood. These characteristics are to do with the anatomy of wood whilst the tree is growing, such as ring width, cell structure, density and the proportion of latewood to earlywood (Alteyrac et al., 2006).

During deformation of wood the load is carried principally by the cellulose microfibrils. Therefore the elastic (reversible) stiffness is dependent on the angle at which the microfibrils are laid down, relative to the axis of the wood. This is known as the microfibril angle. As discussed in Chapter 6 microfibril angle has a huge effect on the mechanical properties of wood. MFA particularly affects the stiffness of wood. Wood will always be stiffer in the direction of the microfibrils than in the transverse direction (Kärenlampi et al., 2003). This often dictates the design of timber structures as stiffness properties are critical to how the wood is used in the design (Varner et al., 2012). Any change in stiffness from old wood to new within a splice or joint will have a critical effect on its success.

The MFA in the wood of a sapling is large, to allow the young tree to flex. As the tree grows the MFA becomes smaller to allow the mature wood to be stiff against the wind. This affects the mechanical properties found throughout the tree and results in varying

properties within a piece of timber, with less stiffness at the central pith and more stiffness in the older wood immediately under the bark (Altaner and Jarvis, 2008). Although wood is an elastic material, the tensile behaviour of isolated single wood cells is not wholly elastic, but has been shown to involve an irreversible 'molecular velcro' effect above its yield stress, as it does not show any loss of strength on elongation. A single cell can actually stretch further than wood without fracturing. The hemicellulose polymers are responsible for this molecular 'velcro' effect by detaching, one hydrogen bond at a time from a microfibril, allowing it to slide further without failure and then to reattach once the strain has stabilised (Altaner and Jarivs, 2008). Alternatively plastic (irreversible) deformation may be caused by shearing of the hemicellulose and lignin matrix between the microfibrils leading to viscous flowing of the matrix material (Keckes et al., 2003; Fratzl et al., 2004; Bjurhager et al., 2010; Bjurhager et al., 2012). The modulus of pure, crystalline cellulose fibres has been estimated at 134 GPa (Burgert, 2006) but this figure, often quoted in the literature, is too high for wood cellulose. It relates to crystalline cellulose which comprises less than 50% of all wood cellulose (Thomas et al., 2014). The matrix polymers only have MOE of around 40 MPa for hemicellulose and possibly about 2GPa for lignin, demonstrating again that wood stiffness is derived from the cellulose microfibrils (Burgert, 2006). Through FTIR experiments cellulose has been shown to have a more elastic response than the other wood polymers when measured by stretching the links between the glucose rings (Altaner et al., 2014a; Hinterstoisser et al., 2000).

The stress strain graph for wood shows an initial steep slope after the slack has been taken up. After the initial steep linear phase, the wood breaks or goes into permanent plastic deformation where the strain flattens out. With increasing load applied beyond this yield point, damage is caused to the material (Burgert, 2006; Lipovszky and Raczkowski, 1971; Schneeweiß and Felber, 2013).

Tensile testing of wood is more difficult than for materials like metals, because of practical problems in attaching the ends of the sample without weaknesses due to splitting or crushing. Bending tests avoid these problems.

Within the literature there are different ways to carry out bending tests on wood. These include 3-point bending, 4 point bending and central loading tests (Schneeweiß and Felber, 2013). Bend testing measures the stiffness of wood using an adapted tensile testing machine.

It is common to calculate the tensile stiffness from the results of a three-point bending test neglecting the shear component and assuming that the tensile and compression moduli are equal. The result is often expressed as the Young's modulus, meaning the elastic stiffness. Elastic properties are measured at low stress levels applied to the

wood, which can completely recover once the load has been removed. If the wood has been loaded to higher stress level the elastic limit is exceeded. The sample then moves into plastic deformation, after which samples cannot recover fully and cannot be re-tested. Finally it leads to wood failure (Kretschmann, 2010; Green, 2001).

One of the important things in 3-point bend testing is to make sure that the sample is aligned in a fixed direction when tested, as the cell-wall structure of wood changes between the radial and tangential directions (Green, 2001).

Bending stiffness is a much needed property in timber. In structural design, new or old beam sizes are calculated based on the stiffness and strength of the wood in question. If a beam has inadequate stiffness for its span it could bend so far as to allow the ends to come out of their recesses in the walls, whereas lack of strength in a beam could result in it breaking in the middle (Kuilen, 2006; Yeomans, 2003). A new piece spliced onto the end of a beam needs to meet the same stiffness requirement as the existing member (Divos et al., 1998).The aim is to produce a new joint which has similar stiffness to the one it has replaced. Different stiffness in replacement joists and rafters could result in unfair stress being applied to the whole structure. This problem could be more serious with rafters as a difference in stiffness could allow local distortion from the weight of the roof and lead to leaks.

Due to the small scale of the samples used here, 3-point bending tests were the most appropriate and had the most available comparisons with previous studies. The static 3-point bending tests are easier to perform than tensile tests and lead to equally good results when calculating the longitudinal modulus of elasticity (Varner et al., 2012) although the bending and tensile moduli are not identical. They also allow for a direct comparison between the historic and modern wood samples to determine if any changes are occurring in MOE with age. The oak and pine samples tested here were expected to show different bending stiffness due to the different characteristics of the species. That is why timber repairs are generally done like for like, but here it was also of interest to see if the difference in stiffness between modern and historic wood could be related not only to age but also to different growing conditions.

MOE determination through 3-point bend testing is based on the deflection between two fixed points, usually with a small actual deflection (Holmqvist and Boström, 2000; Helge, 2000).

The 3-point bend testing experiments are traditionally carried out on wood samples made from what is known as clear wood: that is, areas of the wood which do not contain any knots, splits or any other growth defects. Clear wood samples are usually considered homogeneous in wood mechanics (Kretschmann, 2010; Aydin, 2007). These wood samples are usually a standard size known as small clears, the dimensions of

which are 20 mm x 20 mm x 350 mm (Ilic, 2003; Boey et al., 1985; Fukuta et al., 2011). Small clear samples therefore give an idea of how well the best quality wood from the tree will perform (Straze and Gorisek, 2011; Bendtsen, and Ethington, 1975). But, as the timber beams we were able to obtain were nowhere near this length, a new method using 'micro clears' had to be developed.

There are many reports on the use of conventional small clears in bend tests (Ilic, 2003) but not 'micro clears' of shorter length and proportionate thickness. A prior test needed to be carried out to discover how short we could go before the results were affected by the increase in the depth to span ratio and the resulting shear distortion within the samples (Schneeweiß and Felber, 2013).

8.2 Method Development:

8.2.1 Sample preparation

Micro samples were cut from the historic and modern oak baulks by first cutting a 3 mm strip down the grain. From this strip smaller samples were cut from pith to the bark. These micro samples were standardised at 60 mm x 2 mm x 2 mm after preliminary experiments (see 8.2.2 below) and were cut using a single edge razor and a Japanese pull saw to avoid losing too much of the wood material (Dinh et al., 2008; Farruggia and Perré, 2000). The multiple samples were intended to show the range of properties that change in wood due to the changing MFA and density from pith to bark in growing trees. The samples were made out of clear wood as the effect of any defects in the samples would be exaggerated when using samples as small as this (Straže and Gorigek, 2011; Bohannan, 1966). A consequence of the 2 mm x 2 mm sample dimensions was that many samples comprised mainly earlywood or mainly latewood, especially in the juvenile wood where the growth rings were wide. Due to the greater density of the latewood this led to variation in stiffness from one sample to the next, reflecting the ring structure of the beam. For samples such as this with only a few growth rings the average is easier to deal with (Schneeweiß and Felber, 2013; Farruggia and Perré, 2000).

8.2.2 Procedure

The samples were left for 3 months to equilibrate fully with their environment, which was set at 20°C and 65% RH, and to allow for uniform moisture content over the whole sample set (Yoshihara and Tsunematsu, 2007; Alteyrac et al., 2006).

The samples were first tested at length 100mm and then reduced in length successively in 20 mm intervals and tested again. The cross section of the specimens was kept the same. It was only the length of the samples that was altered. This resulted in a change in the span to depth ratio (Schneeweiß and Felber, 2013).

The 3-point bend tests done here were carried out with the two ends of the samples being supported while the downward load was placed on the middle of the sample (Lopez-Anido et al., 2003; Straže and Gorigek, 2011; Lachenbruch et al., 2010; Wahab and Jumaat, 2014; Lipovszky and Raczkowski, 1971; Schneeweiß and Felber, 2013). These tests were carried out on a Tinius Olsen tensile testing machine with a 250 N load cell. The tests were set up to apply enough force to bend the samples to a deflection of 3mm which is still within the elastic region; they were not tested until breaking point as they were needed for further testing at the shorter lengths. In the load-deformation plots below there is little change to the apparent bending modulus until the sample is below 60 mm. The apparent decrease in the bending modulus at shorter sample lengths could be due to the fact that the bending probe comes to a rounded point which, at the smaller lengths, compresses the wood as well as bending the sample (figure 8.1). From this experiment we were able to discover that it was possible to do 3-point bend testing on the historic oak beam ends as they were around 60-70 mm in length, but unfortunately the majority of the Scots pine samples were less than 40mm and could not be used for this type of testing without the risk of artefacts.

Once the samples were prepared they were tested in the same manner as in the preliminary test using the Tinius Olsen tensile testing machine with a 250 N load cell. The tests were set up to apply enough force to bend the samples to a deflection of 3 mm.
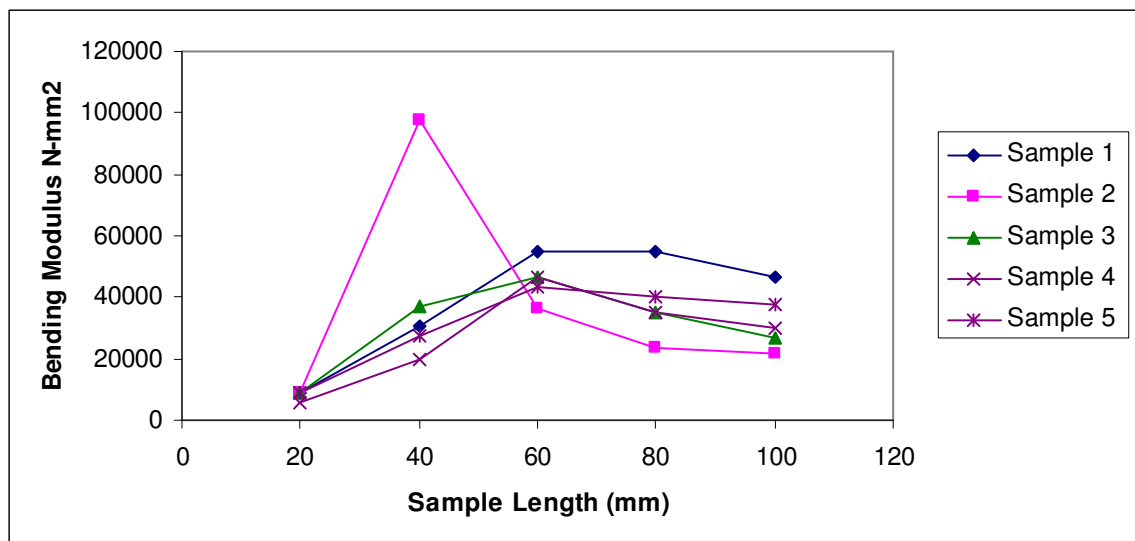
Figure 8.1: Bending modulus of 2 x 2 mm thick oak samples as they were being shortened from an initial length of 100 mm. The bending modulus remained approximately constant until the samples were shortened to 40mm or less.

8.2.3 Final Method:

The final method used on the historic samples was carried out by cutting samples to 2mm by 2mm with a length of 60 mm. As stated above, for this reason only the oak could be tested using this method. They were then set up on the bending rig (figure 8.3) on the Tinius Olsen tensile machine. The samples were placed on 5 mm diameter end supports which were free to rotate as the sample deflected. The probe had a 0.5 mm radius tip and each sample was tested at a deflection rate of 0.002 mm per second to a final deflection of 3mm.

Figure 8.2: The tensile testing machine set up with 3-point bending rig Image: K Hudson-McAulay.

8.3 Results

The results were directly recorded and the load-deformation data were later exported as ASCII files into Excel. The modulus of elasticity was calculated from the linear portion of the graph (Yoshihara and Tsunematsu, 2007) using the following equation 8.1:

Equation 8.1:

$$MOE= (F/S) (L^3/4BH^3)$$

Where MOE is the modulus of elasticity, S is the deflection, F is the load, L is the length (span) of the test piece between the supports, B is the width of the sample and H is the depth of the sample (Wahab and Jumaat, 2014; Ouis, 2002). F/S was taken as the slope of the linear part of the load vs deflection curve.

Equation 8.1 does not take into consideration the shear stress which occurs in bending resistance. To take the effect of shear into account needs much more complicated theory. The value **o**bserved for the bending stiffness is dependent on the span to depth ratio of the samples used. Whichever way the MOE calculations are done, this factor always needs to be included (Schneeweiß and Felber, 2013). The method of calculation chosen is based on ease of use and sometimes not all correlations are perfect (Ouis, 2002).

The samples were not tested to failure as the modulus of elasticity was all that we required to compare stiffness between the old and the new samples, although some did fail during the testing where the grain of the wood was at a steep angle and the samples fractured (Schneeweiß and Felber, 2013). The fracture here occurs near the centre point where the wood sample is reaching its maximum stress (Schneeweiß and Felber, 2013) made worse by the large slope of the grain. Small fractures start from tension stress in the fibrils on the lower edge of the sample which eventually lead to failure (Varner et al., 2012).

After the results were run through the above equation to obtain the modulus of elasticity they were then corrected for the density of each of the samples. Density is known to have a large impact on the stiffness of wood so accounting for it allows a different view of the MOE data. The MOE is divided by the density (Bohannan, 1966). These results were then plotted against radial position (figure 8.4) to compare the stiffness of historic oak with modern oak.

The results from the 3-point bend test on oak shows, that once the MOE was compensated for density there was no significant difference between ages after assessing with a one way analysis of variance. The variation in stiffness is primarily due to the density scatter within the samples, with one historic sample in particular having a much higher density and stiffness than the others tested.
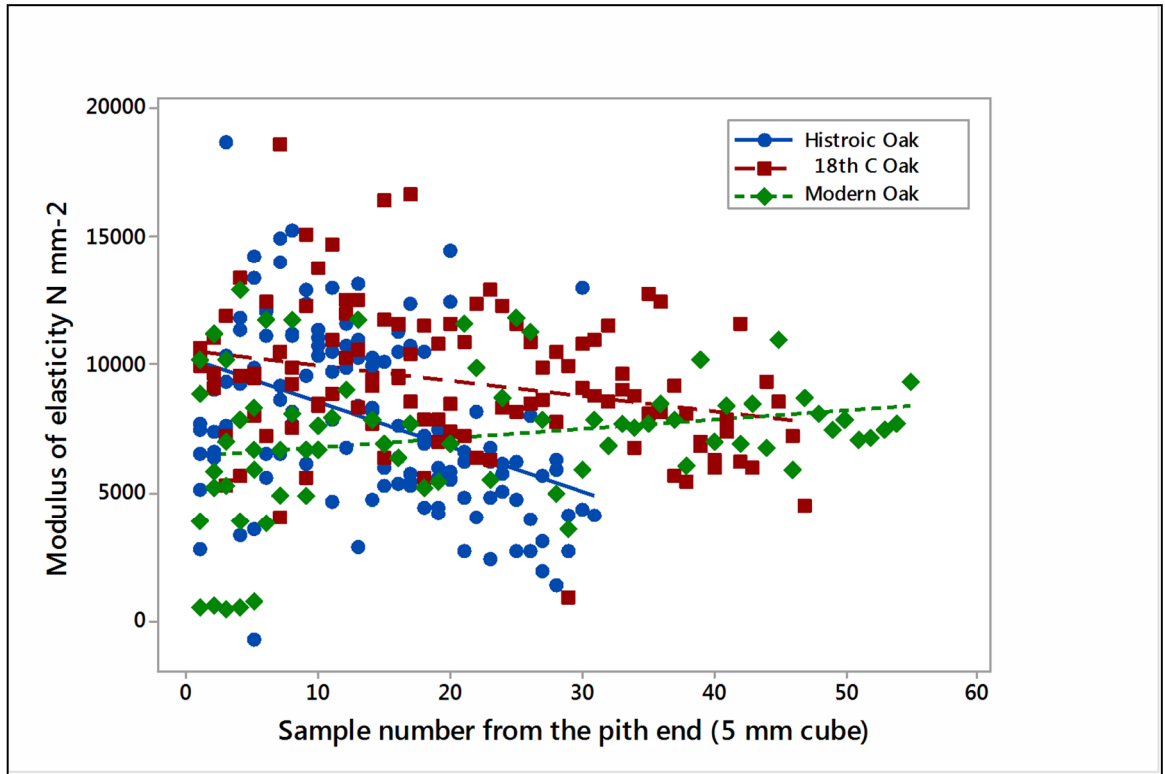
Figure 8.3: Variation in stiffness in oak of different ages from pith to bark.
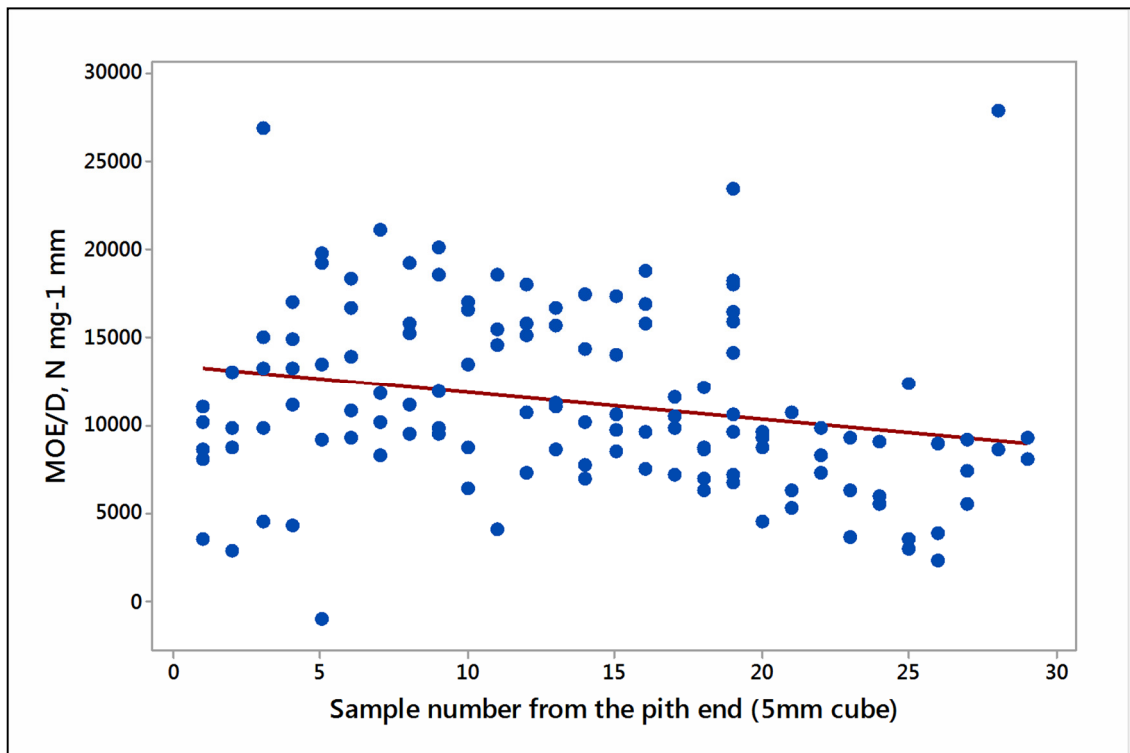
Figure 8.4: Variation in the MOE/D ratio of historic oak from pith to bark.

The scatter graph (figure 8.3) of the modulus of elasticity shows that even though there is a large amount of scatter there does seem to be a loss of stiffness toward the bark in the historic oak samples. When a regression model was fitted to this it showed the difference to be highly significant with a P value of <0.001 and an R^2 Value of 0.259, whereas the slight decline in the 18th C oak from pith to bark was not significant. There was an increase in the MOE/D of the modern oak samples towards the bark end. This again was run through a regression model and came out to be statistically significant with a P value of <0.05 and an R^2 Value of 0.341.

Figure 8.4 shows the MOE again but corrected for density, the drop in the MOE/D ratio at the sapwood can also be seen, although less abrupt than for density (figure 7.3). A *t*-test used to compare the MOE/D ratio of the sapwood and the heartwood showed that there was a difference in the MOE with a very significant P value of <0.01. There was clear weakening by fungi as evidenced in both the density and the MOE even though there were no visual signs on the surface of the wood.

The loss of stiffness in the historic oak samples toward the sapwood is most likely due to biological damage toward the bark edges of the historic beams. But due to the small sample set used this could also be due to the natural variation found in the pith to bark range in the MFA of individual trees. If genuine, the loss of stiffness in historic oak is not down to loss of density alone, but was still observed after correcting for density. The biological decay here is due to fungal decay rather than pests as only one of the historic oak samples has visual evidence of pest decay.
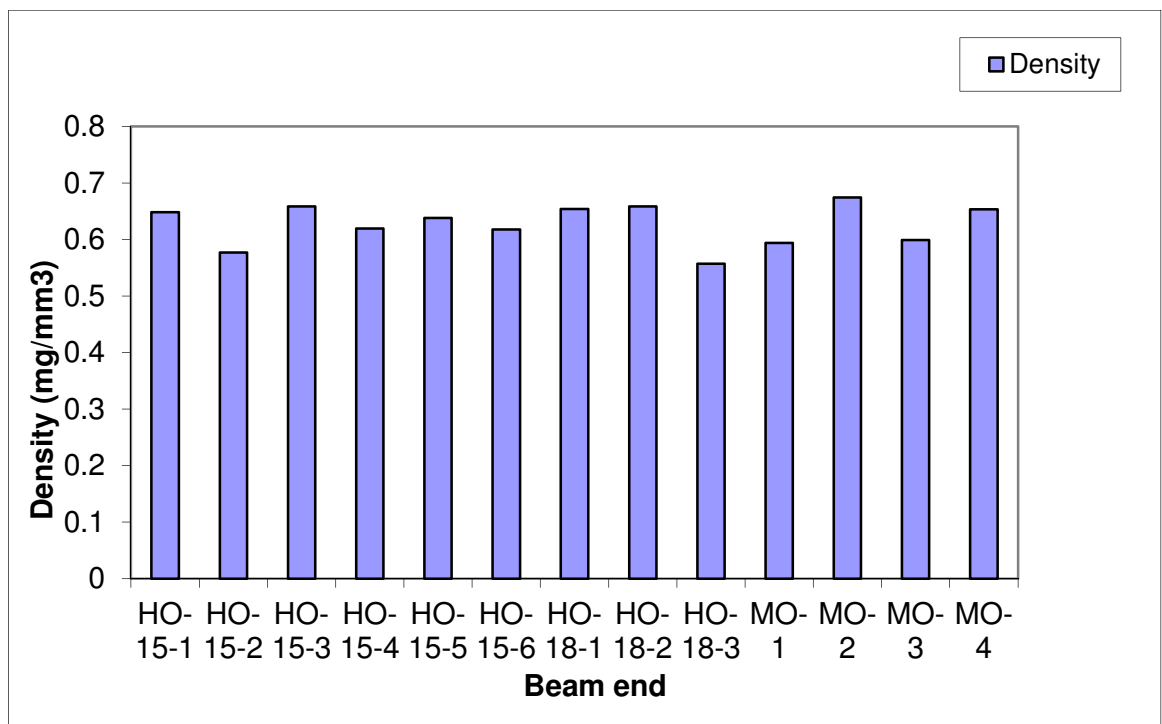
Figure 8.5: The average density of each of the oak beam ends.
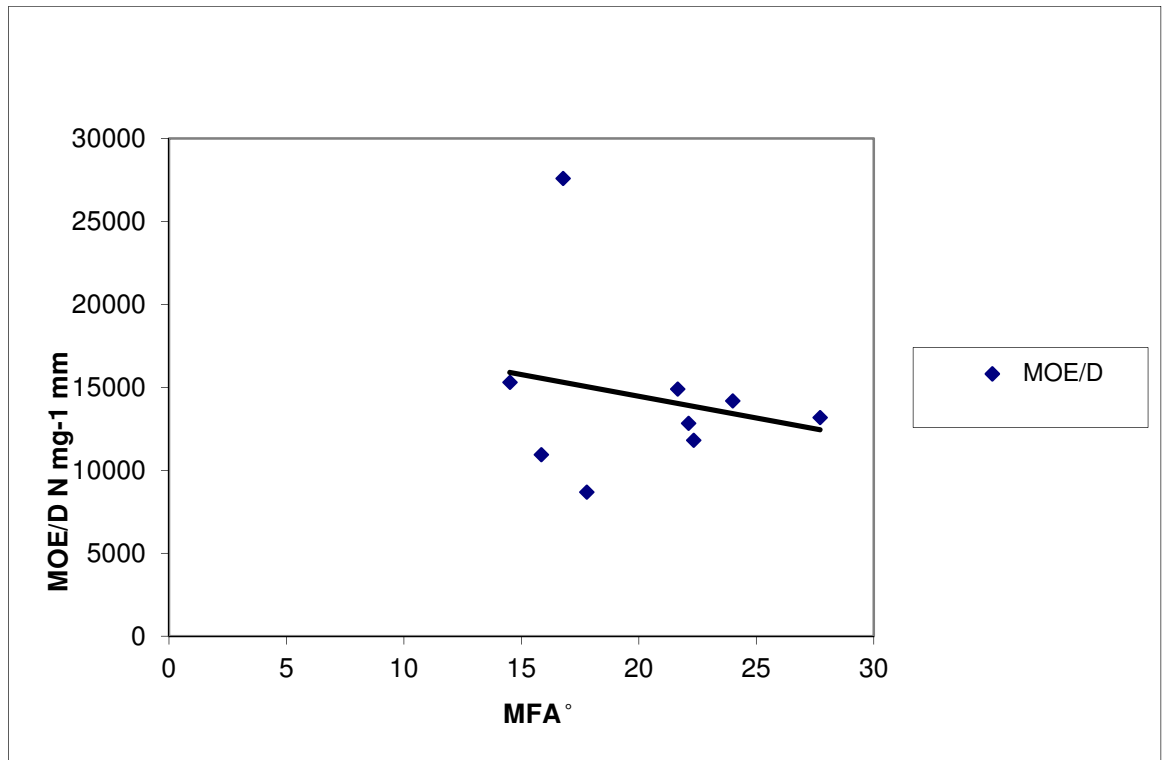
Figure 8.6: The relationship between MFA and oak stiffness measured by 3-point bending, corrected for density.

Figure 8.5 shows that the average density in each of the beam ends was approximately the same. Sample HO-15-5 was in question here as it had an unusually high stiffness when corrected for density. It was initially thought that this might have been an anomaly if the density had been lower than expected, but it appears this was just an extremely stiff piece of oak.

The relationship between the MOE/D and the MFA shown in figure 8.6 had as expected a negative trend in stiffness with increasing MFA, although with oak the slope is not significant.

8.4 Discussion

The results show that there was no real difference in stiffness between the historic and modern oak. This is consistent with the literature on historic oak where little difference other than genetic variation between trees is seen between age groups (Gereke et al., 2011; Aydin, 2007; Wahab and Jumaat, 2014). The difference between the age groups only became apparent when looking at the stiffness of the samples from pith to bark. The regression models showed that the historic wood declined more in stiffness towards the bark of the tree. This is probably due to biological decay (Grabner and Kotlinova, 2008). Usually wood gets stiffer towards the outside of the tree due to increasing density and decreasing MFA, although oak tends to be more even in density than most softwoods (Altaner and Jarvis, 2008). This can be seen in more detail in Chapter 6.

The large amount of scatter in the results is due to genetic variation and other anomalies within individual trees. This is always seen in mechanical testing as no tree or even section of a tree is homogenous (Wahab and Jumaat, 2014; Holmqvist and Boström, 2000).

Adding the load perpendicular to the grain has resulted in splitting along the grain in some of the samples where the grain angle was particularly steep. This is another consideration when examining timber for structural integrity.

Tests on the stiffness of waterlogged wood have shown it has almost half the stiffness of modern wood. Different decay mechanisms in this environment severely degrade its stiffness and strength (Bjurhager et al., 2012), showing again that these two types of wood need to be researched independently. Although historic oak lost stiffness towards the sap edge its overall stiffness was no different from modern wood and it would be perfectly capable of continuing its life in service if properly cared for.

Chapter 9

Compression Testing

The beam ends for the Scots pine were too short along the grain to run a successful bending or tensile test. Their stiffness was measured here using compression testing (Schneeweiß and Felber, 2013). Compression tests on smaller scale pieces of wood have been done regularly on modern clear wood samples. The compression test involves placing the sample end grain up onto a flat surface and then applying downward pressure to the sample (Xavier et al., 2012).

Compression testing of historic wood is of direct importance where the posts supporting a timber frame are loaded in compression. Compression tests can also substitute directly for tensile tests because the tensile and compression moduli are usually considered to be equal, if no fracture or irreversible deformation has occurred. The 3-point bending tests carried out on oak in Chapter 8 measured the stiffness of the top cells in compression and the bottom cells in tension, assuming that the moduli were equal. Therefore the stiffness of the wood can also be measured in compression testing (Yoshihara and Oka, 2001; Hoffmeyer and Davidson, 1989).

Within this chapter we are testing again for wood stiffness not wood strength. To measure wood strength you need to define a mode of fracture. With little material to test we were not testing the historic wood to failure (Le and Nairn, 2014).

It is possible to test compression strength at the nano-scale where the compression test system is so small that the test can be carried out on the S2 layer of a wood cell (Zhang et al., 2010). These nano-scale tests only show the compression strength of the S2 layer as it is the only cell-wall layer thick enough. Considering that nano-scale testing requires an atomic force microscope and that there is little or no information on its application to historic wood, the tests carried out here will be on a larger scale, looking at the wood structure as a whole, not just the S2 layer.

All mechanical properties of wood, when tested on the macro scale are influenced by different factors. For example wood anatomy and slope of grain, microfibril angle (MFA) and density will effect the compression strength of any wood species (Müller et al., 2002).

Mechanical properties of wood are affected by sample orientation. As with other forms of mechanical testing it is also important to consider things such as, distance from the pith and knots, which can all affect the results obtained (Nairn, 2005; Augustin and Schickhofer, 2006). The tests carried out in this chapter were done on a smaller scale than previous work due to the small dimensions of the historic material, but this also enabled us to do more localised testing and see if there was any change in compression stiffness from pith to bark.

<u>Compressive strength and compression failure</u>

Compression strength is a key property of timber when loaded in any compressive direction and is taken into account when designing timber structures (André et al., 2014).

Due to the lack of material available for the compression tests they were restricted for this project to measurements in the linear region of the load deformation curves before any irreversible deformation of the sample could take place.

It is to be expected that compression strength is much greater parallel to the grain than the perpendicular, (Aydin, 2007) which is why posts in timber frames are able to carry such heavy loads.

9.1 Experiment

9.1.1 Sample preparation:

As with many forms of mechanical testing there are universal standards for the testing of modern wood which is intended for building construction. The ASTM 2010 standards for compression tests are set out using a sample size of 50 x 50 x150 mm (Basta et al., 2011). However the samples for the tests here were made much smaller, both to conserve the amount of material used and to give a good overview of possible changes in stiffness from pith to bark (Reiterer and Stanzl-Tschegg, 2001). The samples were cut using a razor blade, again to limit the amount of material lost and, with compression tests, to keep the surface contacting the pressure plates as square, flat and smooth as possible so that distortion, if only part of the surface was in contact, would not interfere with the results (Low, 2001).

Micro samples for this experiment were cut from each of the historic and modern oak and pine samples. They were cut to 5mm x 5mm x 5mm cubes using a single-edge razor blade and scalpel to get the dimensions correct as measured using a digital caliper reading to 2 decimal places (10 μm).

Before testing the samples were left to equilibrate with their environment to ensure uniform moisture content across all the samples. They were left for 3 months at 17.5°C and RH 55% giving a moisture content around 12% (Müller et al, 2002). This process of equilibrating the samples to the same moisture content is important as increasing moisture can increase the plasticity of the wood (Ellis & Steiner, 2002; André et al., 2014), and an increase in temperature has been found to decrease the compression strength of wood (Kutnar and Kamke, 2010) both of which would distort the result.

9.2 Method Development

9.2.1 General Procedure:

The Tinius Olsen H1KS tensile testing machine with a 250N load cell, used in this part of the experiment (Tinius Olsen 6 Perrywood Business Park, Honeycrock Lane, Salford, Surrey RH1 5DZ, England) applies pressure via a load cell above the top of the sample. The sample was placed between 2 flat-ended steel bolts (figure 9.1). The top bolt, directly attached to the load cell measured the amount of force applied as the bottom bolt was pushed up at constant speed of 1 mm per minute, compressing the sample between the two flat faces.

Figure 9.1: Compression testing on the Tinius Olsen machine Image: K Hudson-McAulay.

The data were first recorded from the machine using the Qmat 5.36 software from Tinius Olsen 6 Perrywood Business Park, Honeycrock Lane, Salford, Surrey RH1 5DZ, England and then they were transferred in ASCII format into Excel, where the modulus of elasticity was calculated after selecting the most linear region of the graph as shown in figure 9.2 below.
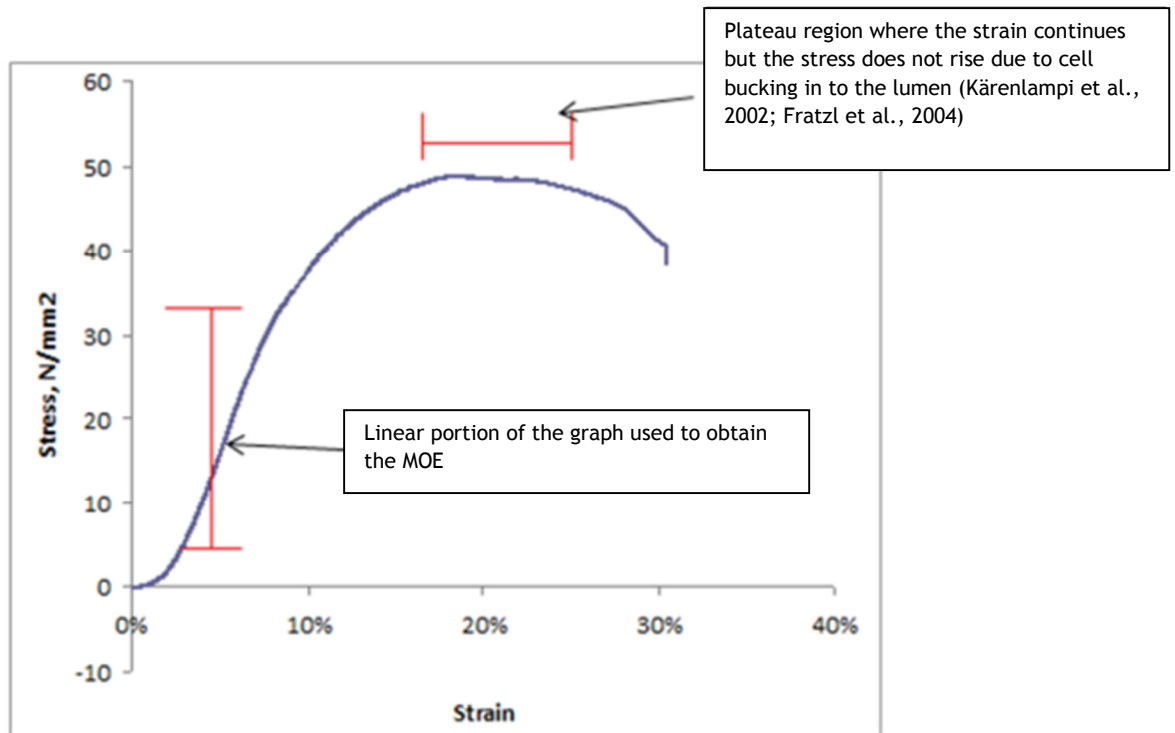
Figure 9.2: Stress/ strain graph showing the linear section from which the MOE is calculated and the plateau where failure has occurred.

The modulus was calculated using Equation 9.1:

Equation 9.1:

$$MOE = S*H/ (W*D)$$

Where S is the slope in N/mm averaged for the linear portion of the graph, H is the height of the sample in mm, W is the width of the sample in mm and D is the depth of the sample in mm (Farruggia and Perré, 2000; Anjos et al., 2014; Lourenço et al., 2007; André et al., 2014).

9.2.2 Potential problems

Wood is a complex material. Compression testing can be affected by variables such as the relative proportions of latewood and earlywood of different density. The orientation of the samples was kept constant (Lourenço et al., 2007). In all the tests described here the stiffness was measured along the grain. As the radial dimension was so small that the samples only included a few growth rings, the ratio of earlywood to latewood and hence the density, showed random variability between samples. This reduced the precision of the measurements.

Compression tests have been criticised in the literature for problems with friction and barrelling effects on the samples. Barrelling effects can occur with any size of sample when it is crushed to near the material's maximum compression strength. As the sample size here was so small and no test was anywhere near the total compression strength of the wood, problems due to the height/width ratio affecting the plateau stress did not occur (Reiterer and Stanzl-Tschegg, 2001). Friction occurs where there are problems at the ends of the samples, such as if there is an unknown substance on the surface or if the surface connecting with the testing machine is uneven. Making sure that the sample is loaded with uniform compression over the whole surface (Leijten, 2010; André et al., 2014; Xavier et al., 2011) appears to be more of a concern when working with smaller samples and this is another possibility affecting the results from the compression tests carried out here.

9.2.3 Initial Procedure
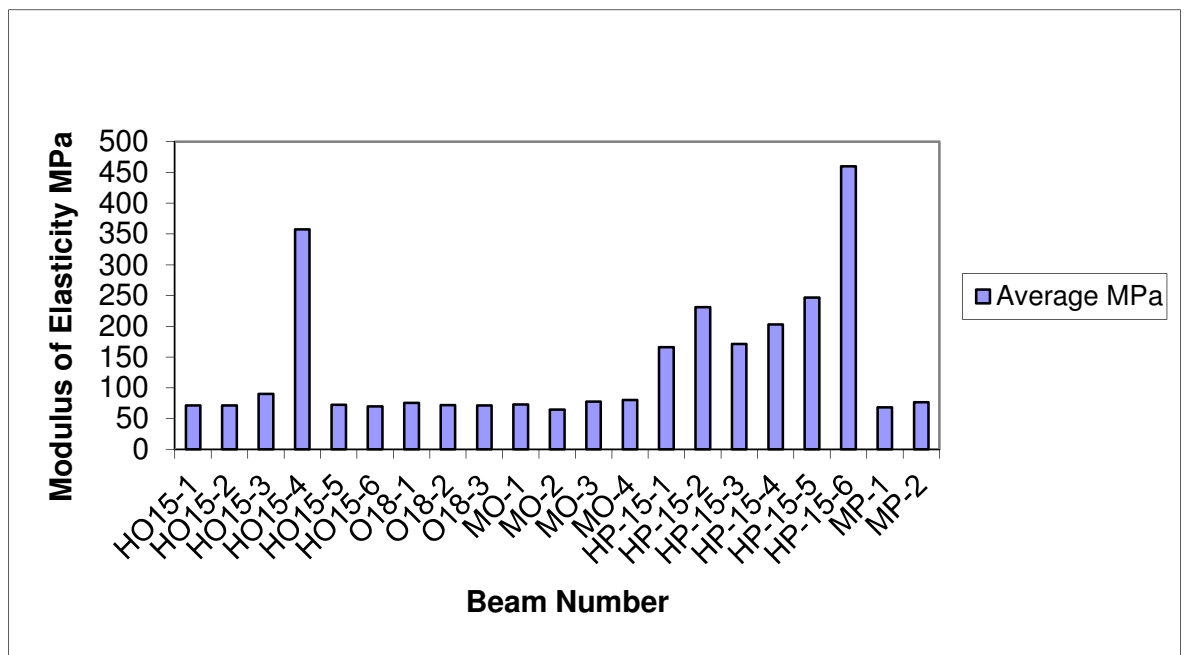
Figure 9.3: Average stiffness for each of the beam ends tested.

These first results implied a range of modulus of elasticity far lower than what would be expected from oak or pine (figure 9.3), for example when related back to the MOE of the oak samples measured in the 3-point bending test in Chapter 8. To investigate what might be causing this problem, the first thing done was to try to overcome the problem of the machine not being stiff enough and the samples' surface not being flat enough, a problem noted in the literature (Dinh et al., 2008; Xavier et al., 2011).

9.2.4 Machine Deflection

The first issue that was tested, in trying to uncover the problems with the compression results, was the machine deflection that would occur due to the smaller machine's frame not being able to stand up to the larger force required in the compression test, causing this movement of the machine to be recorded within the results. Firstly, to test if this could be an issue, the samples were tested on a larger machine which has little machine deflection due to its size.
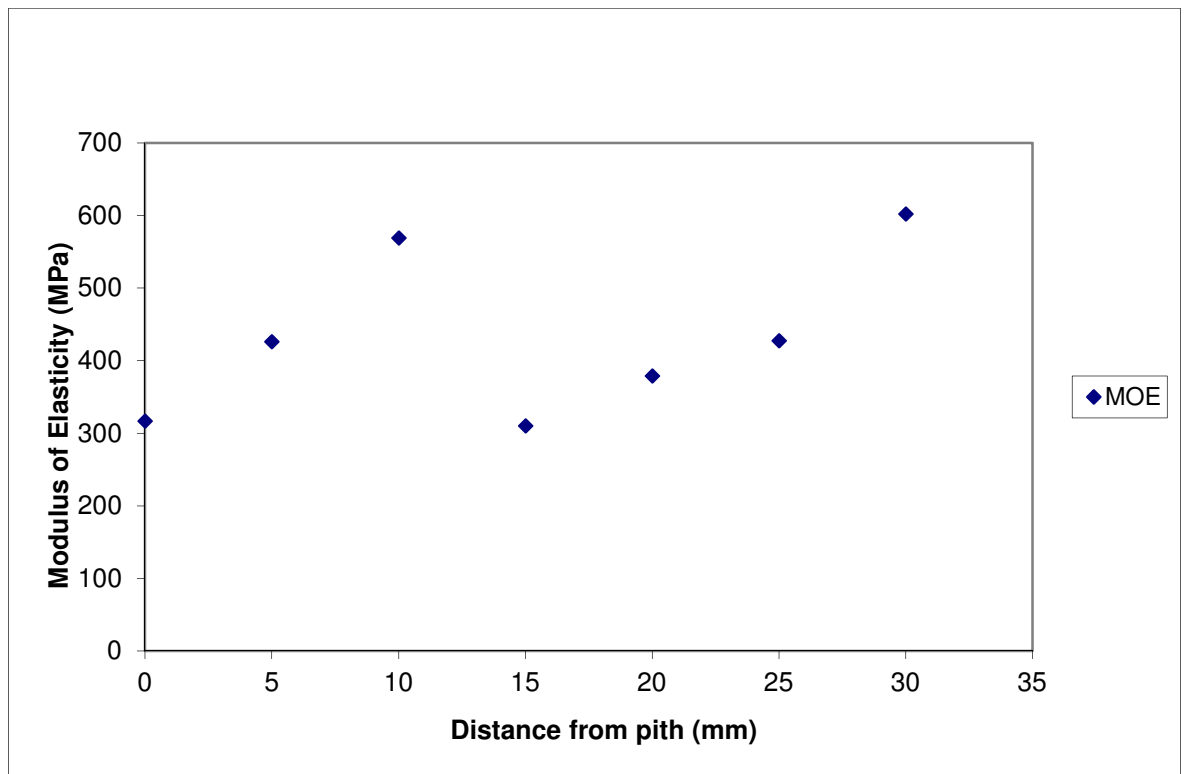
Figure 9.4: MOE of modern Scots pine when tested on the alternate machine.

The Zwick/Reoll Z2.90 with a 2 KN load cell was used to produce the above graph (figure 9.4). Results were recorded by Test Xpert 2 and then transferred into Excel and run through the same process to calculate the MOE. As the samples here were tested to failure the linear part of the graph had to be used to calculate the MOE. Each block was

tested individually at a speed of 0.5 mm per min. A slower speed than on the Tinius Olsen machine was used due to the larger maximum force on the samples. The calculated MOE values were higher than before but still lower than would be expected. This allowed us to assume that surface unevenness is a problem, and that the Tinius Olsen machine first used was not the key problem, although it required a correction for machine deflection and maybe the sample dimensions needed to be changed.

Before the problem of sample dimensions could be faced the deflection of the machine needed to be characterised and accounted for. To do this a steel bolt was used as a mock sample as it is completely rigid and cannot be compressed by the small load exerted by this machine. Any deflection recorded will then be deflection of the machine itself. The bolt was tested in the machine three times to give an average result for the deflection as a function of load. The straight part of the stress strain graph recorded by the machine was transferred to Excel. The slope was calculated in the same way as the original results.

This gave a machine deflection factor (machine deflection / Force) of 0.000173 mm/N which could then be included in the Excel spreadsheet to remove the deflection from the machine. This was done using the equation 9.2 below:

Equation 9.2:

$$E - F*MD = CE$$

Where E is the machine recorded compression, F is the force, MD is the machine deflection factor and CE is the corrected compression. The calculation was done on every compression point recorded by the machine for each sample and the slope of the linear part of the resulting, corrected compression vs force plot was used to calculate the MOE.

9.2.5 Flatness and hardness of the sample ends

The bigger machine also allowed for the testing of another of the key problems pointed out above, the issue of the ends of the sample being uneven and deforming flat before the whole sample was evenly compressed. As the machine is bigger and can apply much more force with the larger load cell it was possible to apply enough force to completely flatten the ends of the samples. As the Tinius Olsen only has a load cell of 250N it was not possible to compress the sample enough to make the surface flat, so the bigger

machine was needed. Each block was tested individually on the Zwick/Reoll Z2.90 machine.

The machine's software recorded the stress strain curve shown in figure 9.2. The linear part of the graph was used, after the discrepancies in the sample's surface had been flattened out. The results in figure 9.3 show that this method along with the correction for machine deflection increased the measured MOE of the samples.

The samples were then re-tested on the Tinius Olsen machine using longer, narrower samples to try and limit the surface in contact with the machine and bring down this error by reducing the surface area over which imperfections could occur.

To discover which sample size would give us the best results a strip was made from one piece of modern Scots pine on which there has been much previous research using the Silviscan which shows the range of MOE to be expected, approximately 6000-15000 MPa (Auty, 2013). This data can be compared to the results obtained here.

The strip was made 80 mm in height along the grain by 2 mm width and 2 mm in thickness. This sample was then tested 4 times on the Tinius Olsen machine using dips in the bolt heads to keep the samples as straight as possible and finding an average. This sample was then cut from 80 mm into two 40 mm sections then retested, then four 20 mm sections which were tested and finally eight 10 mm samples which were individually tested. The results show a decreasing measured MOE with decreasing length, consistent with end effects distorting the measurements, but with a huge standard deviation between samples (table 9.1).

Table 9.1: Relationship of compressive stiffness of Scots pine to sample length, showing the large standard deviation in the first compression testing results.

Sample Length	Average MPa	Standard Deviation
80mm	11804	1563
40mm	7604	3464
20mm	5170	3275
10mm	4266	2579

As the historic beam ends are so short in length only the results below 40mm are applicable to them. As the 20 mm samples appear to be almost in the correct range of MOE, it was decided to try and deal with the unevenness in the ends to see if this would bring the measured MOE into the expected range. This was done by coating the ends

with epoxy resin enabling them to be sanded down more accurately within a specially made jig (figure 9.5).

Figure 9.5: The tool used to flatten the sample ends Image: K Hudson-McAulay.

The samples were re-made starting at 80 mm and the ends were covered in Araldite epoxy resin (Ciba-Geigy) at a ratio of 1/1 hardener to resin, and filed down to make sure they were flat and perpendicular to the axis of the sample.

Table 9.2: Effect on the standard deviation using epoxy resin on the sample ends.

Sample Length	Average MPa	Standard Deviation
80mm	5049	895
20mm	10185	5200

The use of epoxy greatly improved the results from the 20mm samples and brought the MOE into the range expected from modern pine (table 9.2). However, although this greatly improved the result the standard deviation was still much too high, so efforts were then made to improve the stability of the machine itself.

9.2.6 Machine Stability

Force-deflection curves for the deflection of the machine were measured again using a solid steel bolt roughly the same dimensions as the 20 mm x 2mm x 2mm samples tested. The bolt was tested 12 times in different positions. When the results were run

through the machine deflection calculation they showed quite a large standard deviation, as for the samples. Since this result was for a solid bolt it showed that there was too much random deflection coming from the machine itself see table 9.3.

Table 9.3: Random deflection of the machine itself.

Machine Deflection Factor mm/N	Standard Deviation	Standard Error of the Mean (SEM)
0.0025	0.000573	0.000173

The machine was then stabilised further by adding a stronger compression attachment bolt which was more tightly fastened onto the load cell. When the bolt was tested following the same method the standard deviation was greatly lowered as shown in Table 9.4.

Table 9.4: Lowered machine deflection resulting from stabilising the machine itself.

MachineDeflection Factor mm/N	Standard Deviation	SEM
0.001829	0.000047	0.000014

After all this testing to improve the method it was finally decided to test 20mm x 2mm x 2mm specimens of one historic wood sample and one modern sample to see how well the improvements all together would work.

Both the modern and the historic samples were then tested 12 times rotating the sample orientation for each test. The MOE was calculated as described above.

Table 9.5: Compression MOE of historic and modern pine.

Modern pine	Average MPa	Standard Deviation	SEM	Historic pine	Average MPa	Standard Deviation	SEM
	8564	2145	646		3418	519	156

From table 9.5 it can be seen the standard deviation has been lowered by at least half but is still relatively high, and is higher still for the modern samples. Although this standard deviation is still high, this method can be used to compare the historic samples

to the modern samples when tested in the same way. From this first preliminary experiment it can already be seen that the historic samples appear to have half the stiffness of the modern samples.

9.3 Final Method

Using all the experimental modifications and corrections described above, all of the historic pine samples were tested using this method. Four 20 mm x 2 mm x 2 mm samples were cut between the pith and the bark from each of the beam ends and these samples were tested in the fashion described above, along with two modern wood samples for comparison.
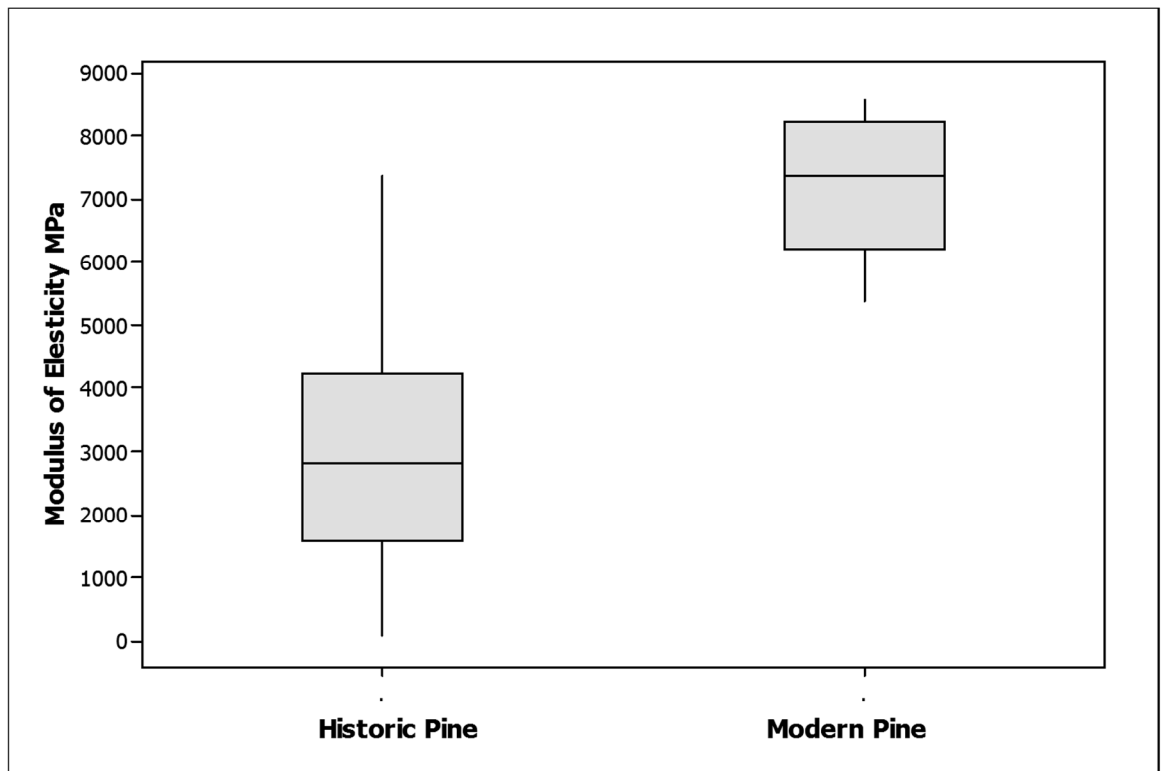
Figure 9.6: Compression MOE of historic and modern Scots pine.

_____

	Historic Pine	Modern Pine
Compression MOE	7239 a	2991 b

_____

Table 9.6: Mean compression MOE of pine samples of different ages.

Means followed by the same letter are not significantly different, Fisher LSD (P>0.05).

The box plot above clearly shows there was a big change in the MOE of Scots pine wood with age using this particular compression test. Although the standard deviation is still a little high the difference is clear: Scots pine does lose stiffness with age (table 9.6). The result was also run through a one way analysis of variance which showed that the difference due to age was statistically highly significant with P value of <0.001. A further *t*-test was run using just the heartwood samples of the historic and modern wood to eliminate the weakness caused by biological decay. This gave a very significant P-value of <0.01 showing the historic pine was less stiff than the modern pine, independent of decay (table 9.7).
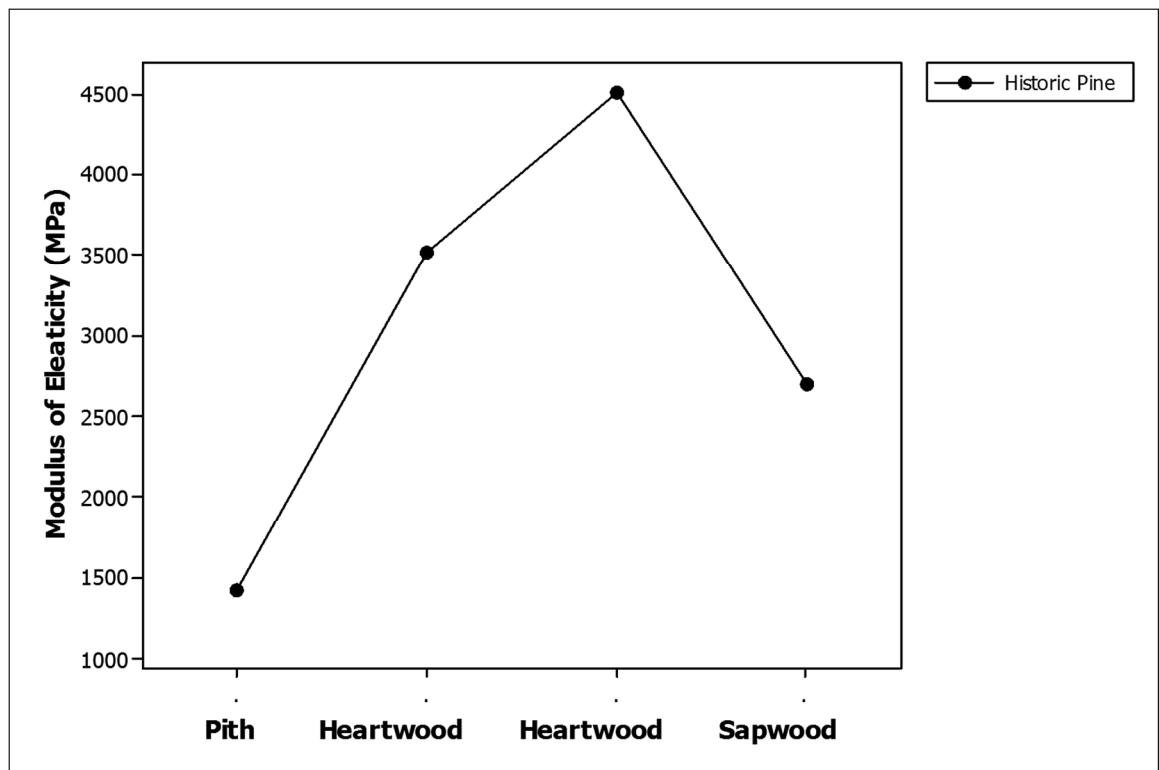
Figure 9.7: Variation in mean stiffness of the historic samples from pith to bark.

	Pith	Heartwood	Heartwood	Sapwood
Compression MOE (radial position)	1592 a	4196 b	3731 b	2445 c

Table 9.7: Mean compression MOE of pine samples in different radial positions.

Means followed by the same letter are not significantly different, Fisher LSD (P>0.05).

The line graph above (figure 9.7) shows the changing stiffness of the historic samples from pith to bark. Although the pith region of a softwood tree is normally observed to have lower MOE than the mature wood (Wagner et al., 2013; Macdonald et al., 2009; André et al., 2014) this is still a low value. As expected the MOE increased moving out towards the bark end of the beam, but there was a decrease in the sapwood. These results were then run through a Fisher test for least significant difference, to see where the significant differences were located in the one way analysis of variance. The test showed that the pith MOE was significantly different from the first heartwood MOE (Fisher $P<0.05$). The Fisher test showed that the second heartwood sample was significantly different from the pith. It also showed that the pith and the sapwood had no significant difference between them, but there was a significant difference between the heartwood samples and the sapwood. This shows that there has probably been a loss of stiffness in the sapwood.

The stiffness of softwoods generally increases from pith to bark (Macdonald et al., 2009), as was observed for the heartwood samples from the historic beams. Normally the pith to bark increase is steep close to the pith and levels out beyond approximately the 15th annual ring. A decrease in MOE in the outward direction is not usually observed except where plantation-grown trees have been severely thinned (Moore et al., 2012; Moore et al., 2009a). The decreased stiffness of the sapwood is most likely due to the influence of biological attack on the sapwood.

9.4 Discussion

The compression tests showed that the old and new wood were significantly different from each other with the historic pine reduced to nearly half the stiffness of the new in some cases. This observation is unusual. Lourenço et al, (2007) showed that there was not much difference in stiffness between old and new chestnut samples. Their old samples had only been in service for 50 years, young compared to the historic samples used in this thesis. Chestnut, like oak, is a ring porous hardwood that might not suffer the same chemical degradation as the historic Scots pine samples here, and is perhaps more likely to show little change in stiffness with age like the historic oak samples tested in Chapter 8 (Sousa et al 2014). Also looking at chestnut, the same authors showed that decay can cause a large decrease in compression stiffness. A similar drop in stiffness, apparently due to decay was found here in the sapwood, but also there was a general decrease in the stiffness of the historic pine wood from pith to bark in comparison to the new wood. As Scots pine loses considerable stiffness with age, after aging over five centuries it could be seen as undesirably low in stiffness for a building

material by modern standards. When pine was beginning to be more widely used in the 1500s in Scotland, it was almost the only wood available in long enough lengths for builders to use. They had no alternative, nor could they know how this material would age, nor even that the buildings they were working on would survive this far into the future.

Chapter 10

Hardness Testing

Carpenters for years have commented on the difference in hardness between green and historic oak. This experiment aimed to objectively assess the hardness of modern and historic oak and Scots pine to see if any quantitative difference in hardness attributable to age could be shown.

Hardness is considered one of the key properties of wood, especially in historic buildings when used as floorboards. Hardness testing can, for example, be based on the use of ridged indenters that act as if causing wear to a floor (Helińska-Raczkowska and Moliński, 2003). Hardness testing can be used to indicate the appropriate use for different timbers. For example, woods that test harder are better for flooring (Silva et al., 2014b). As mentioned throughout this thesis no one wood property stands alone. They all have different impacts on each other. Hardness is very closely linked to the density of wood. Generally speaking the higher the density of the wood the harder it will be (Hoadley, 1990, p.49).

Hardness is not routinely tested by any single method. There are a number of different ways in which is it measured, which correspond to different ideas of the nature of hardness. The choice of method is constrained by national guidelines. The two main types of procedure used are based on the Janka and Brinell tests (Miyajima, 1955), but there are many others based on three main principles. The first is measuring the reaction to a sudden indentation force and the plastic deformation that occurs under the testing implement as a continuous load is applied to the area. The second is known as the rebound hardness test, where an object is dropped directly onto the wood and the height to which it bounces is recorded, testing the elasticity of the material (Oberle et al., 2014; Riggio and Piazza, 2010; Green et al., 2006). The final method is the scratch test where a sharp object - or even your thumbnail, with wood - is dragged down the surface of the grain to see how deeply it will indent the wood. The deeper the scratch the softer the wood (Hoadley, 1990, p.49; Riggio and Piazza, 2010; Doyle and Walker, 1985). This is not commonly used in comparison with the indentation techniques as these are easier to control, give better results and can be done relatively fast (Riggio and Piazza, 2010).

Choosing a hardness testing method suitable for wood:

There are different ways in which the hardness of wood is measured. There is the Meyer (or Piazza and Turrini) hardness method which the Pilodyn instrument is based on, the Brinell hardness test and the Janka test which was developed from the Brinell test method (Riggio and Piazza, 2010). Finally there are nanoindentation tests which test the hardness of a single cell wall (Wimmer et al., 1997).

Brinell hardness test

The Brinell hardness test measures the width of the indentation left behind by a probe driven into the surface by a set fixed force. It was first employed in 1932 by Mörath. It measures the diameter of the depression left behind in the wood by a 10 mm steel ball which is normally forced in by a fixed load of 10 kg (Miyajima, 1955). This load is reached in a minimum of 15 seconds and then kept constant for 30 seconds; then reduced back to zero in a further 15 seconds. The indentation left behind in the wood is measured and its diameter is taken as the hardness result for the wood (Knapic et al., 2012; Riggio and Piazza, 2010; Wimmer and Lucas, 1997). This is the test generally used to determine the hardness of flooring (Miyajima, 1955).

Rockwell (Janka) Hardness test

The Rockwell hardness test or Janka test was developed from the Brinell test. It is accredited by the American Society for Testing and Materials (ASTM) and is a standard test procedure used in Europe (Korkut and Guller, 2008). This test is mainly for use in a laboratory on solid wood with dimensions of 2in by 2in (50 x 50 mm) and a length of 6 in (150 mm), with hardness being tested on the end and side grain of the wood. Testing involves a steel hemisphere with a diameter of 0.444in (11.3 mm) embedded 0.222in (5.7 mm) into the wood. The force recorded from this is the measure of hardness (Green et al., 2006, Riggio and Piazza, 2010, Doyle and Walker, 1985, Salca and Hiziroglu, 2014). For this test the machine needs to be calibrated and set up with the correct testing cycle and indenter (Low, 2001).

Piazza and Turrini (monotron, Mayher) Hardness test

The main method used on timber is the Piazza and Turrini hardness test (Riggio and Piazza, 2010). This is a modified version of the Janka test described above but works more like the Mayer standard of hardness. The force is recorded when a 10 mm cylindrical steel pin is forced 5mm into the wood surface. To obtain a representative measure of the hardness of the entire piece of wood, 5 measurements are averaged over the longitudinal face of the wood. This

method has been specifically developed for the testing of timber on site (Riggio and Piazza, 2010). The same general principle lies behind the Pilodyn instrument commonly used to test the hardness of wet waterlogged wood and to detect decay in standing trees and structural timbers (Clarke and Squirrell, 1985).

<u>Nano Indentation</u>

Micro- or nanoindentation tests are a useful tool in testing the hardness of wood at the cellular level, measuring the hardness of the cell walls and their constituent layers. These tests are more used in biologically based research than in testing of structural timbers, as it is difficult to scale up the data and predict macroscopic properties (Wimmer et al., 1997; Riggio and Piazza, 2010).

The indenter itself forms part of an atomic force microscope, which is suspended on a pneumatic anti-vibration table to isolate it from building vibrations. With a minute pyramid shaped indenter it can penetrate around 0.16μm into the cell wall and is able to determine hardness at the level of a single cell wall (Wimmer and Lucas, 1997).

10.1 Experiment

When testing for hardness there are many things that need to be taken into account. The method used here was based on the Piazza and Turrini test, as it uses the same general principle as Pilodyn testing, the main way in which on-site timber members are tested in conservation (Riggio and Piazza, 2010). This method has been adapted to be used on the small scale samples available from historic material. Because the actual Pilodyn instrument could not be used, the testing principle of the Pilodyn was re-developed for use on the Tinius Olsen H1KS tensile testing machine with a 250N load cell, making it possible to test hardness on a smaller scale.

By reducing the scale of the procedure it was possible to test the samples from the pith to the bark to see if there were any noticeable changes in the level of hardness across the changing anatomy from the pith, through the heartwood and then sapwood if present in the sample. As with most hardness tests it is safe to presume that when the probe is pressed into the flat surface of the test blocks, the applied force increases with the depth of penetration (Miyajima, 1955) allowing the calculation of hardness for each of the samples and wood species.

The hardness of wood can be influenced by many factors such as anisotropy, heterogeneity and moisture content. The test results can also be affected by the type of tool forced into the wood surface. For example sharper tools will increase the level of friction and splitting beneath the indenter compared to a blunter tool. Also on the

macro scale the tool is usually big enough to encompass both early and latewood, giving better averaged results over the annual rings (Wimmer and Lucas, 1997; Riggio and Piazza, 2010). The tool for the machine used here was made on the pin principle of the Pilodyn. On this smaller scale test the shape of the leading edge of the tool is key and the pin used had a hemispherical end.

10.1.2 Sample preparation:

5mm cubes were cut from pith to bark from each of the beam ends using razor blades in order not to lose too much of the original material, and to keep the surface as flat and clean as possible for the best contact with the probe on the machine (Low, 2001). Samples were also cut from modern pine and oak, both of which were well seasoned. Both modern and historic wood samples were left to equilibrate with the environment at a final temperature of 17.5°C and RH 55% for just over a year to make sure that the moisture content was uniform, as changes in moisture content are known to change the hardness results (Low, 2001; Oberle et al., 2014).

10.1.3 Procedure:

First, an adaptation for the tensile testing machine needed to be devised that would mimic the workings of the Pilodyn instrument. A probe pin with a tip 1.3 mm in diameter rounded to 0.5 mm height was attached to the load cell of the tensile testing machine. This probe was then used in the same way as the pin in the Pilodyn. Unlike the Pilodyn in which hardness is measured from the depth of penetration of the pin when fired into the wood with an energy of 6 joules (J), the tensile testing machine drove the pin 0.5 mm into the surface of the wood and the force that was required to do this was recorded.

Each of the samples were tested 3 times in different areas on the surface of the blocks (Doyle and Walker, 1985; Silva et al., 2014b; Helińska-Raczkowska and Moliński, 2003). This was done because the probe was not small enough to test each growth ring, and because latewood is denser, and as a result harder, than earlywood (Miyajima, 1955; Wimmer and Lucas, 1997). Testing one face of the sample 3 times in different places gave a good average of the different densities over the test area.

Each time the test was carried out the indenter had to be checked to make sure that it was correctly in line and in the correct area of the sample to ensure that the indentation was discrete (Yoffe, 1982) and did not interfere with the other tested areas.

All tests were carried out on the wood samples as seen in figure 10.1. The longitudinal-radial surface was tested, as this surface is most commonly tested with the Pilodyn and is the main surface accessible in most historic structures. The end of the beam is generally harder to access than the side (Riggio and Piazza, 2010; Helińska-Raczkowska and Moliński, 2003) as the end is built into the wall or joints.
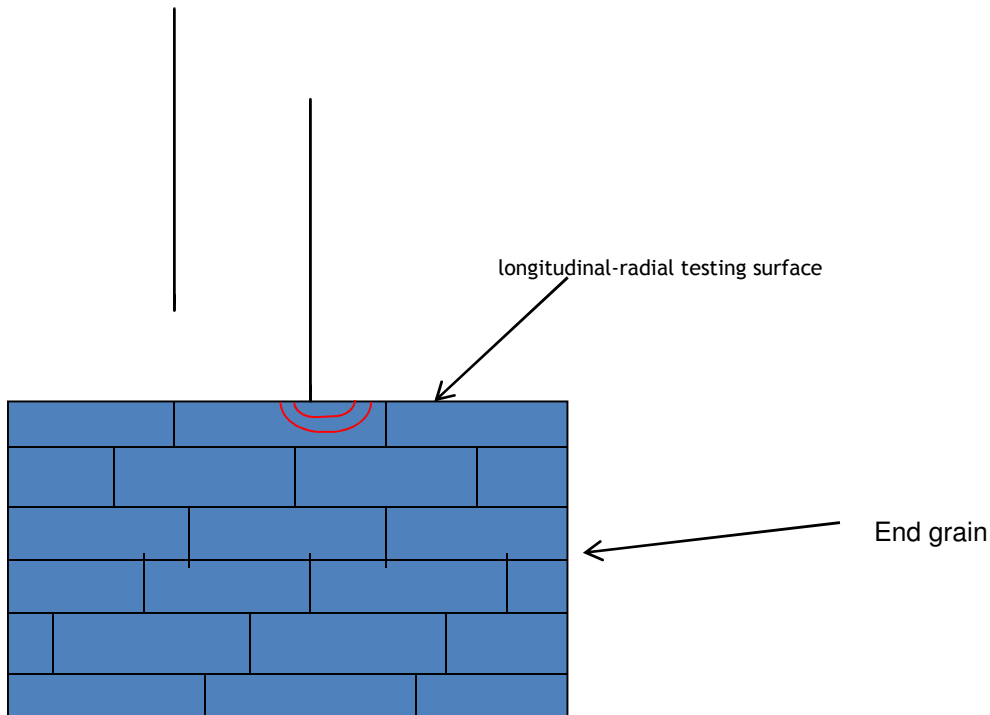
Figure 10.1: The testing probe and wood surface used in hardness testing Image: K Hudson-McAulay.

10.2 Data analysis and results:

Force-displacement data were recorded using the machine software Qmat 5.36 and then transferred in CSV format into Microsoft Excel. Once in Excel, the force recorded on reaching the depth of 0.5 mm for each of the 3 indentations on each sample was taken. These 3 forces were then averaged and assembled in order from pith to bark for each of the beam ends.

10.2.1 Oak
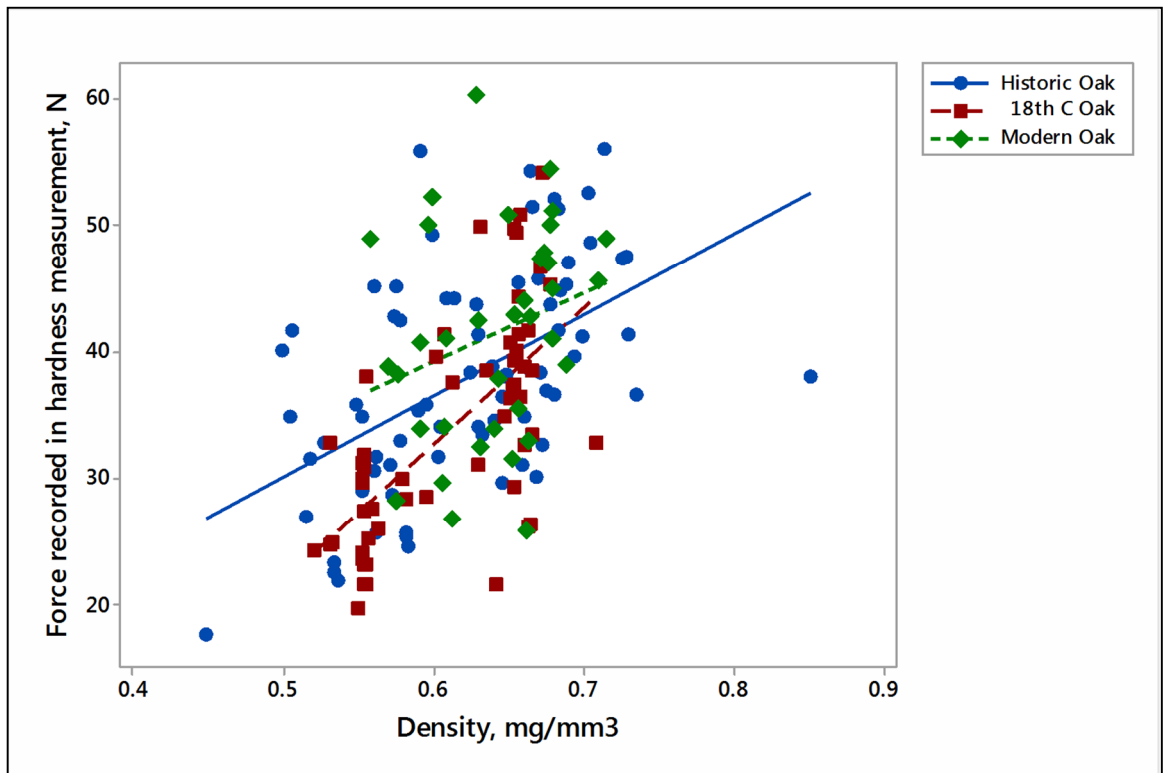
Figure 10.2: Scatter graph with a best fit correlation line showing the relationship of density to hardness in historic and modern oak.

_____

	Modern Oak	18th C Oak	Historic Oak
Hardness (N)	38.01 a	33.86 b	41.47 c

Table 10.1: Mean hardness of oak samples of different ages.

Means followed by the same letter are not significantly different, Fisher LSD (P>0.05).

The results from the hardness test for oak were run through a one way analysis of variance comparing ages. This showed that the difference between the hardness of the different ages of oak was statistically highly significant (table 10.1). The data was then run through a Fisher test for least significant differences. The Fisher tested implied that each age of sample was significantly different from the others (Fisher LSD P<0.05). Figure 10.2 shows that hardness increased as the density of the samples increased. The different aged woods where run separately through the correlation producing figure 10.2 which shows that the R^2 value was 0.276 and P value for the historic samples was <0.001, showing that the increase in hardness with density was statistically highly significant. The 18th C oak had an R^2 value of 0.427 and the P value was also <0.001

making this relationship statistically highly significant as well. The modern samples on the other hand had $R^2 = 0.069$ and $P = >0.05$ making this non significant. In the modern oak there was a smaller range of low densities, reducing the R^2 -value. This would be expected as there is no biological attack to cause lower density areas as with the historic oak. Loss of density through biological decay of the historic oak may also be causing some of the scatter within the samples.
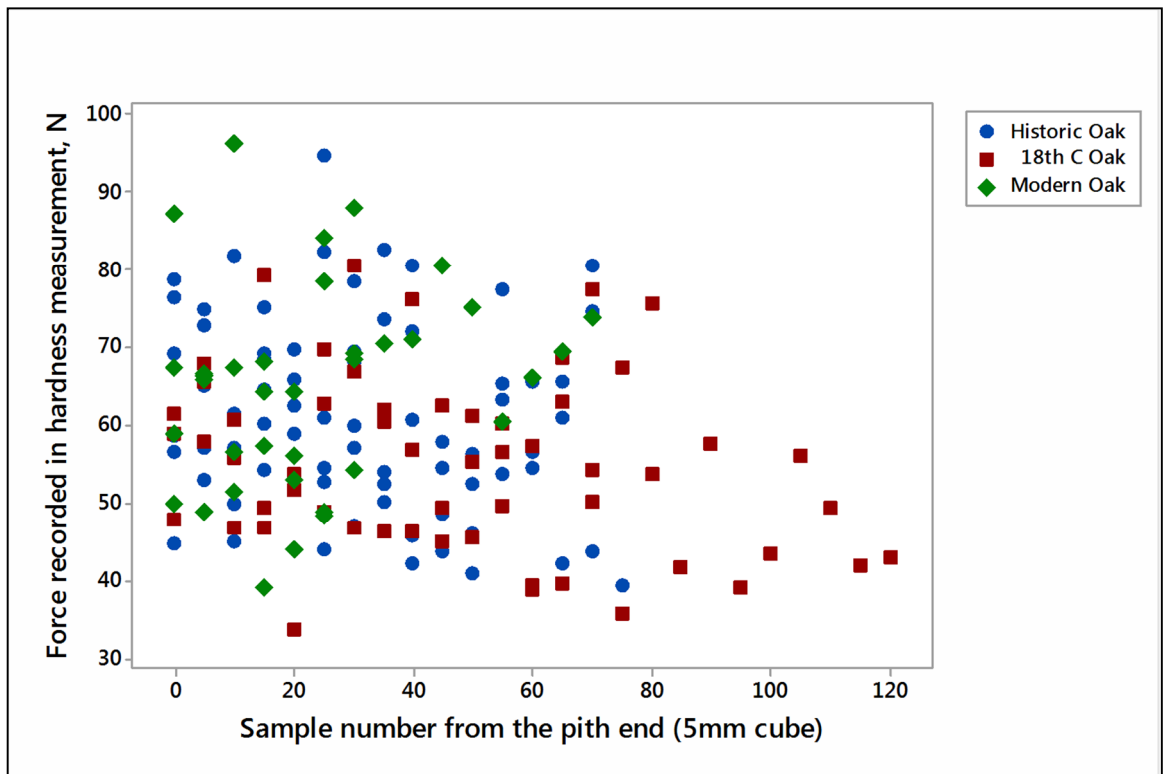
Figure 10.3: Variation in hardness from pith to bark in Oak of different ages.

The scatter graph (figure 10.3) representing the hardness of oak from pith to bark seems to show a slight rise in hardness of the historic oak samples towards the bark, but after running all the different aged samples through a regression model none of them showed a significant trend in hardness from the pith to the bark. This was probably due to the large amount of scatter, as well as oak generally having a rather uniform density from pith to bark. This is discussed further in Chapter 7.

10.2.2 Pine
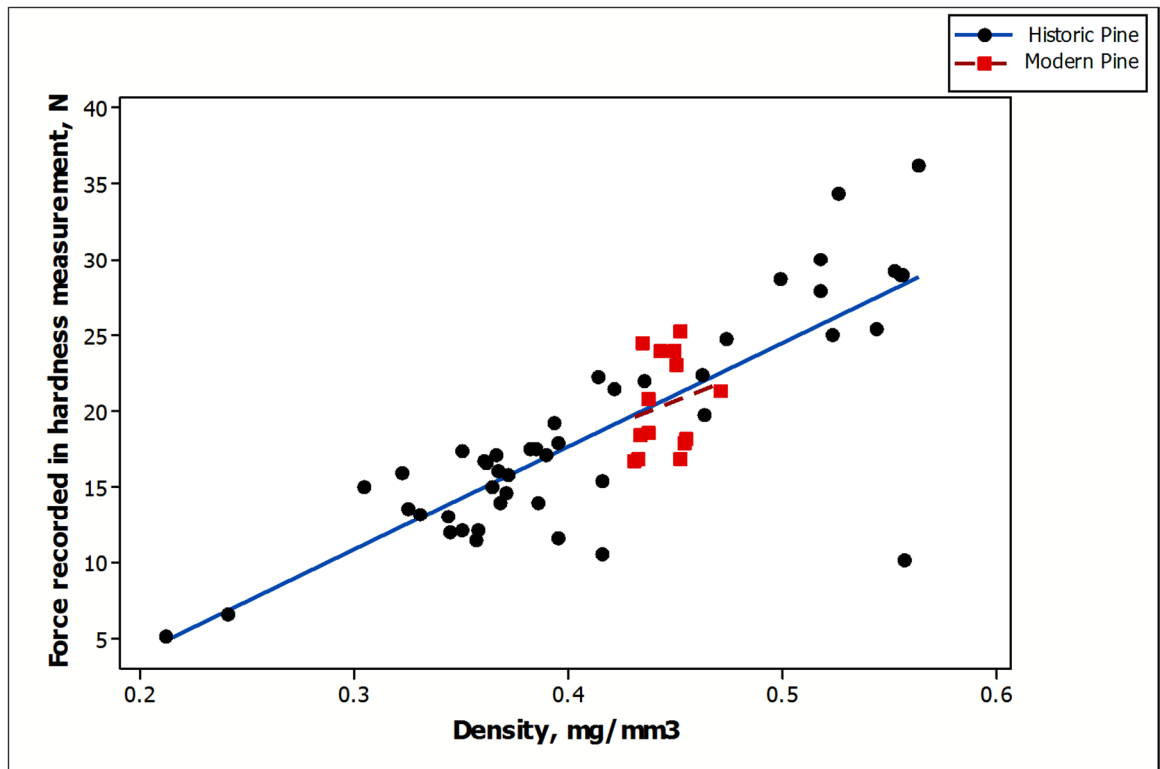
Figure 10.4: Relationship of density to hardness in historic and modern Scots pine.

	Modern Pine	Historic Pine
Hardness (N)	18.46	20.39

Table 10.2: Mean hardness of pine samples of different ages.

There were no significant differences between the means (ANOVA P>0.05).

The *t*- test comparing the historic and modern pine samples showed a P value of >0.05 so there was no significant difference between the two age groups in hardness, unlike the oak samples (table 10.2). This may be due to the large amount of scatter found in the modern samples due to the uneven mix of early and latewood in the area directly tested. There was a larger proportion of low-density earlywood in the modern samples as discussed in Chapter 7.

The comparison of the density and hardness of Scots pine shows that with increasing density the hardness of the wood increased. For the historic pine samples the correlation showed a R^2 Value of 0.677 and a P value of <0.01 but the modern samples show a R^2 Value of 0.043 and P value of 0.475 which is not significant. This may be due to the narrower range of density in the modern samples as they have not lost density

due to decay. The regression line for the pine shows less scatter than the oak. This may be due the fact that density in oak varies less in general than in pine from pith the bark, as is discussed in Chapter 7 The pine sapwood density has already been seen in Chapter 7 to have been reduced by biological attack. This accounts for some of the low densities in figure 10.4.
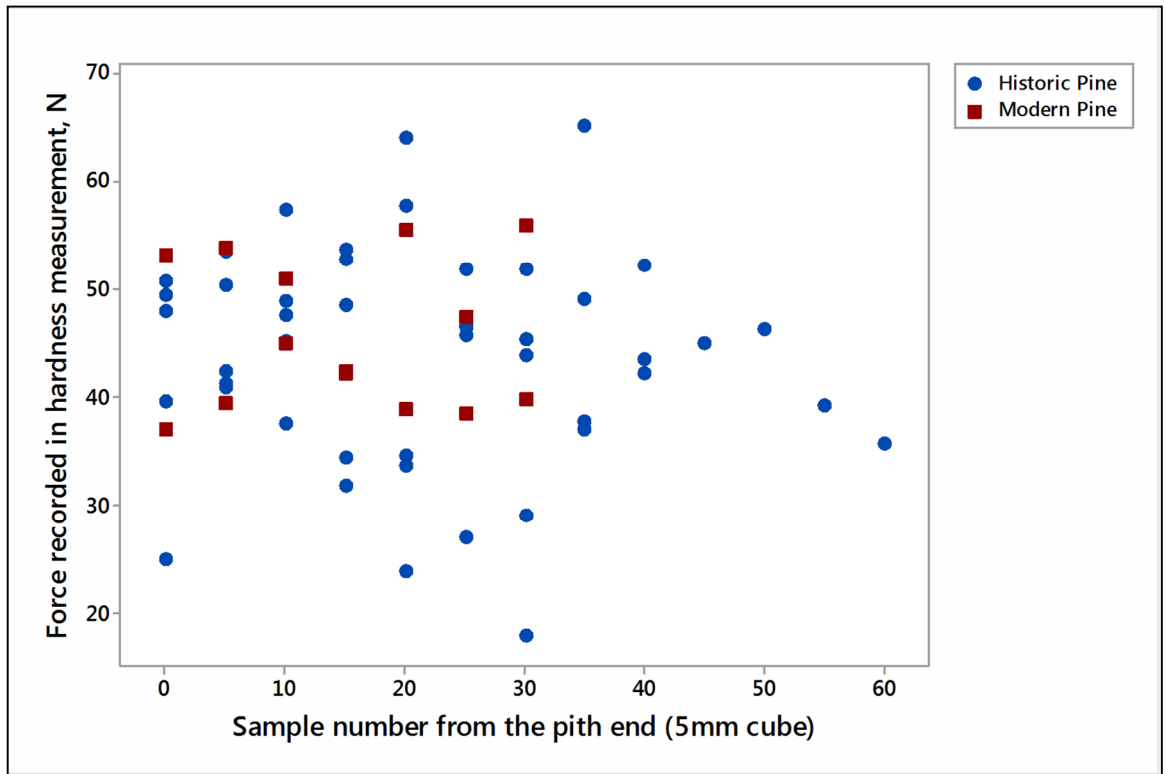
Figure 10.5: Variation in hardness from pith to bark in Scots pine

The scatter graph (figure 10.5) of hardness from the pith to the bark shows no obvious linear relationship in either the modern or the historic samples, and the regression model showed no significant effect of radial position in either age group. This again may be due to the large scatter discussed above, but some of the historic pine samples showed very low hardness which could be explained by loss of material, and hence density, from biological attack.

Hardness, like most wood properties, is affected clearly by density but there is an added possibility that the MFA is affecting the hardness results. If the results had been gathered when testing the samples parallel to the grain, MFA would definitely have been important but when the testing is perpendicular to the grain, MFA is not always considered. Figures 10.6 and 10.7 show the difference in hardness that might be expected between low and high MFA, when testing in this direction. The hardness across the grain would then decrease as the MFA decreased, due to the reduced influence of the more parallel microfibrils.
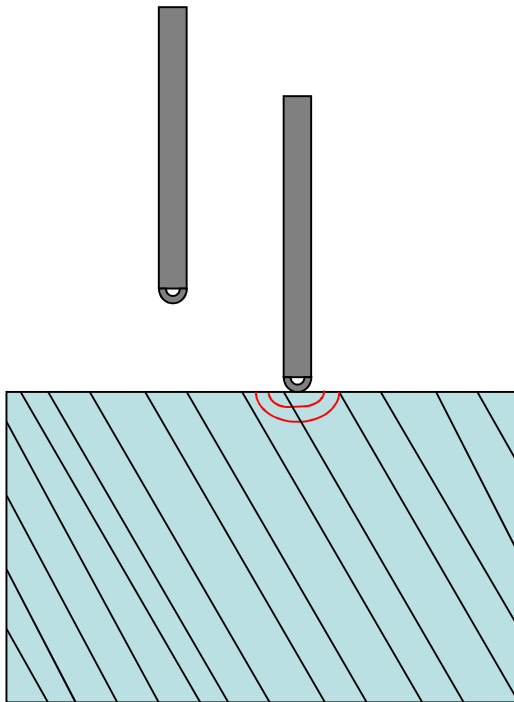
Figure 10.6: Effect of higher MFA on measured hardness when the test probe indents the sample perpendicular to the grain. Diagonal lines show the MFA Image: K Hudson-McAulay.
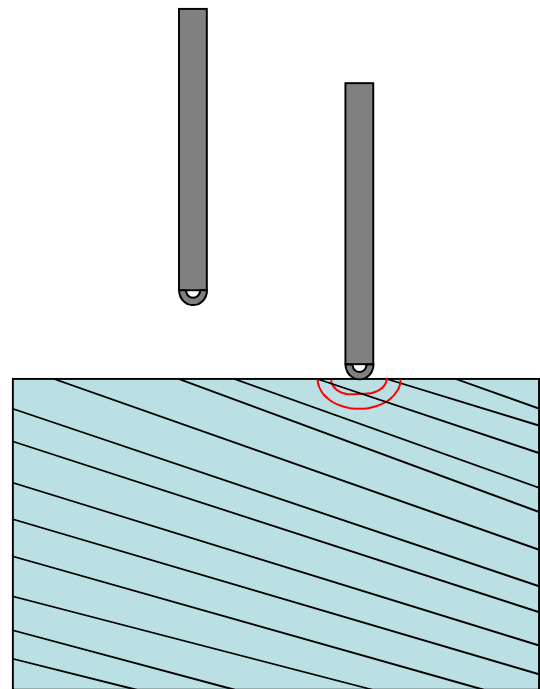
Figure 10.7: Effect of lower MFA on measured hardness when the test probe indents the sample perpendicular to the grain. Diagonal lines show the MFA Image: K Hudson-McAulay.

10.3 Discussion

The results of this experiment showed, as expected from the literature, that the hardness of wood increases with density (Hoadley, 1990; Low, 2001; Oberle et al., 2014). This is what makes this method useful as a way to test indirectly for decay. Although the differences found in wood hardness can be linked to density, this does not mean that other factors do not play a role. For example hardness can also depend on differences between species, such as wood chemistry and anatomy. Cellulose microfibril angle and void space distribution also vary among species (Oberle et al., 2014; Williams et al., 2010, p.42; Silva et al., 2014a), as well as the mass loss due to damage caused by biological attack. All these have different effects on the hardness of the wood. This can be clearly seen from the different hardness measured for the oak and pine samples.
It has been seen that overall, wood has a higher tolerance to the small scale local compression that occurs during hardness tests, than to actual compression testing which can be seen in Chapter 9 (Helińska-Raczkowska and Moliński, 2003). This shows yet

again how remarkable wood is as a building material and as a material in nature. Damage to a few structural cells does not completely compromise the strength and function of wood. This is why wood damaged by pest infestation can still have a long working life if the infestation is prevented from spreading.

Many believe that oak gets harder with age but in the wood tested here the difference in hardness with age, although statistically significant, was in fact very small. An alternative to this accepted idea may be that green wood is softer than historic wood so that possibly, once the green wood has been seasoned and has lost most of the interfering effect of moisture, it shows much the same hardness as historic oak.

It is widely accepted that density has the greatest effect on the hardness of wood (Doyle and Walker, 1985; Riggio and Piazza, 2010). As can be seen from the above data, decay leads to a wider range of low densities in historic wood, causing a loss of hardness that is not seen in sound modern wood. This relationship between hardness and density will change with moisture content and level of decay. Therefore it can be used only qualitatively to assess wet waterlogged timbers (Oberle et al., 2014; Helińska-Raczkowska and Moliński, 2003). The Pilodyn and Resistograph instruments are widely used to test for hardness in this qualitative manner, with the aim of finding any pockets of decay, which will have very low hardness (Sousa et al., 2014; Niemz et al., 2008). For this purpose that form of test is more than adequate and is currently one of the most common 'non destructive' tests used on historic timbers.

Chapter 11

Discussion

Published research on historic wood is very limited compared to that on archaeological or wet waterlogged wood. It is generally assumed that if *in situ* historic wood is visibly free from biological decay, it is sound (Grabner and Kotlinova, 2008; Feio et al., 2008), but wood itself is a biological material and might therefore be subject to aging like any other. This thesis is concerned with natural aging of wood and how historic wood comes to be different from modern wood, as these differences could make the traditional 'like for like' timber replacement repairs unsuitable, indeed potentially dangerous in some cases. When this thesis was first proposed it was hoped to get access to the entire timber beams from a number of painted ceilings that had been salvaged during the demolition of late Medieval Scottish buildings, and were stored in the care of Historic Scotland. Unfortunately this was not possible. In the end I only had access to sections of a few cm in length from the beam ends. This led to the development of more novel, miniaturised methods to enable the testing of the mechanical properties of the timber. There is a constant problem when trying to assess the aging characteristics of historic wood due to lack of material available for scientific testing. Some of the methods developed here will be useful for future researchers in this area.

Any chemical changes that occur with age are likely to change the mechanical properties of historic wood, and as a result cause differences in how it interacts with modern wood. Differences in wood stiffness could cause a repaired joint to be mismatched under load, causing added stress. Differential shrinkage between the modern and historic wood in a joint, under varying humidity, would also put it under stress. Distinguishing between natural aging and effects of biological decay can be difficult towards the sap edge of the wood, as fungal decay, in particular, causes damage much further into the wood than the visible signs. To overcome these issues the experiments were carried out using series of samples from the pith to the bark as biological decay in wood is, in most cases, confined to the sapwood. Therefore, covering the whole period of a tree's growth represented in the cross-section of a beam can allow us to distinguish between changes occurring throughout the wood and changes at the sapwood caused by decay rather than age.

11.1 Differences between historic and modern wood originating from forestry practice.

Before differences to do with any effect of aging are discussed; the natural differences between historic and modern wood need to be taken into account. Both forestry techniques and climate are different today from those in the past. Trees are sensitive to the climate they are grown in. Varying climate will change the properties of the wood (Feilke et al., 2011). This is one of the fundamental tenets of dendrochronology and is used in trying to reconstruct the palaeoclimatic record. Therefore slight differences in the properties of historic and modern wood are expected.

Historic wood generally came from forests which were either natural or slower grown than the plantation trees used for commercial timber production today, giving the wood different properties such as, in most conifers, a higher density and lower microfibril angle (MFA), which are considered to imply better quality wood (André et al., 2014). The historic samples which have been used in this project are all from within the 1500s and 1600s. Matching these timbers to the best modern day equivalent is bound to be difficult, as many of the forests that these trees were taken from do not exist today (Crone, 2011). Dendrochronological evidence from these samples showed that they were from slower grown trees. Wood from slow-growing trees has a smaller annual ring width in comparison to fast-growing trees, as can be seen in figure 12.6. The trees used to produce the beams that the samples were taken from ranged between 88 and 272 years old (Crone, 2011). For the wood samples used in this project the average ring width for historic oak is 1.3 mm, compared to the modern oak with a ring width average of 2.7mm. The historic Scots pine had an average ring width of 0.8 mm whereas the modern pine samples had an average of 3.3mm. It would be expected that this would have a direct impact on the quality of wood produced from these trees. Slow growth in softwoods normally improves wood quality, giving higher density and lower MFA which leads to high stiffness and strength. The effects of slow growth in oak are not as well understood with respect to MFA or mechanical properties, but slower growth in oak leads to lower density (Taylor and Franklin, 2014).

Overall there was no significant difference between the densities of historic and modern oak, from the results shown in Chapter 7 (figure 7.1). The MFA values of modern oak and historic oak are more difficult to compare, as the MFA for oak was produced from a calibration made for Scots pine so that all the MFA values in figure 6.29-34 are very high. These high values may be a result of extractives in oak which influence the baseline correction of the FTIR spectra and which could be changing with age. However it can be seen that the relative MFA of historic oak follows the pattern seen in modern

oak, slightly higher at the pith but then remaining almost constant throughout the tree's growth.

Although there was a difference in overall mean density between the historic and modern pine samples, this was due to decay in the sapwood leading to the lowering of the mean density of the historic wood samples. The heartwood density of the historic Scots pine was not significantly greater than that of the modern wood. This was unexpected in view of the narrow ring width in the historic samples.

Figure 6.18 shows that the MFA in the heartwood of historic pine averaged approximately 10˚. The modern wood shown in figure 6.19 had an average MFA of 14˚, which is not unusual for present-day commercially grown Scots pine. The lower MFA shows that the slow grown historic wood was originally of better quality than most wood produced today. With careful selection it should be possible to select modern Scots pine with similar MFA. The C24 structural grade of Scots pine probably approaches an average MFA of 10˚ and Scots pine exceeding this grading can be obtained to order from some Scottish sawmills. However in some circumstances it might be preferable to select timber with higher MFA, to compensate for loss of stiffness in the historic timber being matched. That is, it could be worth considering matching the stiffness of historic timber rather than matching its MFA.

One area of concern with traditional repairs is the difference in MFA between the modern and historic wood and its effect on swelling and shrinkage. MFA strongly affects shrinkage and the results from Chapter 5 show that there were statistically significant differences between the shrinkage of old and new pine and of old and new oak.

In Chapter 5 only the radial and tangential shrinkage were measured, because longitudinal shrinkage is minimal and cannot be measured on such small samples. Figure 5.1 shows that lateral (tangential and radial) shrinkage is expected to become less with increasing MFA whereas longitudinal shrinkage becomes less at low MFA. Some of these predictions match the shrinkage data in Chapter 5. The tangential shrinkage followed the expected behaviour where the samples had not been affected by biological decay. But the radial shrinkage did not correlate with the tangential shrinkage. The reasons for different patterns of radial shrinkage are unknown but it has been suggested that the ray cells, where the microfibrils run in the radial direction, could be causing different shrinkage patterns (Harris and Meylan, 1965; Treacy et al., 2000; Patera et al., 2013).

11.2 Mechanical weakening of wood through pest infestation.

It is well known that decayed wood is weaker than sound wood, and that pest infestation causes the most damage to wood cells. Pests are usually contained inside

the sapwood (Ridout, 2000, p.180; Unger et al., 2001, p. 62; Desch and Dinwoodie, 1996; p. 251). Within this thesis pest infestation damage can be seen in microscopy images of the historic wood samples (figures 2.14 and 2.19) showing pest holes in both pine and oak sapwood samples.

Loss of density and consequent mechanical weakening from visible pest infestation (although there will also be fungal damage within this) can be inferred from the density data in Chapter 7. Figures 7.6, 7.7, 7.9 and 7.10 show a drop in density due to damage matching the visible decay caused by pest infestation in the sapwood samples of both oak and Scots pine. The drop in sapwood density is reflected in both the compression stiffness of the historic Scots pine samples and the 3-point bending stiffness of the historic oak samples. Figure 9.6 shows the drop in compression stiffness of the historic Scots pine sapwood. This is not seen in modern wood as the sapwood is usually the stiffest region in softwoods, as it has the lowest MFA. Therefore the loss of compression stiffness can be put down to the damage and loss of density resulting from both pest and fungal decay. Figure 8.3 shows the decline of bending stiffness in the historic oak sapwood. This was not quite so sharp as for the historic pine samples and the oak suffered less from pest infestation, having more effective natural defences (Carvalho et al., 2009; Clausen, 2010).

11.3 Polymer breakdown of wood from fungal decay.

Figure 8.4 shows that the MOE/D ratio in oak decreased significantly towards the bark, although with considerable scatter. This is evidence of decay in the sapwood and just beyond the heartwood/sapwood boundary. It did not occur throughout the entire sample and therefore was not a result of natural chemical aging of the wood. As the MFA data in figure 6.35 shows a linear pattern, this loss of stiffness is not due to MFA. Pest damage would be expected to cause weakening in wood as pests completely destroy wood cells. However pest damage will cause loss of density at the same time as loss of stiffness, and the calculation of MOE/D allows for this. Fungal decay is capable of causing loss of stiffness before any loss of density is seen (Bader et al., 2012; Brites et al., 2013; Curling et al., 2001), so that any changes in the MOE/D ratio are most likely due to fungal decay not pest damage. The reduced MOE went deeper into the wood than the loss of density, which can be visibly matched to the pest infestation as is evident from figure 7.3 and figure 8.4.

These graphs show that the effect of fungal decay extends into the wood deeper than can be seen without detailed investigation (Bader et al., 2012; Brites et al., 2013; Curling et al., 2001), and that loss of density alone is not enough to indicate the full

extent of biological damage. This can be seen in figure 8.4 where the lower MOE/D can be seen occurring from sample 20 outward. As each sample is a 5 mm cube this is 40-50 mm from the edge of the beam, which may show that the weakening extends just inside the heartwood/sapwood boundary, although this is not conclusive due to the large amount of scatter within the samples. Therefore incipient decay appears to lower the stiffness of wood before any noticeable mass loss occurs. This can be deduced from my own data but also from experiments carried out by Reinprecht and Hibký, (2011). Enzyme degradation cuts the polymer chains of cellulose and hemicelluloses, especially if the enzymes are from brown rot fungi (Reinprecht and Hibký, 2011; Ridout, 2000, p.30). The loss of cellulose will obviously result in loss of stiffness because the microfibrils that govern wood stiffness consist of cellulose. In the incipient stage of decay the hemicelluloses are the first polymers to be attacked (Curling et al., 2001). Other studies have shown that the loss of hemicelluloses could also be contributing to the loss of stiffness of wood (Bader et al., 2012).

Chapter 4 shows that there were wider effects of polymer breakdown caused by the enzymes produced in the decay mechanisms of fungi, especially in the breakdown of Scots pine. Aside from weakening the wood, the enzymes caused the polymers to be converted to monomeric sugars which the fungi would be expected to metabolise for their own growth and respiration, but some of these sugars may be left in the wood. As these are soluble they are one of the possible causes for increased uptake of moisture. Chapter 4 also shows that historic Scots pine had the ability to absorb 30 – 50% more moisture than modern pine, as can be seen in figure 4.6. In comparison, for oak there was no significant difference in water sorption between modern and historic wood (figure 4.3). Further experimentation into the increased water sorption in historic pine showed that there was a higher concentration of soluble sugars in comparison to modern pine (table 4.2). There are two possible reasons for the higher sugar concentration. One is the preferential breakdown of the hemicellulose, and possibly cellulose, chains by enzymes produced by the fungi. The other potential reason is the hydrolysis of the hemicellulose polymers into monomers by the increased trapped acetic acid in the pine following the detachment of acetyl groups. This is discussed in Section 11.4 below.

Further evidence for the breakdown of cellulose in the S2 layer of the wood cell wall by fungal decay comes from the MFA experiment in Chapter 6. Figure 6.18 shows an increase in MFA in the sapwood of the historic Scots pine samples. This did not occur in modern wood, where the MFA was high at the pith but then became lower throughout the rest of the tree's growth. From the evidence in Chapter 6 it is concluded that the fungi had preferentially attacked the S2 layer which is lower in lignin. The destruction of the S2 layer resulted in the mean MFA being determined mainly by the S1, S3 and

primary wall layers, which have a microfibril orientation much less aligned with the cells. This must be due to fungal breakdown rather than pests, as pests would have completely destroyed many of the cell walls, not just the S2 layer, so that no change in MFA would be predicted.

11.4 Mechanical weakening of wood through age, without biological decay.

All the results showed that with oak there was no statistically significant difference in density or mechanical properties between the modern and historic samples, aside from the damage caused by biological decay. Historic Scots pine on the other hand was different in both density and stiffness from the modern samples. The change in density can be put down to biological decay but the change in stiffness cannot be attributed to decay alone, as it was occurring throughout the entire beam from pith to bark, and not just in the sapwood. Reduced stiffness in the Scots pine heartwood is unexpected as the MFA for historic Scots pine was lower than modern, and thus it would be expected that the stiffness would be higher. Therefore the historic Scots pine has lost stiffness over time. This reduced stiffness in the historic pine heartwood may be due to the effect of acetic acid which is discussed further in section 11.5 below.

Hardness testing of the oak samples also showed no statistically significant difference between the different ages of oak tested. Therefore the widely held notion that oak gets harder with age was not confirmed for the samples tested here. Based on the results of this project (figure 10.3) it can be suggested that oak becomes harder not because of aging, but due to the seasoning process. The prediction that seasoned oak is harder than unseasoned green wood could be tested using methods similar to those used here.

11.5 Chemical breakdown of wood polymers during aging

From this project there is substantial evidence that the hemicellulosic polymers in both the softwood Scots pine and the hardwood oak were degrading with age. The results in Chapter 3 show that both historic oak (figure 3.7) and historic pine (figure 3.11) had a decrease in the acetyl groups associated with the hemicellulose polymers. This is assuming that there was originally a constant amount of acetyl within the wood. There is some evidence supporting a relatively constant amount of acetyl groups with the main difference being between early and latewood (Gorzsas et al., 2011; Kim and Daniel, 2012). From figure 3.8 and 3.12 it can be seen that reduced acetyl content was not a product of decay as the low levels were not localised within the sapwood but occurred throughout the entire wood beam from pith to bark.

Although a reduction in acetyl content occurred in both the oak and the Scots pine it appeared to affect the two species of wood very differently. The breakdown of these acetyl groups by chemical hydrolysis forms acetic acid, which would be released into the wood. Although acetic acid is considered to be a weak acid and does not completely ionize in water, when concentrated in the limited available moisture within wood it may still allow acid hydrolysis of the glycosidic bonds between monomer units in hemicellulose chains. Xylans are more susceptible to acid hydrolysis than glucomannans although all hemicelluloses are more susceptible than cellulose. Studies on historic paper have demonstrated its breakdown with aging due to the effect of acetic acid hydrolysing the cellulose polymers (Dupont and Tétreault, 2000; Tétreault et al., 2013). Acetic acid increases the acidity of the paper, leading to degradation of its mechanical properties (Menart et al., 2014). Therefore, it is logical that acetic acid could have a similar effect on wood. The mechanical testing data on the historic Scots pine do show a loss of stiffness in the historic pine in comparison to the modern pine, as can be seen in figure 9.6. As previously mentioned it would be expected that the historic pine would be stiffer due to its lower MFA. The reduced stiffness therefore shows that the weakening of the Scots pine was due to age, as the loss of stiffness was not confined to the sapwood where it was caused by biological decay.

In oak there was no significant difference in stiffness between the ages tested. It is suggested that due to the large vessel diameter in oak, the acetic acid can escape from the wood structure much more easily than in pine, where it becomes trapped and then acts as a catalyst in the further breakdown of the hemicellulose polymers. This possibly caused the pine wood to lose stiffness and its hemicellulose chains to break down into smaller sugar units. These sugars could be one of the causes of the increased water absorption in the historic pine recorded in Chapter 4. However this experiment showed that hydrolysis by fungal enzymes may be another cause for the increase in free sugars within the historic pine, as well as acid hydrolysis by acetic acid. There was no significant difference in either density or moisture sorption between historic and modern oak.

Another observation in the literature (Popescu et al., 2006; Fackler and Schwanninger, 2012) is that lignin content has been seen in some spectroscopic studies to increase with age. Figure 3.4 does show an increase in the lignin content with age in oak, when its FTIR peak area was ratioed against fingerprint peaks for cellulose and hemicelluloses taken together. The calculation was re-done using only a cellulose peak, and figure 3.6 shows that there was then no significant increase in the relative lignin content with age. The relative increase in lignin content may simply have been due to the loss of the hemicellulose polymers.

11. 5 Conclusions

Evidence was found for both mechanical and chemical differences between historic and modern wood, additional to those resulting from the effect of biological decay due to pests and fungi. Some of these differences originate from the slower growth of the historic samples which were used in this project, leading to lower MFA and hence greater predicted stiffness in the historic pine, but not in oak. Some of the changes with age affected the hardwood oak and the softwood Scots pine in different ways. Chemical degradation of the wood polymers over time could be clearly seen in both oak and pine, which lost acetyl groups from the hemicellulose polymers to form acetic acid. Although the acetic acid appears to have had no real effect on the historic oak, the historic pine lost stiffness compared to the predictions from MFA, probably due to the degradation of the hemicellulose polymers by acid hydrolysis.

The breakdown of the hemicelluloses in decayed Scots pine sapwood, by fungal enzymes, led to further loss of stiffness and also possibly released soluble sugars, allowing the wood to absorb 30-50% more moisture than its modern counterpart.

The added effect of the destruction of the S2 layer in the sapwood by fungal enzyme attack caused the MFA to be recorded as higher than expected, as the measured MFA reflected the microfibril orientation for the other cell wall layers. The loss of the microfibrils from the S2 layer might have an effect on the shrinkage of wood but that is unclear from the evidence in this project.

Overall this project produced evidence of changes to the mechanical and chemical properties of wood with age, some of which could impact the effectiveness of current conservation practice and repair work involving timber replacement.

Chapter 12

Conclusions for Conservation

Conservation science is a fairly new field. The outcomes from projects in conservation science need to be understood by practical conservators to be of use in the conservation field. This chapter aims to put the scientific data from this project into the context of practical conservation issues. As previously mentioned there is very little published research on historic wood, the main reason being that most of the historic wood left in the UK today is part of historic structures or objects, and needs to be preserved for the future, not destroyed by scientific testing. The author was fortunate to obtain some genuine historic oak and pine samples from Historic Scotland, allowing a new look into the aging of historic wood. Determining how historic wood ages is complex as it is necessary to distinguish between biological decay and breakdown of the wood through the direct effect of age (Popescu and Hill, 2013).

Historic wood is often presumed to be stable with time, with nothing happening to affect its properties that is not caused by biological decay (Grabner and Kotlinova, 2008; Feio et al., 2008; Gereke et al., 2011). The first thing that conservators ought to know from this research project is that in both Scots pine and oak, acetyl groups are lost from the hemicellulose polymers with age. Thus like any biological material, wood suffers from chemical breakdown with age, but this effect has very different consequences in oak and in Scots pine.

12.1 Conservation impact on Oak

The array of different tests carried out here showed that oak, despite this chemical breakdown with age, is extremely stable in its mechanical properties. It behaved in mostly the same manner as modern oak without recognisable changes in stiffness or hardness other than the natural variation expected within and between trees. Chemically there were changes, but these were not affecting oak in a physical manner. There is a slight difference in the amount of water that historic oak absorbs in comparison to new oak. This is most likely due to the loss of acetyl groups. Although there is a difference in sorption between the modern and historic oak it is not large and it would only cause damage through differential shrinkage of the two parts of a repaired joint in the most extreme RH fluctuations. When taking into account the variation between trees it is probably negligible within a well cared for building environment.

One other concern about the chemical changes occurring in oak is not so much a concern for the wood repairs themselves, but for surrounding objects. It is common knowledge within the conservation world that oak gives off acetic acid no matter what its age. This is why museum cases are no longer made of wood as metals, especially iron, suffer severe corrosion when in contact with acetic acid (Zelinka et al., 2008). Timber repairs today are not done using iron for these reasons. The concern for conservation here is illustrated by the display of weapons shown in figure 12.1. It is possible that mounting this high up close to the oak panelling could cause corrosion to the metal. It might be an idea to investigate how far the acetic acid produced by oak can spread: in a well ventilated building it might not be an issue.

Figure 12.1: Weaponry displays which may be vulnerable to acetic acid released from wood into their surroundings (Marsden and Winterbottom, 2010, p. 8).

12.2 Conservation Impact on Scots Pine:

The problems implied by the results for Scots pine are of more concern for conservation. The chemical changes to the wood polymers affect Scots pine more than oak. Firstly, the mechanical properties of aged Scots pine were found to be inferior to equivalent modern wood, throughout the beams studied and not just at the sap edge where the changes could be put down to mass loss through pest infestation. Historic Scots pine not only had lower stiffness but also, at high humidity, absorbed 30-50% more moisture than modern wood. This could have a major impact on the traditional splice joints used to repair historic timber structures, where the atmosphere was not well controlled. Excess moisture attracted by the older wood could lead to

water pooling in the joint. This could result in biological decay (Pizzo, 2008) setting in and destroying the new joint. Also the different levels of moisture taken up by the differently aged wood members may cause differential shrinkage between the two and apply even more added stress on the new joint. Both historic oak and historic Scots pine were shown to shrink and swell differently from the modern wood. In modern wood, shrinkage is controlled by MFA (Mansfield et al., 2009; Esteban et al., 2010; Kretschmann, 2010). As there is already a significant difference in their equilibrium shrinkage due to age, this could cause differential movement within a timber repair, and possibly unwanted stress within the joint.

Rigorous control of RH and temperature in a building should be enough to control any problem with the dimensional stability of oak wood and also to control the moisture sorption problem in pine, but 'like for like' pine repairs to joints need to be carefully considered as historic Scots pine is not as invulnerable as people are led to believe. Although it is perfectly capable of completing its service life, repairs need to be done with care making sure that no unnecessary stress is introduced. This requires good control over the building environment and very careful selection of the replacement timber piece for the new joint.

12.3 Consequences for the conservation of joints

Joints are the key to the functioning of timber structures and need to be considered with care (Branco and Descamps, 2015) whether they are old or new. When replacing part of a decayed timber, the new joint between the old and new timber is commonly a scarf or splice joint (figure 12.2). This kind of joint is today usually fastened using both resin adhesive and steel pins, although where possible wooden pegs may be preferred as this was how scarf joints were fastened historically (Brunskill, 2004, p.156).

In Scottish historical timber structures the most common existing joints are dovetail joints (figure12.4), lap and half lap joints (figure12.5) and mortise and tenon joints (figure 12.3). Each of these joints needs careful consideration when one of the joined timbers is to be replaced. For example it is relatively easy to repair a joint if the loads on the structure will be pushing the joint together (under compression). Joints are harder to repair when there are tension forces pulling the joint apart e.g. the joint between a tie or collar beam and a rafter.

12.3.1 Scarf or splice joints

The scarf joint is typically used in repairs where new timber is inserted, for example when a decayed beam end is cut back to remove a short length weakened by decay and

a new piece of timber is scarfed onto the sound part of the beam to make up the lost length. Existing scarf joints (figure 12.2) are also occasionally found in historic structures when a long timber member is made from two or more pieces. There are different types of historical scarf joint but all are pegged together (Brunskill, 2004, p.144) and are never as strong as a continuous solid beam (Branco and Descamps, 2015). Further strain will be put on a scarf joint if the new and old timbers are not compatible. From this research we can say that very strong forces along the grain will develop if one part of the joint swells or shrinks longitudinally more than the other in changing levels of humidity. The force produced from this mismatch is capable of destroying a pegged joint or even bending a whole timber if it has been glued. Differences in longitudinal shrinkage will occur if the timber members making up the joint are responding differently to moisture, or if one is wet and the other dry. Unfortunately this research cannot say more about matching new to old in this respect, as longitudinal shrinkage was not tested due to the small scale of the sample material.
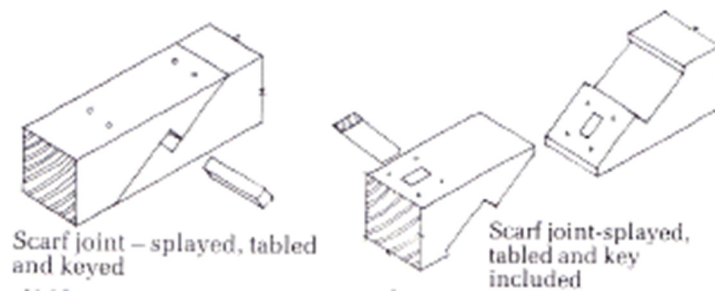
Figure 12.2: Example of a typical historic scarf joint (Brunskill, 2004, p. 145).

12.3.2 Mortise and tenon Joints

In a mortise and tenon joint (figure 12.3), the tenon formed on the end of one timber slots into the mortise cut into the other. Both of the timbers are weakened as the joint is cut into them (Brunskill, 2004, p.140). There are a number of variations of the joint and the tenon can be formed one- or two-shouldered (Brunskill, 2004, p.143; Branco and Descamps, 2015). If the fit is slightly slack, these joints undergo a little movement and rotation when under load, and work like hinges (Bulleit et al., 1999; Sangree, et al 2008). The tenon can be pinned into position to prevent it from coming out once it is positioned. The dovetail tenon joint also achieves this but without the need for extra pinning (Brunskill, 2004, p. 143; Branco and Descamps, 2015). A mortise and tenon was generally favoured for beam to column joints between load bearing timbers. When these joints fail, it is generally a result of flexing in the beam itself away from the joint (Bulleit et al., 1999). Lateral shrinkage is the key to the success of a repaired joint. This research shows that lateral shrinkage changes with age. Although the detail is

complicated it can be said that lateral shrinkage will cause this type of joint to slacken if the timber member that is forming the tenon shrinks more than the mortise. If the member that contains the mortise shrinks more it could split as a result of the pressure from the tenon. There are several ways to mismatch timber in lateral shrinkage: (1) Difference in moisture content between the old and new timber pieces when the new piece is being shaped for the repair; (2) Changes in shrinkage due to the different ages of the samples; (3) Any difference in MFA between the two pieces will result in a difference in lateral shrinkage; (4) The difference between longitudinal and transverse shrinkage or between tangential and radial shrinkage.
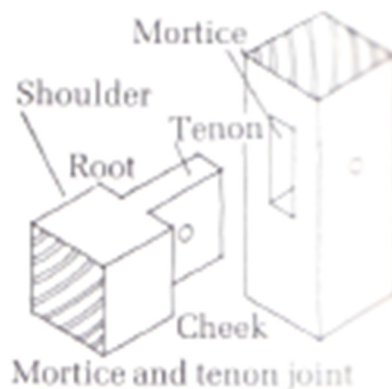
Figure 12.3: Example of a typical mortise and tenon joint (Brunskill, 2004, p. 142).

12.3.3 Dovetail joints

The dovetail joint (figure 12.4) was traditionally used in Scotland as the favoured joint in the jointed cruck frame. A dovetail joint is commonly used between collar and rafter beams or between struts and other members. It is one of the very few older joints which can deal with tensile as well as compression forces (Kunecký et al 2015). The dovetail joint relies on an exact fit: if the contact area becomes small and the gaps large it can slip under tension (Branco and Descamps, 2015; Kunecký et al., 2015). Another common type of failure in a dovetail joint is the splitting of one of the members due to forces produced by the wedge shape of the joint under tension (Branco and Descamps, 2015). The same shrinkage issues found with the mortise and tenon joints apply to dovetail joints. The only key difference is that the dovetail joint must stay tight if it is to work correctly in tension.
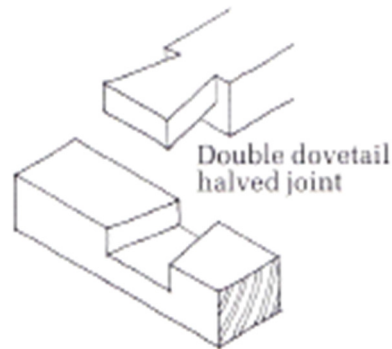
Figure 12.4: Example of a typical dovetail joint (Brunskill, 2004, p. 141).

12.3.4 Lap joints

Lap joints (figure 1.6) and half-lap joints again have variations but are generally used when one lighter timber member is passing over another. For example when a brace meets a rafter, usually one member will be rebated to allow the other to slot in (Brunskill, 2004, p.142). Lap and half-lap joints are usually held together with pins. Occasionally one member will be dovetailed into the other, which is another way to reinforce this joint against tensile forces (Branco and Descamps, 2015). Otherwise, as the joint is heavily reliant on the strength of the pins its efficiency can be very low. The wooden pins need to fit perfectly in the joint for it to function well, but over time the pins can slacken due to movement of the structure (Branco and Descamps, 2015). The pins will suffer from extra shear stress produced by differential shrinkage if a new, mismatched piece of timber is substituted on one side of the joint (Sjödin and Johansson, 2007). Loosened pins need to be repaired or replaced, otherwise shear failure can occur reducing the load capacity of the joint (Branco and Descamps, 2015). Gaps between timbers mean that the members are not in full contact with each other and will need reinforcement to avoid failure within the frame. Traditionally this was done with wooden wedges or additional pegs (Branco and Descamps, 2015). Well matched timber and good control of the surrounding RH environment will reduce stress on the new joint from differential shrinkage between the old and new wood, but the difficultly of assessing old timber to facilitate a good match needs to be overcome by future research (Branco and Descamps, 2015).

12.4 Suggestions for improvements in current conservation methods

A new timber joint requires careful selection of the replacement piece. There are many things that should be taken into account to provide the best match for both oak and Scots pine, but this is both more difficult and more important for Scots pine. Even in oak, it is obvious that the moisture content of the new wood should be matched with the old. For example, due to difficulties in sourcing seasoned oak in large dimensions, green wood is sometimes used to repair a historic structure, and having an initially high moisture content it dries out once it is in service. This can cause loosening of joints, particularly mortise joints, when the green wood shrinks as it dries over time in contrast to the historic wood which is already completely seasoned.

One of the key things to be taken into account is the microfibril angle (MFA) of the wood. The MFA, as discussed in detail in Chapter 6, governs the stiffness and shrinkage of timber (Lachenbruch et al., 2010; Bader et al., 2012). The MFA changes through the growth of a tree. That is why it is important to match the MFA of the historic material. Juvenile softwood has a higher MFA as it needs to bend with the wind. The MFA then gets smaller as the tree matures, to provide support for the larger crown (Auty et al., 2014; Gryc et al., 2011). Therefore, if a piece of juvenile wood is inserted into a joint along with mature wood it will cause a huge amount of stress to the structure.

MFA is also important when the replacement of a whole structural timber is needed. As MFA governs the stiffness of each piece of timber, it needs to be matched as closely as possible to the timber removed, as a piece of new timber with a large difference in stiffness, added into a structure, could lead to the loads within the historic structure being badly distributed and cause unwanted movement and stress in the other supporting timbers. An example of this is the replacement of floor joists, if the replacement timber is stiffer or less stiff than the original, the floor will deflect unevenly under load and there will be local bending stress on the floorboards.

As mentioned in Chapter 6 MFA is difficult and expensive to measure, out of reach of most conservation budgets, but the approximate MFA can be gauged by looking at the growth rings on the end grain of the timber, and seeing which part of the tree the original beam was cut from and how wide the growth rings were. The replacement piece can then be cut from the same part of a similar tree. As the average MFA recorded from the historic Scots pine was 10° it is possible to achieve a similar MFA by careful selection of good quality modern Scots pine, even though trees were generally grown more slowly in the past producing a higher average quality of wood than today. Much present-day Scots pine contains a large amount of fast grown juvenile wood which is easily spotted from the wide growth rings (Gryc et al., 2011).

Figure 12.5: Comparison of growth rings between the slow grown wood on the left and the fast grown wood on the right (Science Photo Library, 2013).

It is possible to select for both density and MFA as these are separately governed by the physiology of the tree (Wagner et al., 2013). However, finding the best match for historic timber can be very difficult today for the above reasons and because many trees from medieval forests were of much greater diameter. Trying to find wood to match even the thickness of some historic beams is difficult to start with, but close co-operation with UK saw millers would be helpful in sourcing suitable Scots pine.

Wood will always continue to draw water into its structure, no matter what its age but depending on the environment surrounding it. Water absorption may become slower as in the case of historic oak, but wood never loses the ability to absorb and desorb water (Buck, 1952). Control of RH and temperature is the best course of action for any wooden material. Wood tolerates natural fluctuation in RH just as a tree tolerates seasonal change, but constantly changing RH is like going through thousands of seasonal changes in a short space of time, which can be damaging to the wood structure and to joints (Erhardt et al., 1996; Kozlov and Kitsernaya, 2013). Differential movement in historic wood is not a problem except in joints, but it is also a concern for the survival of historic wooden artefacts, especially polychrome statues, painted wooden panels and anything else with a paint coating that does not move with the wood, leading to susceptibility to a whole range of issues including cracking, paint flaking and hidden moulds developing on the back or under paint layers. Maintenance is a key thing for both historic buildings and museums (Buck, 1952).

12.5 Summarised implications for conservation.

The original aim of this thesis was to discover if there were any differences in quality between historic and modern wood which could have been caused by the different growing conditions in medieval forests compared to today's forests. From the results it could be seen that there are differences resulting from different growing conditions, but these were not large enough to require changes to the current conservation practice of sourcing modern timber for traditional repairs using 'like for like' replacement, provided that the replacement timber has properties similar to those of the historic timber when it was felled.

However, unexpectedly it was discovered that the mechanical performance of Scots pine deteriorates with age, caused by a chemical mechanism that is not connected with fungal decay or pest damage, but is caused by the natural aging of the wood. The loss of stiffness in pine is described in Chapter 9, but the results of this research project can only suggest what practical conservation problems might result. It was out of its remit to test large timbers or timber structures, and the pine samples were only tested for stiffness, not strength. Calculations of the structural safety factors for historic floor or roof structures using stiffness figures published for modern Scots pine may therefore be unreliable, but further testing of larger samples would be needed before stiffness and strength data for historic pine could be derived. A suggested alternative which may be more appropriate is to measure the sag of pine floors *in situ*. None of these problems were demonstrated to apply to oak.

Both historic pine and historic oak show differential shrinkage in comparison to their modern equivalents (Chapter 5). Differential shrinkage can potentially cause a range of problems, discussed in Section 12.3, in joints between old and new timber. The most important recommendation is to make sure the moisture content of wood used in a 'like for like' repair is similar that of the historic timber. This means not using green oak in such repairs as it will cause added strain on the joint, as one side of it dries out. Matching the timber as closely as possible in grain direction and microfibril angle (MFA) (discussed in Chapter 6) is also recommended if possible.

Matching moisture content and MFA is more difficult in repairs using Scots pine than in oak, due to the loss of stiffness in pine over historic time, and because historic Scots pine can absorb 30-50% more moisture than modern pine (Chapter 4) whereas in oak the difference in moisture-absorbing capacity with age is very small.

Careful matching of new timbers in MFA and moisture content will improve the future success of repairs. These measures need to be backed up with proper maintenance and monitoring of the humidity environment of historic buildings, making sure that relative

humidity does not fluctuate to extreme values. This will keep the wood's moisture content constant and therefore restrict movement via swelling and shrinkage to a minimum.

For these reasons, an understanding of the behaviour of aged and new wood is crucial to carrying out successful conservation on historic wooden structures. Applying the findings of this thesis will give appropriate longevity to conservation treatments carried out on historic wooden structures.

12. 6 Future Research

In the course of the research done during this PhD project, a number of areas were identified that were out of reach in terms of both time and resources, but would justify further research.

As already mentioned in Chapters 8 and 9 all the tests described here were carried out on micro scale samples, due to lack of material. Although it could be difficult to make larger samples available, it would be important to carry out mechanical testing of historic Scots pine timber on a larger scale. The miniaturised compression test described in Chapter 9 showed that pine loses stiffness with age, in relative terms, but it cannot reliably estimate the absolute remaining stiffness for pine of any particular age. To calculate the remaining stiffness of historic timber structures, structural engineers need MOE data validated according to the Eurocode system (EN 14081-1). The industry standard bending test needs 'small clear' samples 30 cm long. Because a clear loss of stiffness was demonstrated in the results of this thesis, historic Scots pine material of sufficient dimensions should be released to allow these tests to go forward, for reasons of public safety. As stated before, only stiffness testing was carried out and breaking strength was not measured, but if the hemicellulose and cellulose polymers suffer from degradation due to acetic acid trapped in the wood this might reduce the strength of the wood as well as its stiffness. Strength and stiffness can be measured simultaneously in the standard bending test on 30 cm 'small clear' samples. Testing for loss of strength in historic wood, especially pine should be done urgently. In addition, it maybe possible to load test existing Scots pine timber present in buildings.

Acoustic and ultrasonic testing are non-destructive methods which can used to measure the stiffness of straight beams (Tsang and Chan, 2008; Bucur, 1985). They are best suited to beams which have their ends exposed, but these are hard to find *in situ*. There have been a number of experiments using acoustic and ultrasonic methods to test timber *in situ* but the measurements are difficult to calibrate due to interference from

holes cut into the wood for joints (Kandemir-Yucel, 2007; Chapman et al., 2006). Joints make the sound wave paths difficult to determine due to interference effects.

Load testing is another form of non-destructive testing. This can be done in a variety of ways but the principle is to weigh down the timber with either buckets of water or people. The amount of deflection is measured for a known load and the stiffness can then be calculated (Hume, 1998).

There needs to be far more research into the use of 'like for like' repairs to structural timbers especially Scots pine. As a result of this project it can be said that more research is needed into possible alternative species or the use of different repair methods such as resins. This project alone cannot determine what conservation strategy would be best.

Some of the 'like for like' matching problems are due to modern and historic timbers, both oak and Scots pine, having different densities, ring widths and MFA from their modern counterparts. This is due to historic wood being extracted mostly from slower grown, natural or semi-natural forest. Matching the properties of historic timber rather than, or as well as, the species could help maintain the same structural stability, after repair, but the properties of historic timber need to be researched in more detail. It may be easier find suitable matches for oak than for pine, as the properties of historic and modern oak differ less than Scots pine. This can be looked at as a possible approach, starting with the literature on modern oak. There are further issues in terms of locating the best piece from vast amounts of planting and then the time it would take to season new oak from green to the same moisture content as that of the historic timber. There is an argument for using re-purposed timber from Victorian buildings, and mechanical testing could be done on this material to see if it would be appropriate. Scots pine needs more research due to the more complicated nature of the aging properties.

Hardness of oak is something that has been commented on for years. Carpenters generally say that historic oak is a lot harder than green oak. In the research here quantitative measures were used to see if science would back this up (Chapter 10). It was found that there was no difference in hardness between modern and historic oak, but by the time of testing, the blocks cut from the green oak would have seasoned. Therefore maybe the difference is between unseasoned green oak and seasoned oak. Further research could look at this question using a range of hardness testing methods to see if they concur.

Further research into production of soluble sugars and acetic acid in Scots pine would provide more understanding of the large increase in moisture sorption that was observed. It would be worthwhile further research to look into the breakdown of

hemicelluloses to produce small sugar units, and determine their molecular size and osmotic potential. More research in this area would be required to determine if the problem is widespread or serious and could also be applied to modern timber technonlogy as there is little research in both modern and historic wood in the area. During this research a calibration enabling MFA to be measured using FTIR spectra was developed for historic Scots pine. It would be fantastic for research and conservation if more of these calibrations could be made on different species of wood used in timber structures in Europe. This would allow matching for MFA in like for like repairs without expense outside the reach of a conservation budget.

List of references

Abadie, M. and Mendonce, K., 2009. Moisture performance of building materials: From material characterization to building simulation using the moisture buffer value concept. *Building and Environment,* 44, pp. 388–401.

Adams, S., 2014. *The impact of changing climate on tree growth and wood quality of Sitka spruce.* Doctoral thesis, University of Glasgow.

Åkerholm, M. and Salmén, L., 2004. Softening of wood polymers induced by moisture studied by dynamic FTIR spectroscopy. *Journal of Applied Polymer Science*, 94, pp. 2032–2040.

Ali, M., Emsley, A.M., Herman, H. and Heywood, R.J., 2001. Spectroscopic studies of the ageing of cellulosic paper. *Polymer*, 42, pp. 2893–2900.

Altaner, C.M. and Jarvis, M.C., 2008. Modelling polymer interactions of the 'molecular Velcro' type in wood under mechanical stress. *Journal of Theoretical Biology*, 253, pp. 434–45.

Altaner, C.M., Thomas, L., Fernandes, A. and Jarvis, M., 2014a. How cellulose stretches: synergism between covalent and hydrogen bonding. *Biomacromolecules*, 15, pp. 791–798.

Altaner, C.M., Horikawa, Y., Sugiyama, J. and Jarvis, M., 2014b. Cellulose Iß investigated by IR-spectroscopy at low temperatures. *Cellulose*, 21, pp. 3171–3179.

Altaner, C.M., Tokareva, E., Jarvis, M. and Harris, P., 2010. Distribution of (1→4)-ß-galactans, arabinogalactan proteins, xylans and (1→3)-ß-glucans in tracheid cell walls of softwoods. *Tree Physiology*, 30, pp. 782–793.

Altaner, C.M., Tokareva, E., Wong, J., Hapca, A., McLean, P. and Jarvis, M., 2008. Measuring compression wood severity in spruce. *Wood Science and Technology*, 43, pp. 279–290.

Alteyrac, J., Cloutier, A., Zhang, S.and Ung, C., 2006. Mechanical properties in relation to selected wood characteristics of black spruce. *Wood and Fiber Science*, 38, pp. 229–237.

American Society for Testing and Materials (ASTM). 2010 D 143 Standard methods of testing small clear specimens of timber. *ASTM, West Conshohocken,* PA, USA.

Anagnost, S.1998. Light microscopic diagnosis of wood decay. *IAWA Journal (NS)* 19, pp. 141-167.

André, A., Kliger, R. and Asp, L.E., 2014. Compression failure mechanism in small scale timber specimens. *Construction and Building Materials*, 50, pp. 130–139.

André, A., Kliger, R. and Olsson, R., 2013. Compression failure mechanism in small-scale wood specimens reinforced with CFRP: An experimental study. *Construction and Building Materials*, 41, pp. 790–800.

Anjos, O., Rodrigues, C., Morais, J. and Pereira, H., 2014. Effect of density on the compression behaviour of cork. *Materials and Design*, 53, pp. 1089–1096.

List of references

Anjos, O., Pereira, H. and Rosa, M.E., 2008. Effect of quality, porosity and density on the compression properties of cork. *Holz als Roh- und Werkstoff*, 66, pp. 295–301.

Ashby, M. and Medalist, R., 1983. The mechanical properties of cellular solids. *Metallurgical Transactions A*, 14, pp. 1755–1769.

Ashour, T., Georg, H. and Heiko, W., 2011. An experimental investigation on equilibrium moisture content of earth plaster with natural reinforcement fibres for straw bale buildings. *Applied Thermal Engineering,* 31, pp. 293-303.

Augustin, M. and Schickhofer, G., 2006. Behavior of glulam in compression perpendicular to grain in different strength grades and load configurations. *Proceedings of CIB-W* 18, pp. 1–16.

Auty, D., Achim, A., Macdonald, E., Cameron, D. and Gardiner, B., 2014. Models for predicting wood density variation in Scots pine. *Forestry*, 87, pp. 449–458.

Auty, D., Achim, A., Macdonald, E., Cameron, D. and Gardiner, B., 2013. Models for predicting microfibril angle variation in Scots pine. *Annals of Forest Science*, 70, pp. 209–218.

Auty, D., 2011. *Modelling the effects of forest management on the wood properties and branch characteristics of UK-grown Scots pine.* Doctoral Thesis, Univsersity of Aberdeen.

Aydin, S., 2007. Mechanical properties of four timber species commonly used in Turkey. *Turkish Journal of Engineering,* 31, pp. 19-27.

Ayers, T., 2000. *Salisbury Cathedral: The West Front.* Phillimore.

Babiński, L., 2011. Investigations on pre-treatment prior to freeze-drying of archaeological pine wood with abnormal shrinkage anisotropy. *Journal of Archaeological Science*, 38, pp. 1709–1715.

Babiński, L., Izdebska-Mucha, D. and Waliszewska, B., 2014. Evaluation of the state of preservation of waterlogged archaeological wood based on its physical properties: basic density vs. wood substance density. *Journal of Archaeological Science*, 46, pp. 372–383.

Badel, É. and Perré, P., 2002. Predicting oak wood properties using X-ray inspection: representation, homogenisation and localisation. Part I: Digital X-ray imaging and representation by finite elements. *Annals of Forest Science*, 59, pp. 767–776.

Badel, E., Bakour, R. and Perré, P., 2006. Investigation of the relationships between anatomical pattern, density and local swelling of oak wood. *IAWA Journal*, 27, pp. 55–71.

Bader, T.K., Hofstetter, K., Alfredsen, G. and Bollmus, S., 2012. Changes in microstructure and stiffness of Scots pine *(Pinus sylvestris* L.*)* sapwood degraded by *Gloeophyllum trabeum and Trametes versicolor* – Part II: Anisotropic stiffness properties. *Holzforschung*, 66, pp. 199–206.

Bailey, M.J., Biely, P. and Poutanen, K., 1992. Interlaboratory testing of methods for assay of xylanase activity. *Journal of Biotechnology*, 23, pp. 257–270.

List of references

Barber, N.F. and Meylan, B.A., 1964. The anisotropic shrinkage of wood: A theoretical model. *Holzforschung,* 18, pp. 146-156.

Barker, B. and Owen, N.L., 1999. Identifying softwoods and hardwoods by infrared spectroscopy. *Journal of Chemical Education,* 76, p.1706-1709.

Barnett, J.R. and Bonham, V. A., 2004. Cellulose microfibril angle in the cell wall of wood fibres. *Biological Reviews of the Cambridge Philosophical Society,* 79, pp. 461–72.

Basta, C.T., Gupta, R., Leichti, R. And Sinha, A., 2011. Characterizing perpendicular-to-grain compression (C⊥) behavior in wood construction. *Holzforschung,* 65, pp. 845–853.

Beaulieu, J., Zhang, S., Yu, Q. and Rainville, A., 2006. Comparison between genetic and environmental influences on lumber bending properties in young white spruce. *Wood and Fiber Science,* 38, pp. 553–564.

Beck, M.J. and Strickland, R.C.,1984. Production of ethanol by bioconversion of wood sugars derived from two-stage dilute acid hydrolysis of hardwood. *Biomass,* 6, pp. 101–110.

Beets, P.N., Gilchrist, K. and Jeffreys, M.P., 2001. Wood density of Radiata pine: effect of nitrogen supply. *Forest Ecology and Management,* 145, pp. 173–180.

Bell, T., 1992. Extended use of timber frame structures. *Construction and Building Materials,* 6, pp. 153- 157.

Benabou, L., 2012. Finite strain analysis of wood species under compressive failure due to kinking. *International Journal of Solids and Structures,* 49, pp. 408–419.

Bendtsen, B. and Ethington, R., 1975. Mechanical properties of 23 species of Eastern hardwoods. *USDA Forest Service,* pp. 1–12.

Bergander, A., Brändström, J., Daniel, G. and Sahnen, L., 2002. Fibril angle variability in earlywood of Norway spruce using soft rot cavities and polarization confocal microscopy. *Journal of Wood Science,* 48, pp. 255–263.

Bergès, L., Nepveu, G. and Franc, A., 2008. Effects of ecological factors on radial growth and wood density components of sessile oak (*Quercus petraea* Liebl.) in Northern France. *Forest Ecology and Management,* 255, pp. 567–579.

Bergsten, U., Lindeberg, J., Rindby, A. and Evans, R., 2001. Batch measurements of wood density on intact or prepared drill cores using x-ray microdensitometry. *Wood Science and Technology,* 35, pp. 435–452.

Bhadusha, N. and Ananthabaskaran, T., 2011. Kinetic, thermodynamic and equilibrium studies on uptake of Rhodamine B onto $ZnCl_2$ activated low cost carbon. *E-Journal of Chemistry,* 9, pp. 137–144.

Bikova, T. and Treimanis, A., 2001. Solubility and molecular weight of hemicelluloses from *Alnus incana* and *Alnus glutinosa:* effect of tree age. *Plant Physiology and Biochemistry,* 40, pp. 347–353.

List of references

Björdal, C., Nilsson, T. and Bardage, S., 2005. Three-dimensional visualisation of bacterial decay in individual tracheids of *Pinus sylvestris. Holzforschung*, 59, pp. 178–182.

Bjurhager, I., Halonen, H., Lindfors, E., Iversen, T., Almkvist, G., Gamstedt, K. and Berglund, L., 2012. State of degradation in archeological oak from the 17th century Vasa ship: substantial strength loss correlates with reduction in (holo)cellulose molecular weight. *Biomacromolecules*,13, pp. 2521–7.

Bjurhager, I., Ljungdahl, J., Wallström, L., Gamstedt, K. and Berglund, L., 2010. Towards improved understanding of PEG-impregnated waterlogged archaeological wood: A model study on recent oak. *Holzforschung*, 64, pp. 243–250.

Blanchette, R., Otjen, L., Effland, M. and Eslyn, W., 1985. Changes in structural and chemical components of wood delignified by fungi. *Wood Science and Technology*, 19, pp. 35–46.

Blanchette, R., 1995. Degradation of the lignocellulose complex in wood. *Canadian Journal of Botany*, 73, pp. 999–1010.

Blanchette, R., 2000. A review of microbial deterioration found in archaeological wood from different environments. *International Biodeterioration and Biodegradation*, 46, pp. 189–204.

Boey, F., Chia, L. and Teoh, S., 1985. Compression, bend and impact testing of some tropical wood polymer composites. *Radiation Physics and Chemistry,* 26, pp. 415–421.

Bohannan, B., 1966. *Effect of size on bending strength of wood members*. U.S Forest Service. Madison, Wisc

Borgin, K., Faix, O. and Schweer, W., 1975. The effect of aging on lignins of wood. *Wood Science and Technology*, 9, pp. 207–211.

Borgin, K., Tsoumis, G. and Passialis, C., 1979. Density and shrinkage of old wood. *Wood Science and Technology,* 13, pp. 49–57.

Borri, A. and Corradi, M., 2011. Strengthening of timber beams with high strength steel cords. *Composites: Part B,* 42, pp. 1480–1491.

Boström, L., 1999. Determination of the modulus of elasticity in bending of structural timber–comparison of two methods. *European Journal of Wood and Wood Products*, 57, pp. 145–149.

Bouriaud, O., Bréda, N., Le Moguédec, G. and Nepveu, G., 2003. Modelling variability of wood density in beech as affected by ring age, radial growth and climate. *Trees*, 18, pp. 264–276.

Branco, J.M. and Descamps, T., 2015. Analysis and strengthening of carpentry joints. *Construction and Building Materials,* 97, pp. 34–47.

Brazier. D., 1985.Timber. In: Sunley, J and Bedding, B (ed.) *Timber in Construction,* pp. 13-21, TRADA, High Wycombe.

List of references

Brentnall, C., 2008.Timber. In: Forsyth (ed) *Materials and Skills for Historic Building Conservation,* pp. 167-175, Blackwell, Oxford.

Breuil, C. and Saddler, J., 1985. Comparison of the 3, 5-dinitrosalicylic acid and Nelson-Somogyi methods of assaying for reducing sugars and determining cellulase activity. *Enzyme and Microbial Technology*, 7, pp. 327–332.

Britannica., 2006. *Wood* [Online]. [Accessed 12/06/12] Available from: http://kids.britannica.com/elementary/art-66141/Cross-section-of-a-tree-trunk.

Brites, R.D., Neves, L., Saporiti Machado, J., Lourenço, P. and Sousa, H., 2013. Reliability analysis of a timber truss system subjected to decay. *Engineering Structures*, 46, pp. 184–192.

Bromley, J.R., Busse-Wicher, M., Tryfona, T., Mortimer, J., Zhang, Z., Brown, D. and Dupree, P., 2013. GUX1 and GUX2 glucuronyltransferases decorate distinct domains of glucuronoxylan with different substitution patterns. *The Plant Journal*, 74, pp. 423–434.

Broughton, J.G. and Hutchinson, A.R. 2001. Effect of timber moisture content on bonded-in rods. *Construction and Building Materials*, 15, pp. 17–25.

Brunskill, R., 2004. *Timber building in Britain.* 2nd edition. Cassell. London

Buck, R., 1952. A note on the effect of age on the hygroscopic behaviour of wood. *Studies in Conservation*, 1, pp. 39–44.

Bucşa, L. and Bucşa, C., 2008. Roman wooden churches wall painting bio deterioration. In: Gril, J, (ed). *Wood science for conservation of cultural heritage,* Proceedings of the international conference held by COST Action IE0601 in Braga (Portugal), pp. 75-80.

Bucur, V., 1985. Ultrasonic, hardness and X-ray densitometric analysis of wood. *Ultrasonics*, 23, pp. 269–275.

Bulleit, B., Sandberg, L., Drewek, M. and Bryant, T., 1999. Behaviour and modelling of wood-pegged timber frames. *Journal of Structural Engineering* 125, pp. 3-9

Busse-Wicher, M., Gomes, T., Tryfona, T., Nikolovski, N., Stott, K., Grantham, N., Bolam, D., Skaf, M. and Dupree, P., 2014. The pattern of xylan acetylation suggests xylan may interact with cellulose microfibrils as a twofold helical screw in the secondary plant cell wall of *Arabidopsis thaliana. The Plant Journal ,* 79, pp. 492–506.

Burgert, I. and Fra tzl, P., 2009. Plants control the properties and actuation of their organs through the orientation of cellulose fibrils in their cell walls. *Integrative and Comparative Biology*, 49, pp. 69–79.

Burgert, I., 2006. Exploring the micromechanical design of plant cell walls. *American Journal of Botany*, 93, pp. 1391–1401.

Burnett, J., 1964. *The Vegetation of Scotland.* Edinburgh: Oliver and Boyd, pp. 562-565.

Canmore, 2008. *Carnock House* [Online]. [Accessed 04/04/13] Available from: http://canmore.org.uk/site/46828/carnock-house.

List of references

Canmore, 2013. *Dysart, Panhall, 1 Pan Ha', Bay House* [Online]. [Accessed 04/04/13]
Available from: http://canmore.org.uk/site/53989/dysart-panhall-1-pan-
ha-bay-house.

Carbó, M., Martínez, V. and Adelantado, J., 1997. Fourier transform infrared
spectroscopy and the analytical study of sculptures and wall decoration. *Journal
of Molecular Spectroscopy* 2860, pp. 559-563.

Carlquist, S., 2010. Caryophyllales: a key group for understanding wood anatomy
characterstates and their evolution. *Botanical Journal of the Linnean Society*,
164, pp. 342–393.

Carpenter Oak and Woodland., 2003. *Stirling Castle* [Online]. [Accessed: 10/02/2012]
Available from: carpenteroakandwoodland.com/conservation/gallery/restored-
oak-framed-roof-stirling-castle-scotland.

Carvalho, J., Santos, J. and Santos, J., 2009. Quality control and productivity in oak
timber-from forest to the primary processing. *COST Action E53* conference 22nd -
23rd October 2009, Lisbon, Portugal, pp. 1-16

Casadio, F. and Toniolo, L., 2001. The analysis of polychrome works of art: 40 years of
infrared spectroscopic investigations. *Journal of Cultural Heritage*, 2, pp. 71–78.

Cave, I., 1968. The anisotropic elasticity of the plant cell wall. *Wood Science and
Technology*, 2, pp. 268–278.

Cave, I.D., 1972. A theory of the shrinkage of wood. *Wood Science and Technology*, 6,
pp. 284–292.

Cawthorne, R., 2012. *10 things you might not know about the Mary Rose* [Online].
[Accessed 23/04/2014]. Available from:
http://www.archaeology.co.uk/articles/features/10-things-you-might-not-know-
about-the-mary-rose.htm.

Čejková, A. and Kolář, T., 2009. Extreme radial growth reaction of Norway spruce
along an altitudinal gradient in the Šumava Mountains. *Geochronometria*, 33,
pp. 41–47.

Cestari, C.B., Biglione, G., Cestari, L., Corradino, G., Crivellaro, A., Luca, D., Marzi,
T., Panosch, P. and Pasquino, R., 2011. Learning from a case study: the great
timber roof structures of the Cathedral of Vercelli. *International Conference on
Structural Health Assessment of Timber Structures* - Lisbon, Portugal - June
2011 pp.1–13.

Chaffey, N., 2000. Microfibril orientation in wood cells: new angles on an old topic.
Trends in Plant Science, 5, pp. 360-362.

Chang, H.-T. and Chang, S.T., 2002. Moisture excluding efficiency and dimensional
stability of wood improved by acylation. *Bioresource Technology*, 85, pp. 201–4.

Chang, S., Salmén, L., Olsson, A. and Clair, B., 2014. Deposition and organisation of
cell wall polymers during maturation of poplar tension wood by FTIR
microspectroscopy. *Planta*, 239, pp. 243–54.

List of references

Chapman, M., Norton, B., Taylor, J. and Lavery, D., 2006. The reduction in errors associated with ultrasonic non-destructive testing of timber arising from differential pressure on and movement of transducers. *Construction and Building Materials*, 20, pp. 841–848.

Charles, F. W. B. and Charles, M., 1990. *Conservation of timber buildings*. Stanley Thornes Ltd, Cheltenham.

Chauhan, S.S., Aggarwal, P., Karmarkar, A. and Pandey, K. K., 2001. Moisture adsorption behaviour of esterified rubber wood (*Hevea brasiliensis*). *Holz als Roh- und Werkstoff*, 59, pp. 250–253.

Chirkova, J., Irbe, I, Andersons, B. and Andersone, I., 2006. Study of the structure of biodegraded wood using the water vapour sorption method. *International Journal of Biodeterioration and Biodegradation*, 58, pp. 162–167.

Clarke, R. and Squirrell, J., 1985. An instrument for assessing the condition of waterlogged wooden objects. *Studies in Conservation*, 30, pp. 177-183.

Clausen, C., 2010. Biodeterioration of wood, In: Forest Service (ed), *Wood Hand Book: Wood as an Engineering Material*. USDA, pp. 14.1-14.16.

Cosgrove, D.J. and Jarvis, M.C., 2012. Comparative structure and biomechanics of plant primary and secondary cell walls. *Frontiers in Plant Science*, 3, pp.1-6.

Courtenay, L., 1999. Where roofs meet wall: structural innovations and hammer-beam antecedents, 1150-1250. In: Yeomans, D (ed) *The Development of Timber as a Structural Material*. Routledge, Oxford, pp. 91-126.

Cowdrey, D.R. and Preston, R.D., 1966. Elasticity and microfibrillar angle in the wood of Sitka spruce. *Proceedings of the Royal Society B: Biological Sciences*, 166, pp. 245–272.

Cown, D., Ball, R. and Riddell, M., 2005. Wood density and microfibril angle in 10 *Pinus radiata* clones: distribution and influence on product performance. *New Zealand Journal of Forestry*, 34, pp. 293-315.

Crone, A., 1998. The development of an Early Historic tree-ring chronology for Scotland. *Proceedings of the Society of Antiquaries of Scotland*, 128, pp. 485–493.

Crone, A. and Mills, C., 2002. Seeing the wood and the trees: dendrochronological studies in Scotland. *Antiquity*, 76, pp. 788-793.

Crone, A., 2008 Stirling Castle Palace, dendrochronological analysis of oak and pine timbers. *Archaeological and Historical Research*. Historic Scotland, Edinburgh.

Crone, A., 2011. *Carnock House, Stirling; Dendrochronological analysis of the painted oak beams*. AOC Archaeology Group, Edinburgh.

Čufar, K., Gričar, J., Zupančič, M., Koch, G. and Schmitt, U., 2008. Anatomy, cell wall structure and topochemistry of water-logged archaeological wood aged 5,200 and 4,500 years. *IAWA Journal*, 29, pp. 55–68.

Čufar, K., Merela, M. and Erič, M., 2014. A Roman barge in the Ljubljanica River (Slovenia): wood identification, dendrochronological dating and wood preservation research. *Journal of Archaeological Science*, 44, pp. 128–135.

List of references

Cullen C., 1996. In search of concealed timber decay. *Context,* 49, pp. 13-16.

Curling, S., Clausen, C. and Winandy J., 2001. The effect of hemicellulose degradation on the mechanical properties of wood during brown rot decay. *International Research Group on Wood Preservation* IRG/WP 01-20219, pp. 1-10

Custódio, J. and Broughton, J., 2008. Factors influencing bond performance In: Richter, K.and Cruz, H., (ed). *COST Action E34, Bonding of timber,* pp. 62-79.

Custodio, J., Broughton, J. and Cruz, H., 2009. A review of factors influencing the durability of structural bonded timber joints. *International Journal of Adhesion and Adhesives,* 29, pp. 173-185.

Davidson, M., 2014.Sanctuary: A modern legal anachronism. *Capital University Law Review,* 42, pp. 583-618.

Davis, A., 2011. Long-term approaches to native woodland restoration: Palaeoecological and stakeholder perspectives on Atlantic forests of Northern Europe. *Forest Ecology and Management,* 261, pp. 751–763.

Davies, A and Watson, F., 2007. Understanding the changing value of natural resources: an integrated palaeoecological–historical investigation into grazing–woodland interactions by Loch Awe, Western Highlands of Scotland, *Journal of Biogeography,* 34, pp. 1777-1791.

Deacon, J., 2005. *Fungal Biology* [online].[Accessed 05/03/2011] Available from: http://archive.bio.ed.ac.uk/jdeacon/FungalBiology/chapters.htm#top.

De Borst, K. and Bader, T.K., 2014. Structure-function relationships in hardwood-insight from micromechanical modelling. *Journal of Theoretical Biology,* 345, pp. 78–91.

De Borst, K., Jenkel, C., Montero, C., Colmars, J., Gril, J., Kaliske, M. and Eberhardsteiner, J., 2013. Mechanical characterization of wood: An integrative approach ranging from nanoscale to structure. *Computers and Structures,* 127, pp. 53-67.

Decoux, V., Varcin, É. and Leban, J., 2004. Tree-ring wood density assessed by X-ray densitometry and optical anatomical measurements in conifers. Consequences for the cell wall apparent density determination. *Annals of Forest Science,* 61, pp. 251–262.

Demaus, R., 1995. *Precision treatment of death watch beetle attack. The Conservation and Repair of Ecclesiastical Buildings* [Online]. [Accessed *17/10/2009]* Available at: www.buildingconservation.com.

Derrick, M., Stulik, D. and Landry, J., 1999. *Infrared Spectroscopy in Conservation Science,* The Getty Conservation Institute, Los Angeles.

Desch, H. and Dinwoodie, J., 1996. *Timber; Structure, Properties, Convservation and Use.* 7th edition. Macmillan Press Ltd, London.

Dinh, A., Pilate, G., Assor, C. and Perré, P., 2008. Measurement of the elastic properties of the minute samples of wood along the three material directions In: Gril, J. (ed). *Wood Science for Conservation.* COST Action IE0601 in Braga (Portugal), pp. 30-35.

List of references

Dinwoodie, J.M., 1966. Induction of cell wall dislocation (slip planes) during the preparation of microscope sections of wood. *Nature,* 212, pp. 525-527.

Divos, F., Tanaka, T. and Kato, H.N.H., 1998. Determination of shear modulus on construction size timber. *Wood Science and Technology,* 32, pp. 393–402.

Dixon, P., 2002. *Puir Labourers and Busy Husbandmen. The Countryside of Lowland Scotland in the Middle Ages.* Edinburgh: Birlinn Press, pp. 24-29.

Doménech Carbó, M., Periz Martínez, V. and Gimeno Adelantado, J. V., 1997. Fourier transform infrared spectroscopy and the analytical study of sculptures and wall decoration. *Journal of Molecular Structure*, 2860, pp. 559–563.

Doménech Carbó, M.T., Bosch Reig, F., Gimeno Adelantado, J. V. and Periz Martínez, V., 1996. Fourier transform infrared spectroscopy and the analytical study of works of art for purposes of diagnosis and conservation. *Analytica Chimica Acta*, 330, pp. 207–215.

Donaldson, L., 2008. Review –microfibril angle: measurement, variation and relationships. *IAWA Journal,* 29, pp. 345-386.

Dover Museum., 2000. *Bronze Age boat [*Online]. [Accessed 14/07/15]Available from; http://www.dovermuseum.co.uk/Bronze-Age-Boat/Bronze-Age-Boat.aspx.

Downes, G. and Nyakuengama, J., 2002. Relationship between wood density, microfibril angle and stiffness in thinned and fertilized *Pinus radiata. IAWA Journal*, 23, pp. 253–265.

Downes, G.M., Wimmer, R. and Evans, R., 2002. Understanding wood formation: gains to commercial forestry through tree-ring research. *Dendrochronologia*, 20, pp. 37–51.

Doyle, J. and Walker, J., 1985. Indentation of wood by wedges. *Wood Science and Technology*, 55, pp. 47–55.

Driftwood Forest Products., 2011. *Knotty pine paneling* [Online]. [Accessed 14/07/15] Available from: http://www.draftwood.com/knotty-pine-paneling.html.

Dupont, A. and Tétreault, J., 2010. Cellulose degradation environment VOCs. *Studies in Conservation*, 45, pp. 201–210.

Dutilleul, P., Herman, M. and Avella-Shaw, T., 1998. Growth rate effects on correlations among ring width, wooddensity, and mean tracheid length. *Canadian Journal of Forest Research*, 28, pp. 56–68.

Dutta, S., De, S., Saha, B. and Alama, I., 2012. Advances in conversion of hemicellulosic biomass to furfural and upgrading to biofuels. *Catalysis Science and Technology* 10, pp. 2025-2036.

Edith, J. and Maryse, M., 2009. *Application of FTIR Microscopy to Cultural Heritage Materials.* Alma Mater Studiorum, Università di Bologna.

Edwards, C. and Mason W.L. 2006., Stand structure and dynamics of four native Scots pine *(Pinus sylvestris* L.*)* woodlands in northeast Scotland. *Forestry, 79,* pp. 261-277.

List of references

El-Hosseiny, F. and Page, D., 1973. The measurement of fibril angle of wood fibres using polarized light. *Wood and Fiber Science*, 5, pp. 9–12.

Ellis, S. and Steiner, P., 2002. The behaviour of five wood species in compression. *IAWA Journal*, 23, pp. 201–211.

Ellison, R., 2000. *The effects of daylight* [Online].[Accessed 12/06/13] Available from: http://www.buildingconservation.com/articles/daylight/daylight.htm.

Encyclopaedia Britannica., 2000. *Wood: Shrinkage and Swelling* [Online]. [Accessed 14/06/2015] Available from: http://www.britannica.com/science/wood-plant-tissue/images-videos/Distortions-in-sawn-wood-due-to-shrinkage-and-swelling-At/55254.

Engelund, E.T., Thygesen, L., Svensson, S. and Hill, C., 2013. A critical discussion of the physics of wood–water interactions. *Wood Science and Technology*, 47, pp. 141–161.

Enoki, A., Tanaka, H. and Fuse, G., 1988. Degradation of lignin-related compounds, pure cellulose, and wood components by white-rot and brown-rot fungi. *Holzforschung*, 42, pp. 85-93.

Enoki, A., Tanaka, H. and Fuse, G., 1989. Relationship between degradation of wood and production of H_2O_2-producing or one-electron oxidases by brown-rot fungi. *Wood Science and Technology*, 12, pp. 1–12.

Erhardt, D., Mecklenburg, M. and Tumosa, C., 1996. New versus old wood: Differences and similarities in physical, mechanical, and chemical properties. In: *ICOM Committee for Conservation, 11th Triennial meeting in Edinburgh, Scotland, 1-6 September 1996: Preprints*, pp. 903–910.

Esau, K., 1977. *Anatomy of seed plants. 2nd edition* John Wiley and sons Inc., New York, pp.101-106.

Esteban, L., Fernándezb, F., Casasúsa, A., De Palaciosa, P. and Grilc, J., 2006. Comparison of the hygroscopic behaviour of 205-year-old and recently cut juvenile wood from *Pinus sylvestris*. L. *Annals of Forest Science,* 63, pp. 309-317.

Esteban, L., Gril, J., De Palaciosa, P. and Casasúsa, A., 2005. Reduction of wood hygroscopicity and associated dimensional response by repeated humidity cycles. *Annals of Forest Science,* 62, pp. 175-184.

Esteban, L.G., de Palacios, P., García Fernández, F., Martín, Juan A., Génova, M. and Fernández-Golfín, J., 2009. Sorption and thermodynamic properties of buried juvenile *Pinus sylvestris* L. wood aged 1,170 ± 40 BP. *Wood Science and Technology*, 43, pp. 679–690.

Esteban, L.G., de Palacios, P., García Fernández, F. and García-Amorena, I., 2010. Effects of burial of *Quercus* spp. wood aged 5910±250 BP on sorption and thermodynamic properties. *International Biodeterioration and Biodegradation*, 64, pp. 371–377.

Ethington, R.L., Eskelsen, V. and Gupta, R., 1996. Relationship between compression strength perpendicular to grain and ring orientation. *Forest Products Journal*, 46, pp. 84–86.

Evans, P., Michell, A. and Schmalzl, K., 1992. Studies of the degradation and protection of wood surfaces. *Wood Science and Technology*, 163, pp. 151-163.

Evans, R. and Ilic, J., 2001. Rapid prediction of wood stiffness from microfibril angle and density. *Forest Products Journal,* 51, pp. 53-57.

Evans, R., 1999. A variance approach to the X-ray diffractometric estimation of microfibril angle in wood. *Appita*, 52, pp. 283–289.

Evans, R., Stringer, S. and Kibblewhite, R.P., 2000. Variation of microfibril angle, density and fibre orientation in twenty-nine *Eucalyptus nitens* trees. *Appita*, 53, pp. 450–457.

Fackler, K. and Schwanninger, M., 2012. How spectroscopy and microspectroscopy of degraded wood contribute to understand fungal wood decay. *Applied Microbiology and Biotechnology,* 96, pp. 587–99.

Faix, O. and Böttcher, J., 1992. The influence of particle size and concentration in transmission and diffuse reflectance spectroscopy of wood. *Holz als Roh-und Werkstoff*, 50, pp. 221-226.

Faix, O., Bremer, J., Schmidt, O. and Tatjana, S., 1991. Monitoring of chemical changes in white-rot degraded beech wood by pyrolysis—gas chromatography and Fourier-transform infrared spectroscopy. *Journal of Analytical and Applied Pyrolysis*, 21, pp. 147–162.

Faix, O., 1991. Classification of lignins from different botanical origins by FT-IR spectroscopy. *Holzforschung*, 45, pp. 21–28.

Farruggia, F. and Perré, P., 2000. Microscopic tensile tests in the transverse plane of earlywood and latewood parts of spruce. *Wood Science and Technology*, 34, pp. 65–82.

Fawcett, R., 2002. *Scottish Medieval Churches: Architecture & Furnishings*. The History Press, Gloucestershire.

Feilden, M. B., 2003. *Conservation of Historic Buildings*. Architectural Press, London.

Feio, A.O., Lourenço, P.B. and Machado, J.S., 2008. Structural behaviour of traditional mortise-and-tenon timber joints. In: *Wood science for conservation of cultural heritage: Braga 2008: Proceedings of the international conference held by COST Action IE0601 in Braga (Portugal), 5-7 November 2008*, pp. 309–315.

Fenton, A., 1976. *Scottish Country Life*. John Donald, Edinburgh. pp. 181-192.

Fernandes, A., Thomas, L., Altaner, C., Callow, P., Forsyth, T., Apperley, D., Kennedy, C. and Jarvis, M., 2011. Nanostructure of cellulose microfibrils in spruce wood. *Proceedings of the National Academy of Sciences of the United States of America,* 108, pp. E1195–203.

Ferraz, A., Córdova, A.M. and Machuca, A., 2003. Wood biodegradation and enzyme production by *Ceriporiopsis subvermispora* during solid-state fermentation of *Eucalyptus grandis. Enzyme and Microbial Technology*, 32, pp. 59–65.

Fielke, T., Zimmer, K., Fromm, J. and Larnøy, E., 2011. Sorption behaviour of Scots Pine in Northern Europe. In: *Proceedings of the 7th Meeting of the Nordic-*

Baltic Network in Wood Material Science and Engineering (WSE), October 27-28, 2011, Oslo Norway. pp. 131–136.

Fowler, J.2002. *Landscapes and Lives. The Scottish Forest through the Ages.* Edinburgh: Canongate. pp. 27-32.

Fratzl, P., Burgert, I. and Gupta, H., 2004. On the role of interface polymers for the mechanics of natural polymeric composites. *Physical Chemistry Chemical Physics*, 6, pp. 5575–5579.

Frew, C., 2013. Lime Harling, *Building Conservation* [Online]. [Accessed 04/08/15] Available from: www.buildingconservation.com/articles/lime-harling/lime-harling.htm.

Frihart, C. and Hunt, C., 2010. Adhesives with Wood Materials: Bond Formation and Performance. In: Forestry Service (ed.) *Wood Handbook: Wood as an engineering material*, United States Department of Agriculture. pp. 228-251.

Fukuta, S., Watanabe, A., Akahori, Y., Makita, A., Imamura, Y. and Sasaki, Y., 2011. Biegeeigenschaften von Pressholz imprägniert mit Phenolharz über gebohrte Löcher. *European Journal of Wood and Wood Products*, 69, pp. 633–639.

Gabrielii, I., Gatenholm, P., Glasser, W.G., Jain, R.K. and Kenne, L., 2000. Separation characterization and hydrogel-formation of hemicellulose from aspen wood. *Carbohydrate Polymers*, 43, pp. 367–374.

Gapare, W., Ivković, M. and Dillon, S., 2012. Genetic parameters and provenance variation of *Pinus radiata* D. Don. 'Eldridge collection'in Australia 1: growth and form traits. *Tree Genetics and Genomes,* 8, pp. 1–17.

Gelbrich, J., Gaur, R. and Bansal, N., 2002. Effects of moisture transfer across building components on room temperature. *Building and Environment*, 37, pp. 11-17.

Gelbrich, J., Mai, C. and Militz, H., 2012. Evaluation of bacterial wood degradation by Fourier Transform Infrared (FTIR) measurements. *Journal of Cultural Heritage,* 13, pp. S135-S138.

Gelbrich, J., Mai, C. and Militz, H., 2008. Chemical changes in wood degraded by bacteria. *International Biodeterioration and Biodegradation,* 6, pp. 24–32.

General Botany Laboratory., 2011. *Heartwood and Sapwood* [Online]. [Assessed: 14/04/2012] Available from: emp.byui.edu/wellerg/Secondary%20Gro wth/Instructions/Secondary%20Growth%20Instructions%2003.html

Gereke, T., Anheuser, K. and Lehmann, E., 2011. Moisture behaviour of recent and naturally aged wood. *Wood Research,* 56, pp. 33–42.

Gerhards, C., 1980. Effect of moisture content and temperature on the mechanical properties of wood: an analysis of immediate effects. *Wood and Fiber Science,* 14, pp. 4–36.

Gerrish. S., 2011. Architectural Joinery. *The Building Conservation Directory* Cathedral Communications, Wiltshire pp. 134-136.

List of references

Giorgi, R., Chelazzi, D. and Baglioni, P., 2005. Nanoparticles of calcium hydroxide for wood conservation. The deacidification of the Vasa warship. *Langmuir : the ACS Journal of Surfaces and Colloids*, 21, pp. 10743-8.

Glass, S. and Zelinka S., 2010. Moisture relations and physical properties of wood. In: Forest Service (ed) *Wood Handbook: Wood as an Engineering Material*. USDA. pp. 14.1-14.19.

Gomme, A., 2002.Scottish hammerbeam roofs, and one that isn't. *Architectural Heritage*. 13, pp. 20-35.

Gorzsas, H., Stenlund, P., Persson, J., Trygg, B. and Sundberg, B., 2011. Cell-specific chemotyping and multivariate imaging by combined FT-IR microspectroscopy and orthogonal projections to latent structures (OPLS) analysis reveals the chemical landscape of secondary xylem. *Plant Journal*, 66, pp. 903–914.

Grabner, M. and Kotlinova, M., 2008. Ageing of wood –Described by the analysis of old beams. In: Gril, J. (ed). *Wood Science for Conservation of Cultural Heritage. Proceedings of the International Conference held by COST Action IE0601 in Braga (Portugal)*, pp. 57-61.

Grabner, M., Müller, U., Gierlinger, N. and Wimmer, R., 2005. Effects of heartwood extractives on mechanical properties of larch. *IAWA Journal*, 26, pp. 211–220.

Grant, I., 1961. *Highland Folk Ways*. Routledge and Kegan Paul, London, pp. 141-160.

Greaves, H., 1971. The bacterial factor in wood decay. *Wood Science and Technology*, 5, pp. 6–16.

Green, D E., 2001. *Wood: Strength and Stiffness*. Encyclopedia of Materials: Science and Technology, Elsevier, Amsterdam. pp. 9732–9736.

Green, D., Begel, M. and Nelson, W. 2006. Janka hardness using nonstandard specimens. *Forest Products Laboratory Research note* FLP-RN-0303 USDA, pp. 2-13.

Grimsdale., 1985. Timber frame construction. In: Sunley, J. and Bedding, B., *Timber in Construction*, TRADA, High Wycombe, pp. 105-119.

Gross, M., 2010. *Biofuels: the next generation* [Online]. [Accessed 06/03/14] Available from; www.rsc.org/education/eic/issues/2009May/Biofuelsthenextgeneration.asp.

Gruchow, F., Machill, S., Thiele, S., Herm, C. and Salzer, R., 2009. Imaging FTIR spectroscopic investigations of wood: paint interface of aged polychrome art objects. *e-Preservation Science*, 6, pp. 145–150.

Gryc, V., Vavrčík, H. and Horn, K., 2011. Density of juvenile and mature wood of selected coniferous species. *Journal of Forest Science*, 57, pp. 123–130.

Guilley, É., Hervé, J., Huber, F. and Nepveu, G., 1999. Modelling variability of within-ring density components in *Quercus petraea* Liebl. with mixed-effect models and simulating the influence of contrasting silvicultures on wood density. *Annals of Forest Science*, 56, pp. 449-458.

List of references

Guilley, E., Hervé, J.-C. and Nepveu, G., 2004. The influence of site quality, silviculture and region on wood density mixed model in *Quercus petraea* Liebl. *Forest Ecology and Management*, 189, pp. 111–121.

Hanke, T., 2008a. Scotland: The Case of Stirling Palace. *Archaeological and Historical Research*. Historic Scotland, Edinburgh.

Hanke, T., 2008b. Stirling Castle: The construction of the ceilings over the royal bed chambers. *Archaeological and Historical Research*. Historic Scotland. Edinburgh.

Hannrup, B., Wilhemsson, L. and Danell, Ö., 1998. Time trends for genetic parameters of wood density and growth traits in *Pinus sylvestris* L. *Silvae Genetica*, 47, pp. 214-219.

Harris, J. and Meylan, B., 1965. The influence of microfibril angle on longitudinal and tangential shrinkage in *Pinus radiata. Holzforschung,* 19, pp. 144–153.

Harris, R., 2010. *Discovering Timber-Framed Buildings*. 3rd Edition. Shire Publications, Oxford.

Hastrup, A. Howell, C., Larsen, F., Sathitsuksanoh, N., Goodell, B. and Jellison, J., 2012. Differences in crystalline cellulose modification due to degradation by brown and white rot fungi. *Fungal Biology,* 116, pp. 1052–1063.

Hay, G., 1976. Some aspects of timber construction in Scotland. In: Fenton, (ed). *Building Construction in Scotland: some historical and regional aspects Scottish vernacular buildings* working group Dundee and Edinburgh, pp. 28-38.

Hayden, J. and Lund, I., 1998 Restoration of a timber framed threshing barn. *Context,* 59, pp. 33-35.

He, X., Lau, A., Sokhansanj, S., Lim, C., Bi, X. and Melin, S., 2013. Moisture sorption isotherms and drying characteristics of aspen (*Populus tremuloides*). *Biomass and Bioenergy*, 57, pp.161–167.

Hein, P.R. and Lima, J., 2012. Relationships between microfibril angle, modulus of elasticity and compressive strength in Eucalyptus wood. *Maderas, Ciencia y Tecnología,* 14, pp. 267–274.

Hein, P.R., Silva, J.R. and Brancheriau, L., 2013. Correlations among microfibril angle, density, modulus of elasticity, modulus of rupture and shrinkage in 6-year-old *Eucalyptus urophylla × E. grandis. Madera,. Ciencia y Tecnología,* 15, pp. 171–182.

Helińska-Raczkowska, L. and Moliński, W., 2003. The effect of the Janka ball indentation depth on the hardness number determined for selected wood species. *Folia Forestalia Polonica*, 1990, pp. 27–36.

Helge, S.K., 2000. Modulus of elasticity – local or global values. *Proceedings of the 6th World Conference on Timber engineering,* Canada, 408, pp. 1–6.

Historic Scotland., 2012. *Holyrood Abbey* [Online]. [Accessed 06/06/12] Available from: http://www.historic-scotland.gov.uk/propertyresults/propertydetail. htm?PropID=PL_124.

List of references

Hittmeier, M., 1967. Effect of structural direction and initial moisture content on swelling rate of wood. *Wood Science and Technology*, 1, pp. 109–121.

Hiziroglu, S., 2009. *Strength Properties of Wood for Practical Applications.* Fact Sheet FAPC-162 Oklahoma State University,

Hoadley, B., 1990. *Identifying Wood: Accurate Results with Simple Tools.* Taunton Press Inc. Newtown, Connecticut.

Hoffmeyer, P. and Davidson, R.W., 1989. Mechano-sorptive creep mechanism of wood in compression and bending. *Wood Science and Technology,* 23, pp. 215-227.

Holmqvist, C. and Boström, L., 2000. Determination of the modulus of elasticity in bending of structural timber - comparison of two methods. *Holz als Roh- und Werkstoff*, 57, pp. 145–149.

Horie, C. V., 1987. *Materials for Conservation: Organic Consolidants, Adhesives and Coatings*. Butterworth and Heinemann, Oxford.

Hosseinaei, O., Wang, S. and Rials, T., 2012. Effect of hemicellulose extraction on physical and mechanical properties and mold susceptibility of flakeboard. *Forest Product*, 61, pp. 31–37.

Hume, I., 1998 Load testing and historic structure. *Context,* 57, pp. 23-25.

Ikonen, V.P., Peltola, H., Wilhelmsson, L., Kilpeläinen, A., Väisänen, H., Nuutinen, T. and Kellomäki, S., 2008. Modelling the distribution of wood properties along the stems of Scots pine (*Pinus sylvestris* L.) and Norway spruce (*Picea abies* (L.) Karst.) as affected by silvicultural management. *Forest Ecology and Management*, 256, pp. 1356-1371.

Ilic, J., 2003. Dynamic MOE of 55 species using small wood beams. *Holz als Roh-und Werkstoff*, 61, pp. 167–172.

Ispas, M., 2013. Experimental investigations on swelling pressure of natural and heat-treated ash wood. Bulletin of the Transilvania University of Brasov, Series II: Forestry, *Wood Industry, Agricultural Food Engineering*, 6, pp. 55–62.

Jackson, A. and Day, D., 1989. *Collins Complete Woodworkers Manual,* HarperCollins, London.

Jakub, G., Magdalena, S. and Tomasz, Z., 2012. Cellulose crystallinity index examination in oak wood originated for antique woodwork. *Komunik,* 55, pp. 109-113.

Jarvis, M.C., 2012. Cellulose crystallinity: perspectives from spectroscopy and diffraction. In: Harding, S.E. (ed.) *Stability of Complex Carbohydrate Structures: Biofuels, Foods, Vaccines and Shipwrecks*. Royal Society of Chemistry, London, UK.

Ji, Z. Ma, J., Zhang, Z., Xu, F. and Sun, R., 2013. Distribution of lignin and cellulose in compression wood tracheids of *Pinus yunnanensis* determined by fluorescence microscopy and confocal Raman microscopy. *Industrial Crops and Products*, 47, pp. 212–217.

List of references

Joseleau, J.P., Imai, T., Kuroda, K. and Ruel, K., 2004. Detection *in situ* and characterization of lignin in the G-layer of tension wood fibres of *Populus deltoides*. *Planta,* 219, pp. 338–345.

Kačuráková, M. and Wilson, R.H., 2001. Developments in mid-infrared FT-IR spectroscopy of selected carbohydrates. *Carbohydrate Polymers,* 44, pp. 291–303.

Kandemir-Yucel, A., 2007. *In situ* assessment of structural timber elements of a historic building by infrared thermography and ultrasonic velocity. *Infrared Physics and Technology*, 49, pp. 243-248.

Kärenlampi, P., Tynjälä, P. and Ström, P., 2003. Molecular reorganization in wood. *Mechanics of Materials*, 35, pp. 1149–1159.

Keckes, J., Burgert, I., Frühmann, K., Müller, M., Kölln, K., Hamilton, M., Burghammer, M., Roth, S., Stanzl-Tschegg, S. and Fratzl, P., 2003. Cell-wall recovery after irreversible deformation of wood. *Nature Materials*, 2, pp. 810–814.

Kellomäki, S., Ikonen, V., Peltola, H. and Kolström, T., 1999. Modelling the structural growth of Scots pine with implications for wood quality. *Ecological Modelling*, 122, pp. 117-134.

Kennedy, A. and Pennington, E.R., 2014. Conservation of chemically degraded waterlogged wood with sugars. *Studies in Conservation,* 59, pp. 194–201.

Khali, D.P. and Rawat, S.P.S., 2000. Clustering of water molecules during adsorption of water in brown rot decayed and undecayed wood blocks of *Pinus sylvestris. Holz als Roh- und Werkstoff*, 58, pp.340–341.

Khalili, S., Nilsson, T. and Daniel, G., 2001. The use of soft rot fungi for determining the microfibrillar orientation in the S2 layer of pine tracheids. *Holz als Roh- und Werkstoff,* 58, pp.439–447.

Khan, W., Tremblay, D. and LeDuy, A., 1986. Assay of xylanase and xylosidase activities in bacterial and fungal cultures. *Enzyme and Microbial Technology*, 8, pp.373–377.

Kifetew, G., Thuvander, F., Berglund, L. and Lindberg, H., 1998. The effect of drying on wood fracture surfaces from specimens loaded in wet condition. *Wood Science and Technology,* 32, pp. 83–94.

Kim, J. and Daniel, G., 2012. Distribution of glucomannans and xylans in poplar xylem and their changes under tension stress. *Planta*, 236, pp. 35–50.

Kisternaya, M. And Kozlov, V., 2010. Chemical protection of historic timber structures: Results and Future Needs. *International Research Group on Wood Protection pp 4 Biarritz*,9th-13th May 2010 France, pp. 10-40

Kisternaya, M. and Kozlov, V., 2006. Russian wooden architectural heritage: century-old traditions to use forest products. *Cultural Heritage and Sustainable Forest Management. Proceedings of Conference 8-11 June 2006 Florence* Italy, pp. 465-469.

Kisternaya, M. and Kozlov, V., 2007. Wood science approach for the preservation of historic timber structures. *Petrozavodsk: Izd-ro KarRC RAS-Russia*. pp. 132-139.

List of references

Klaassen, R., 2014. Speed of bacterial decay in waterlogged wood in soil and open water. *International Biodeterioration and Biodegradation,* 86, pp.129–135.

Knapic, S., Louzada, J., Leal, S. and Pereira, H., 2007. Radial variation of wood density components and ring width in cork oak trees. *Annals of Forest Science*, 64, pp. 211–218.

Knapic, S., Machado, J.S. and Pereira, H., 2012. Properties of cork oak wood related to solid wood flooring performance. *Construction and Building Materials,* 30, pp. 569–573.

Knut, L. and Marstien, N., 2000. *Conservation of Historic Timber Structures: An Ecological Approach.* Bulten and Hein, London.

Kolář, T., Rybníček, M. and Střelcová, M., 2014. The changes in chemical composition and properties of subfossil oak deposited in Holocene sediments. *Wood Research,* 59, pp. 149–166.

Kolin, B. and Janezic, T., 1996. The effect of temperature, density and chemical composition upon the limit of hygroscopicity of wood. *Holzforschung*, 50, pp. 263–268.

Kong, F., Engler, C.R. and Soltes, E.J., 1992. Effects of cell-wall acetate, xylan backbone, and lignin on enzymatic hydrolysis of aspen wood. *Applied Biochemistry and Biotechnology*, 34-35, pp. 23–35.

Koponen, S. and Virta, J., 2004. Stress relaxation and failure behaviour under swelling and shrinkage loads in transverse directions. *COST E35 Workshop* I, *8 - 9 September 2004, Vila Real, Portugal 1*, pp.1–4.

Koponen, S., Toratti, T. and Kanerva, P., 1989. Modelling longitudinal elastic and shrinkage properties of wood. *Wood Science and Technology,* 63, pp. 55–63.

Korkut, S. and Guller, B., 2008. Physical and mechanical properties of European hophornbeam (*Ostrya carpinifolia* Scop.) wood. *Bioresource Technology*, 99, pp. 4780–4785.

Kostiainen, K., Kaakinen, S., Saranpaa, P., Sigurdsson, D., Lundqvist, O., Linder, S. and Vapaavuori, E. 2009. Stem wood properties of mature Norway spruce after 3 years of continuous exposure to elevated [CO_2] and temperature. *Global Change Biology*, 15, pp. 368-379.

Kozlov, V. and Kitsernaya, M., 2013. Sorption properties of historic and recent pine wood. *International Biodeterioration and Biodegradation,* 86, pp. 153-157.

Krauss, A., Moliński, W., Kúdela, J. and Čunderlík, I., 2011. Differences in the mechanical properties of early and latewood within individual annual rings in dominant pine tree (*Pinus sylvestris* L.). *Wood Research*, 56, pp. 1–12.

Kretschmann, D., 2010. Mechanical properties of wood. In Forest Service (ed.) *Wood Handbook: Wood as an Engineering Material*. USDA. Madison, pp. 5.1-5.46.

Kretschmar, E., Gelbrich, J., Militz, H. andLamersdorf, N., 2008. Studying bacterial wood decay under low oxygen conditions—results of microcosm experiments. *International Biodeterioration & Biodegradation,* 61, pp. 69–84.

Kuilen, J., 2006. Service life modelling of timber structures. *Materials and Structures,* 40, pp. 151–161.

Kulkarni, A.R. Peña, M., Avci, U., Mazumder, K., Urbanowicz, B., Pattathil, S., Yin, Y., O'Neill, M., Roberts, A., Hahn, M., Xu, Y., Darvill, A. and York, W., 2012. The ability of land plants to synthesize glucuronoxylans predates the evolution of tracheophytes. *Glycobiology,* 22, pp. 439–451.

Kunecký, J., Arciszewska-Kędzior, A., Sebera, V., and Hasníková, H., 2015. Mechanical performance of dovetail joint related to the global stiffness of timber roof structures. *Materials and Structures,* 10.1617/s11527-015-0651-1, pp. 1-13.

Kutnar, A. and Kamke, F.A., 2010. Transverse compression behavior of wood in saturated steam. In: *First Serbian Forestry Congress*. pp. 1571–1577.

Lachenbruch, B., Johnson, G. R., Downes, G. M. and Evans, R., 2010. Relationships of density, microfibril angle, and sound velocity with stiffness and strength in mature wood of Douglas fir. *Canadian Journal of Forest Research,* 40, pp. 55–64.

Langan, P., Sangha, A.,Wymore, T., Parks, J.,Yang, Z.,Hanson, B., Fisher, Z., Mason, S., Blakeley, M., Forsyth, T., Glusker, J., Carrell, H., Smith, J., Keen, D.,Graham, D. and Kovalevsky, A., 2014. Epimerization by D-xylose isomerase: X-ray, / neutron crystallographic and molecular simulation study. *Structure,* 22, pp. 1287-1300.

Larsen, K. and Marstein, N., 2000. *Conservation of Historic Timber Structures: An Ecological Approach*. Butterworth and Heinemann, Oxford.

Lasserre, J.P., Mason, E., Watt, M. and Moore, J., 2009. Influence of initial planting spacing and genotype on microfibril angle, wood density, fibre properties and modulus of elasticity in *Pinus radiata* D. Don corewood. *Forest Ecology and Management*, 258, pp. 1924-1931.

Le, E. and Nairn, J., 2014. Measuring interfacial stiffness of adhesively bonded wood. *Wood Science and Technology*, 48, pp. 1109–1121.

Leal, S., Sousa, V., Knapic, S., Louzada, J. and Pereira, H., 2011. Vessel size and number are contributors to define wood density in cork oak. *European Journal of Forest Research,* 130, pp. 1023-1029.

Lee, S.H., Doherty, T., Linhardt, R. and Dordick, J., 2008. Ionic liquid-mediated selective extraction of lignin from wood leading to enhanced enzymatic cellulose hydrolysis. *Biotechnology and Bioengineering,* 102, pp. 1368–76.

Lehringer, C., Daniel, G. and Schmitt, U., 2009. TEM/FE-SEM studies on tension wood fibres of *Acer* spp., *Fagus sylvatica* L. and *Quercus robur* L. *Wood Science and Technology*, 43, pp.691–702.

Leijten, J.M., Larsen, H.J. and Van der Put, T., 2010. Structural design for compression strength perpendicular to the grain of timber beams. *Construction and Building Materials,* 24, pp. 252–257.

Leney, L., 1981. A technique for measuring fibril angle using polarized light. *Wood and Fiber Science*, 13, pp. 13-16.

List of references

Leonardon, M., Altaner, C., Vihermaa, L. and Jarvis, M., 2009. Wood shrinkage: influence of anatomy, cell wall architecture, chemical composition and cambial age. *European Journal of Wood and Wood Products,* 68, pp. 87–94.

Lipovszky, G. and Raczkowski, J., 1971. Stress relaxation in wood periodically reloaded to attain initial stress. *Holzforschung*, 25, pp. 47–49.

Lionetto, F. and Frigione, M., 2012. Effect of novel consolidants on mechanical and absorption properties of deteriorated wood by insect attack. *Journal of Cultural Heritage,* 13, pp. 195–203.

Lionetto, F., Sole,R., Cannoletta, D., Vasapollo, G. and Maffezzoli, A., 2012, Monitoring wood degradation during weathering by cellulose crystallinity. *Materials*, 5, pp.1910-1922.

Lionetto, F., Quarta, G., Cataldi, A., Cossa, A., Auriemma, R., Calcagnile, L. and Frigione, M., 2013. Characterization and dating of waterlogged woods from an ancient harbor in Italy. *Journal of Cultural Heritage*, 15, pp. 213-217.

Logan, J., 2013. *Sensitivity to Fundamental Wood Properties in the Metriguard Model 7200 HCLT and the CLT* [Online]. [Accessed 14/04/1013] Available from: http://www.metriguard.com/fiber.php.

Long, J., Conn, A., Batchelor, W. and Evans, R., 1999. Comparison of techniques to measure the fibril angle. *Appita Journal,* 53, pp. 432-437.

Lopez-Anido, R., Michael, A.P. and Sandford, T.C., 2003. Experimental characterization of FRP composite-wood pile structural response by bending tests. *Marine Structures*, 16, pp. 257–274.

Lourenço, P.B., Feio, A.O. and Machado, J.S., 2007. Chestnut wood in compression perpendicular to the grain: Non-destructive correlations for test results in new and old wood. *Construction and Building Materials,* 21, pp. 1617–1627.

Low, S.R. 2001. *Rockwell Hardness Measurement of Metallic Materials*, National Institute of Standards and Technology Special publication 960-5, Washington.

Lythe, S.and Butt, J., 1975. *An Economic History of Scotland 1100-1939*. Blackie. Glasgow, pp. 58-60.

Macchioni, N., Capretti, C., Sozzi, L. and Pizzo, B., 2013. Grading the decay of waterlogged archaeological wood according to anatomical characterisation. The case of the Fiavé site (N-E Italy). *International Biodeterioration and Biodegradation*, 84, pp. 54-64.

MacDonald, E., Moore, J. and Gardiner, B., 2009. Developing methods for assessing Scots pine timber quality. *Research Note-Forestry*, pp. 1–8.

MacKinnon, I., Šturcová, A., Sugimoto-Shirasu K., His, I., McCann, M. and Jarvis, M., 2006. Cell-wall structure and anisotropy in *procuste*, a cellulose synthase mutant of *Arabidopsis thaliana*. *Planta*,224, pp. 438–448.

Machado, J.S., Louzada, J., Santos, A., Nunes, L., Anjos, O., Rodrigues, J., Simões, R.and Pereira, H., 2014. Variation of wood density and mechanical properties of blackwood (*Acacia melanoxylon* R. Br.). *Materials and Design,* 56, pp. 975–980.

List of references

Mäkinen, H., Nöjd, P., Kahle, H. P., Neumann, U., Tveite, B., Mielikäinen, K., Röhle, H. and Spiecker, H., 2003. Large-scale climatic variability and radial increment variation of *Picea abies* (L.) Karst. in central and northern Europe. *Trees - Structure and Function,* 17, pp. 173–184.

Mansfield, S.D., Parish, R., Di Lucca, C., Goudie, J., Kang, K. and Ott, P., 2009. Revisiting the transition between juvenile and mature wood: a comparison of fibre length, microfibril angle and relative wood density in lodgepole pine. *Holzforschung,* 63, pp. 449-456.

Marchessault, R.H., 1962. Application of infra-red spectroscopy to cellulose and wood polysaccharides. *Pure and Applied Chemistry,* 5, pp.107–130.

Marsden, J. and Winterbottom, M., 2010. *Windsor Castle,* Royal Collection Enterprises Ltd. London.

Martin, A., 1987. *Kintyre Country Life.* John Donald, Edinburgh, pp. 142-147.

Mather, R. and Savill, P., 1994. The commercial impact of oak shake in Great Britain. *Forestry,* 67, pp. 119-131.

Mather, R.A., Kanowski, P.J. and Savill, P.S., 1993. Genetic determination of vessel area in oak (*Quercus robur* L and *Q. petraea* Liebl): a characteristic related to the occurrence of stem shakes. *Annales des Sciences Forestiéres,* 50, pp. 395–398.

Mattheck, C., Bethge, K. and Albrecht, W., 1995. Failure modes of trees and related failure criteria. *Wind and Trees, September 16-18, 2003,* University of Karlsruhe, Germany. pp. 195–203.

Mazzanti, P., 2012. Drying shrinkage and mechanical properties of poplar wood (*Populus alba* L.) across the grain. *Journal of Cultural Heritage* 13, pp. 89-92.

McCaig, I., 2006. Using synthetic resin to conserve and repair timber. *Context,* 95, pp. 25-26.

McConnachie, G., Eaton, R. and Jones, M., 2008. A re-evaluation of the use of maximum moisture content data for assessing the condition of waterlogged archaeological wood. *E-preservation Science*, pp. 29–35.

McGowan, A., 1999. *HMS Victory: Her Conservation, Career and Restoration,* Caxton Editions. London.

McLean, J.P., Evans, R. and Moore, J.R., 2010. Predicting the longitudinal modulus of elasticity of Sitka spruce from cellulose orientation and abundance. *Holzforschung,* 64, pp. 1–6.

Meinert, M.C. and Delmer, D.P., 1977. Changes in biochemical composition of the cell wall of the cotton fiber during development. *Plant Physiology,* 59, pp. 1088–1097.

Menart, E., de Bruin, G. and Strlič, M., 2014. Effects of NO_2 and acetic acid on the stability of historic paper. *Cellulose*, 21, pp. 3701–3713.

Meylan, B., 1972. The influence of microfibril angle on the longitudinal shrinkage-moisture content relationship. *Wood Science and Technology,* 6, pp. 293–301.

List of references

Mihranyan, A., Llagostera, A,. Karmhag, R., Strømme, M. and Ek, R., 2004. Moisture sorption by cellulose powders of varying crystallinity. *International Journal of Pharmaceutics*, 269, pp. 433–442.

Milek, K and Jones, R., 2015. *SCARF Science Panel Report* [Online]. [Accessed: 26/11/15] Available from:http://www.scottishheritagehub.com/content/15-dendrochronology-scotland.

Miller, G.L., 1959. Use of dinitrosalicylic acid reagent for determination of reducing sugar. *Analytical Chemistry,* 31, pp. 426-428.

Mills, C., 2008. Historic pine and dendrochronology in Scotland. In: *Thirteenth meeting, October 2008, Scottish Natural Heritage Centre Perth*. Woodland History Section. pp. 4-8.

Mills, C. and Crone, A., 2012. Dendrochronological evidence for Scotland's native timber resources over the last 1000 years. *Scottish Forestry*, 66, pp. 18-33.

Mitchell, G., 1985. Domestic carpentry. In: Sunley, J and Bedding, B ed. *Timber in Construction,* TRADA, High Wycombe, pp. 119-140.

Miyajima, H., 1955. The hardness test by static ball for wood, especially for Nara-wood under various moisture conditions.研究報告= *Research Bulletins of the College Experiment Forests,* 17, pp. 749-768.

Monaco, A., Mattei, E., Pelosi, C. and Santancini, M., 2013. The scientific investigation for the study and conservation of the wooden model of S. Maria della Consolazione's church (Todi, Italy). *Journal of Cultural Heritage*, 14, pp. 537–543.

Moore, J., Achim, A., Lyon, A., Mochan, S. and Gardiner, B., 2009a. Effects of early re-spacing on the physical and mechanical properties of Sitka spruce structural timber. *Forest Ecology and Management*, 258, pp. 1174–1180.

Moore, J., 2011. *Wood properties and uses of Sitka spruce in Britain,* Research report, SIRT, Forestry Commission, Edinbrough.

Moore, J.R., Lyon, A., Searles, G. and Vihermaa, L., 2009b. The effects of site and stand factors on the tree and wood quality of Sitka spruce growing in the United Kingdom. *Silva Fennica,* 43, pp. 383–396.

Moore, J.R., Cown, D.J. and McKinley, R.B., 2014. Modelling microfibril angle variation in New Zealand-grown Radiata pine. *New Zealand Journal of Forestry Science,* 44, pp. 25-36.

Mörath, E., 1932. Studien über die hygroskopischen Eigenschaften und die Härte der Hölzer. *Mitteilung der Holzforschungsstelle an der TH Darmstadt*. Hannover: Schape.

Morton, B., 2009. Bell-frames under threat. *Context*, 110, pp. 11-12.

Müller, U., Sretenovic, A., Gindl, W., Grabner, M., Wimmer, R. and Teischinger, A., 2002. Effects of macro- and micro-structural variability on the shear behaviour of softwood. *IAWA Journal*. 25, pp. 231-243.

List of references

Nagpure, A. Choudhary, B. Kumar, S. Gupta, R., 2014. Isolation and characterization of chitinolytic *Streptomyces* sp. MT7 and its antagonism towards wood-rotting fungi. *Annals of Microbiology,* 64, pp. 531–541.

Nairn, J., 2005. Numerical simulations of transverse compression and densification in wood. *Wood and Fiber Science,* 38, pp. 576–591.

Naumann, A. and Polle, A,. 2006. FTIR imaging as a new tool for cell wall analysis of wood. *New Zealand Journal of Forestry Science*, 36, pp. 54–59.

Newland, K., 2010. *The acquisition and use of Norwegian timber in seventeenth century Scotland, with reference to the principal building works of James Baine, His Majesty's Master Wright*. Unpublished PhD thesis, University of Dundee.

Newton, F., 2011. *Stopping the Rot: a Guide to Enforcement Action to Save Historic Buildings.* 2nd edition. English Heritage, London.

Niemz, P., 2008. Methods of non-destructive wood testing In: Gril J (ed) *Wood science for Conservation of Cultural Heritage-* Proceedings of the international conference held by COST action ie0601 in Braga (Portugal), pp. 30-35.

Nilsson, T. and Rowell, R., 2007. Historical Wood. In: Uzielli, L., (ed) *Wood Science for Conservation of Cultural Heritage-Florence 2007*: Proceedings of the International Conference held by COST Action IE0601 in Florence (Italy), 8-10 November 2007, pp. 11-15.

Oberle, B., Dunham, K., Milo, A., Walton, M., Young, D. and Zanne, A., 2014. Progressive, idiosyncratic changes in wood hardness during decay: Implications for dead wood inventory and cycling. *Forest Ecology and Management*, 323, pp. 1–9.

Oldrieve, W. and Scot, F., 1916. The ancient roof of Glasgow cathedral: Its condition and restoration. *Proceedings of the Society of Antiquaries of Scotland.* 50, pp. 155-172

Olsson, A.M. and Salmén, L., 2004. The association of water to cellulose and hemicellulose in paper examined by FTIR spectroscopy. *Carbohydrate Research,* 339, pp. 813–8.

Ouis, D., 2002. On the frequency dependence of the modulus of elasticity of wood. *Wood Science and Technology*, 36, pp. 335–346.

Ozdemir, F., Ayrilmis, N., Kaymakci, A. and Kwon, J., 2014. Improving dimensional stability of injection molded wood plastic composites using cold and hot water extraction methods. *Maderas,Ciencia y tecnología*, 16, pp. 365–372.

Page, D.H., 1969. A method for determining the fibrillar angle in wood tracheids. *Journal of Microscopy,* 90, pp. 137–143.

Palaia, L., 2007. Structural failure analysis of timber floors and roofs in ancient buildings at Valencia (Spain) In: *Material to Structure - Mechanical Behaviour and Failures of the Timber Structures ICOMOS IWC - XVI International Symposium* – Florence, Venice and Vicenza 11th -16th November 2007, pp. 1-11.

List of references

Palviainen, J., Silvennoinen,R. and Rouvinen, J., 2004. Analysis of microfibril angle of wood fibers using laser microscope polarimetry. *Optical Engineering*, 43, pp. 186-191.

Pandey, K., 1998. A study of chemical structure of soft and harwood and wood polymers by FTIR spectrscopy. *Journal of Applied Polymer Science,* 71, pp.1969–1975.

Pandey, K. and Theagarajan, K., 1997. Analysis of wood surfaces and ground wood by diffuse reflectance (DRIFT) and photoacoustic (PAS) Fourier transform infrared spectroscopic techniques. *Holz als Roh-und Werkstoff*. 55, pp. 383-390.

Pandey. K. and Pitman. A., 2003. FTIR studies of the changes in wood chemistry following decay by brown-rot and white-rot fungi. *International Biodeterioration and Biodegradation,* 52, pp. 151-160.

Parente, J.P., Adão, C., da Silva, B. and Tinoco, L., 2014. Structural characterization of an acetylatedglucomannan with antiinflammatory activity and gastroprotective property from *Cyrtopodiumandersonii*. *Carbohydrate Research,* 391, pp. 16–21.

Paris, O., Burgert, I. and Fratzl, P., 2010. Biomimetics and biotemplating of natural materials. *MRS Bulletin*, 35, pp. 219-226.

Park, S., Baker, J., Himmel, M., Parilla, P. and Johnson, D., 2010. Cellulose crystallinity index: measurement techniques and their impact on interpreting cellulase performance. *Biotechnology for Biofuels,* 3, pp. 10-20.

Passialis, C., 1997. Physico-chemical characteristics of waterlogged archaeological wood. *Biology, Chemistry, Physics and Technology of Wood*, 51, pp. 111–113.

Patera, A., Derome, D., Griffa, M. and Carmeliet, J., 2013. Hysteresis in swelling and in sorption of wood tissue. *Journal of Structural Biology,* 182, pp. 226–34.

Pawar, P., Koutaniemi, S., Tenkanen, M. and Mellerowicz, E., 2013. Acetylation of woody lignocellulose: significance and regulation. *Frontiers in Plant Science*, 4, pp. 1-8.

Penttilä, P., Várnai, A., Pere, J., Tammelin, T., Salmén, L., Siika-aho, M., Viikari, L. and Serimaa, R., 2013. Xylan as limiting factor in enzymatic hydrolysis of nanocellulose. *Bioresource Technology,* 129, pp. 135–41.

Pérez, J., Muñoz-Dorado, J., de la Rubia, T. and Martínez, J., 2002. Biodegradation and biological treatments of cellulose, hemicellulose and lignin: an overview. *International Microbiology : The Official Journal of the Spanish Society for Microbiology*, 5, pp. 53–63.

Perré, P. and Huber, F., 2007. Measurement of free shrinkage at the tissue level using an optical microscope with an immersion objective: results obtained for Douglas fir (*Pseudotsuga menziesii*). *Annals of Forest Science,* 64, pp. 255–265.

Piazza, M. and Riggio, M., 2008. Visual strength-grading and NDT of timber in traditional structures. *Journal of Building Appraisal*, 3, pp. 267–296.

Pinto, P.C., Evtuguin, D. V. and Neto, C.P., 2005. Structure of hardwood glucuronoxylans: Modifications and impact on pulp retention during wood kraft pulping. *Carbohydrate Polymers*, 60, pp. 489-497.

List of references

Pizzo B. and Schober, K., 2008. On site interventions on decayed beam ends In: Richter, K and Cruz, H (ed). *COST Action E3,4 Bonding of Timber,* Brussels, pp. 46-55.

Pizzo, B., 2008. Durability of historic structures repaired with adhesives In: Richter, K and Cruz, H (ed). *COST Action E34, Bonding of Timber,* Brussels, pp. 80-85.

Popescu, C.M. and Hill, C., 2013. The water vapour adsorption–desorption behaviour of naturally aged *Tilia cordata* Mill. wood. *Polymer Degradation and Stability,* 98, pp. 1804–1813.

Popescu, C.M., Dobele, G., Rossinskaja, G., Dizhbite, T. and Vasile, C., 2006. Degradation of lime wood painting supports. *Journal of Analytical and Applied Pyrolysis,* 79, pp. 71–77.

Popescu, M., Froidevaux, J., Navi, P. and Popescu, C., 2013. Structural modifications of *Tilia cordata* wood during heat treatment investigated by FT-IR and 2D IR correlation spectroscopy. *Journal of Molecular Structure*, 1033, pp. 176–186.

Preston, J., Smith, A., Schofield, E., Chadwick, A., Jones. M. and Watts, J., 2014. The effects of Mary Rose conservation treatment on iron oxidation processes and microbial communities contributing to acid production in marine archaeological timbers. *PloS One*, 9, e84169.

RCAHMS., 2013. *Abbey Strand, Palace of Hoylrood* [Online]. [Accessed 12/01/13] Available from:http://www.scotlandsplaces.gov.uk/record/rcahms/52391 /edinburgh- holyrood-palace-holyrood -abbey-abbey-pend/rcahms.

Rackham, O., 1990.*Trees and Woodland in the British Landscape*. Revised Edition. Phoenix Press, London, pp. 87-88.

Raphael, B., 1877. *The open timber roof of the Middle Ages: illustrated by perspective and working drawing of some of the best varieties of church roof: with descriptive letter-press*, David Bogue, S6, Fleet Street, London.

Reffner, J. A., Martoglio, P. A. and Williams, G.P., 1995. Fourier transform infrared microscopical analysis with synchrotron radiation. The microscope optics and system performance. *Review of Scientific Instruments,* 66, pp. 1298-1310.

Reinprecht, L. and Hibký, M., 2011. The type and degree of decay in spruce wood analyzed by the ultrasonic method in three anatomical directions. *BioResources,* 6, pp. 4953–4968.

Reiterer, A. and Stanzl-Tschegg, S., 2001. Compressive behaviour of softwood under uniaxial loading at different orientations to the grain. *Mechanics of Materials,* 33, pp. 705–715.

Repola, J., 2006. Models for vertical wood density of Scots pine, Norway spruce and birch stems and their application to determine average wood density. *Silva Fennica*, 40, pp. 673–685.

Ricardo, P., Hein, P. and Brancheriau, L., 2011. Radial variation of microfibril angle and wood density and their relationships in 14-year-old *Eucalyptus urophylla* St Blake wood. *BioResources,* 6, pp. 3352-3362.

Ridout, B., 2000. Timber decay in buildings: the conservation approach to treatment. E. and F.N. Spon, London.

List of references

Ridout, B. 2005. Insect damage to timber: re thinking control mechanisms [Online]. [Accessed: 08/03/12] Available from: http://www.buildingconservation.com/articles/insectdamage/insectdamage.htm.

Ridout, B., 2008. Understanding decay in building timbers. In: Forsyth, M (ed) *Materials and Skills for Historic Building Conservation*. Blackwell, Oxford, pp. 160-166.

Riggio, M. and Piazza, M., 2010. Hardess test. In: Kasal, B and Tannert, T (ed.) *In Situ Assessment of Structural Timber,* Springer, Berlin, pp. 87-97.

Rinn, F., Schweingruber, F. and Schär, E., 1996. Resistograph and X-ray density charts of wood. Comparative evaluation of drill resistance profiles and X-ray density charts of different wood species. *Holzforschung*, 50, pp. 303–311.

Roliński, W. and Fabisiak, E., 2013. Radial variation of mechanical properties of pine wood (*Pinus sylvestris* L.) determined upon tensile stress. *Wood Research,* 58, pp. 329–342.

Rosner, S., Karlsson, B., Konnerth, J. and Hansmann, C., 2009. Shrinkage processes in standard-size Norway spruce wood specimens with different vulnerability to cavitation. *Tree Physiology,* 29, pp. 1419-31.

Ross, R.J. and Pellerin, R.E., 1993. Nondestructive testing for in-place assessment of wood members. *Wood Products for Engineered Structures,* 70, pp.176–179.

Roszyk, E., Moliński, W. and Jasińska, M., 2010. The effect of microfibril angle on hygromechanic creep of wood under tensile stress along the grain. *Wood Research*, 55, pp. 13-24.

Rusinb, A. and Tulika, M., 2005. Micro fibril angle in wood of Scots pine trees (*Pinus sylvestris*) after irradiation from the Chernobyl nuclear reactor accident'. *Environmental Pollution,* 134, pp. 195–199.

Russell, P., 1993. *Timber framed buildings and roofs.* [Online]. [Accessed 19/10/2009] Available from: The Building Conservation Directory http://www.buildingconservation.com/articles/timber/wood93.htm

Salca, E.A. and Hiziroglu, S., 2014. Evaluation of hardness and surface quality of different wood species as function of heat treatment. *Materials and Design*, 62, pp. 416–423.

Salmén, L., 2004. Micromechanical understanding of the cell-wall structure. *Comptes Rendues Biologies,* 327, pp. 873-880.

Sandu, I., Brebu, M., Luca, C., Sandu, I. and Vasile, C., 2003. Thermogravimetric study on the ageing of lime wood supports of old paintings. *Polymer Degradation and Stability,* 80, pp. 83–91.

Sarén, M.P. and Serimaa, R., 2006. Determination of microfibril angle distribution by X-ray diffraction. *Wood Science and Technology,* 40, pp. 445–460.

Schädel, C., Blöchl, A., Richter, A. and Hoch, G., 2010. Quantification and monosaccharide composition of hemicelluloses from different plant functional types. *Plant Physiology and Biochemistry,* 48, pp. 1–8.

List of references

Schimleck, L., Evans, R. and Jones, P., 2005. Estimation of microfibril angle and stiffness by near infrared spectroscopy using sample sets having limited wood density variation. *IAWA Journal,* 26, pp. 175–187.

Schimleck, L.R., Sussenbach, E. and Leaf, G., 2007. Microfibril angle prediction of *Pinus taeda* wood samples based on tangential face NIR spectra. *IAWA Journal*, 28, pp. 1–12.

Schneeweiß, G. and Felber, S., 2013. Review on the bending strength of wood and influencing factors. *American Journal of Materials Science,* 3, pp. 41–54.

Schniewind, A. and Cal, R. 1968. Recent progress in the study of the rheology of wood. *Wood Science and Technology,* 2, pp. 188–206.

Schober, K., 2008. Timber with passive reinforcement. In: Richter, K. and Cruz, H. (ed). *COST Action E34 Bonding of Timber,* Brussels, pp. 22-28.

Schoch, W.,Heller,I.,Schweingruber,F.H. and Kienast,F., 2004. *Wood anatomy of central   European species.* [Online]. [Accessed 06/08/15] Available from: www.woodanatomy.ch.

Science photo library., 2013. *Growth rings* [Online].[Accessed 30/07/2013]. Available from:http://www.sciencephoto.com/search?subtype=keywords&searchstring=growth+rings&sort_results=&per_page=48&page=5&previews=1&media_type=images&matchtype=fuzzy&license=M&license=F&people=yes&people=no&orientation=all&closed=search_motion_filters&shot_audio=yes&shot_audio=no&shot_aspect_ratio=all&shot_speed=all&shot_type=all&channel=all.

ScotWeb., 2013. *Sinclair* [Online]. [Accessed 09/03/13] Available from: http://www.scotweb.co.uk/info/sinclair/.

Sedighi-Gilani, M. and Navi, P., 2007. Experimental observations and micromechanical modeling of successive-damaging phenomenon in wood cells' tensile behavior. *Wood Science and Technology,* 41, pp. 69–85.

Sjödin, J. and Johansson, C., 2007. Influence of initial moisture induced stresses in multiple steel-to-timber dowel joints. *Holz als Roh- und Werkstoffe,* 65, pp. 71–77.

Serafini, A. and González-Longo, C., 2015. The design and construction techniques of eighteenth century timber roofs in Scotland; Glasgow Trades Hall and Tweeddale House in Edinburgh. *Paper presented at 5th International Congress on Construction History, Chicago, United States,* 3/06/15 - 7/06/15,

Silva, C., Branco, J., Camões, A. and Lourenço, P., 2014a. Dimensional variation of three softwoods due to hygroscopic behavior. *Construction and Building Materials,* 59, pp. 25–31.

Silva, F. and Higuchi, N., Nascimento, C., Matos, J., Paula, E. and Santos, J., 2014b. Non-destructive evaluation of hardness in tropical wood. *Journal of Tropical Forestry*, 26, pp. 69–74.

Simonović, J., Stevanic, J., Djikanović, D., Salmén, L. and Radotić, K., 2011. Anisotropy of cell wall polymers in branches of hardwood and softwood: a polarized FTIR study. *Cellulose,* 18, pp. 1433-1440.

Simons, P., 2007. Timber Crosses. In *Historical churches* [Online]. [Accessed 31/01/2012]   Available from: www.building conservation directory.com.

Singh, A.P., 2012. A review of microbial decay types found in wooden objects of cultural heritage recovered from buried and waterlogged environments. *Journal of Cultural Heritage,* 13, pp. 16–20.

Simpson, W.T., 1993. Specific Gravity, Moisture Content, and Density Relationship for Wood. *General Technical Report FPLGTR76 Madison WI* US Department of Agriculture Forest Service, Forest Products Laboratory. Madison.

Sousa, H.S., Branco, J.M. and Lourenço, P.B., 2014. Characterization of cross-sections from old chestnut beams weakened by decay. *International Journal of Architectural Heritage*, 8, pp. 436–451.

Smout, T.C., MacDonald, A. and Watson, F. 2005. *A history of the native woodlands of Scotland, 1500 –1920.* EUP. Edinburgh.

Smout, C. 2008. A handful of lost pinewoods, 1600-1800 In: *Thirteenth meeting, October 2008, Scottish Natural Heritage Centre Perth. Woodland History Section,* pp. 1-3.

Smout, C., 2015. The history and the myth of Scots pine. *Scottish Forestry,* 69, pp. 7-10.

Spicer, R. and Groover, A., 2010. Evolution of development of vascular cambia and secondary growth. *New Phytologist,* 186, pp. 577–592.

Srivilai, P., Chaiseana, W., Loutchanwoot, P. and Dornbundit, P., 2013. Comparison of differences between the wood degradation by Monokaryons (n) and Dikaryons (2n) of white rot fungus (Cambodian *Phellinus linteus*). *Journal of Biological Sciences,* 13, pp. 131-138.

Srpčič, J., 2008. Biological deterioration of historical wooden roof and floor structures and their renovation. In: Gril, J. (ed). *Wood science for conservation of cultural heritage*. Proceedings of the international conference held by COST action ie0601 in Braga (Portugal), pp. 142 –147.

Stevanic, J. and Salmén, L., 2009. Orientation of the wood polymers in the cell wall of spruce wood fibres. *Holzforschung,* 63, pp. 497–503.

Stevenson, N., 2009. Early joinery. Historic churches. *Context,* 16, pp. 27-29.

Stoeckel, F., Konnerth, J. and Gindl-Altmutter, W., 2013. Mechanical properties of adhesives for bonding wood—A review. *International Journal of Adhesion and Adhesives*, 45, pp. 32–41.

Strätling, M., 2008. Orientated investigation to kill the mycelia of the dry rot fungus, *Serpula lacrymans*, with microwaves. In: Gril, J. (ed). *Wood science for conservation of cultural heritage* - Proceedings of the international conference held by COST action IE0601 in Braga (Portugal), pp. 148-152.

Straže, A. and Gorišek, Z., 2011. Analysis of size effect on determination of mechanical properties of Norway spruce wood. *Wood is Good*: *EU Preaccession Challenges*, pp. 183–190.

Sturcova, A., Eichhorn, S., and Jarvis, M. 2006. Vibrational spectroscopy of biopolymers under mechanical stress: processing cellulose spectra using bandshift difference integrals. *Biomacromolecules,* 7, pp. 2688-2691.

Sun, R., Fang, J. M., Tomkinson, J., Geng, Z. C. and Liu, J. C., 2001. Fractional isolation, physico-chemical characterization and homogeneous esterification of hemicelluloses from fast-growing poplar wood. *Carbohydrate Polymers,* 44, pp. 29–39.

Svedström, K., Bjurhager, I., Kallonen, A., Peura, M. and Serimaa, R., 2012. Structure of oak wood from the Swedish warship Vasa revealed by X-ray scattering and microtomography. *Holzforschung*, 66, pp. 355–363.

Szabo, O.E., Csiszar, E., Toth, K., Szakacs, G. and Koczka, B., 2015. Ultrasound-assisted extraction and characterization of hydrolytic and oxidative enzymes produced by solid state fermentation. *Ultrasonics Sonochemistry*, 22, pp. 249–56.

Tabet, T. and Aziz, F., 2013. Cellulose microfibril angle in wood and its dynamic mechanical significance. In: *Cellulose - Fundamental Aspects*. pp. 113–142.

Tabraham, C., 1986. *Scottish Castles and Fortifications*. HMSO. Edinburgh.

Tamburini, D., Łucejko, J., Modugno, F. and Colombini, M., 2014. Characterisation of archaeological waterlogged wood from Herculaneum by pyrolysis and mass spectrometry. *International Biodeterioration and Biodegradation,* 86, pp. 142–149.

Taylor, and Franklin, J., 2014. Are fast-grown trees of low quality? [Online]. [Accessed 31/07/2015] Available from: https://extension.tennessee.edu/publications /Documents/W253.

Taylor, J., 1999. The George Inn. [Online]. [Accessed 19/10/2009] Available from: http://www.buildingconservation.com/articles/george/inn_conservation.htm:

Tétreault, J., Dupont, A. L., Bégin, P. and Paris, S., 2013. The impact of volatile compounds released by paper on cellulose degradation in ambient hygrothermal conditions. *Polymer Degradation and Stability,* 98, pp. 1827–1837.

Thibaut, B., Gril, J. and Fournier, M., 2001. Mechanics of wood and trees: Some new highlights for an old story. *Comptes Rendus de l'Academie de Sciences - Serie IIb: Mecanique*, 329, pp. 701–716.

Thomas, L., Forsyth, T., Martel, A., Grillo, I., Altaner, C. and Jarvis, M., 2014. Structure and spacing of cellulose microfibrils in woody cell walls of dicots. *Cellulose*, 21, pp. 3887–3895.

Thomas, L., Forsyth, V Trevor Adriana, Š., Kennedy, C., May, R., Altaner, C., Apperley, D., Wess, T. and Jarvis, M., 2013. Structure of cellulose microfibrils in primary cell walls. *Plant Physiology*, 161, pp. 465–476.

Tolvaj, L., 2009. Monitoring of photodegradation for wood by infrared spectroscopy. In: *COST Action IE0601 International Conference on Wooden Cultural Heritage: Evaluation of Deterioration and Management of Change*, Hamburg, 7–10 October. pp.1-7

List of references

Tomback, D., 2007. Valuing our heritage. In: Forsyth, M. (ed) *Understanding historic building conservation*. Blackwell Publishing. Oxford. pp. 204-210.

Thomson, A., 1991. *The Scottish Timber Trade 1680 to 1800.* Unpublished PhD thesis, St Andrews University, Scotland.

Treacy, M., Evertsen, J. and Dhubháin, A., 2000. *A Comparison of Mechanical and Physical Wood Properties*. COFORD, Finland.

Tredgold, T., 1985. *Elementary Principles of Carpentry*, E. and F. N. Spon: London.

Tsang, K. and Chan, W., 2008. Overhead line wooden pole condition sensing by acoustic method, *Sensors and Actuators*, 143, pp. 251-255.

Ulvcrona, T. and Ulvcrona, K., 2011. The effects of pre-commercial thinning and fertilization on characteristics of juvenile clearwood of Scots pine (*Pinus sylvestris* L.). *Forestry,* 84, pp. 207–219.

Unger, A., Schniewind, A. and Unger, W., 2001. *Conservation of Wooden Artefacts: A Handbook*. Springer, Berlin.

Varner, D., Černý, M., Varner, M. and Fajman, M., 2012. Possible sources of acoustic emission during static bending test of wood specimens. *Acta Universitatis Agriculturae et Silviculturae Mendelianae Brunensis*, 60, pp. 199–206.

Vats, P. and Banerjee, U., 2002. Studies on the production of phytase by a newly isolated strain of *Aspergillus niger* var *teigham* obtained from rotten wood-logs. *Process Biochemistry,* 38, pp. 211–217.

Vavrčík, H., Gryc, V. and Koňas, P., 2009. Comparison of wood density in relation to growth rings of English oak and Sessile oak. In: *Proceedings of Abstracts of TRACE* 2009. pp. 66-72.

Verrill, S. and Kretschmann, D., 2011. Concerns about a variance approach to X-ray diffractometric estimation of microfibril angle in wood. *Wood and Fiber Science,* 43, pp. 153-168.

Via, B.K., So, C., Shupe, T., Groom, L. and Wikaira, J., 2009. Mechanical response of longleaf pine to variation in microfibril angle, chemistry associated wavelengths, density, and radial position. *Composites Part A: Applied Science and Manufacturing*, 40, pp. 60–66.

Wagner, L., Bader, T., Auty, D. and de Borst, K., 2013. Key parameters controlling stiffness variability within trees: a multiscale experimental–numerical approach. *Trees,* 27, pp. 321–336.

Wahab, M. and Jumaat, M., 2014. Investigation of linearity between mechanical properties of wood using graphical method. *Sains Malaysiana,* 43, pp. 211–218.

Walker, B., 1976. Some regional variations in building techniques in Angus, Fife and Perthshire. In: A. Fenton (ed.) *Building Construction in Scotland: some Historical and Regional Aspects.* Scottish vernacular buildings working group, Dundee and Edinburgh, pp. 52-64

Warren, R., 2002. Restoring a Comper and Bucknall Church. *Context,* 74, pp. 65-67.

List of references

Weldon J., 2009. Timber floors. *The Building Conservation Directory,* Cathedral Communications, Wiltshire, pp. 190-193.

What When How., 2008. *Wood Analysis* [Online]. [Assessed: 13/04/2012] Available from: http://what-when-how.com/forensic-sciences/wood-analysis/.

Wiedenhoeft, A., 2010. Structure and function of wood (handbook). In: Rowell, R. (ed) *Handbook of Wood Chemistry and Wood Composites,* General Technical Report FPL–GTR–190. Forest Products Laboratory, Madison, pp. 9-30.

Wikipedia., 2011. Mary Rose [Online]. [Accessed 18/01/2011] Available from; https://en.wikipedia.org/wiki/Mary_Rose.

Williams, R., 2010. Finishing of Wood. In: Forest Service (ed.) *Wood Hand Book: Wood as an engineering material*. USDA. Madison, pp. 16.1-16.37.

Williams, J., Meaden, M., Simm, J.and Dupray, S., 2010. *Assessment of the Durability and Engineering Properties of Lesser-known Hardwood Timber Species for use in Marine and Freshwater Construction. A Research Report*, TRADA Technology Ltd, High Wycombe

Wilson, R., Gunnarson, B., Loader, N., Rydval, M., Patton, H., Frith, A., Mills, C. M., Crone, A. and Edwards, C., 2011. Reconstructing Holocene climate from tree rings: The potential for a long chronology from the Scottish Highlands. *The Holocene*, 22, pp. 3–11.

Wilson, K. And White, D., 1986. *The Anatomy of Wood,* Stobart and Son Ltd, London.

Wimmer, R. and Lucas, B.N., 1997. Comparing mechanical properties of secondary wall and cell corner middle lamella in spruce wood. *IAWA Journal,* 18, pp. 77–88.

Wimmer, R., Lucas, B. N., Tsui, T. Y. and Oliver, W. C.k 1997. Longitudinal hardness and Young's modulus of spruce tracheid secondary walls using nanoindentation technique. *Wood Science and Technology,* 31, pp. 131–141.

Wright, G., 2005. *Ancient Building Technology*, Vol 2, Materials, BRILL

Xavier, J., de Jesus, A., Morais, J. and Pinto, J., 2012. Stereovision measurements on evaluating the modulus of elasticity of wood by compression tests parallel to the grain. *Construction and Building Materials*, 26, pp. 207–215.

Xu, G. and Goodell, B., 2001. Mechanisms of wood degradation by brown rot fungi: chelator-mediated cellulose degradation and binding of iron by cellulose. *Journal of Biotechnology,* 87, pp. 43-57.

Yamamoto, H., Sassus, F., Ninomiya, M. and Gril, J., 2001. A model of anisotropic swelling and shrinking process of wood. *Wood Science and Technology,* 35, pp. 167–181.

Yamashita, K., Hirakawa, Y., Nakatani, H. and Ikeda, M., 2009. Tangential and radial shrinkage variation within trees in sugi (*Cryptomeria japonica*) cultivars. *Journal of Wood Science,* 55, pp. 161–168.

Yang, J.L. and Evans, R., 2003. Prediction of MOE of eucalypt wood from microfibril angle and density. *Holz als Roh- und Werkstoff,* 61, pp. 449-452.

List of references

Yang, D and Normand, D., 2012. Element 4: Hardwood Initiative — Development of new processes and technologies in the hardwood industry. *Transformative Technologies*, FPInnovations, pp. 1-25.

Yang, L., Fazio, P. and Rao, J., 2012. An investigation of moisture buffering performance of wood panelling at room level and its buffering effect on a test room. *Building and Environment*, 47, pp. 205-216.

Yao, J., 1969. Shrinkage properties of second-growth Southern yellow pine. *Wood Science and Technology*, 3, pp. 25–39.

Yeomans, D., 1985. Historic development of timber structures. In: Sunley, J. and Bedding, B. (ed). *Timber in Construction*, TRADA, High Wycombe. pp. 62-83.

Yeomans, D., 2003. *Strength Grading Historic Timbers* [Online]. [Accessed 01/10/2012] Available at: www.buildingconservation.com.

Yeomans, D., 2009. *How Structures Work: Design and Behaviour from Bridges to Buildings.* Wiley-Blackwell, Oxford.

Yilgor, N., Dogu, D., Moore, R., Terzi, E. and Kartal, S. 2013. Evaluation of fungal deterioration in *Liquidambar orientalis* Mill. heartwood by FT-IR and light microscopy. *BioResources,* 8, pp. 2805–2826.

Yoffe, E. H., 1982. Elastic stress fields caused by indenting brittle materials. *Philosophical Magazine A*, 46, pp. 617-628.

Yoshihara, H. and Oka, S., 2001. Measurement of bending properties of wood by compression bending tests. *Journal of Wood Science,* 47, pp. 262–268.

Yoshihara, H. and Tsunematsu, S., 2007. Bending and shear properties of compressed Sitka spruce. *Wood Science and Technology,* 41, pp. 117–131.

Yu, E., 1982. Production of 2, 3 - butanediol by *Klebsiella pneumoniae* grown on acid hydrolyzed wood hemicellulose. *Zhurnal Eksperimental'noi i Teoreticheskoi Fiziki*, 4, pp. 110-115.

Zabler, S., Zabler, S., Paris, O., Burgert, I and Fratzl, P., 2010. Moisture changes in the plant cell wall force cellulose crystallites to deform. *Journal of Structural Biology,* 171, pp. 133–41.

Zelinka, S., Rammer, D. and Stone, D., 2008. *Corrosion of metals in contact with treated wood: developing test methods*. New Orleans, LA, NACE,

Zhang, S.Y. 1993. Modelling wood density in European oak (*Quercus petraea* and *Quercus robur*) and simulating the silvicultural influence. *Canadian Journal of Forest Research,* 23, pp. 2587-2593.

Zhang, X., Zhao, Q., Wang, S., Trejo, R., Lara-Curzio, E. and Du, G., 2010. Characterizing strength and fracture of wood cell wall through uniaxial micro-compression test. *Composites Part A: Applied Science and Manufacturing,* 41, pp. 632–638.

Zhou, C., Smith, G.D. and Dai, C., 2009. Characterizing hydro-thermal compression behavior of aspen wood strands. *Holzforschung,* 63, pp. 609–617.

List of references

Zwerger, K., 1997. *Wood and Wood joints: building traditions of Europe, Japan and China.* Walter de Gruyter, Germany.